NASA CR-
144639

MCR-75-212
NAS9-13578

FINAL REPORT

October 1975

The Detection of Tightly Closed Flaws by Nondestructive Testing (NDT) Methods

Ward D. Rummel, Richard A. Rathke,
Paul H. Todd, Jr., and Steve J. Mullen

Mr. W. L. Castner
NASA Technical Monitor

Final Report of Research Performed
under Contract NAS9-13578
for the

National Aeronautics and Space Administration
Lyndon B. Johnson Space Center
Houston, Texas 77058

MARTIN MARIETTA

1. Report No.	2. Government Accession No.	3. Recipient's Catalog No.

4. Title and Subtitle	5. Report Date
THE DETECTION OF TIGHTLY CLOSED FLAWS BY NONDESTRUCTIVE TESTING (NDT) METHODS	October 1975
	6. Performing Organization Code
7. Author(s) Ward D. Rummel, Richard A. Rathke, Paul H. Todd, Jr., and Steve J. Mullen	8. Performing Organization Report No. MCR-75-212
9. Performing Organization Name and Address Martin Marietta Aerospace Denver Division Denver, Colorado 80201	10. Work Unit No. 11. Contract or Grant No. NAS9-13578
12. Sponsoring Agency Name and Address National Aeronautics and Space Administration Washington, D.C. 20546	13. Type of Report and Period Covered Contractor Report June 1973 - October 1975 Final 14. Sponsoring Agency Code

15. Supplementary Notes

16. Abstract

Liquid penetrant, ultrasonic, eddy current and x-radiographic techniques were optimized and applied to the evaluation of 2219-T87 aluminum alloy test specimens in integrally stiffened panel, and weld panel configurations. Fatigue cracks in integrally stiffened panels, lack-of-fusion in weld panels, and fatigue cracks in weld panels were the flaw types used for evaluation. 2319 aluminum alloy weld filler rod was used for all welding to produce the test specimens. Forty seven integrally stiffened panels containing a total of 146 fatigue cracks, ninety three lack-of-penetration (LOP) specimens containing a total of 239 LOP flaws and one-hundred seventeen welded specimens containing a total of 293 fatigue cracks were evaluated. Specimen thickness were nominally 0.317 cm (0.125 inch) and 1.27 cm. (0.500 inch) for welded specimens and 0.710 cm (0.280 inch) for the integrally stiffened panels. NDT detection reliability enhancement was evaluated during separate inspection sequences in the specimens in the "as-machined or as-welded", post etched and post proof loaded conditions. Results of the nondestructive test (NDT) evaluations were compared to the actual flaw size obtained by measurement of the fracture specimens after completing all inspection sequences. Inspection data were then analyzed to provide a statistical basis for determining the flaw detection reliability. Analyses were performed at 95% probability and 95% confidence levels and one sided lower confidence limits were calculated by the binomial method. The data were plotted for each inspection technique, specimen type and flaw type as a function of actual flaw length and depth.

PRICES SUBJECT TO CHANGE

17. Key Words		18. Distribution Statement
Nondestructive Testing	2219 Aluminum	Unclassified - Unlimited
Flaw Detection Reliability	Welding	
Liquid Penetrant	Fracture Cont.	
Ultrasonic	Fatigue Crack	
Eddy Current		
x-Radiography		Cat. 18

19. Security Classif. (of this report)	20. Security Classif. (of this page)
Unclassified	Unclassified

PREFACE

This report was prepared by Martin Marietta Aerospace under contract NAS 9-13578. Work reported was initiated by National Aeronautics and Space Administration, Lyndon B. Johnson Space Center to evaluate the capability of nondestructive evaluation techniques to detect flaws in weldments and stringer stiffended panels. The work described herein was completed between June 30, 1973 and October 30, 1975. Work was conducted under the technical direction of Mr. W. L. Castner of the Johnson Space Center.

At Martin Marietta Aerospace, Mr. Ward D. Rummel provided technical direction and program management. Mr. Richard A. Rathke was Principle Investigator for eddy current and statistical data analysis. Mr. Paul H. Todd, Jr. was principle investigator for other nondestructive evaluation techniques. Dr. Conrad F. Fiftal, C. Toth, W. Post, R. Chihoski, and W. Phillips provided support in all sample preparation; Messrs Thomas L. Tedrow, H. D. Brinkerhoff, S. Mullen and S. R. Marston provided support in X-radiographic investigations. Additional inspection and analysis support were provided by Messrs. L. Gentry, H. Lovinsone, R. Stadler and J. Neri, Jr. Special X-radiograph analysis was provided by Mr. H. Ridder, Magnaflux, Corporation.

Management support was provided by Messrs G. McGee, R. Morra, C. Duclon, C. Cancallosi and R. Daum.

Editing and typing were done by Ms B. Beddinger and J. Dummer.

The assistance and cooperation of all contributing personnel are appreciated and gratefully acknowledged. We also appreciate the program direction, support and contributions of Mr. W. L. Castner and gratefully acknowledge his continuing participation.

CONTENTS

	Page
PREFACE	
INTRODUCTION	I-1 and I-2
STATE-OF-THE-ART NONDESTRUCTIVE TESTING (NDT) METHODS	II-1
X-radiography	II-2
Penetrant	II-5
Ultrasonic Inspection	II-6
Eddy Current	II-8 thru II-11
INTEGRALLY STIFFENED STRINGER PANEL EVALUATION	III-1
Specimen Preparation	III-4
NDT Optimization	III-9
Test Specimen Evaluation	III-17
Panel Fracture	III-20
Data Analysis	III-20
Data Results	III-29 thru III-32
EVALUATION OF LACK OF PENETRATION (LOP) PANELS	IV-1
Specimen Preparation	IV-4
NDT Optimization	IV-5
Test Specimen Evaluation	IV-10
Panel Fracture	IV-12
Data Analysis	IV-12
Data Results	IV-23 thru IV-34
FATIGUE-CRACKED WELD PANEL EVALUATION	
Specimen Preparation	V-1
NDT Optimization	V-5
Test Specimen Evaluation	V-7
Panel Fracture	V-9
Data Analysis	V-9
Data Results	V-25 thru V-41
CONCLUSIONS AND RECOMMENDATIONS	VI-1 and VI-2

Page

APPENDIX A.- LIQUID PENETRANT INSPECTION PROCEDURE FOR WELD PANELS, STIFFENED PANELS AND LOP PANELS A-1

APPENDIX B.- ULTRASONIC INSPECTION FOR "TIGHT FLAW DETECTION BY NDT" PROGRAM - INTEGRALLY STIFFENED PANELS B-1

APPENDIX C.- EDDY CURRENT INSPECTION AND RECORDING FOR INTEGRALLY STIFFENED ALUMINUM PANELS C-1

APPENDIX D.- X-RADIOGRAPHIC INSPECTION PROCEDURES FOR DETECTION OF FATIGUE CRACKS AND LOP IN WELDED PANELS D-1

APPENDIX E.- ULTRASONIC INSPECTION FOR "TIGHT FLAWS DETECTION BY NDT" PROGRAM - LOP PANELS E-1

APPENDIX F.- EDDY CURRENT INSPECTION AND RECORDING OF LACK OF PENETRATION (LOP) ALUMINUM PANELS, UNSCARFED CONDITION. F-1

APPENDIX G.- EDDY CURRENT INSPECTION AND C SCAN RECORDING OF LOP, ALUMINUM PANELS, SCARFED CONDITION . . G-1

APPENDIX H.- ULTRASONIC INSPECTION FOR "TIGHT FLAWS DETECTED BY NDT" PROGRAM - WELD PANELS HAVING CROWNS. H-1

APPENDIX I.- ULTRASONIC INSPECTION FOR TIGHT FLAWS IN PANELS WITH FLUSH WELDS. I-1

APPENDIX J.- EDDY CURRENT INSPECTION AND RECORDING OF WELD CRACK ALUMINUM PANELS HAVING CROWNS . . . J-1

APPENDIX K.- EDDY CURRENT INSPECTION AND C-SCAN RECORDING OF FLUSH WELD ALUMINUM PANELS. K-1

Figure

III-1	Anticipated Surface Stress Distribution for Axially Loaded 2219-T87 Integrally Stiffened Panel	III-2
III-2	NDT Evaluation Sequence for Integrally Stiffened Panels	III-3
III-3	Integrally Stiffened Panel Configuration	III-5
III-4	Schematic Side View of the Starter Flaw and Final Crack Configurations, Integrally Stiffened Panels.	III-6
III-5	Ultrasonic Reflected Energy Response	III-12
III-6	Eddy Current Probe	III-14
III-7	Typical Eddy Current Scanning setup for Stringer Panels	III-15
III-8	Typical Eddy Current Recordings.	III-16
III-9	Stringer-to-Subpanel Attachment.	III-18
III-10	Integrally Stiffened Panel Layout and Riveted Panel Configuration.	III-19
III-11	Crack Detection Probability for Integrally Stiffened Panels by the Penetrant Method. Plotted at 95% Probability and 95% Confidence Level	III-30
III-12	Crack Detection Probability for Integrally Stiffened Panels by the Ultrasonic Method Plotted at 95% Probability and 95% Confidence Level	III-31
III-13	Crack Detection Probability for Integrally Stiffened Panels by the Eddy Current Method Plotted at 95% Probability and 95% Confidence Level	III-32
IV-1	Typical Weldment Lack of Penetration Defects	IV-1
IV-2	NDT Evaluation Sequence for Lack of Penetration Panels	IV-3
IV-3	Schematic View of a Buried LOP in a Weld, with Representative Photomicrograph Crossectional Views of a Defect.	IV-6
IV-4	Spring-Loaded Eddy Current Scanning Probe Holder for Welded Panels with Crowns.	IV-8
IV-5	Spring-Loaded Eddy Current Scanning Probe Holder for Flat Panels.	IV-9
IV-6	Schematic Side View of a LOP (Lune) Flaw Showing Critical Dimensions.	IV-13
IV-7	Flaw Detection Probability for LOP Panels by the Penetrant Method Plotted at 95% Probability and 95% Confidence	IV-31
IV-8	Flaw Detection Probability for LOP Panels by the Ultrasonic Method Plotted at 95% Probability and 95% Confidence	IV-32
IV-9	Flaw Detection Probability for LOP Panels by the Eddy Current Method Plotted at 95% Probability and 95% Confidence	IV-33

IV-10	Flaw Detection Probability for LOP Panels by the X-radiograph Method Plotted at 95% Probability and 95% Confidence	IV-34
V-1	NDT Evaluation Sequence for Fatigue-Cracked Welded Panels.	V-2
V-2	Fatigue-Cracked Weld Panels.	V-3
V-3	Schematic Side View of the Starter Flaw and Final Flaw Configurations for Fatigue-Cracked Weld Panels. .	V-4
V-4	Crack Detection Probability for Longitudinal Welds With Crowns by the Penetrant Method Plotted at 95% Probability and 95% Confidence	V-26
V-5	Crack Detection Probability for Longitudinal Welds With Crowns by the Ultrasonic Method Plotted at 95% Probability and 95% Confidence	V-27
V-6	Crack Detection Probability for Longitudinal Welds With Crowns by the Eddy Current Method Plotted at 95% Probability and 95% Confidence	V-28
V-7	Crack Detection Probability for Longitudinal Welds With Crowns by the X-radiograph Method Plotted at 95% Probability and 95% Confidence	V-29
V-8	Crack Detection Probability for Transverse Welds with Crowns by the Penetrant Method Plotted at 95% Probability and 95% Confidence	V-30
V-9	Crack Detection Probability for Transverse Welds with Crowns by the Ultrasonic Method Plotted at 95% Probability and 95% Confidence	V-31
V-10	Crack Detection Probability for Transverse Welds with Crowns by the Eddy Current Method Plotted at 95% Probability and 95% Confidence	V-32
V-11	Crack Detection Probability for Transverse Welds with Crowns by the X-radiograph Method Plotted at 95% Probability and 95% Confidence	V-33
V-12	Crack Detection Probability for Flush, Longitudinal Welds by the Penetrant Method Plotted at 95% Probability and 95% Confidence	V-34
V-13	Crack Detection Probability for Flush, Longitudinal Welds by the Ultrasonic Method Plotted at 95% Probability and 95% Confidence	V-35
V-14	Crack Detection Probability for Flush, Longitudinal Welds by the Eddy Current Method Plotted at 95% Probability and 95% Confidence	V-36
V-15	Crack Detection Probability for Flush, Longitudinal Welds by the X-radiograph Method Plotted at 95% Probability and 95% Confidence	V-37
V-16	Crack Detection Probability for Flush, Transverse Welds by the Penetrant Method Plotted at 95% Probability and 95% Confidence	V-38

V-17 Crack Detection Probability for Flush, Transverse Welds by the Ultrasonic Method Plotted at 95% Probability and 95% Confidence V-39
V-18 Crack Detection Probability for Flush, Transverse Welds by the Eddy Current Method Plotted at 95% Probability and 95% Confidence V-40
V-19 Crack Detection Probability for Flush, Transverse Welds by the X-radiograph Method Plotted at 95% Probability and 95% Confidence V-41

Table

III-1	Parameters for Fatigue Crack Growth in Integrally Stiffened Panels	III-7
III-2	Stringer Panel Flaw Distribution	III-8
III-3	Actual Crack Data, Integrally Stiffened Panels	III-21
III-4	NDT Observations, Integrally Stiffened Panels	III-23
IV-1	Actual Flaw Data, LOP Panels	IV-14
IV-2	NDT Observations, LOP Panels	IV-18
IV-3	NDT Observation by the Penetrant Method, LOP Panels	IV-22
IV-4	NDT Observations by the Ultrasonic Method, Merged Data, LOP Panels	IV-26
V-1	Parameters for Fatigue Crack Growth in Welded Panels	V-6
V-2	Actual Crack Data, Fatigue Cracked Longitudinal Welded Panels with Crowns	V-10
V-3	Actual Crack Data, Fatigue Cracked Transverse Welded Panels with Crowns	V-12
V-4	Actual Crack Data, Fatigue Cracked Flush, Longitudinal Welded Panels	V-13
V-5	Actual Crack Data, Fatigue Cracked Flush Transverse Welded Panels	V-15
V-6	NDT Observations, Fatigue Cracked Longitudinal Welded Panels with Crowns	V-17
V-7	NDT Observations, Fatigue Cracked Transverse Welded Panels with Crowns	V-19
V-8	NDT Observations, Fatigue Cracked Flush, Longitudinal Welded Panels	V-21
V-9	NDT Observations, Fatigue Cracked Flush, Transverse Welded Panels	V-24

I. INTRODUCTION

Recent advances in engineering structural design and quality assurance techniques have incorporated material fracture characteristics as major elements in design criteria. Fracture control design criteria, in a simplified form, are the largest (or critical) flaw size(s) that a given material can sustain without fracture when subjected to service stresses and environmental conditions. To produce hardware to fracture control design criteria, it is necessary to assure that the hardware contains no flaws larger than the critical.

Many critical structural hardware components, including some pressure vessels, do not lend themselves to proof testing for flaw screening purposes. Other methods must be used to establish maximum flaw sizes that can exist in these structures so fracture analysis predictions can be made regarding structural integrity.

Nondestructive testing (NDT) is the only practical way in which included flaws may be detected and characterized. The challenge to nondestructive testing engineering technology is thus to (1) detect the flaw, (2) determine its size and orientation, and (3) precisely locate the flaw. Reliance on NDT methods for flaw hardware assurance requires a knowledge of the flaw size that each NDT method can reliably find. The need for establishing a knowledge of flaw detection reliability, i.e., the maximum size flaw that can be missed, has been identified and has been the subject of other programs* involving flat 2219 aluminum alloy specimens. The next logical step in terms of NASA Space Shuttle program requirements was to evaluate flaw detection reliability in other space hardware elements. This area of need and the lack of such data were pointed out in NASA TMX-64706, which is a recent state-of-the-art assessment of NDT methods.

---

*Donald E. Pettit and David W. Hoeppner: *Fatigue Flaw Growth and NDI Evaluation for Preventing Through-Cracks in Spacecraft Tankage Structures*. NASA CR-128560, September 25, 1972.

R. T. Anderson, T. J. DeLacy, and R. C. Stewart: *Detection of Fatigue Cracks by Nondestructive Testing Methods*. NASA CR-128946, March 1973.

Ward D. Rummel, Paul H. Todd, Jr., Sandor A. Frecska, and Richard A. Rathke: *The Detection of Fatigue Cracks by Nondestructive Testing Methods*. NASA CR-2369, February 1974.

The program reported here was conducted to determine the reliability of nondestructive testing methods in detecting tightly closed flaws in three Space Shuttle structural elements, i.e., (1) cracks in the radii of integrally stiffened 2219 aluminum alloy structures, (2) lack of penetration (LOP) in welded 2219 aluminum alloy structures, and (3) cracks in the weld area in welded 2219 aluminum alloy structures. X-radiographic, penetrant, ultrasonic, and eddy current methods were evaluated.

As a secondary objective, production processing steps were simulated to assess the effects of various operations and constraints on inspection sensitivity and to aid in analysis and planning of inspection operations at optimum points in the production sequence.

Experience has shown that one of the most difficult flaws to detect by NDT techniques is a small tightly closed flaw and that this is one of the flaw types most detrimental to load-carrying structures. Tightly closed flaws may be simulated by artificially induced fatigue cracks and by lack of penetration (LOP) in two opposing pass weldments. By using these primary flaw types, the influences of crack orientation, location, etc can be evaluated by systematic variation of sample preparation and inspection sequences. Methods previously developed were used to prepare test specimens. NDT methods were optimized for these specimens in accordance with industry practices. NDT evaluation of samples was conducted and documented to establish a data base for rigorous analysis of NDT capabilities. Statistical analysis methods established previously under NASA contract NAS9-12276 and in current investigation under NASA contract NAS3-18907* were used to analyze and present the data.

Since the output of the program was engineering data, care was taken in the program to randomize samples, inspection sequences, and data reporting. Inspection analyses were performed independently by operators who had no knowledge of the number of flaws in test panels. Blank panels were introduced to further randomize data and to negate anticipation of flaws. The results are intended to reflect attainable detection sensitivities and reliabilities when NDT techniques are directed toward specific flaw types.

The program was functionally divided into three elements relating to the panel and flaw types. These elements are discussed separately in the following chapters.

---

*S. Klima: *Assessment of NDT Reliability Data.* NAS3-18907. (to be completed in June 1975)

II. STATE-OF-THE-ART NONDESTRUCTIVE TESTING (NDT) METHODS

Nondestructive testing, nondestructive inspection, and nondestructive evaluation in the broadest sense denote testing, inspection, and/or evaluation of a material, component, or system without altering or destroying the functional capability of the tested item. Like other forms of testing, NDT is used to reduce risk in the functional performance of the item and as such provides a measure of insurance for the producer, evaluator, and/or operator of the item. Unlike other forms of testing, it offers the capability for 100% testing or sampling and provides economic advantage by assurance of no loss of any part of the item. These advantages have been both aids and liabilities in the orderly development of the technology. Although nondestructive testing methods are widely used, little quantitative information concerning testing capabilities has been produced.* This program was directed toward quantitative assessment of NDT methods. It was not intended to advance the state of the art in terms of new methods or increased sensitivity. It was intended to provide a practical engineering tool for application of methods now used in the industry. The X-radiography (X-ray), liquid penetrant, ultrasonic, and eddy current test methods generally used for assurance of aluminum alloy materials, components, and assemblies were selected for this study. Many testing options are available in application of these methods. This report addresses generally applied techniques as used in state-of-the-art engineering technologies.

---

*Robert B. Neuschaefer and James B. Beal: *Assessment of and Standardization for Quantitative Nondestructive Testing.* NASA TM-X-64706, September 30, 1972.

ASME Boiler and Pressure Vessel Code (Sections I, III, VIII, and IX), 1968.

Military Standard: Radiographic Inspection, Soundness Requirements for Fusion Welds in Aluminum and Magnesium Missile Components. MIL-R-45774, October 1963.

J. R. Alburger: "A New, Significant Penetrant Parameter - Indication Depletion Time Constant." Paper presented before the American Society for Nondestructive Testing, Spring Conference, Los Angeles, California, 1973.

B. G. Martin and C. J. Adams: *Detection of Lack of Fusion in Aluminum Alloy Weldments by Ultrasonic Shear Waves.* Technical Paper 3499, Douglas Aircraft Company, 1965.

A. X-RADIOGRAPHY

X-radiography is well established as a nondestructive evaluation tool and has been used indiscriminately as an all-encompassing inspection method for detecting flaws and describing flaw size. While pressure vessel specifications* frequently require X-radiographic inspection and the criteria allow no evidence of crack, lack of penetration, or lack of fusion on radiographs, little attempt has been made to establish or control defect detection sensitivity. Further, an analysis of the factors involved clearly demonstrates that X-radiography is one of the least reliable of the nondestructive techniques available for crack detection. The "quality" or "sensitivity" of a radiograph is measured by reference to a penetrameter image on the film at a location of maximum obliquity from the source. A penetrameter is a physical standard made of material radiographically similar to the test object, with a thickness less than or equal to 2% of the test object thickness and containing three holes of diameters four times (4T), two times (2T), and equal to (1T) the penetrameter thickness. Normal space vehicle sensitivity is 2% as noted by perception of the 2T hole (Fig. II-1).

In theory, such a radiograph should reveal a defect with a depth equal to or greater than 2% of the test object thickness. Since it is, however, oriented to defects of measureable volume, tight defects of low volume such as cracks and lack of penetration may not be detected.

---

*Op cit. *ASME Boiler and Pressure Vessel Code.*

MIL R-45774.

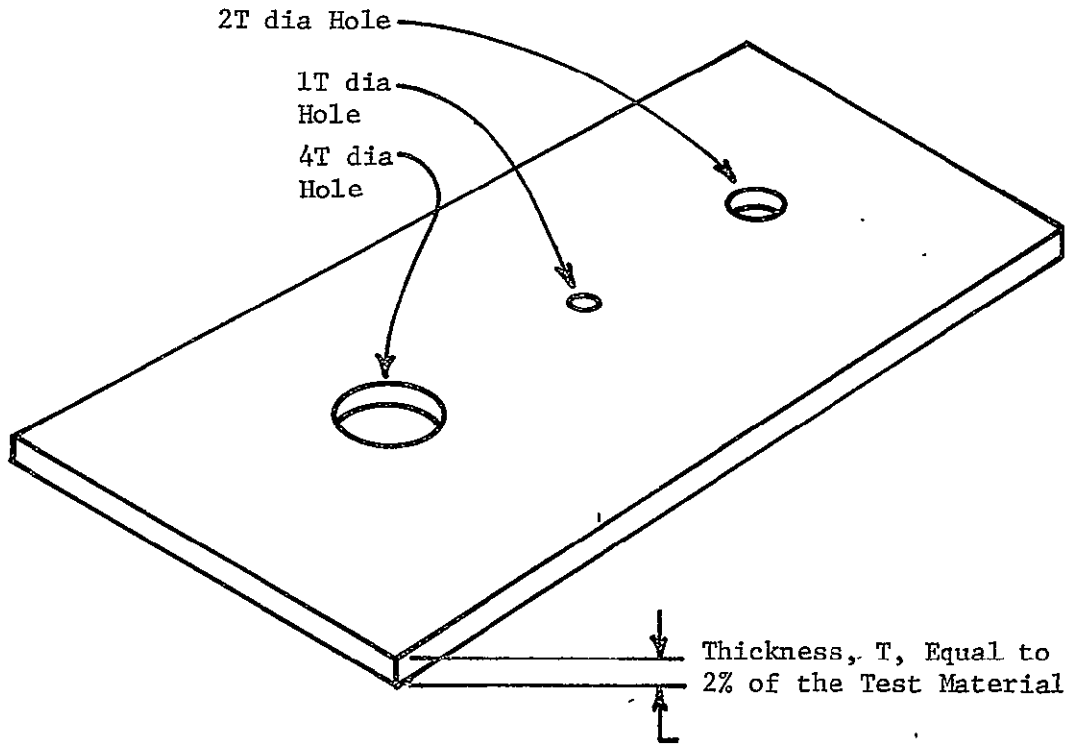

Figure II-1 Conventional Penetrameter (MIL-STD-453)

In practice, cracks and lack of penetration defects are detected only if the axis of the crack is located along the axis of the incident radiation. Consider for example a test object (Fig. II-2) that contains defects A, B, and C. Defect A lies along the axis of the cone of radiation and should be readily detected at depths approaching the 2% sensitivity requirement. Defect B, whose depth may approach the plate thickness, will not be detected since it lies at an oblique angle to incident radiation. Defect C lies along the axis of radiation but will not be detected over its total length. This variable-angle property of X-radiation accounts for a higher crack detection record than would be predicted by geometric analysis and at the same time emphasizes the fallacy of depending on X-radiography for total defect detection and evaluation.

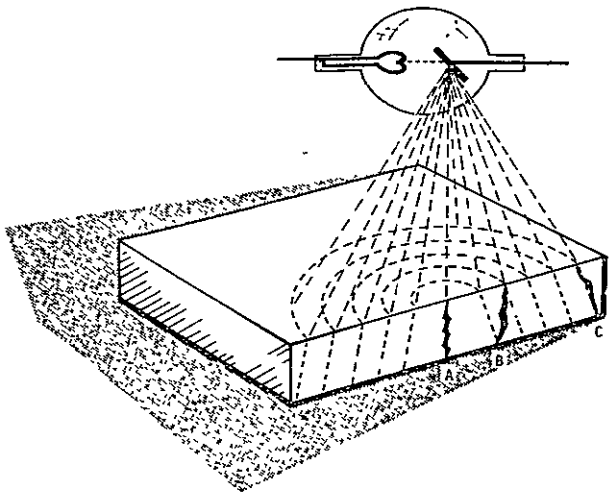

Figure II-2
Schematic View of Crack Orientation with Respect to the Cone of Radiation from an X-ray Tube (Half Section)

Variables in the X-ray technique include such parameters as kilovoltage, exposure time, source film distance and orientation, film type, etc. Sensitivity to orientation of fatigue cracks has been demonstrated by Martin Marietta in 2219-T87 parent metal. Six different crack types were used. An off-axis exposure of 6 degrees resulted in missing all but one of the cracks. A 15-degree offset caused total crack insensitivity. Sensitivity to tight LOP is predicted to be poorer than for fatigue cracks. "Quick-look" inspection of known test specimens showed X-radiography to be insensitive to some LOP but revealed a porosity associated with the lack of penetration.

Advanced radiographic techniques have been applied to analysis of tight cracks including high-resolution X-ray film (Kodak Hi-Rel) and electronic image amplification. Exposure times for high-resolution films are currently too long for practical application (24 hr. 0.200-in. aluminum). The technique as it stands now may be considered to be a special engineering tool.

Electronic image processing has shown some promise for image analysis when used in the derivative enhancement mode but is affected by the same geometric limitations as in producing the basic X-radiograph. The image processing technique may also be considered as a useful engineering tool but does not in itself offer promise of reliable crack or lack of penetration detection by X-radiography.

This program addressed conventional film X-radiography as generally applied in industry.

B. PENETRANT

Penetrants are also used for inspection of pressure vessels to detect flaws and describe flaw length. Numerous penetrant materials are available for general and special applications. The differences between materials are essentially in penetration and subsequent visibility, which in turn affect the overall sensitivity to small defects. In general, fluorescent penetrants are more sensitive than visible dye penetrant materials and are used for critical inspection applications. Six fluorescent penetrant materials are in current use for inspection of Saturn hardware, i.e., SKL-4, SKL-HF, ZL-22, ZL-44B, P545, and P149.

To be successful, penetrant inspection requires that discontinuities be open to the surface and that the surface be free of contamination. Flowed material from previous machining or scarfing operations may require removal by light buffing with emery paper or by light chemical etching. Contamination may be removed by solvent wiping, by vapor degreasing, and by ultrasonic cleaning in a Freon bath. Since ultrasonic cleaning is impractical for large structures, solvent wipe and vapor degreasing are most commonly used and are most applicable to this program.

Factors affecting sensitivity include not only the material surface condition and type of penetrant system used but also the specific sequence and procedures used in performing the inspection. Parameters such as penetrant dwell time, penetrant removal technique, developer application and thickness, and visual inspection procedure are controlled by the inspector. This in turn must be controlled by training the inspector in the discipline to maintain optimum inspection sensitivities.

In Martin Marietta work with fatigue cracks (2219-T87 aluminum), small tight cracks were often undetectable by high-sensitivity penetrant materials but were rendered visible by proof loading the samples to 85% of yield strength.

In recent work, Alburger* reports that controlling crack width to 6 to 8 microns results in good evaluation of penetrant materials, while tight cracks having widths of less than 0.1 micron in width are undetected by state-of-the-art penetrants. These values may be used as qualitative benchmarks for estimation of crack tightness in surface-flawed specimens and for comparison of inspection techniques. This program addressed conventional fluorescent penetrant techniques as they may be generally applied in industry.

Op cit. J. R. Alburger.

C. ULTRASONIC INSPECTION

Ultrasonic inspection involves generation of an acoustical wave in a test object; detection of resultant reflected, transmitted, and scattered energy from the volume of the test object; and evaluation by comparison with "known" physical reference standards. Traditional techniques utilize shear waves for inspection. Figure II-3 illustrates a typical shear wave technique and corresponding oscilloscope presentation. An acoustical wave is generated at an angle to the part surface, travels through the part, and is reflected successively by boundaries of the part and also by included flaw surfaces. The presence of a reflected signal from the volume of the material indicates the presence of a flaw. The relative position of the reflected signal locates the flaw while the relative amplitude describes the size of the flaw. Shear wave inspection is a logical tool for evaluating welded specimens and for tankage.

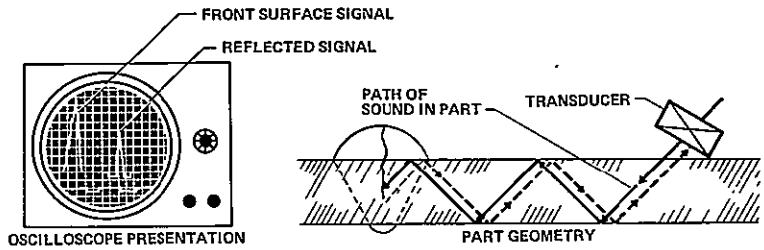

Figure II-3 Shear Wave Inspection

By scanning and electronically gating signals obtained from the volume of a part, a plan view of a C-scan recording may be generated to provide uniform scanning and control of the inspection and to provide a permanent record of inspection.

The shear wave technique and related modes are applicable to detection of tight cracks. Planar (crack life) interfaces were reported to be detectable by ultrasonic shear wave techniques when a test specimen was loaded in compression up to the yield point.* Variable parameters influencing the sensitivity of shear wave inspection include test specimen thickness, frequency and type, and incident sound angle. A technique is best optimized by analysis and by evaluation of representative reference specimens.

It was noted that a shear wave is generated by placing a transducer at an angle to a part surface. Variation of the incident angle results in variation in ultrasonic wave propagation modes and variation of the technique. In aluminum, a variation in incident angle between approximately 14- to 29-degree (water immersion) inclination to the normal results in propagation of energy in the shear mode (particulate motion transverse to the direction of propagation).

Op cit. B. G. Martin and C. J. Adams.

At an angle of approximately 30 degrees, surface or Rayleigh waves that have a circular particulate motion in a plane transverse to the direction of propagation and a penetration of about one-half wavelength are generated. At angles of approximately 7.8, 12.6, 14.7, 19.6, 25.6, and 31.0 to 33.0 degrees, complex Lamb waves that have a particulate motion in symmetrical or asymmetrical sinusoidal paths along the axis of propagation and that penetrate through the material thickness are generated in the thin (0.060-in.) materials.

In recent years, a technique known as "Delta" inspection has gained considerable attention in weldment evaluation. The technique consists of irradiating a part with ultrasonic energy propagated in the shear mode and detecting redirected, scattered, and mode-converted energy from an included flaw at a point directly above the flaw (Fig. II-4). The advantage of the technique is the ability to detect crack-like flaws at random orientations.

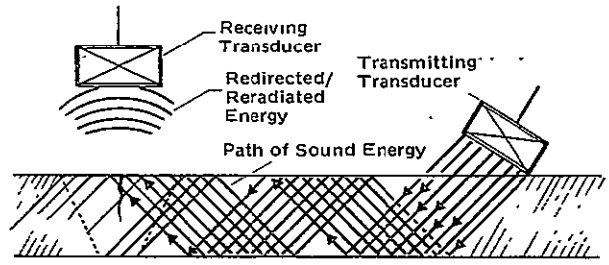

Figure II-4
Schematic View of the Delta Inspection Technique

In addition to variations in the ultrasonic energy propagation modes, variations in application may include immersion or contact, variation in frequency, and variation in transducer size and focus. For optimum detection sensitivity and reliability, an immersion technique is superior to a contact technique because several inspection variables are eliminated and a permanent recording may be obtained. Although greater inspection sensitivity is obtained at higher ultrasonic frequencies, noise and attenuation problems increase and may blank out a defect indication. Large transducer size in general decreases the noise problems but also decreases the selectivity because of an averaging over the total transducer face area. Focusing improves the selectivity of a larger transducer for interrogation of a specific material volume, but decreases the sensitivity in the material volume located outside the focal plane.

This program addressed the conventional shear wave technique as generally applied in industry.

D. EDDY CURRENT

Eddy current inspection has been demonstrated to be very sensitive to small flaws in thin aluminum materials* and offers considerable potential for routine application. Flaw detection by eddy current methods involves scanning the surface of a test object with a coil probe, electronically monitoring the effect of such scanning, and noting the variation of the test frequency to ascertain flaw depth. In principle, if a probe coil is energized with an alternating current, an alternating magnetic field will be generated along the axis of the coil (Fig. II-5). If the coil is placed in contact with a conductor, eddy currents will be generated in the plane of the conductor around the axis of the coil. The eddy currents will in turn generate a magnetic field of opposite sign along the coil. This effect will "load" the coil and cause a resultant shift in impedance of the coil (phase and amplitude). Eddy currents generated in the material depend on conductivity ρ, the thickness T, the magnetic permeability μ, and the material's continuity. For aluminum alloys, the permeability is unity and need not be considered.

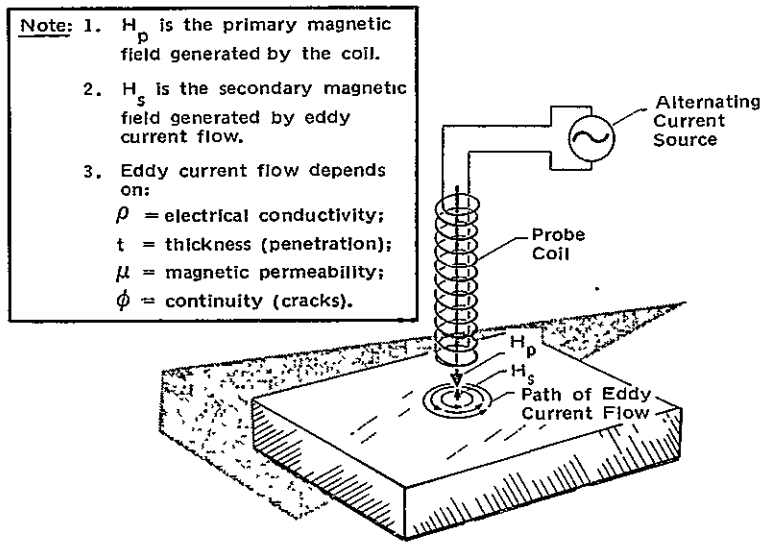

Figure II-5
Schematic View of an Eddy Current Inspection

**Recommended Practice for Standardizing Equipment for Electromagnetic Testing of Seamless Aluminum Alloy Tube.* ASTM E-215-67, September 1967.

The conductivity of 2219-T87 aluminum alloy varies slightly from sheet to sheet but may be considered to be a constant for a given sheet. Overheating due to manufacturing processes* will change the conductivity and therefore must be considered as a variable parameter. The thickness (penetration) parameter may be controlled by proper selection of a test frequency. This variable may also be used to evaluate defect depth and to detect part-through cracks from the opposite side. For example, since at 60 kHz the eddy current penetration depth is approximately 0.060 inch in 2219-T87 aluminum alloy, cracks should be readily detected from either available surface. As the frequency decreases, the penetration increases so the maximum penetration in 2219 aluminum is calculated to be on the order of 0.200 to 0.300 inch.

In practical application of eddy currents, both the material parameters must be known and defined and the system parameters known and controlled. Liftoff (i.e., the spacing between the probe and material surface) must be held constant or must be factored into the results. Electronic readout of coil response must be held constant or defined by reference to calibration samples. Inspection speeds must be held constant or accounted for. Probe orientation must be constant or the effects defined, and probe wear must be minimized. Quantitative inspection results are obtained by accounting for all material and system variables and by reference to physically similar "known standards."

In current Martin Marietta studies of fatigue cracks, the eddy current method is effectively used in describing the crack sizes. Figure II-6 illustrates an eddy current description of two surface fatigue cracks in the 2219-T87 aluminum alloy. Note the discrimination capability of the method for two cracks that range in size only by a minor amount. The double-peak readout in the case of the smaller crack is due to the eddy current probe size and geometry. For deep buried flaws, the eddy current technique may not describe the crack volume but will describe the location of the crack with respect to the test sample surface. By applying conventional ultrasonic C-scan gating and recording techniques, a permanent C-scan recording of defect location and size may be obtained as illustrated in Figure II-7.

Since the eddy current technique detects local changes in material continuity, the visibility of tight defects is greater than with other techniques. The eddy current technique will be used as a benchmark for other techniques due to its inherently greater sensitivity.

---

*Ward D. Rummel: "Monitor of the Heat-Affected Zone in 2219-T87 Aluminum Alloy Weldments." *Transactions of the 1968 Symposium on NDT of Welds and Materials Joining*, Los Angeles, California, March 11-13, 1968.

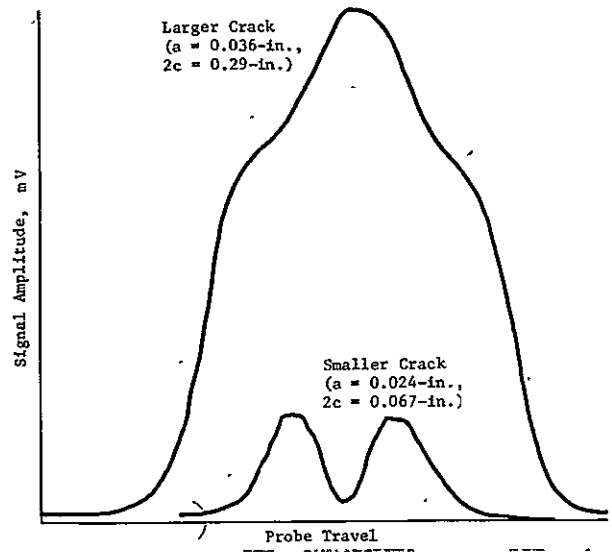

Figure II-6
Eddy Current Detection of Two Fatigue Cracks in 2219-T87 Aluminum Alloy

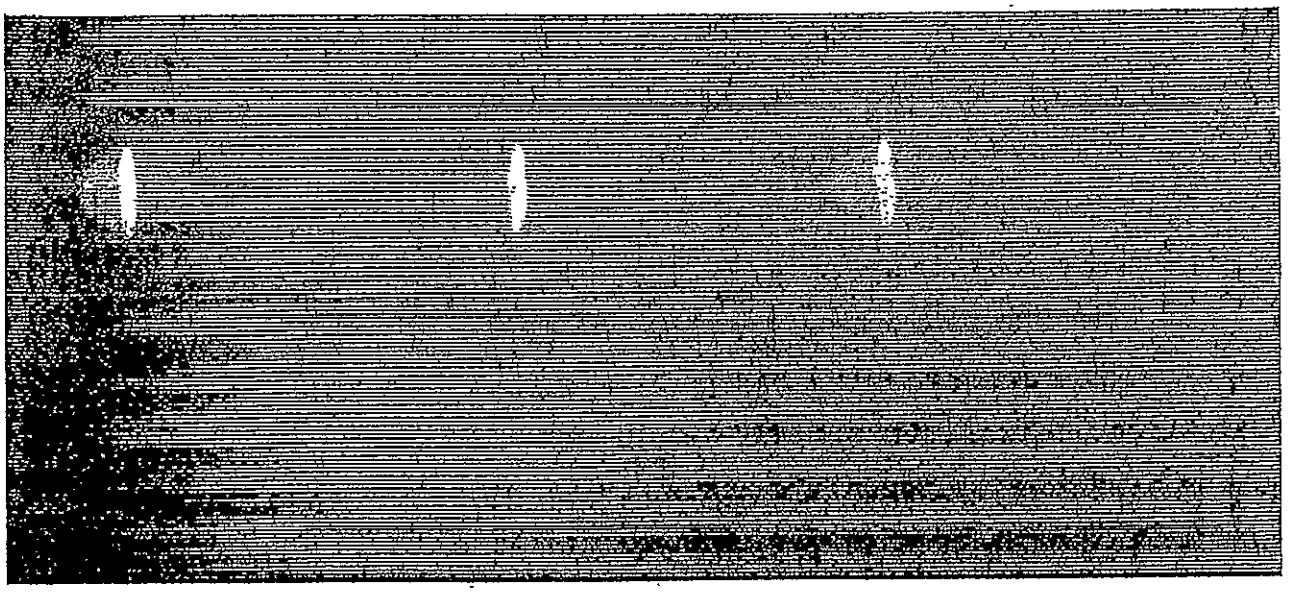

Figure II-7
Eddy Current C-Scan Recording of a 2219-T87 Aluminum Alloy Panel Containing Three Fatigue Cracks (0.820 inch long and 0.105 inch deep)

Although eddy current scanning of irregular shapes is not a general industrial practice, the techniques and methods applied are in general usage and interpretation may be aided by recorded data collection and analysis in future programs.

III. INTEGRALLY STIFFENED STRINGER PANEL EVALUATION

Integrally machined stiffened panels and riveted T-stiffened panels are common aerospace structural design elements and are representive of Space Shuttle structure. Cracks in stiffened panels may be the result of a raw material (plate) anomaly, or may be a product of machining, heat treating, forming operations, or service loading. If they are service induced, cracks will most likely form at the tangency point of the rib radius as shown schematically in Figure III-1. Note in this figure that a rather sharp stress concentration occurs at the junction of the stress and fillet radii (the nominal membrane stress in this figure is 30 ksi). This stress concentration extends through the thickness but decreases from a K_t of about 1.4 on the rib side to 1.2 on the opposite side. Note also the extremely sharp decrease in stress at points along the curvature of the fillet. Fatigue flaw growth in stiffened panels was evaluated under a previous NASA contract* in which flaw growth in the rib side was assessed.

In a practical sense, the difficulty encountered by artificially extending flaws occurring on the rib side of the fillet means that these flaws should not be of major concern in flight hardware subjected to a similar loading state. Thus the most critical area to be examined by NDT is at the fillet tangency point and the back surface behind this position because of the severity of cracks occurring in the region of stress concentration.

Cracks in the radius area normally open to the surface and are effectively simulated by the tightly closed fatigue crack as a worst-case condition. Artificially induced fatigue cracks in the radius area were selected for evaluation. After the flaw type and location were established, a program plan for test panel preparation, evaluation, and analysis was established as shown schematically in Figure III-2.†

---

*E. J. Beck: *Fatigue Flaw Growth Behavior in Stiffened and Unstiffened Panels Loaded in Biaxial Tension.* Martin Marietta Aerospace, Denver, Colorado, February 1973. (Contract NAS9-12439)

†All panels prepared in this program were evaluated independently by Rockwell International, Space Division. Only the results of the Martin Marietta studies are shown in this report.

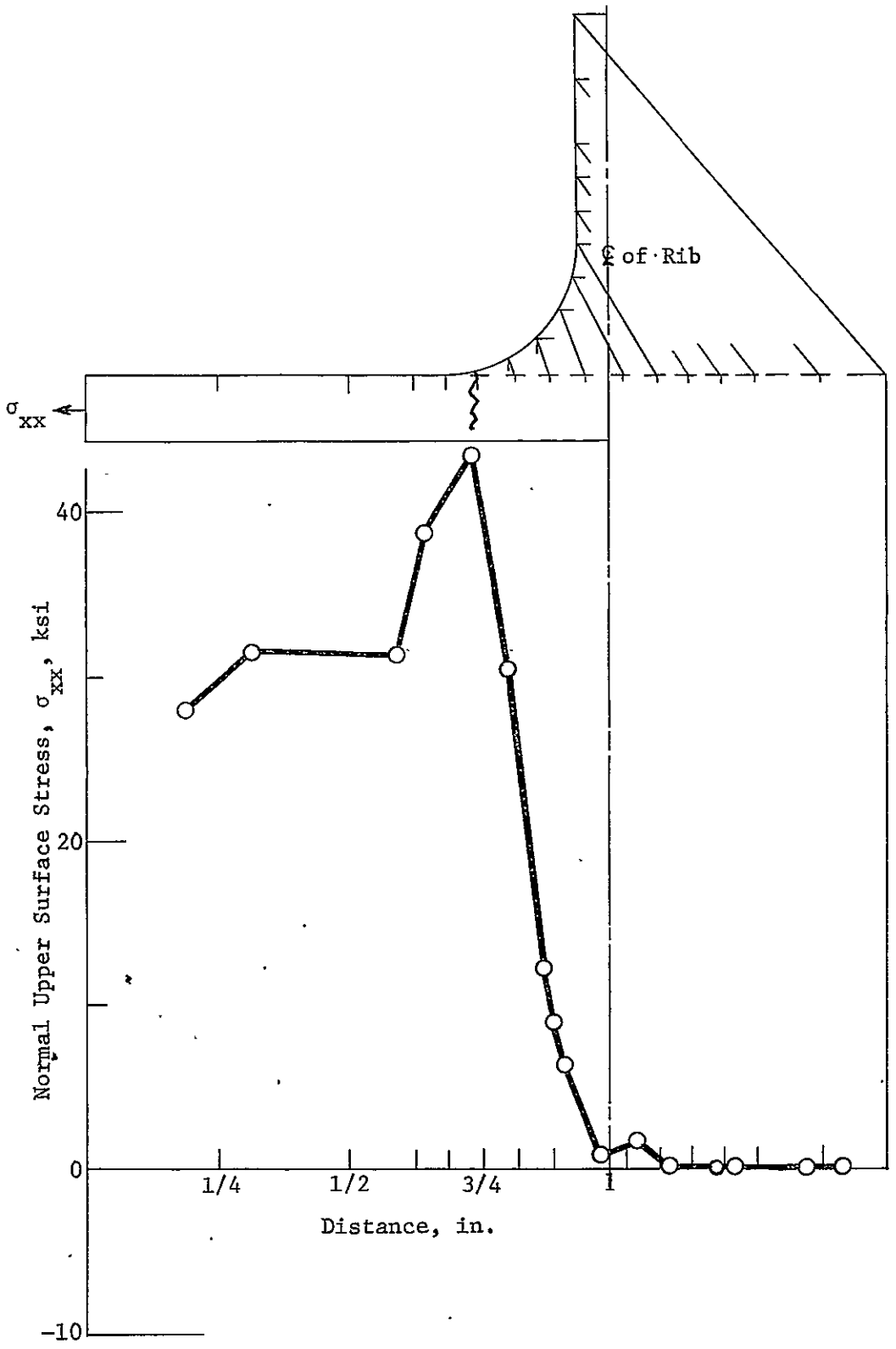

Figure III-1
Anticipated Surface Stress Distribution for Axially Loaded 2219-T87 Integrally Stiffened Panel

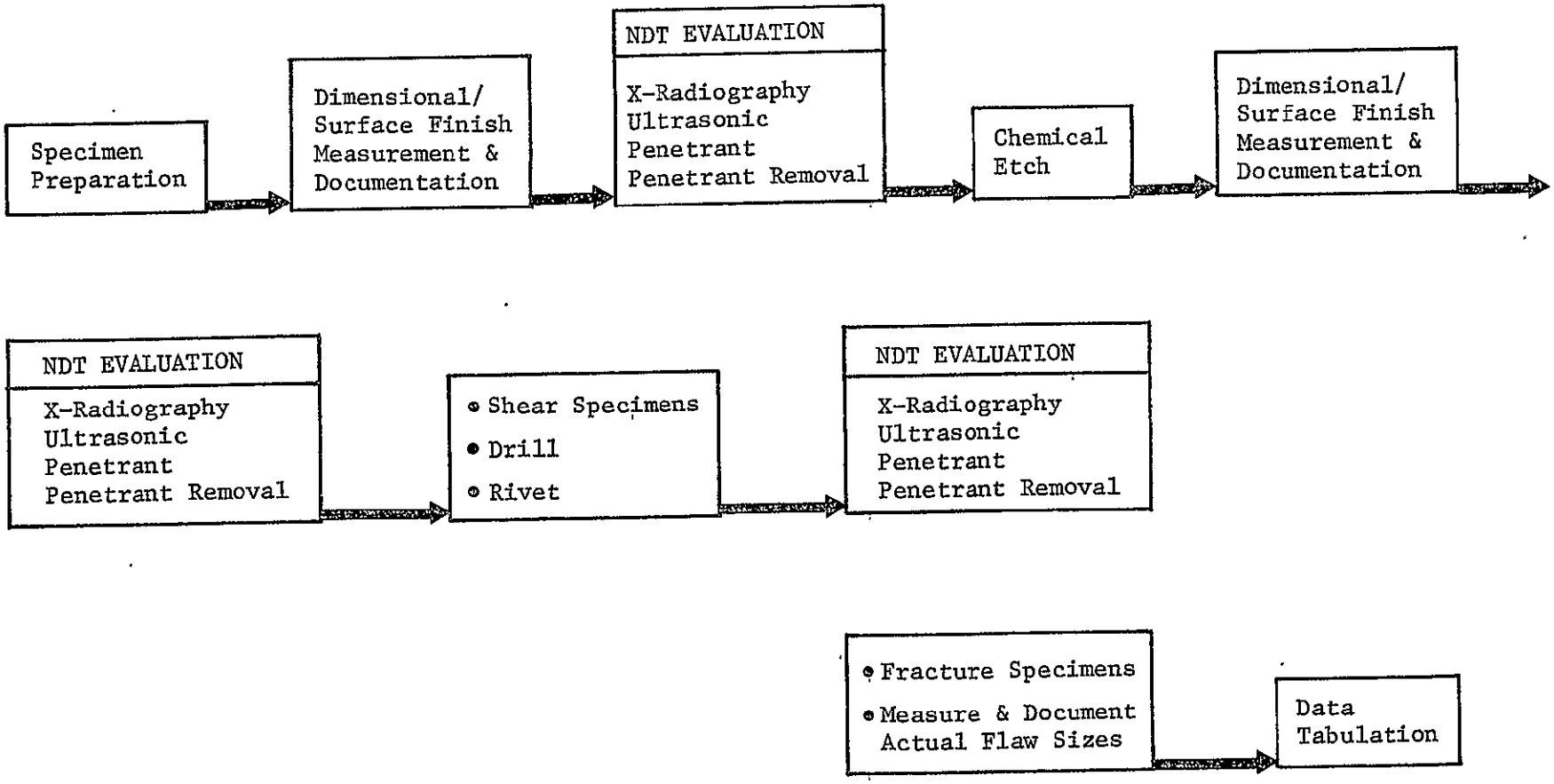

Figure III-2 NDT Evaluation Sequence for Integrally Stiffened Panels

A. SPECIMEN PREPARATION

Integrally stiffened panel blanks were machined from 3.81-centimeter (1½-in.) thick 2219-T87 aluminum alloy plate to a final stringer height of 2.54 centimeters (1 in.) and an initial skin thickness of 0.780 centimeter (0.310 in.). The stringers were located asymmetrically to provide a 15.1-centimeter (5.97-in.) band on the lower stringer and a 12.6-centimeter (4.97-in.) band on the upper stringer, thereby orienting the panel for inspection reference (Fig. III-3). A nominal 63 rms (root-mean-square) surface finish was maintained. All stringers were 0.635-centimeter (0.250-in.) thick and were located perpendicular to the plate rolling direction.

Fatigue cracks were grown in the stiffener/rib area of panel blanks at random locations along the ribs. Starter flaws were introduced by electrodischarge machining (EDM) using shaped electrodes to control final flaw shape. Cracks were then extended by fatigue and the surface crack length visually monitored and controlled to the required final flaw size and configuration requirements as shown schematically in Figure III-4. Nominal flaw sizes and growth parameters are as shown in Table III-1.

Following growth of flaws, 0.076 centimeter (0.030 in.) was machined off the stringer side of the panel using a shell cutter to produce a final membrane thickness of 0.710 centimeter (0.280 in.), a 0.317-centimeter (0.125-in.) radius at the rib, and a nominal 63 rms surface finish. Use of a shell cutter randomized the surface finish pattern and is representative of techniques used in hardware production. Grip ends were then cut off each panel and the panels were cleaned by vapor degreasing and submitted for inspection. Forty-three flawed panels and four unflawed panels were prepared and submitted for inspection. Three additional panels were prepared for use in establishing flaw growth parameters and were destroyed to verify growth parameters and techniques. Distribution of flaws in the panels is as shown in Table III-2.

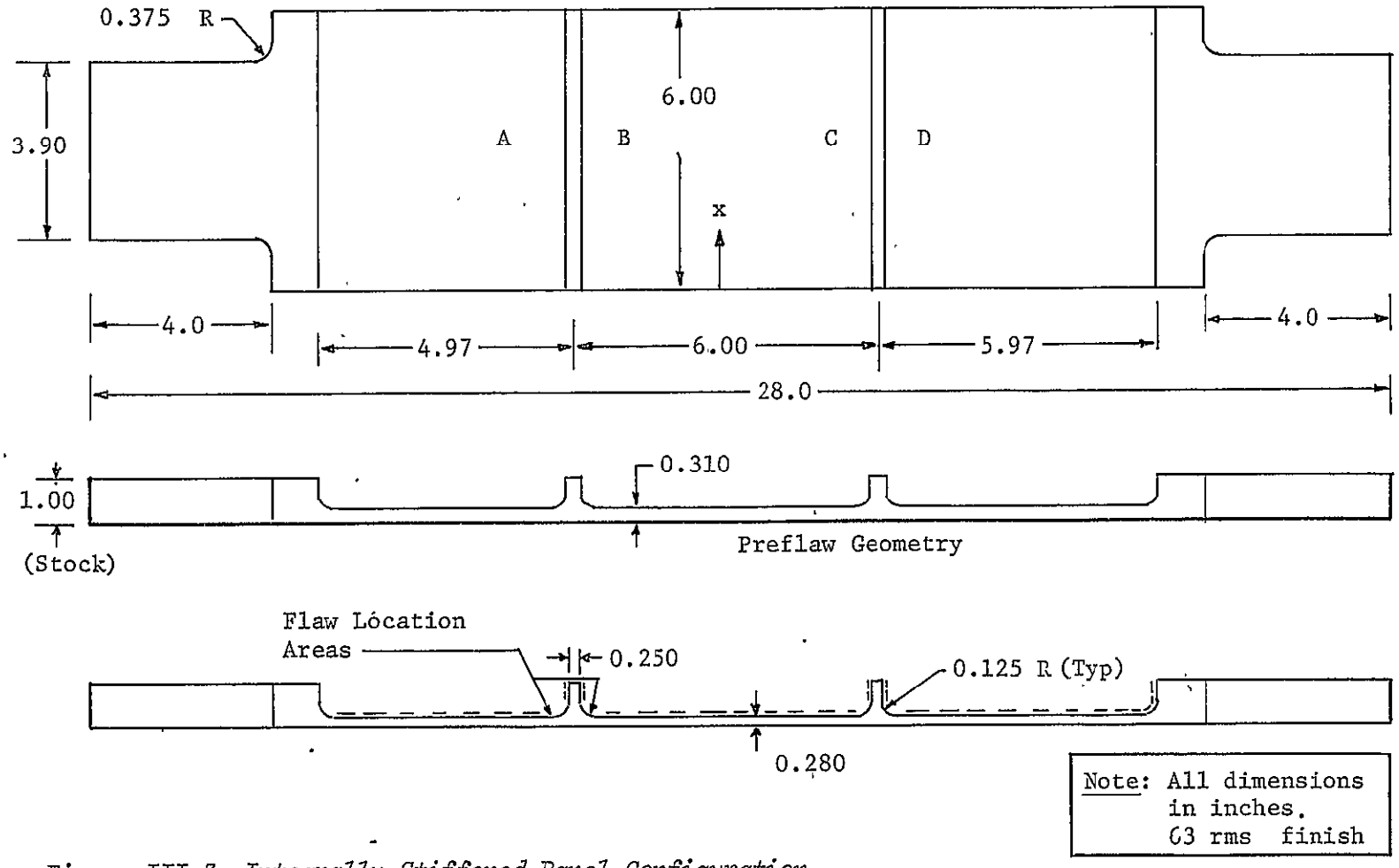

Figure III-3 Integrally Stiffened Panel Configuration

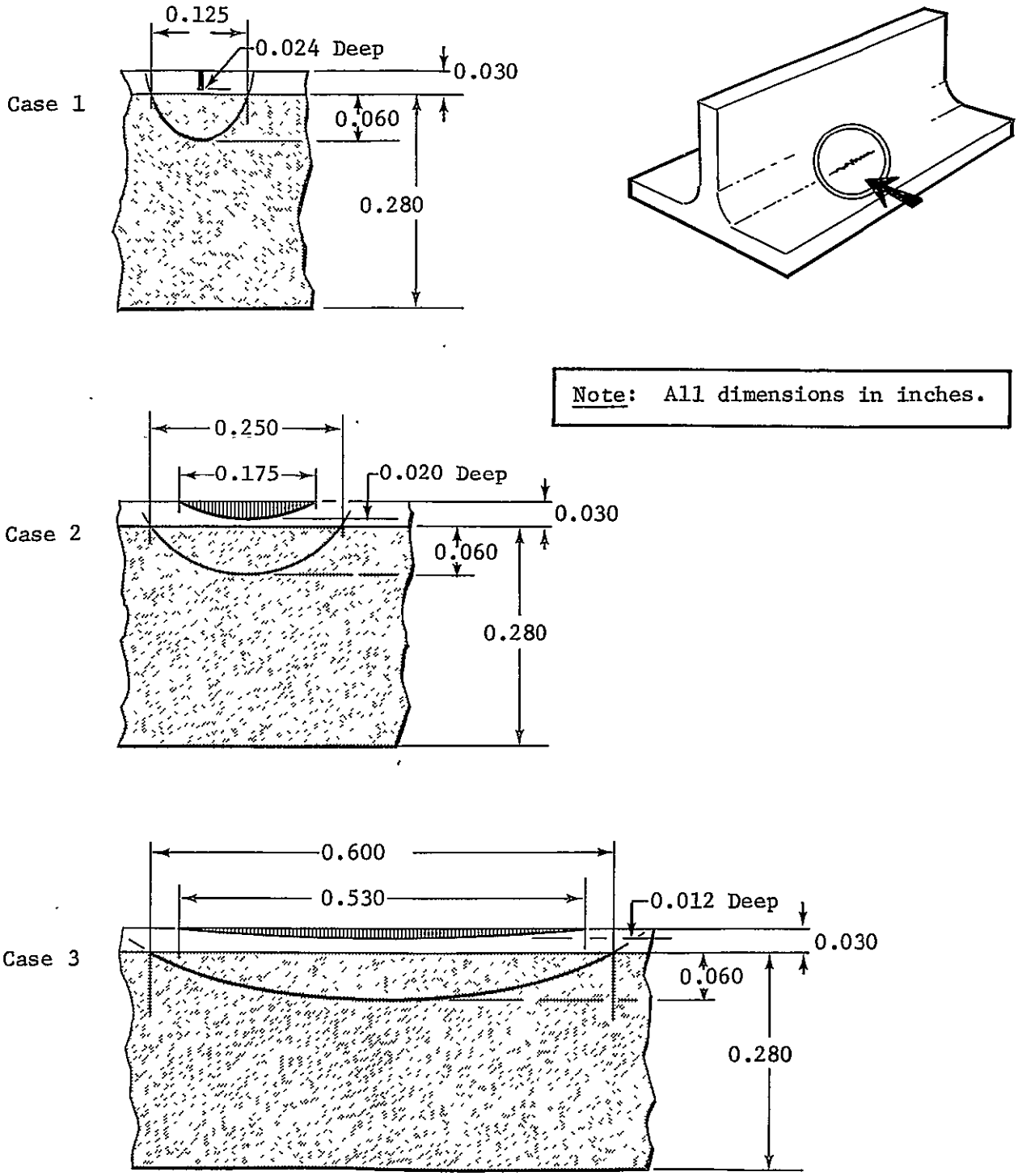

Figure III-4
Schematic, Side View of Starter Flaw and Final Crack Configurations, Integrally Stiffened Panels

Table III-1 Parameters for Fatigue Crack Growth in Integrally Stiffened Panels

CASE	a/2C	a/t	EDM Starter Notch Depth	Width	Measured Fatigue Flaw Length	Final Specimen Thickness	Type of Loading	Stress	Stress Cycles (avg)	No. of Panels	No. of Flaws
1	0.5	0.2	0.061 cm (0.024 in.)	0.045 cm (0.018 in.)	0.508 cm (0.200 in.)	0.710 cm (0.280 in.)	3-Point Bending	20.7×10^6 N/m^2 (30 ksi)	80,000	22	102
2	0.25	0.2	0.051 cm (0.020 in.)	0.445 cm (0.175 in.)	0.760 cm (0.300 in.)	0.710 cm (0.280 in.)	3-Point Bending	20.7×10^6 N/m^2 (30 ksi)	25,000	22	22
3	0.1	0.2	0.031 cm (0.012 in.)	1.34 cm (0.530 in.)	1.52 cm (0.600 in.)	0.710 cm (0.280 in.)	3-Point Bending	20.7×10^6 N/m^2 (30 ksi)	22,000	10	22

Note: a = final depth of flaw,
2C = final length of flaw,
t = final panel thickness.

Table III-2 Stringer Panel Flaw Distribution

Crack Designation	Number of Panels	Number of Flaws	Flaw Depth (a)	Flaw Length (2c)
1	23	102	0.152 cm (0.060 in)	0.289 cm (0.125 in)
2	10	22	0.152 cm (0.060 in)	0.630 cm (0.250 in)
3	10	22	0.152 cm (0.060 in)	1.520 cm (0.600 in)
Blanks	4	0		
TOTALS	47	146		

B. NDT OPTIMIZATION

Following preparation of integrally stiffened fatigue-flawed panels, an NDT optimization and calibration program was initiated. One panel containing cracks of each flaw type (case) was selected for experimental and system evaluations. Criteria for establishment of specific NDT procedures were (1) penetrant, ultrasonic, and eddy current inspection from the stringer (rib) side only, and (2) NDT evaluation using state-of-the-art practices for initial evaluation and for system calibrations prior to actual inspection. Human factors were minimized by the use of automated C-scan recording of ultrasonic and eddy current inspections and through redundant evaluation by three different and independent operators. External sensitivity indicators were used to provide an additional measurement of sensitivity and control.

1. X-radiography

Initial attempts to detect cracks in the stringer panels by X-radiography were totally unsuccessful. A 1% penetrameter sensitivity was obtained using a Norelco 150 beryllium window X-ray tube and the following exposure parameters with no success in crack detection:

1) 50 kV ;

2) 20 MA;

3) 5-minute exposure;

4) 48-in. film focal distance (Kodak, type M, industrial X-ray film).

Various masking techniques were tried using the above exposure parameters with no success.

After completion of the initial ultrasonic inspection sequence, two panels were selected that contained flaws of the greatest depth as indicated by the ultrasonic evaluations. Flaws were marginally resolved in one panel using Kodak single-emulsion, type-R film and extended exposure times. Flaws could not be resolved in the second panel using the same exposure techniques.

Special X-radiographic analysis was provided through the courtesy of Mr. Henry Ridder, Magnaflux Corporation, in evaluation of case 2 and case 3 panels using a recently developed microfocus X-ray system.* This system decreases image unsharpness, which is inherent in conventional X-ray units. Although this system thus has a greater potential for crack detection, no success was achieved.

Two factors are responsible for the poor results with X-radiography: (1) fatigue flaws were very tight and were located at the transition point of the stringer (rib) radius, and (2) cracks grew at a slight angle (from normal) under the stringer. Such angulation decreases the X-ray detection potential using normal exposures. The potential for detection at an angle was evaluated by making exposures in 1-degree increments at angles from 0 to 15 degrees by applying optimum exposure parameters established by penetrameter resolution. No crack image was obtained. Two panels were evaluated using X-ray opaque penetrant fluids for enhancement. No crack image was obtained.

As a result of the poor success in crack detection with these panels, the X-radiographic technique was eliminated from the integrally stiffened panel evaluation program.

2. Penetrant Evaluation

In our previous work with penetrant materials and optimization for fatigue crack detection under contract NAS9-12276,† we selected Uresco P-151, a group VII solvent removable, fluorescent penetrant system, for evaluation. Storage (separation and precipitation of constituents) difficulties with this material and recommendations from Uresco resulted in selection of the Uresco P-149 material for use in this program. In previous tests, the P-149 material was rated similar in performance to the P-151 material and is more easily handled. Three materials, Uresco P-133, P-149, and P-151, were evaluated with known cracks in stringer and welded panels and all were determined to be capable of resolving the required flaw types, thus providing a backup (P-133) material and an assessment of P-151 versus P-149 capabilities. A procedure was written for use of the P-149 material

---

*Henry J. Ridder: "High-Sensitivity Radiography with Variable Microfocus X-ray Unit." Paper presented at the WESTEC 1975 ASNT Spring Conference, Los Angeles, California. (Magnaflux Corporation MX-100 Microfocus X-ray System)

†Ward D. Rummel, Paul H. Todd, Jr., Sandor A. Frecska, and Richard A. Rathke: *The Detection of Fatigue Cracks by Nondestructive Testing Methods*. NASA CR-2369, February 1974, pp 28-35.

for all panels in this program. This procedure is shown in Appendix A.

Removal of penetrant materials between inspections was a major concern for both evaluation of reference panels and the subsequent test panels. Ultrasonic cleaning using a solvent mixture of 70% 1,1,1-trichloroethane and 30% isopropyl alcohol was used initially but was found to attack welded panels and some areas of the stringer panels. The procedure was modified to ultrasonic cleaning in 100% (technical grade) isopropyl alcohol. The technique was verified by application of developer to known cracks with no evidence of "bleedout" and by continuous monitoring of inspection results. The panel cleaning procedure was incorporated as an integral part of the penetrant procedure and is included in Appendix A.

3. Ultrasonic Evaluation

Optimization of ultrasonic techniques using panels containing cases 1, 2, and 3 cracks was accomplished by analysis and by experimental assessment of the best overall signal-to-noise ratio. Primary consideration was given to the control and reproducibility offered by shear wave, surface wave, Lamb wave, and Delta techniques. On the basis of panel configuration and previous experience, Lamb wave and Delta techniques were eliminated for this work. Initial comparison of signal amplitudes at 5 and 10 MHz, and previous experience with the 2219-787 aluminum alloy, resulted in selection of 10 MHz for further evaluation.

Panels were hand-scanned in the shear mode at incident angles varying from 12 to 36 degrees in the immersion mode using the C-scan recording bridge manipulator. Noise from the radius of the stringer made analysis of separation signals difficult. A flat reference panel containing an 0.180-inch long by 0.090-inch deep fatigue crack was selected for use in further analyses of flat and focused transducers at various angles. Two possible paths for primary energy reflection were evaluated with respect to energy reflection. The first path is the direct reflection of energy from the crack at the initial material interface. The second is the energy reflection off the back surface of the panel and subsequent reflection from the crack. The reflected energy distribution for two 10-MHz transducers was plotted as shown in Figure III-5. Subsequent C-scan recordings of a case 1 stringer panel resulted in selection of an 18-degree angle of incidence using a 10-MHz 0.635-centimeter diameter flat transducer. Recording techniques, test setup, and test controls were optimized and an inspection evaluation procedure written. Details of this procedure are shown in Appendix B.

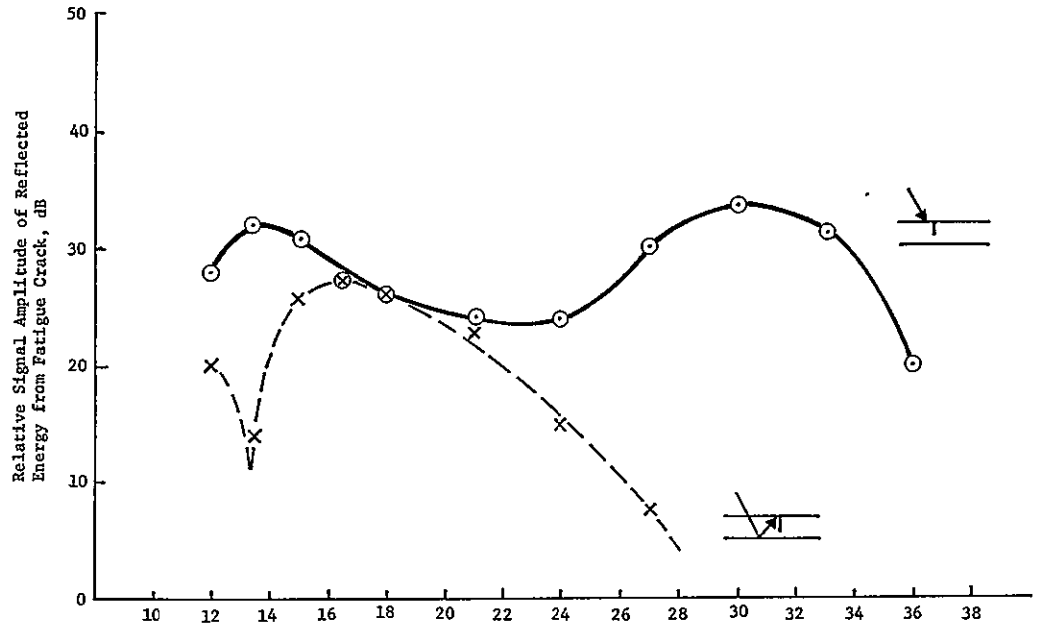

(b) 10-MHz 1/4-in. Diameter Flat Transducer

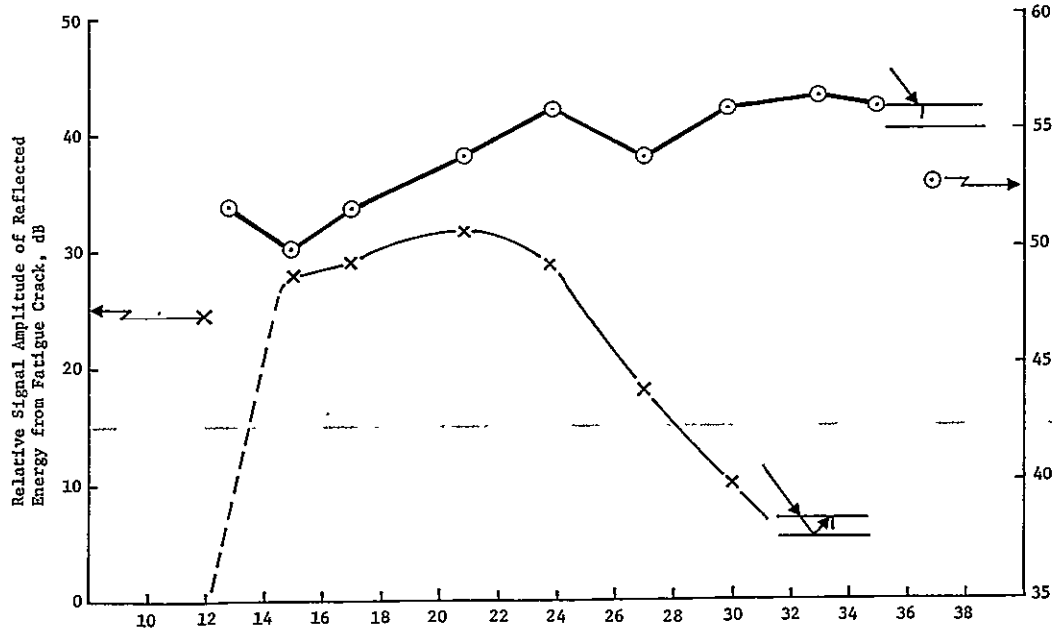

(a) 10-MHz 3/8-in.

Figure III-5 Ultrasonic Reflected Energy Response

4. Eddy Current Evaluation

For eddy current inspection, we selected the NDT Instruments Vector III instrument* for its long-term electronic stability and selected 100 kHz as the test frequency based on the results of previous work and the required depth of penetration in the aluminum panels. The 100-kHz probe has a 0.063-inch core diameter and is a single-coil helically wound probe. Automatic C-scan recording was required and the necessary electronic interfaces were fabricated to utilize the Budd SR-150 ultrasonic scanning bridge and recorder system. Two critical controls were necessary to assure uniform readout--alignment and liftoff controls. A spring-loaded probe holder and scanning fixture were fabricated to enable alignment of the probe on the radius area of the stringer and to provide constant probe pressure as the probe is scanned over a panel. Fluorolin tape was used on the sides and bottom of the probe holder to minimize friction and probe wear. Figure III-6 illustrates the configuration of the probe holder and Figure III-7 illustrates a typical eddy current scanning setup.

Various recording techniques were evaluated. Conventional C-scan in which the probe is scanned incrementally in both the x and y directions was not entirely satisfactory because of the rapid decrease in response as the probe was scanned away from the stringer. A second raster scan recording technique was also evaluated and used for initial inspections. In this technique the probe scans the panel in only one direction (x-axis) while the other direction (y-axis) is held constant. The recorded output is indicative of changes in the x-axis direction while the y-axis, driven at a constant stepping speed, builds a repetitive pattern to emphasize anomalies in the x-direction. In this technique, the sensitivity of the eddy current instrument is held constant.

A procedure written for inspection using the raster scan technique was initially verified on case 1, 2, and 3 panels. Details of this procedure are shown in Appendix C.

An improvement in the recording technique was made by implementing an analog scan technique. This recording is identical to the raster scan technique with the following exceptions. The sensitivity of the eddy current instrument (amplifier gain) is stepped up in discrete increments each time a line scan in the x-direction is completed. This technique provides a broad amplifier gain range and allows the operator to detect small and large flaws on

---

*NDT Instruments Inc, 705 Coastline Drive, Seal Beach, California, 90740.

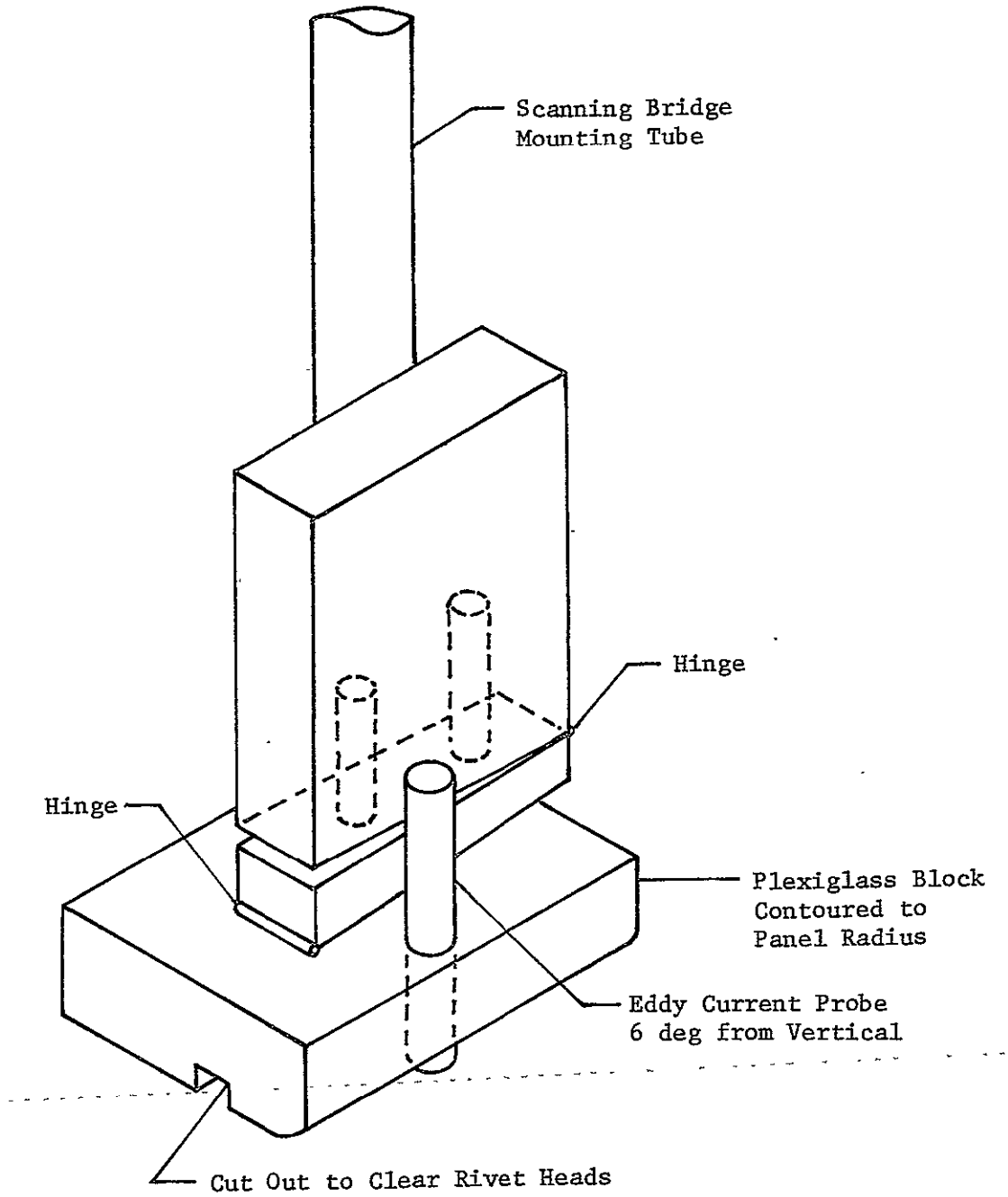

Figure III-6 Eddy Current Probe

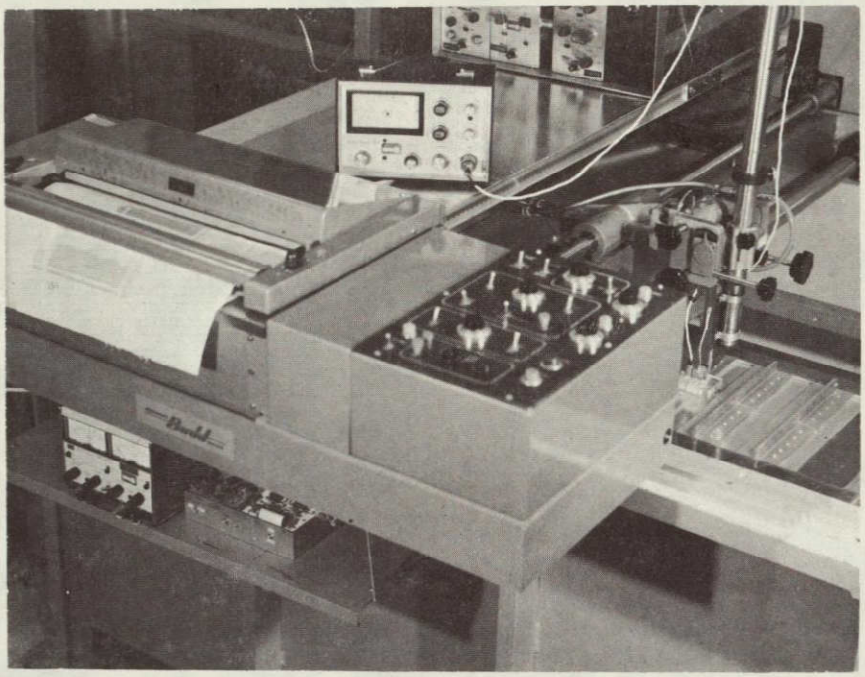

Figure III-7
Typical Eddy Current Scanning Setup for Stringer Panels

the same recording. It also accommodates some system noise due to panel smoothness and probe backlash. Examples of the raster scan and analog scan recordings are shown in Figure III-8. The dual or shadow trace is due to backlash in the probe holder. The inspection procedure was modified and implemented as shown in Appendix C.

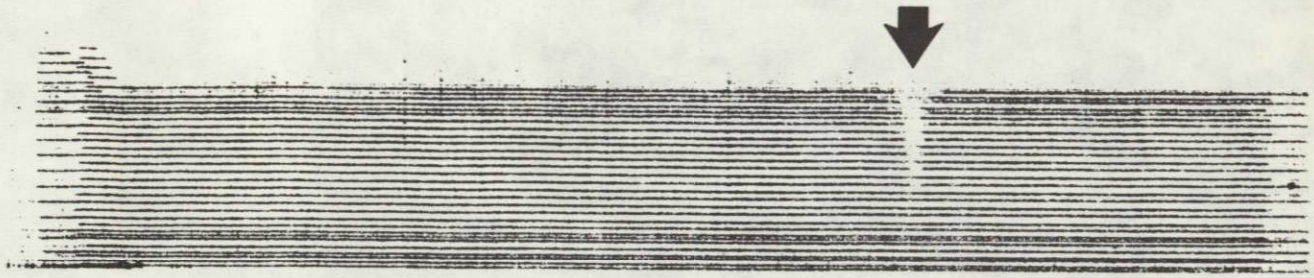

Raster Scan

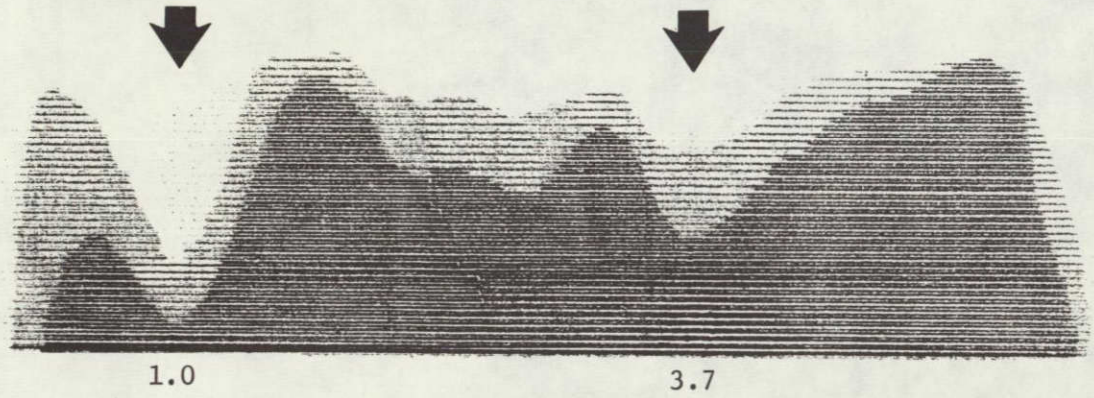

Analog Scan

Figure III-8 Typical Eddy Current Recordings

C. TEST SPECIMEN EVALUATION

Test specimens were evaluated by optimized penetrant, ultrasonic, and eddy current inspection procedures in three separate inspection sequences. After familiarization with the specific procedures to be used, the 47 specimens (94 stringers) were evaluated by three different operators for each inspection sequence. Inspection records were analyzed and recorded by each operator without a knowledge of the total number of cracks present, the identity of previous operators, or previous inspection results. Panel identification tags were changed between inspection sequence 1 and 2 to further randomize inspection results.

Sequence 1 - Inspection of As-Machined Panels

The Sequence 1 inspection included penetrant, ultrasonic, and eddy current procedures by three different operators. Each operator independently performed the entire inspection sequence, i.e., made his own ultrasonic and eddy current recordings, interpreted his own recordings, and interpreted and reported his own results.

Inspections were carried out using the optimized methods established and documented in Appendices A thru C. Crack length and depth (ultrasonic only) were estimated to the nearest 0.16 centimeter (1/16 in.) and were reported in tabular form for data processing.

Cracks in the integrally stiffened (stringer) panels were very tightly closed and few cracks could be visually detected in the as-machined condition.

Sequence 2, Inspection after Etching

On completion of the first inspection sequence, all specimens were cleaned, the radius (flaw) area of each stringer was given a light metallurgical etch using "Flicks" etchant solution, and the specimens were recleaned. Less than 0.0013 centimeter (0.0005 in.) of material was removed by this process. Panel thickness and surface roughness were again measured and recorded. Few cracks were visible in the etched condition. The specimens were again inspected using the optimized methods. Panels were evaluated by three independent operators. Each operator independently performed each entire inspection operation, i.e., made his own ultrasonic and eddy current recordings and reported his own results. Some difficulty encountered with penetrant was attributed to "clogging" of the cracks by the various evaluation fluids. A mild alkaline cleaning was used to improve penetrant results. No measurable change in panel thickness or surface roughness resulted from this cleaning cycle.

Sequence 3, Inspection of Riveted Stringers

Following completion of sequence 2, the stringer (rib) sections were cut out of all panels so a T-shaped section remained. Panels were cut to form a 3.17-centimeter (1.25-in.) web on either side of the stringer. The web (cap) section was then drilled on 2.54-centimeter (1-in.) centers and riveted to a 0.317-centimeter (0.125-in.) thick subpanel with the up-set portion of the rivets projecting on the web side (Fig. III-9). The resultant panel simulated a skin-to-stringer joint that is common in built-up aerospace structures. Panel layout prior to cutting and after riveting to subpanels is shown in Figure III-10.

Riveted panels were again inspected by penetrant, ultrasonic, and eddy current techniques using the established procedures. The eddy current scanning shoe was modified to pass over the rivet heads and an initial check was made to verify that the rivet heads were not influencing the inspection. Penetrant inspection was performed independently by three different operators. One set of ultrasonic and eddy current (analog scan) recordings was made and the results analyzed by three independent operators.

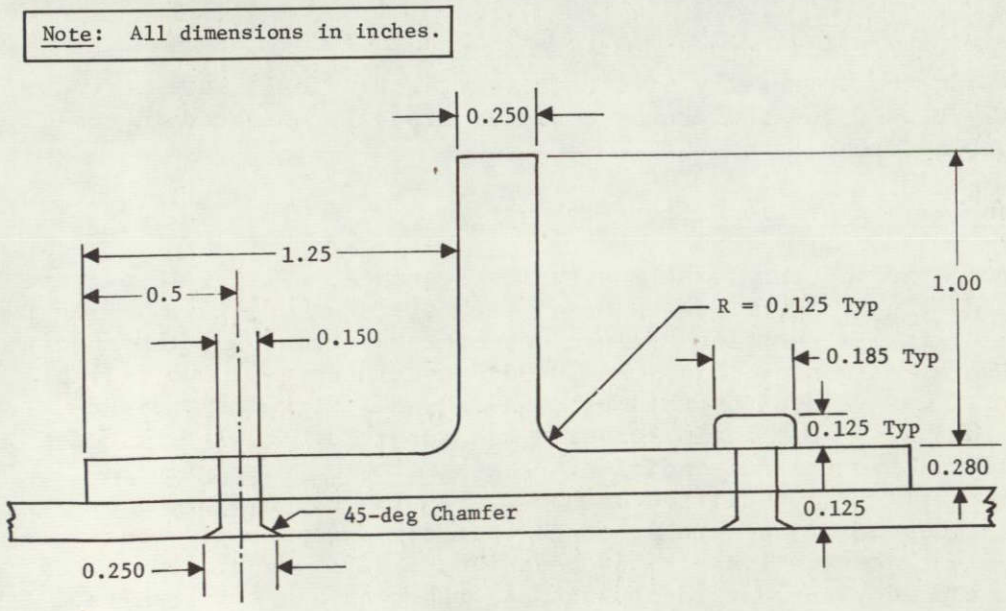

Figure III-9 Stringer-to-Subpanel Attachment

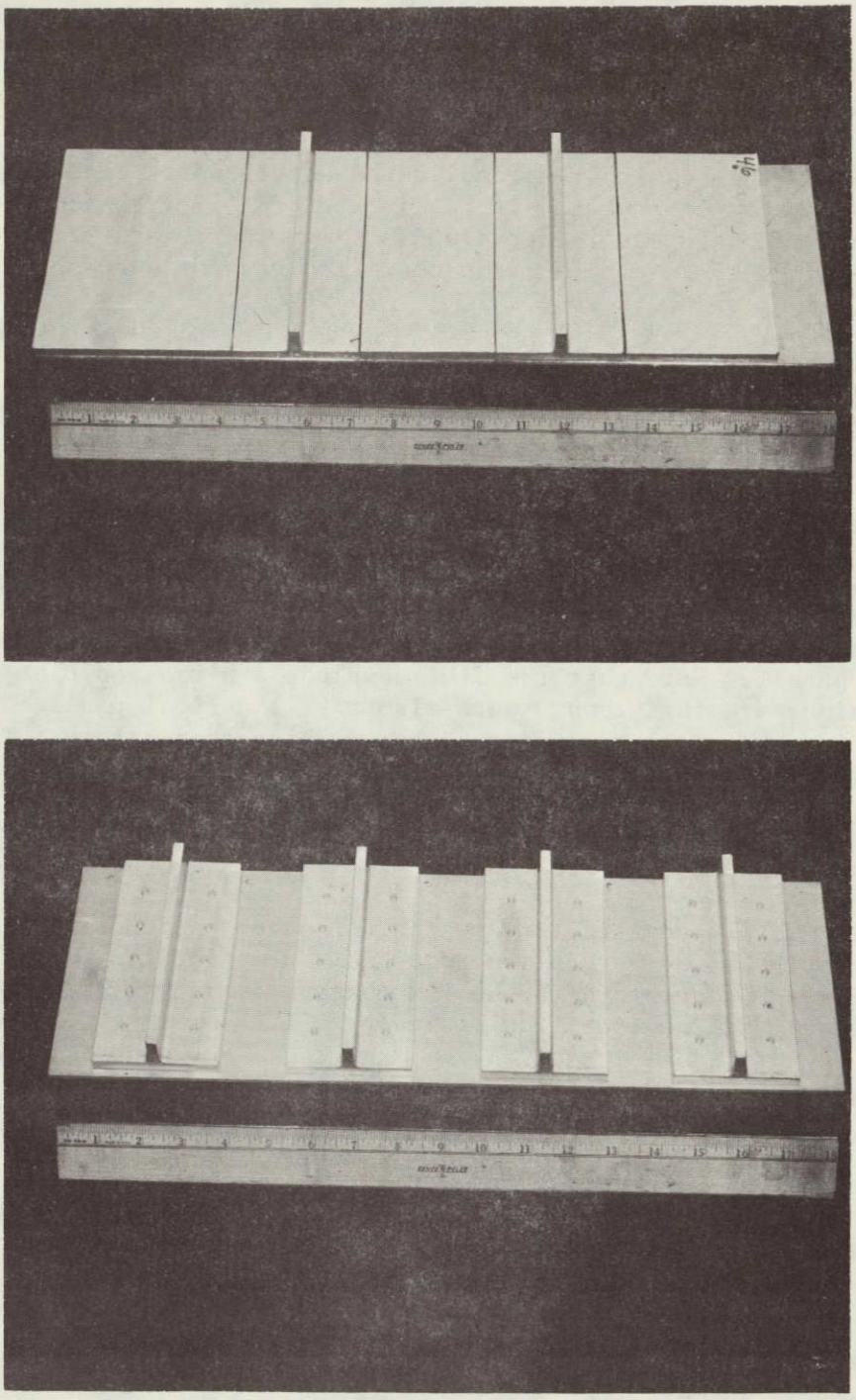

Figure III-10
Integrally Stiffened Panel Layout and Riveted Panel Configuration

D. PANEL FRACTURE

Following the final inspection in the riveted panel configuration, the stringer sections were removed from the subpanels and the web section broken off to reveal the actual flaws. Flaw length, depth, and location were measured visually using a traveling microscope and the results recorded in the actual data file. Four of the flaws were not revealed in panel fracture. For these, the actual surface length was recorded and attempts were made to grind down and open up these flaws. This operation was not successful and all of the flaws were lost.

E. DATA ANALYSIS

1. Data Tabulation

Actual crack data and NDT observations were keypunched and input to a computer for data tabulation, data ordering, and data analysis sequences. Table III-3 lists actual crack data for integrally stiffened panels. Note that the finish values are rms and that all dimensions are in inches. Note also that the final panel thickness is greater in some cases after etching than before. This lack of agreement is the average of thickness measurements at three locations and is not an actual thickness increase. Likewise the change in surface finish is not significant due to variation in measurement at the radius location.

Table III-4 lists nondestructive test observations as ordered according to the actual crack length. An X "0" indicates that there were no misses by any of the three NDT observers. Conversely, a "3" indicates that the crack was missed by all observers.

2. Data Ordering.

Actual crack data (Table III-3) were used as a basis for all subsequent calculations, ordering, and analysis. Cracks were initially ordered by decreasing actual crack length, crack depth, and crack area. These data were then stored for use in statistical analysis sequences.

Table III-3 Actual Crack Data, Integrally Stiffened Panels

PANEL NO.	CRACK NO.	CRACK LENGTH	CRACK DEPTH	INITIAL FINISH	INITIAL THICKNESS	FINAL FINISH	FINAL THICKNESS	CRACK POSITION X	CRACK POSITION Y
1 B	1	0.157	0.030	52	0.2780	32	0.2810	4.07	-0.
1 C	2	0.193	0.037	52	0.2780	22	0.2810	1.72	-0.
2 D	3	0.182	0.051	38	0.2800	18	0.2840	3.04	-0.
3 C	4	0.531	0.095	57	0.2790	30	0.2820	2.96	-0.
4 B	5	0.175	0.028	47	0.2790	32	0.2810	3.00	-0.
4 C	6	0.170	0.032	47	0.2790	30	0.2800	3.01	-0.
5 A	7	0.085	0.032	77	0.2790	32	0.2800	1.97	-0.
5 D	8	0.170	0.032	77	0.2790	42	0.2790	2.08	-0.
6 A	9	0.174	0.033	65	0.2780	38	0.2810	1.73	-0.
6 C	10	0.160	0.033	65	0.2780	40	0.2830	1.70	-0.
6 D	11	0.172	0.036	65	0.2780	46	0.2830	4.45	-0.
7 A	12	0.179	0.039	58	0.2770	22	0.2790	4.23	-0.
7 B	13	0.180	0.030	58	0.2770	30	0.2750	1.68	-0.
7 C	14	0.142	0.036	58	0.2770	40	0.2790	1.73	-0.
8 A	15	0.142	0.027	72	0.2780	26	0.2800	1.67	-0.
8 A	16	0.050	0.027	72	0.2780	26	0.2800	4.57	-0.
8 B	17	0.183	0.039	72	0.2780	30	0.2800	2.62	-0.
8 C	18	0.194	0.046	72	0.2780	24	0.2800	3.57	-0.
8XD	19	0.200	0.046	72	0.2780	30	0.2800	1.39	-0.
8XD	20	0.166	0.046	72	0.2780	30	0.2800	4.50	-0.
9 A	21	0.187	0.040	73	0.2790	28	0.2790	2.47	-0.
9 B	22	0.149	0.034	73	0.2790	22	0.2790	3.74	-0.
9 B	23	0.202	0.043	73	0.2790	22	0.2790	4.60	-0.
9 C	24	0.195	0.042	73	0.2790	26	0.2790	1.66	-0.
9 C	25	0.163	0.037	73	0.2790	26	0.2790	2.63	-0.
9 D	26	0.100	0.037	73	0.2790	26	0.2790	4.00	-0.
10 A	27	0.262	0.048	37	0.2800	20	0.2830	1.46	-0.
11 D	28	0.273	0.055	17	0.2800	22	0.2810	2.44	-0.
12 B	29	0.269	0.051	32	0.2800	24	0.2790	3.84	-0.
13 B	30	0.271	0.052	28	0.2790	20	0.2830	1.92	-0.
13 D	31	0.273	0.053	28	0.2790	20	0.2810	3.80	-0.
14 A	32	0.275	0.051	31	0.2800	24	0.2820	4.19	-0.
14 C	33	0.286	0.062	31	0.2800	20	0.2810	3.98	-0.
15 A	34	0.272	0.051	39	0.2790	26	0.2810	3.89	-0.
15 D	35	0.275	0.053	39	0.2790	22	0.2810	1.36	-0.
16 B	36	0.276	0.050	53	0.2800	22	0.2820	2.40	-0.
16 C	37	0.208	0.038	53	0.2800	23	0.2820	1.55	-0.
16 D	38	0.302	0.080	53	0.2800	18	0.2820	4.46	-0.
17 A	39	0.265	0.043	38	0.2760	36	0.2680	1.72	-0.
17 C	40	0.275	0.049	38	0.2760	20	0.2820	3.87	-0.
17 D	41	0.266	0.049	38	0.2760	24	0.2810	1.37	-0.
18 A	42	0.276	0.046	38	0.2800	30	0.2820	4.43	-0.
18 B	43	0.291	0.052	38	0.2800	18	0.2830	1.37	-0.
18 C	44	0.321	0.060	38	0.2800	25	0.2840	4.47	-0.
19 A	46	0.277	0.053	35	0.2810	12	0.2820	1.58	-0.
19 B	47	0.269	0.047	35	0.2810	25	0.2820	4.33	-0.
19 C	48	0.268	0.054	35	0.2810	26	0.2820	4.56	-0.
19 D	49	0.288	0.056	35	0.2810	16	0.2820	1.45	-0.
20 A	50	0.561	0.064	30	0.2800	22	0.2830	4.00	-0.
21 D	51	0.569	0.065	33	0.2780	52	0.2790	2.56	-0.
22 C	52	0.593	0.070	20	0.2800	20	0.2800	3.47	-0.
23 B	53	0.551	0.043	31	0.2790	22	0.2800	3.90	-0.
23 C	54	0.549	0.042	31	0.2790	22	0.2820	3.92	-0.
24 A	55	0.576	0.061	32	0.2800	16	0.2850	1.60	-0.
24 D	56	0.576	0.059	32	0.2800	32	0.2790	4.00	-0.
25 A	57	0.566	0.047	44	0.2800	44	0.2800	2.54	-0.
25 C	58	0.563	0.050	32	0.3040	32	0.3040	3.57	-0.
26 A	59	0.528	0.045	34	0.2790	25	0.2790	1.57	-0.
26 B	60	0.560	0.055	34	0.2790	14	0.2780	4.36	-0.
26 D	61	0.579	0.076	34	0.2790	22	0.2790	1.50	-0.
27 A	62	0.572	0.056	29	0.2760	22	0.2780	4.27	-0.
27 B	63	0.573	0.059	29	0.2760	20	0.2770	1.67	-0.
27 D	64	0.550	0.048	29	0.2760	25	0.2770	4.58	-0.
28 B	65	0.578	0.054	33	0.2780	18	0.2780	2.50	-0.
28 C	66	0.542	0.052	33	0.2780	24	0.2780	4.43	-0.
28 D	67	0.612	0.073	33	0.2780	18	0.2790	1.72	-0.
29 A	68	0.569	0.063	52	0.2790	30	0.2770	4.16	-0.
29 B	69	0.476	0.034	52	0.2790	41	0.2780	1.61	-0.
29 C	70	0.684	0.056	52	0.2790	38	0.2780	1.59	-0.
29 D	71	0.451	0.062	52	0.2790	30	0.2800	4.37	-0.
31 B	72	0.255	0.047	18	0.2780	18	0.2780	1.97	-0.

Table III-3 (concl)

31 B	73	0.571	0.039	22	0.2770	22	0.2770	2.21	-0.
35 C	74	0.274	0.068	35	0.2790	35	0.2790	3.78	-0.
36 A	75	0.126	0.025	45	0.2780	42	0.2780	1.78	-0.
36 A	76	0.179	0.038	45	0.2780	42	0.2780	4.51	-0.
36 C	77	0.186	0.038	45	0.2780	33	0.2780	2.77	-0.
36 D	78	0.193	0.047	45	0.2780	40	0.2780	4.30	-0.
37 A	79	0.140	0.029	50	0.2790	50	0.2780	2.46	-0.
37XA	80	0.215	0.029	50	0.2790	50	0.2780	4.69	-0.
37 B	81	0.113	0.024	50	0.2790	40	0.2790	1.51	-0.
37 B	82	0.182	0.045	50	0.2790	40	0.2790	3.54	-0.
37 C	83	0.109	0.026	50	0.2790	41	0.2790	1.24	-0.
37 C	84	0.063	0.016	50	0.2790	41	0.2790	2.05	-0.
37 D	85	0.164	0.045	50	0.2790	18	0.2790	3.62	-0.
37 D	86	0.190	0.024	50	0.2790	18	0.2790	4.64	-0.
38 A	87	0.089	0.018	42	0.2790	24	0.2790	1.65	-0.
38 A	88	0.175	0.039	42	0.2790	24	0.2790	4.58	-0.
38 B	89	0.078	0.016	42	0.2790	16	0.2780	2.80	-0.
38 C	90	0.140	0.031	42	0.2790	21	0.2790	2.07	-0.
38 C	91	0.164	0.036	42	0.2790	21	0.2790	4.75	-0.
38 D	92	0.169	0.033	42	0.2790	29	0.2780	1.19	-0.
38 D	93	0.125	0.024	42	0.2790	29	0.2780	3.80	-0.
39 A	94	0.274	0.056	17	0.2780	17	0.2780	1.72	-0.
39 C	95	0.181	0.042	19	0.2790	19	0.2790	1.26	-0.
39 D	97	0.181	0.049	24	0.2790	24	0.2790	2.17	-0.
39 D	98	0.142	0.030	24	0.2790	24	0.2790	4.62	-0.
40 A	99	0.112	0.026	50	0.2780	50	0.2790	4.03	-0.
40 B	100	0.172	0.040	50	0.2780	32	0.2770	1.54	-0.
40 B	101	0.134	0.033	50	0.2780	32	0.2770	2.56	-0.
40 C	102	0.114	0.024	50	0.2780	36	0.2780	1.27	-0.
40 D	103	0.061	0.009	50	0.2780	34	0.2770	3.71	-0.
40 D	104	0.160	0.037	50	0.2780	34	0.2770	4.46	-0.
41 A	105	0.183	0.038	44	0.2790	28	0.2790	2.05	-0.
41 A	106	0.120	0.022	44	0.2790	28	0.2790	4.62	-0.
41 B	107	0.127	0.028	44	0.2790	25	0.2790	1.34	-0.
41 B	108	0.097	0.021	44	0.2790	25	0.2790	4.04	-0.
41 C	109	0.136	0.033	44	0.2790	22	0.2790	1.56	-0.
41 C	110	0.200	0.040	44	0.2790	22	0.2790	4.84	-0.
42 B	111	0.182	0.044	33	0.2780	30	0.2780	2.46	
42 C	112	0.126	0.028	33	0.2780	32	0.2780	2.18	-0.
42 C	113	0.158	0.041	33	0.2780	32	0.2780	4.74	-0.
42 D	114	0.191	0.047	33	0.2780	35	0.2780	1.35	-0.
42 D	115	0.098	0.032	33	0.2780	35	0.2780	4.03	-0.
43 A	116	0.415	0.100	30	0.2800	36	0.2780	2.65	-0.
43 A	117	0.184	0.041	30	0.2800	36	0.2780	4.60	-0.
43 B	118	0.177	0.041	30	0.2800	24	0.2770	1.54	-0.
43 B	119	0.163	0.036	30	0.2800	24	0.2770	4.11	-0.
43 C	120	0.095	0.019	30	0.2800	30	0.2790	3.53	-0.
43 D	121	0.076	0.018	30	0.2800	22	0.2780	1.88	-0.
43 D	122	0.200	0.023	30	0.2800	22	0.2780	4.40	-0.
44 A	123	0.106	0.019	33	0.2790	21	0.2790	3.72	-0.
44 A	124	0.178	0.036	33	0.2790	21	0.2790	4.69	-0.
44 B	125	0.138	0.024	33	0.2790	23	0.2770	2.13	-0.
44 B	126	0.132	0.031	33	0.2790	23	0.2770	4.23	-0.
44 C	127	0.160	0.037	33	0.2790	24	0.2780	1.07	-0.
44 C	128	0.113	0.026	33	0.2790	24	0.2780	4.86	-0.
44 D	129	0.179	0.040	33	0.2790	21	0.2780	1.46	-0.
44 D	130	0.147	0.033	33	0.2790	21	0.2780	3.52	-0.
45 A	131	0.164	0.034	28	0.2770	25	0.2790	1.62	-0.
45 B	132	0.162	0.036	28	0.2770	29	0.2760	4.27	-0.
45 C	133	0.161	0.033	28	0.2770	23	0.2780	4.42	-0.
46 A	135	0.083	0.017	31	0.2780	24	0.2770	3.46	-0.
46 A	136	0.176	0.036	31	0.2780	24	0.2770	4.55	-0.
46 C	137	0.158	0.035	31	0.2780	25	0.2780	1.44	-0.
46 C	138	0.085	0.017	31	0.2780	25	0.2780	2.33	-0.
46 D	139	0.184	0.045	31	0.2780	23	0.2770	4.54	-0.
47 A	140	0.136	0.026	33	0.2780	28	0.2780	2.43	-0.
47 A	141	0.087	0.017	33	0.2780	28	0.2780	4.72	-0.
47 B	142	0.167	0.031	33	0.2780	27	0.2780	1.18	-0.
47 B	143	0.059	0.011	33	0.2780	27	0.2780	3.43	-0.
47 C	144	0.126	0.030	33	0.2780	20	0.2780	3.58	-0.
47 D	145	0.139	0.035	33	0.2780	26	0.2780	2.54	-0.
47 D	146	0.187	0.044	33	0.2780	26	0.2780	4.75	-0.

Table III-4 NDT Observations, Integrally Stiffened Panels

		PENETRANT			ULTRASONIC			EDDY CURRENT		
INSPECTION SEQUENCE		1	2	3	1	2	3	1	2	3
CRACK NUMBER	ACTUAL VALUE									
70	.684	0	0	0	0	0	0	0	1	0
67	.612	0	1	0	0	0	0	3	0	1
52	.593	3	0	0	3	0	0	3	1	1
61	.579	0	0	0	0	0	0	1	0	0
65	.578	0	0	0	0	0	0	1	0	3
55	.576	0	0	0	0	0	3	1	0	0
56	.576	0	0	0	0	0	0	0	0	1
63	.573	1	0	0	0	0	0	2	1	3
62	.572	0	0	0	0	0	0	2	0	0
73	.571	0	1	0	0	0	3	2	0	3
51	.569	1	0	0	2	0	0	0	0	2
68	.569	0	0	0	0	0	0	0	0	0
57	.566	1	0	0	1	0	0	0	0	2
58	.563	0	0	0	1	0	0	0	0	0
50	.561	0	0	0	0	0	0	0	0	0
60	.560	0	1	0	0	0	0	0	0	0
53	.551	0	0	0	0	0	0	3	2	3
54	.549	0	0	0	0	0	0	1	1	1
66	.542	0	0	0	1	0	0	0	0	0
4	.531	0	1	0	0	0	0	0	0	0
59	.528	0	1	0	0	0	3	0	1	0
69	.476	0	0	0	0	0	0	2	0	0
71	.451	0	0	0	0	0	3	0	0	1
44	.321	0	0	0	0	0	0	2	1	1
38	.302	0	0	0	0	0	0	0	1	0
43	.291	0	1	0	0	0	0	1	0	1
49	.288	1	0	0	0	0	0	1	0	1
33	.286	3	1	0	3	0	2	3	0	0
46	.277	0	0	0	0	1	0	2	3	3
36	.276	0	1	0	1	0	0	2	2	1
42	.276	0	0	0	1	0	0	1	1	0
32	.275	0	1	2	0	0	0	1	1	1
35	.275	0	0	0	0	1	0	2	1	1
40	.275	0	1	0	0	0	0	1	0	2
74	.274	0	0	0	0	0	0	2	2	1
94	.274	0	0	1	1	0	3	0	0	0
31	.273	0	1	0	0	0	0	1	1	2
28	.273	0	2	3	0	0	0	0	0	0
34	.272	0	0	0	0	0	0	2	1	1
30	.271	0	0	3	0	1	0	2	0	3
47	.269	1	0	0	0	0	0	1	0	1
29	.269	0	1	2	0	0	0	2	0	2
48	.268	0	1	2	1	0	0	1	1	2
41	.266	0	0	0	0	0	0	1	1	1

Table III-4 (cont)

CK NO	ACT VAL	1	2	3	1	2	3	1	2	3
27	.262	0	0	0	0	0	0	2	2	1
80	.215	3	0	0	0	0	3	0	0	0
37	.208	0	0	0	0	1	0	3	3	3
23	.202	0	0	1	1	0	0	0	0	2
19	.200	0	0	0	0	0	0	1	1	3
110	.200	1	0	0	0	0	0	1	0	0
122	.200	1	0	1	0	0	0	0	0	2
24	.195	1	0	1	0	0	0	1	0	0
18	.194	0	0	1	0	0	0	0	0	0
2	.193	1	1	3	0	0	0	0	0	0
78	.193	0	0	0	0	0	0	0	0	0
114	.191	0	0	0	0	0	0	1	0	1
86	.190	3	3	3	0	0	3	1	1	2
21	.187	0	0	3	0	2	0	0	0	0
146	.187	0	0	0	0	0	3	2	0	1
77	.186	0	0	0	0	0	0	0	0	0
139	.184	2	0	0	0	0	0	1	0	2
117	.184	0	0	0	0	0	0	0	0	0
17	.183	0	0	0	0	0	0	1	1	0
105	.183	0	0	0	0	2	3	2	1	0
111	.182	3	1	2	0	0	0	0	1	3
3	.182	0	0	0	0	0	0	0	0	0
82	.182	3	0	0	0	0	0	1	0	3
95	.181	0	0	1	1	0	0	0	0	2
97	.181	2	2	1	1	0	3	1	1	3
13	.180	0	0	0	1	2	2	1	2	2
129	.179	0	0	1	1	0	0	1	0	3
12	.179	0	0	0	0	0	1	1	0	1
76	.179	0	0	0	0	0	0	2	1	2
124	.178	0	0	0	0	0	3	1	0	0
118	.177	0	0	0	0	0	0	0	1	2
136	.176	2	1	0	0	3	3	1	0	2
88	.175	3	3	3	1	0	0	2	2	2
5	.175	0	1	0	0	1	3	2	1	2
9	.174	0	0	1	1	0	0	1	0	1
11	.172	1	1	3	0	2	3	0	0	1
100	.172	0	0	0	0	0	0	1	0	1
8	.170	0	1	0	0	1	0	0	0	1
6	.170	0	1	0	0	1	0	0	0	0
92	.169	3	1	1	0	1	0	3	3	3
142	.167	0	1	0	1	0	0	1	0	0
20	.166	0	1	0	0	1	0	1	0	2
91	.164	3	2	3	0	0	0	2	2	3
131	.164	2	0	1	0	1	0	0	0	0
85	.164	3	3	3	0	2	3	1	1	3
25	.163	0	2	3	0	2	0	1	0	0

Table III-4 (concl)

CK NO	ACT VAL	1	2	3	1	2	3	1	2	3
119	.163	0	1	1	0	0	3	0	1	0
132	.162	0	1	1	0	0	0	0	1	3
133	.161	0	1	1	0	0	0	1	1	2
127	.160	1	1	1	0	0	3	0	0	0
104	.160	0	0	0	0	1	3	0	0	2
10	.160	0	0	1	0	0	0	0	0	0
137	.158	3	2	0	0	2	3	2	0	2
113	.158	0	1	0	0	0	0	1	0	0
1	.157	1	0	3	0	0	0	0	0	1
22	.149	1	2	2	0	0	0	0	0	2
130	.147	0	0	1	1	0	0	1	0	3
98	.142	2	3	3	1	3	3	1	1	3
14	.142	0	0	0	1	2	1	0	0	0
15	.142	0	0	2	0	0	2	2	3	3
90	.140	1	2	3	1	0	3	3	2	3
79	.140	1	1	0	0	3	3	2	1	3
145	.139	2	0	0	0	1	3	2	2	2
125	.138	0	0	0	0	0	3	1	1	3
140	.136	0	0	0	0	0	0	1	1	2
109	.136	0	0	0	0	0	0	0	0	3
101	.134	1	1	0	0	0	3	0	0	2
126	.132	0	0	0	0	1	0	1	0	3
107	.127	0	0	0	0	3	3	2	3	3
144	.126	0	2	0	0	0	0	2	0	2
75	.126	3	0	1	3	0	3	1	2	3
112	.126	2	0	0	0	0	0	0	0	0
93	.125	1	0	1	0	0	0	2	3	3
106	.120	0	0	0	3	3	3	3	3	3
102	.114	1	0	0	0	0	0	0	1	3
128	.113	0	0	1	0	0	3	1	0	3
81	.113	1	0	0	0	1	3	2	3	3
99	.112	0	0	0	3	0	3	3	1	2
83	.109	2	0	0	0	1	3	0	2	3
123	.106	0	1	0	2	3	3	3	3	3
26	.100	0	0	1	1	0	3	0	1	0
115	.098	3	1	1	0	0	3	2	0	1
108	.097	0	0	0	3	3	3	2	3	3
120	.095	1	0	2	3	3	1	3	3	3
87	.089	0	2	0	2	3	3	3	3	2
141	.087	1	2	1	3	3	3	3	3	1
138	.085	3	0	1	0	3	3	3	3	3
7	.085	0	1	0	1	3	3	0	1	0
135	.083	3	2	2	3	3	3	3	3	3
89	.078	3	0	2	3	3	3	3	3	3
121	.076	0	0	1	3	3	3	3	3	2
84	.063	3	0	1	3	2	3	2	3	3
103	.061	0	2	1	3	3	3	3	3	3
143	.059	3	1	1	3	3	3	3	3	2
16	.050	0	3	3	0	0	0	2	1	1

3. Statistical Analysis

There are four possible results when an inspection is performed:

1) detection of a defect that is present (true positive)

2) failure to detect a defect that is not present (true negative)

3) detection of a defect that is not present (false positive)

4) failure to detect a defect that is present (false negative)

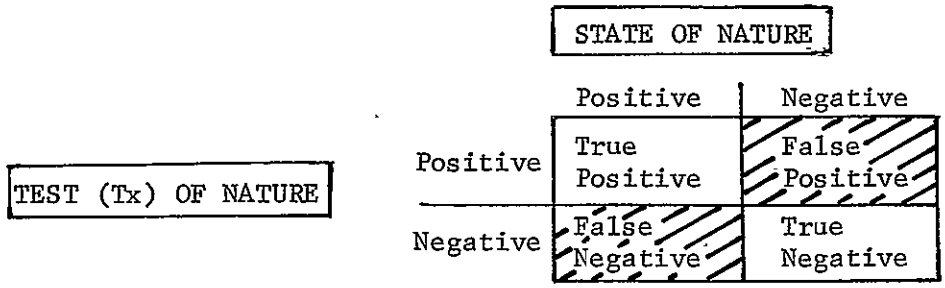

Although reporting of false indications (false positive) has a significant impact on the cost and hence the practicality of an inspection method, it was beyond the scope of this investigation.* Factors conducive to false reporting, i.e. low signal to noise ratio, were minimized by the initial work to optimize inspection techniques. An inspection may be referred to as a binomial event if we assume that it can produce only two possible results, i.e. success in detection (true positive) or failure to detect (false negative).

Analysis of data was oriented to demonstrating the sensitivity and reliability of state-of-the-art NDT methods for the detection of small, tightly closed flaws. Analysis was separated to evaluate the influences of etching and interference caused by rivets in the inspection area. Flaw size parameters of primary importance in the use of NDT data for fracture control are crack length (2C) and crack depth (a). Analysis was directed to determining the flaw size that would be detected by NDT inspection with a high probability and confidence.

---

*For a discussion on false reporting see Jamieson, John A., et al.: Infrared Physics and Engineering, McGraw-Hill Book Company Inc, page 330.

To establish detection probabilities from the data available, traditional reliability methods were applied. Reliability is concerned with the probability that a failure will not occur when an inspection method is applied. One of the ways to measure reliability is to measure the ratio of the number of successes to the number of trail (or number of chances for failure). This ratio times 100% gives us an estimate of the reliability of an inspection process and is termed a point estimate. A point estimate is independent of sample size and may or may not constitute a statistically significant measurement. If we assume a totally successful inspection process (no failures) we may use standard reliability tables to select a sample size. A reliability of 95% at 95% confidence level was selected for processing all combined data, and analyses were based on these conditions. For a 95% reliability at 95% confidence level, 60 successful inspection trials with no failure are required to establish a valid sampling and hence a statistically significant data point. For large crack sizes where detection reliability would be expected to be high, this criteria would be expected to be reasonable. For smaller crack sizes where detection reliability would be expected to be low, the required sample size to meet the 95% reliability/95 confidence level criteria would be very large.

To establish a reasonable sample size and to maintain some continuity of data we held the sample size constant at 60 NDT observations (trials). We then applied confidence limits to the data generated to provide a basis for comparison and analysis of detection successes, and to provide an estimate of the true proportion of cracks of a particular size that can be detected. Confidence limits are statistical determinations based on sampling theory and are values (boundaries) within which we expect the true reliability value to lie. For a given sample size, the higher our confidence level, the wider our confidence simply means that the more we know about anything, the better our chances are of being right. It is a mathematical probability relating the true value of a parameter to an estimate of that parameter and is based on history repeating itself.

4. Plotting Methods

In plotting data graphically, we have attempted to summarize the results of our studies in a few rigorous analyses. Plots were generated by referring to the tables of ordered values by actual flaw dimension, i.e., crack length.

Starting at the longest crack length, we counted down 60 inspection observations and calculated a detection reliability (successes divided by trails). A single data point was plotted at the largest crack (length in this group). This plotting technique biases

data in the conservative direction. We then backed up 30 observations, counted down 60 observations and plotted the data point at the longest crack in this group. The process was repeated for the remaining observations in each inspection operation. By use of the overlapping sampling technique, the total amount of data required could be reduced. The overlapping method is applicable since all observations are independent and hence may be included in any data sampling group. An added advantage is the "smoothing" of the curve resulting from such a plotting technique.

5. Calculation of Confidence Limits

The analysis and data plotting methods used to assess the variation in flaw detection reliability with flaw dimension becomes increasingly less rigorous as detection failures increase. To maintain continuity of data analysis and penetration using the same analysis and plotting methods, we have calculated and plotted confidence limits for each plot point using the available data sample in that sample group. Confidence limits are values within which we expect the true reliability value to be if an infinitely large sample is taken. For a given sample size, the higher our confidence level, the wider our confidence limits. Confidence limits are statistical determinations based on sampling theory.

The statistics that are used to determine confidence limits are dependent up the distribution of whatever characteristic we are measuring. Data based on success/failure criteria can be best described statistically by applying the binomial distribution. The normal, Chi-square and Poisson distributions are sometimes used as approximations to the binomial and are selected on the basis of available sample size. If the sample size is held constant, confidence limits may be applied to these data to establish the true reliability values. A binomial distribution analysis was applied to the data to find the lower or one-sided confidence limit based on the proportion of successes in each sample group.

Lower confidence limits were calculated by standard statistical methods* and is compatible with the method described by Yee et al.+ The lower confidence level, P_ℓ , is obtained by solving the equation:

---

*Alexander McFarlane Mood: *Introduction to the Theory of Statistics*. McGraw-Hill Book Company, Inc, 1950, pp 233-237.

B.G.W. Yee, J. C. Couchman, F. H. Chang, and D. F. Packman: *Assessment of NDE Reliability Data*. CR-134834. General Dynamics Corporation, Fort Worth Division, September 1975.

$$G = \sum_{i=o}^{n-1} \binom{N}{i} P_\ell^i \quad (1-P_\ell)^{N-i},$$

where G is the confidence level desired,
N is the number of tests performed,
n is the number of successes in N tests,
and P_ℓ is the lower confidence level.

Lower confidence limits were determined at a confidence level of 95% (G=.95) using 60 trials (N=60) for all calculations. The lower confidence limits are plotted as (-) points on all graphical presentations of data reported herein.

F. DATA RESULTS

The results of inspection and data analysis are shown graphically in Figures III-11, III-12 and III-13. The results clearly indicate an influence of inspection geometry on crack detection reliability when compared to results obtained on flat aluminum panels.* Although some of the change in reliability may be attributed to a change flaw tightness and/or slight changes in the angle of flaw growth, most of the change is attributed to geometric interference at the stringer radius. Effects of flaw variability were minimized by verifying the location of each flaw at the tangency point of the stringer radius before accepting the flaw/inspection data. Four flaws were eliminated by such analysis.

Changes in detection reliability due to the presence of rivets as revealed in the Sequence 3 evaluation further illustrates that obstacles in the inspection area will influence detection results.

---

* Op cit. Ward D. Rummel, Paul H. Todd, Jr., Sandor A. Frecska, and Richard A. Rathke.

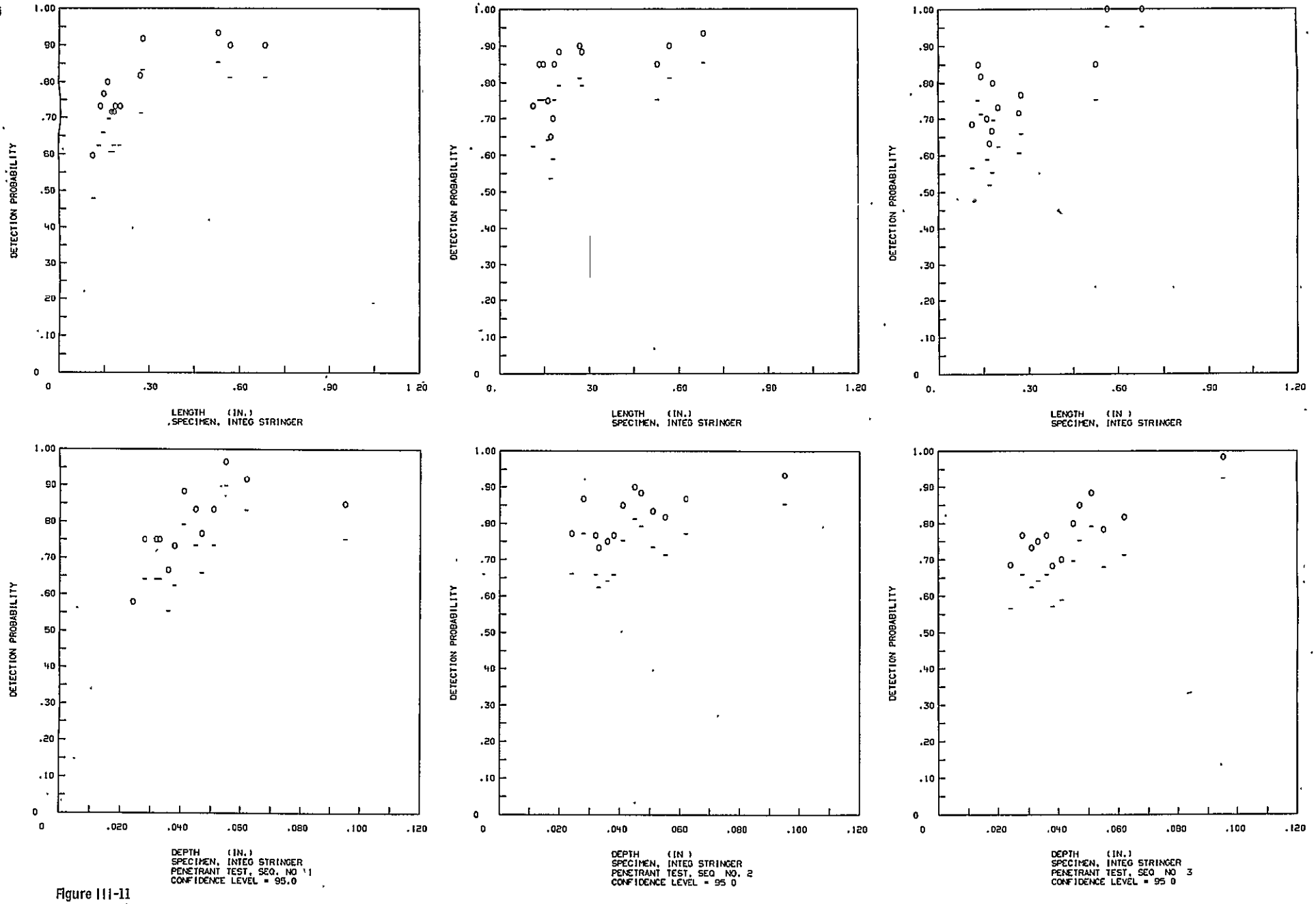

Figure III-11
Crack Detection Probability for Integrally Stiffened Panels by the Penetrant Method Plotted at 95% Probability and 95% Confidence Level

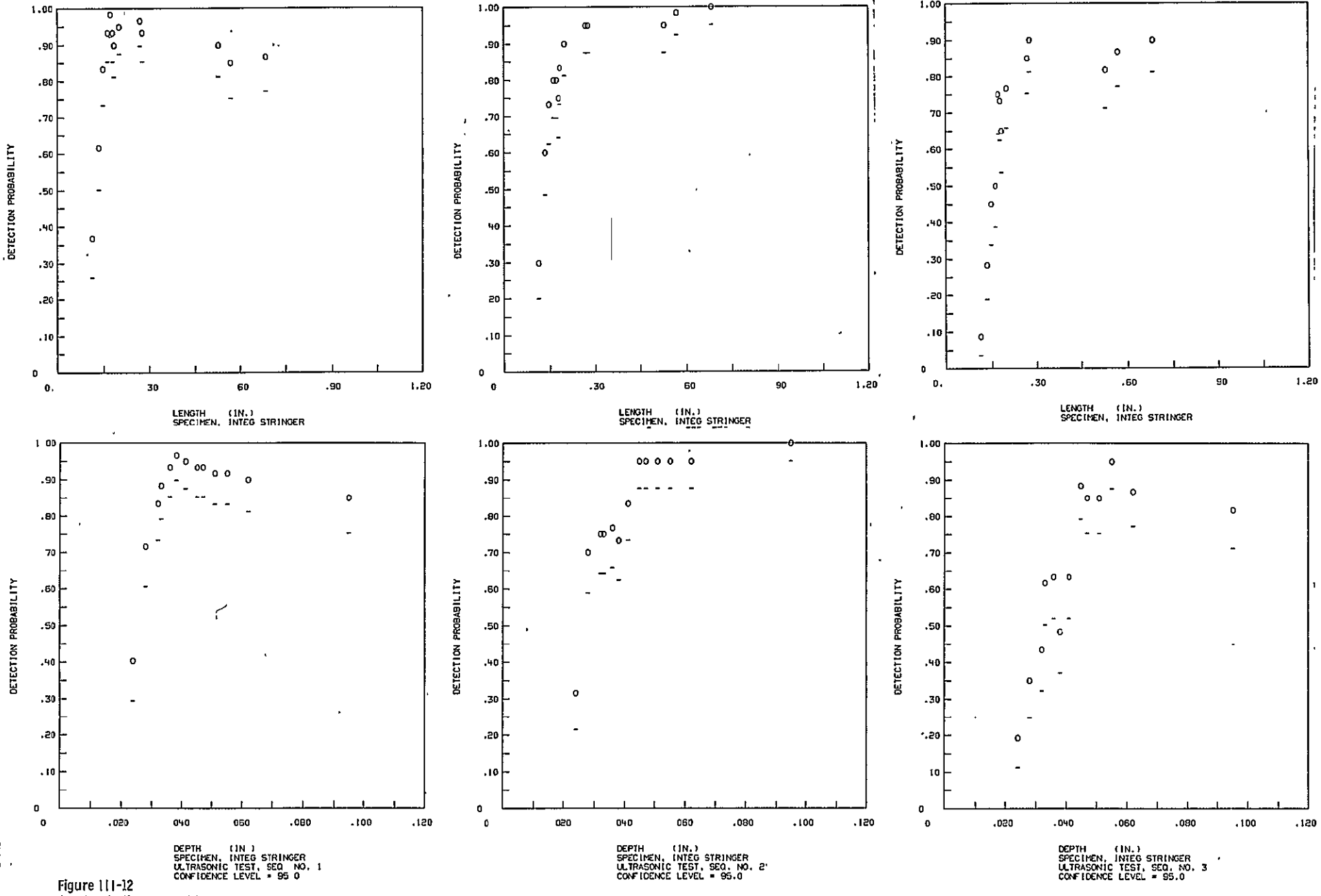

Figure III-12
Crack Detection Probability for Integrally Stiffened Panels by the Ultrasonic Method Plotted at 95% Probability and 95% Confidence Level

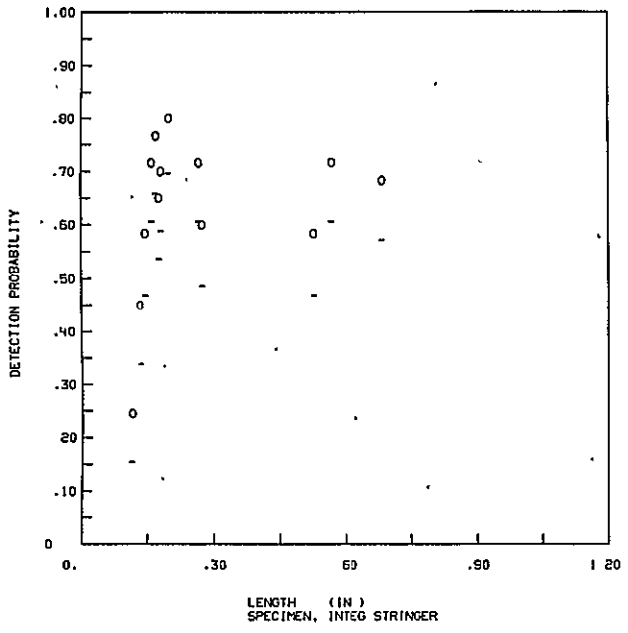

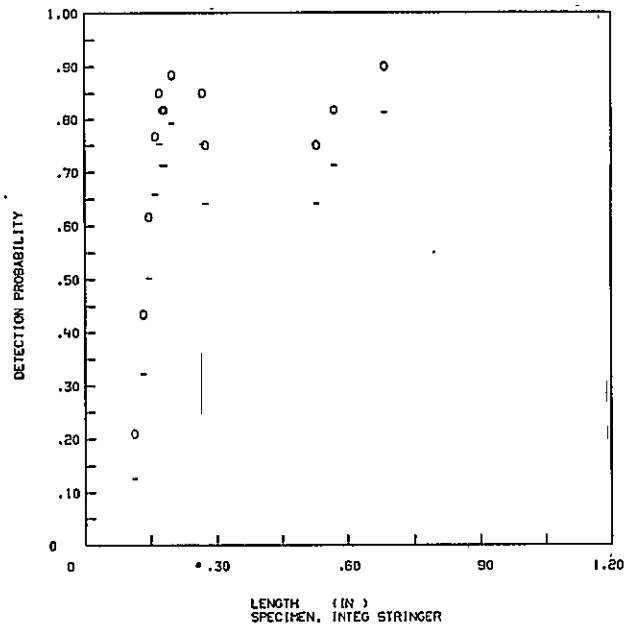

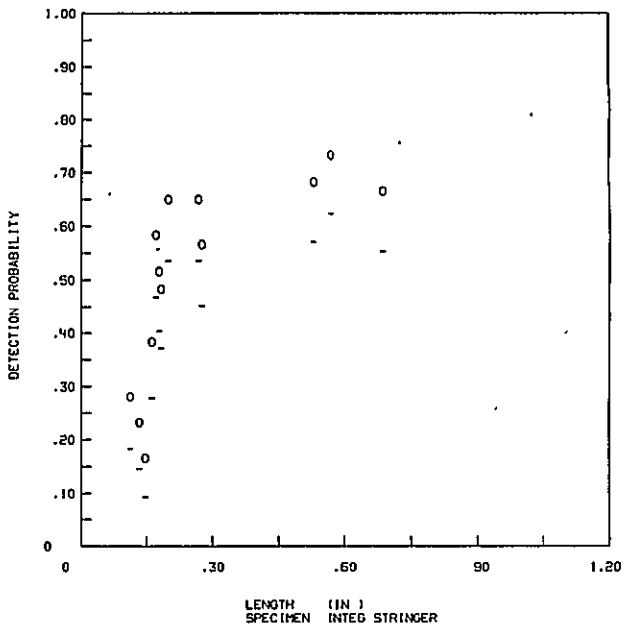

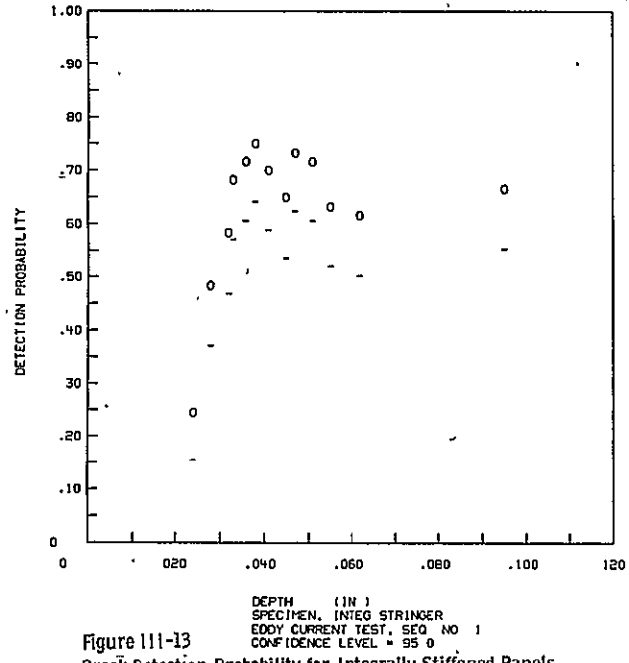

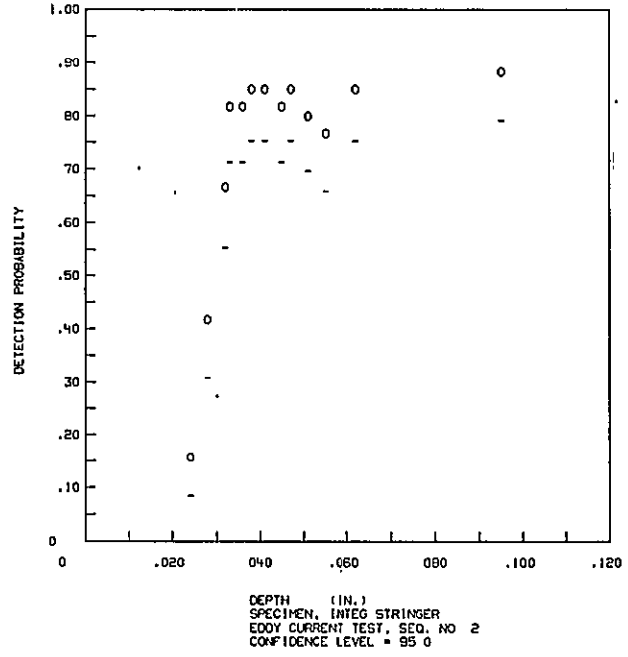

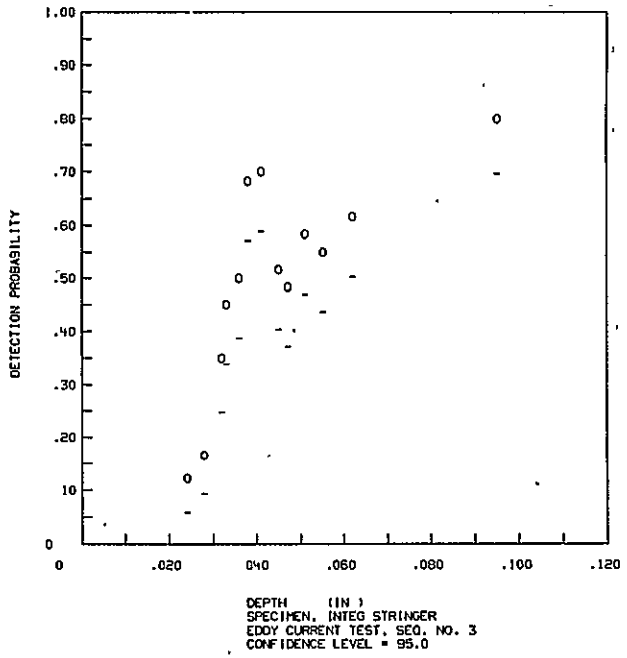

Figure III-13
Crack Detection Probability for Integrally Stiffened Panels by the Eddy Current Method Plotted at 95% Probability and 95% Confidence Level

IV. EVALUATION OF LACK OF PENETRATION (LOP) PANELS

Welding is a common method of joining major elements in the fabrication of structures. Tightly closed flaws may be included in a joint during the welding process. A lack of penetration (LOP) flaw is one of several types of tightly closed flaws that can form in a weld joint and is representative of the types that commonly occur.

Lack of penetration flaws (defects) may be the product of slight variations in welding parameters or of slight variations in welding parameters or of slight variations in weld joint geometry and/or fit up. Lack of penetration defects are illustrated schematically

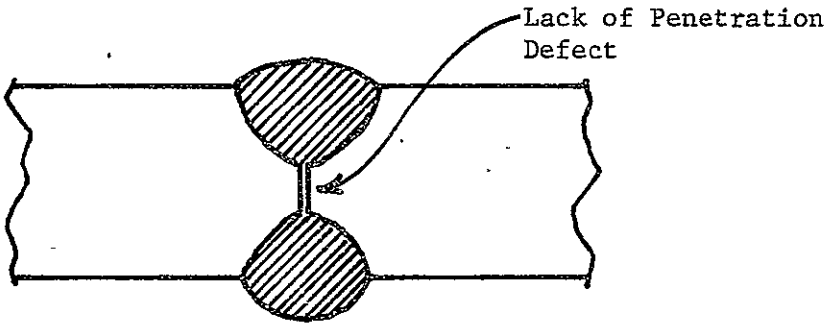

(a) Straight Butt Joint Weldment with One Pass from Each Side

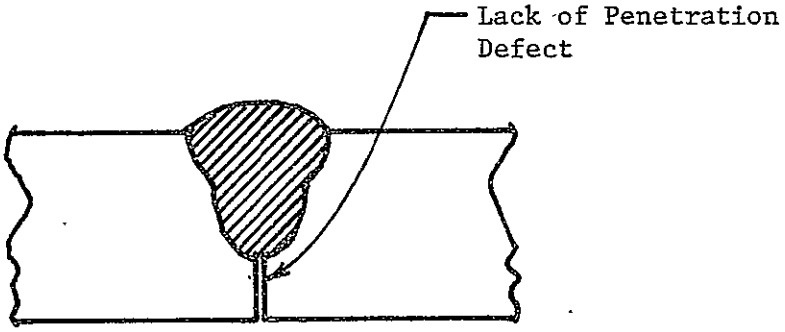

(b) Straight Butt Joint Weldment with Two Passes from One Side

Figure II-1 Typical Weldment Lack of Penetration Defects

Figure IV-1(a) is the result of a failure to penetrate the weld joint fully by single passes from each side of the joint. This type of defect is also termed lack of fusion and may be referred to as such in the literature. Figure IV-1(b) is the result of a failure to penetrate the weld joint fully by two passes from the same side of a joint.

A lack of penetration defect has been shown to be one of the most difficult flaws to detect by conventional nondestructive inspection techniques. Because of the high residual compressive stresses present in weldments containing this defect and the tendency of the defect to form a diffusion bond under its combined heat and stress exposure, it is possible to miss it using X-radiographic and ultrasonic inspection methods. Even if the defect is open to the surface, it is possible for the joint to be so tightly closed that penetrants will not reveal it. Various investigators have conducted studies to enhance L.O.P. defect detection*. A difficult experiment variable in such programs is the tightness of the defect. Lack of penetration in straight butt joint weldments with one pass from each side was selected for evaluation. This configuration provided the greatest option in varying defect location through the thickness of the weld, i.e. open, near the surface and buried, and provided the greatest chance for obtaining tightly closed flaws. After the flaw type was established, a program plan for test panel preparation, evaluation and analysis was established as shown schematically in Figure IV-2.

---

*B. G. Martin and C. J. Adams: *Detection of Lack of Fusion in Aluminum Alloy Weldments by Ultrasonic Shear Waves*. Technical Paper No. 3499. Douglas Aircraft Company, 1965.

J. L. Cook: *Detection of Lack of Fusion Using Opaque Additives, Phase I Progress Report*. Contract NAS8-28708. McDonnell Douglas Astronautics Company, November 1972.

Definition of Mutually Optimum NDI and Proof Test Criteria for 2219 Aluminum Pressure Vessels, Work in progress, Contract NAS3-17790, Martin Marietta Aerospace, Denver, Colorado.

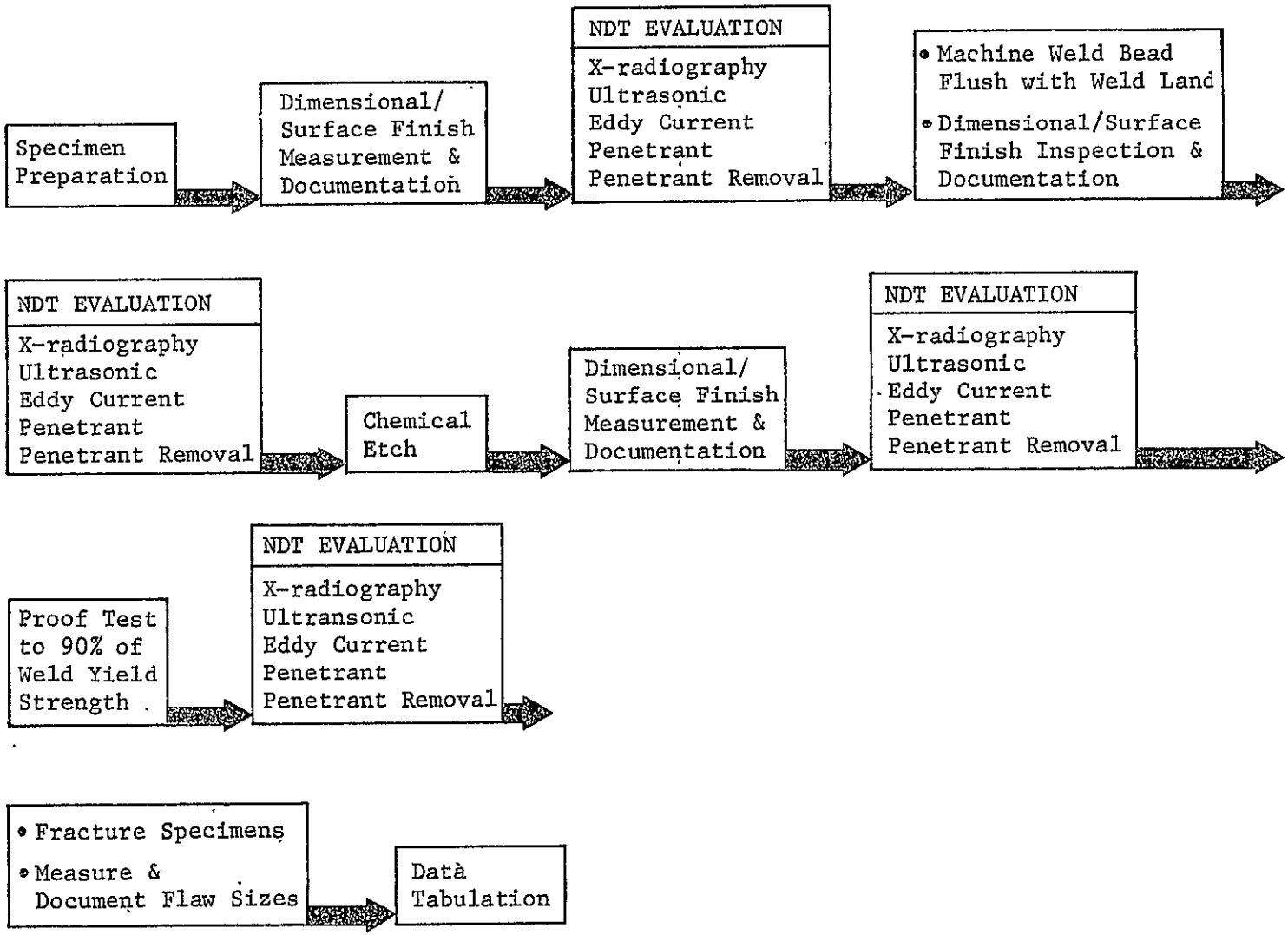

Figure IV-2 NDT Evaluation Sequence for Lack of Penetration Panels

A. SPECIMEN PREPARATION

The direct current, gas tungsten arc (GTA) weld technique was selected as the most appropriate method for producing LOP flaws in 2219-T87 panels and is commonly used in aerospace construction. The tungsten arc allows independent variation of current, voltage, electrode tip shape, and weld travel. This allows for a specific reproduction of weld conditions from time to time as well as several degrees of freedom for producing nominally proportioned welds and specific weld deviations. The dc GTA can be relied on to produce a bead of uniform depth and width and always produce a single specific response to a programmed change in the course of welding.

In experiments that are run to measure or observe the presence of lack of penetration flaws, the most trying task is to produce the LOP predictably. Further, a control is desired that can alter the length and width and sometimes the shape of the defect. Commonly an LOP is produced deliberately by a momentary reduction of current or some other vital weld parameter. Such a reduction of heat naturally reduces the penetration of the melt. But even when the degree of cutback and the duration of cutback are precisely executed, the results are variable.

Instead of varying the weld process controls to produce the desired LOP defects, we chose to locally vary the weld joint thickness. At a desired defect location, we locally increased the thickness of the weld joint in accordance with the desired height and length of the defect.

A constant penetration (say 80%) in a plate can be decreased to 30% of the original parent metal plate thickness when the arc hits this thickness increase. It will then return to the original penetration, after a lag, when it runs off the reinforcement pad. The height of the pad was programmed to vary the LOP size in a constant weld run.

An experimental program was completed to determine the appropriate pad configuration and welding parameters necessary to produce the required defects. Test panels were welded in 4-foot lengths using the direct-current gas tungsten arc welding technique and 2319 aluminum alloy filler wire. Buried flaws were produced by balanced, 60% penetration passes from both sides of a panel. Near-surface and open flaws were produced by unbalanced (i.e., 80%/30%) penetration passes from both sides of a panel. Defect length and depth were controlled by controlling the reinforcement pad configuration. Flaws produced by this method are lune shaped as

illustrated by the in-plane cross-sectional microphotograph in Figure IV-3.

The 4-foot long panels were x-radiographed to assure general weld process control and weld acceptability. Panels were then sawed to produce test specimens, 15.1 centimeters (6 in.) wide and approximately 22.7 (9 in.) long with the weld running across the 15.1 centimeter dimension. At this point, one test specimen from each weld panel produced was fractured to verify defect type and size. The reinforcement pads were mechanically ground off to match the contour of the continuous weld bead. Seventy 1/8-inch (0.32) and seventy 1/2-inch (1.27-cm) thick specimens were produced containing an average of two flaws per specimen and having both open and buried defects in 0.250, 0.500, and 1.000-inch (0.64, 1.27, 2.54-cm) lengths. Ninety-three of these specimens were selected for NDT evaluation.

B. NDT OPTIMIZATION

Following preparation of LOP test specimens, an NDT optimization and calibration program was initiated. Panels containing 0.250-inch long open and buried flaws in 1/8-inch and 1/2-inch material thicknesses were selected for evaluation.

1. X-Radiography

X-radiographic techniques used for typical production weld inspection were selected for LOP panel evaluation. Details of the procedure for evaluation of LOP panels are included in Appendix D. This procedure was applied to all weld panel evaluations. Extra attention was given to panel alignment to provide optimum exposure geometry for detection of the LOP defects.

2. Penetrant Evaluation

The penetrant inspection procedure used for evaluation of LOP specimens was the same as that used for evaluation of integrally stiffened panels. This procedure is shown in Appendix A.

Figure IV-3
Schematic View of a Buried LOP in a Weld, with Representative Photomicrograph Crossectional Views of Defect

3. Ultrasonic Evaluation

Panels used for optimization of X-radiographic evaluation were also used for optimization of ultrasonic evaluation methods. Comparison of the techniques was difficult due to apparent differences in the tightness of the defects. Additional weld panels containing 1/64-inch holes drilled at the centerline along the axis of the weld were used to provide an additional comparison of sensitivities.

Single and double transducer combinations operating at 5 and 10 megahertz were evaluated for sensitivity and for recorded signal-to-noise responses. A two-transducer automated C-scan technique was selected for panel evaluation. This procedure is shown in Appendix E. Following the Sequence 1 evaluation cycle (as-welded condition) one of the weld beads was shaved off flush with the specimen surface (Sequence 2, scarfed condition). The ultrasonic evaluation procedure was again optimized. This procedure is shown in Appendix F.

4. Eddy Current Evaluation

Panels used for optimization of x-radiographic evaluation were also used for optimization of eddy current methods. Depth of penetration in the panel and noise resulting from variations in probe lift-off were primary considerations in selecting an optimum technique. A Vector 111 instrument was selected for its stability. A 100-kilohertz probe was selected for evaluation of 1/8-inch specimens and a 20-kilohertz probe was selected for evaluation of 1/2-inch specimens. These operating frequencies were chosen to enable penetration to the midpoint of each specimens configuration. Automated C-scan recording was accomplished with the aid of a spring-loaded probe holder as shown in Figure IV-4. A procedure was established for evaluating welded panels with the crown intact. This procedure is shown in Appendix G. Following the Sequence 1 evaluation cycle (as-welded condition), one of the weld beads was shaved off flush with the specimen surface (Sequence 2, scarfed condition). The eddy current evaluation procedure was again optimized. Automated C-scan recording was accomplished with the aid of a spring-loaded probe holder as shown in Figure IV-5. The procedure for eddy current evaluation of welded, flat panels is shown in Appendix H.

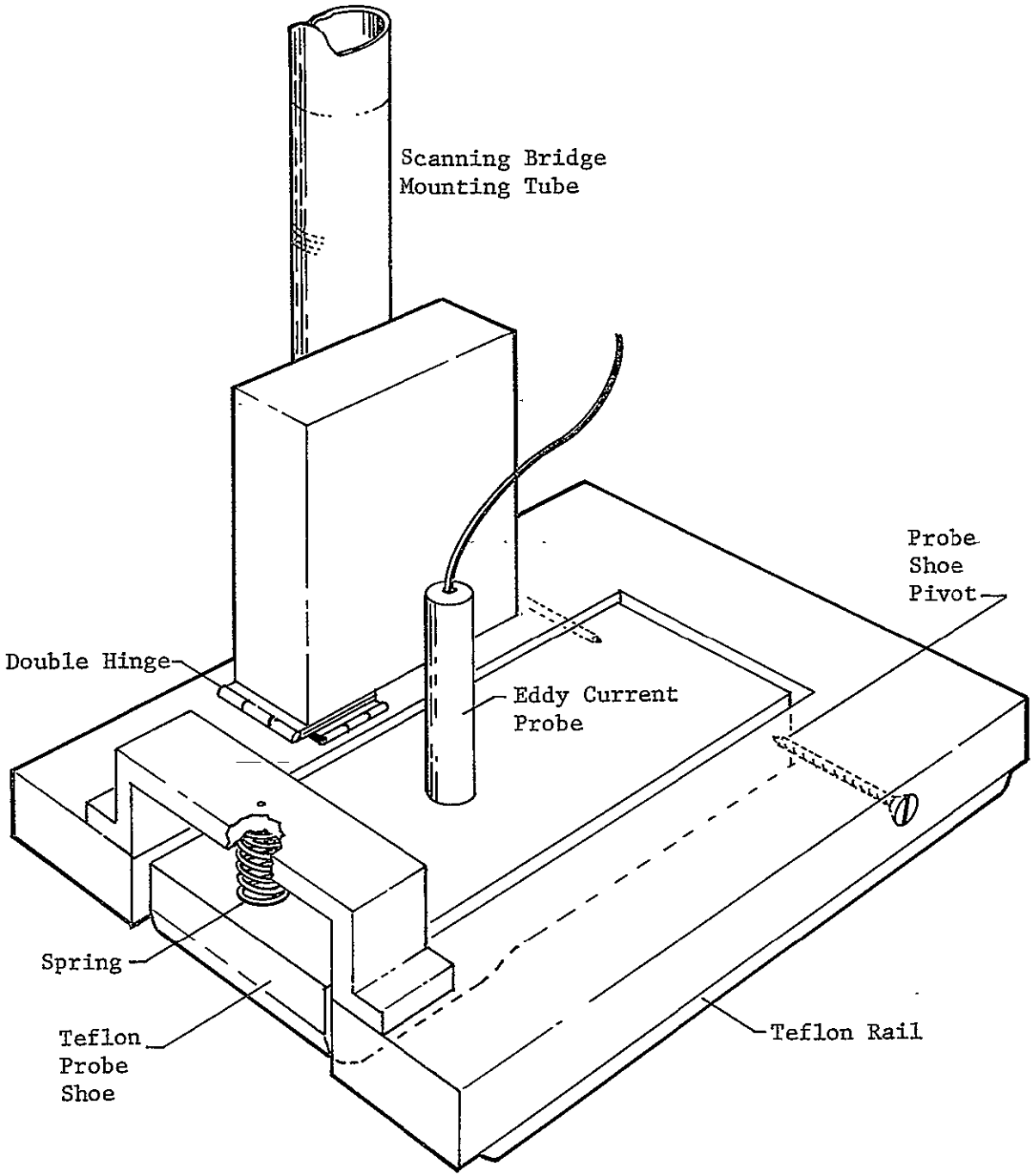

Figure IV-4
Spring-Loaded Eddy Current Scanning Probe Holder for Welded Panels with Crowns

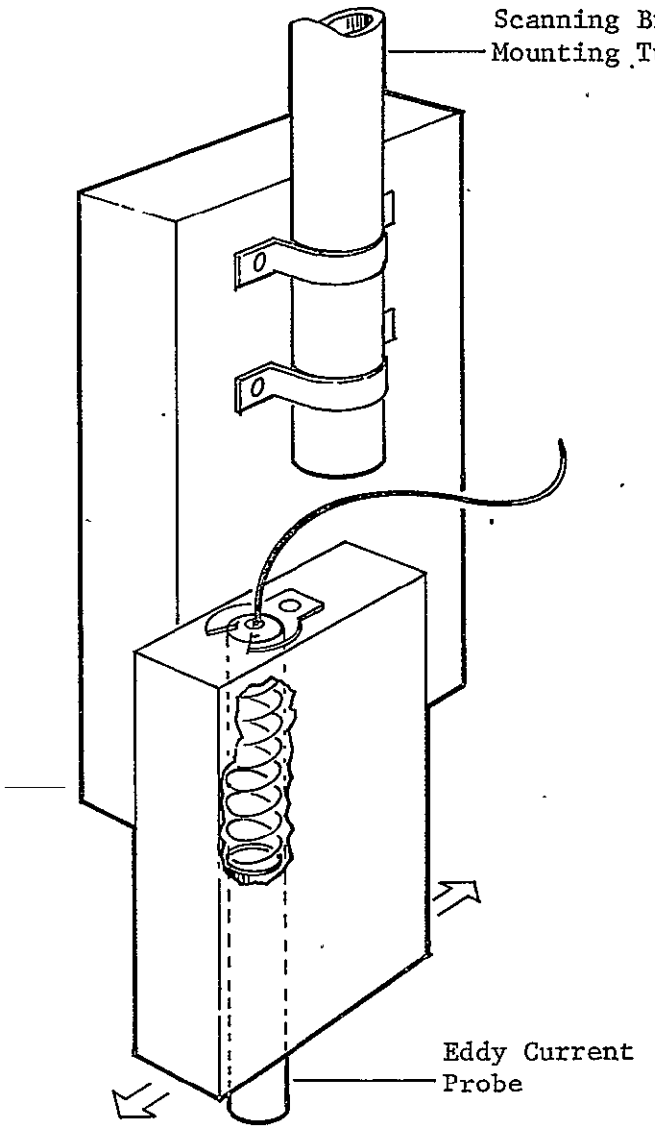

Figure IV-5
Spring-Loaded Eddy Current Scanning Probe Holder for Flat Panels

C. TEST SPECIMEN EVALUATION

Test specimens were evaluated by optimized x-radiographic, penetrant, ultrasonic, and eddy current inspection procedures in three separate inspection sequences. Two additional penetrant cycles were completed after etching panels in the as-welded condition and after etching in the scarfed condition. After familiarization with the specific procedures to be used, the 93 specimens were evaluated by three different operators for each inspection sequence. Inspection records were analyzed and recorded by each operator without a knowledge of the total number of defects present or of the previous inspection results.

1. Sequence 1 - Inspection of As-Welded Specimens

The Sequence 1 inspection included x-radiographic, penetrant, ultrasonic, and eddy current inspection procedures. One set of x-radiographs was made. The radiographs were then evaluated independently by three different operators. Each operator interpreted the x-radiographic image and reported his own results.

Penetrant inspection of specimens in the "as-welded" condition was performed by one operator. Few defects were detected and results were not included in the data. This inspection was somewhat biased due to the mechanical grinding on the beads to remove the reinforcement pads. The specimens were etched using a light metallurgical etch ("Flicks" etchant solution), recleaned using a mild alkaline cleaner, and reinspected. Penetrant inspection was performed independently by three different operators who completed the entire penetrant inspection process and reported their own results.

One set of C-scan ultrasonic and eddy current recordings were made. The recordings were then evaluated and the results recorded independently by three different operators.

Inspections were carried out using the optimized methods established and documented in Appendices A, D, E, and F. The locations and relative magnitudes of the NDT indications were recorded by each operator and coded for data processing.

2. Sequence 2 - Inspection after Scarfing

On completion of the first inspection sequence, the weld crown on one side of each LOP panel was removed by scarfing. In all cases the weld crown was removed flush with the parent metal surface. For near-surface LOP flaws, the weld crown was removed from the side nearest to the LOP to open it to the scarfed surface. Panels were cleaned and inspected by the optimized NDT methods. One set of x-radiographs was made. The radiographs were then evaluated independently by three different operators. Each operator interpreted the information on the x-ray film and reported his own results.

Penetrant inspection was performed independently by three different operators who completed the entire penetrant inspection procedure and reported their own results. Scarfing of the weld crown resulted in mechanical smearing of the aluminum material, thus decreasing the chances for the penetrant to reveal the flaws. The surface was therefore etched using a light metallurgical etch ("Flick's" etchant solution), recleaned using a milk alkaline cleaner, and reinspected by three different operators.

One set of C-scan ultrasonic and eddy current recordings was made. The recordings were then evaluated independently by three different operators. Inspections and readout were carried out using the optimized methods established and documented in Appendices A, D, E, and G. The locations and relative magnitudes of the NDT indications were recorded by each operator and were coded for data processing.

3. Sequence 3 - Inspection after Proof Loading

Following completion of Sequence 2, the LOP panels were proof-loaded to approximately 90% of the yield strength for the weld. This loading cycle was performed to simulate a proof load cycle on functional hardware and to evaluate the enhancement of flaw detection provided by NDT methods. Panels were cleaned and inspected by optimized NDT methods. One set of x-radiographs was made. This set was evaluated independently by three different operators. Each operator interpreted the information on the x-ray film and reported his own results.

Penetrant inspections were performed independently by three different operators who completed the entire penetrant inspection procedure and reported his own results.

One set of C-scan ultrasonic and eddy current recordings was made. The recordings were then evaluated independently by three different operators. Inspections and readout were carried out using the optimized methods established and documented in Appendices A, D, E, and G. The locations and relative magnitudes of the NDT indications were recorded by each operator and were coded for data processing.

D. PANEL FRACTURE

Following final inspection in the post proof-loaded configuration, the panels were fractured and the actual flaw sizes measured. Flaw sizes and locations were measured with the aid of a traveling microscope and the results were recorded in the actual data file. The lengths from the tip to the tip of the lunes were measured and recorded as actual flaw length and were used in processing data by the x-ray, ultrasonic, and eddy current methods. The lengths of the flaw open to the panel surface were measured and recorded as the actual flaw lengths and were used in processing data by the penetrant method.

The heights of the lunes were measured and recorded as actual flaw depth and were used in processing all data. In addition to the plan view location within the panel, the depth or location of the lune beneath the surface for buried flaws was recorded. This depth below the surface was used as a criterion for accepting data observed by the eddy current method. Figure IV-6 schematically shows the measurements taken for the LOP specimens.

E. DATA ANALYSIS

1. Data Tabulation

Actual LOP flaw data and NDT observations were coded, keypunched, and input to a computer for data tabulation, data ordering, and data analysis sequences. Table IV-1 lists actual flaw data for LOP specimens. Note that all dimensions are in inches.

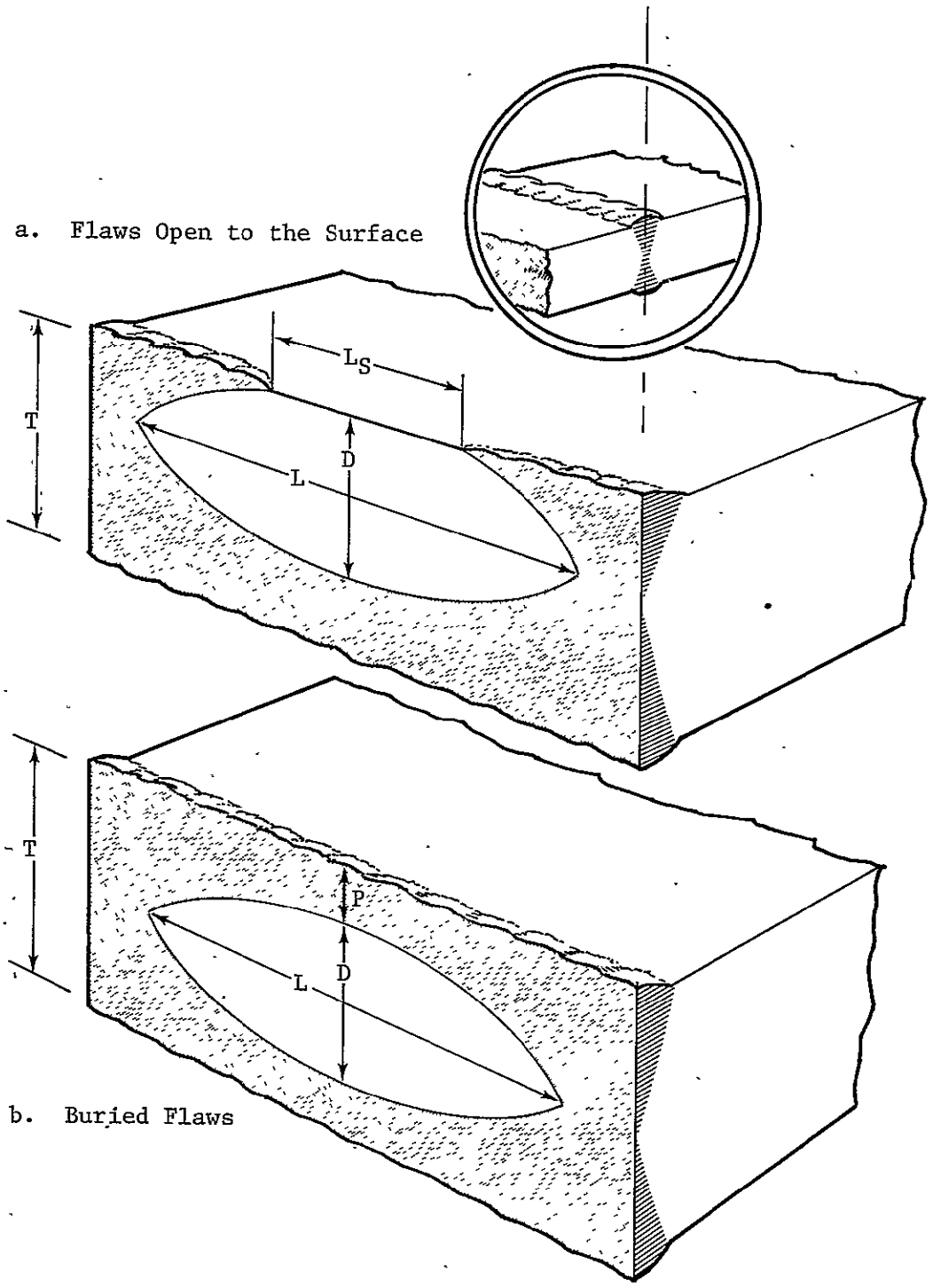

Figure IV-6
Schematic Side View of a LOP (Lune) Flaw Showing Critical Dimensions

Table IV-1 Actual Flaw Data, LOP Panels

PANEL NO.	CRACK NO.	CRACK LENGTH	CRACK DEPTH	INITIAL FINISH	INITIAL THICKNESS	FINAL FINISH	FINAL THICKNESS	CRACK POSITION X	CRACK POSITION Y	F DEPTH
1C	1	.517	.035	51	.1380	50	.1060	1.23	4.43	0.0238
1CA	2	.504	.040	51	.1380	50	.1060	2.85	4.48	0.0201
8CA	17	.542	.042	51	.1380	50	.1060	2.30	4.32	0.0224
10CA	19	.498	.046	62	.1500	25	.1330	2.33	4.38	0.0173
10CA	20	.569	.047	62	.1500	25	.1330	3.82	4.38	0.0210
13CB	24	.194	.050	53	.1300	50	.1150	2.12	3.40	
16CB	28	.133	.042	87	.1840	20	.1440	4.99	3.42	
16CB	29	.231	.042	88	.1660	32	.1390	4.09	3.45	
16CB	30	.268	.050	88	.1660	32	.1390	3.22	3.45	
19CA	35	.346	.076	60	.1750	40	.1460	1.94	3.20	0.0108
20CA	36	.318	.057	77	.1690	28	.1510	2.00	3.27	0.0033
21CB	37	.263	.053	76	.1720	50	.1510	2.86	3.28	
21CB	38	.341	.066	76	.1720	50	.1510	1.95	3.27	
22CB	39	.345	.065	65	.1620	30	.1540	3.92	3.27	
22CB	40	.258	.057	65	.1620	30	.1540	3.01	3.27	
24CB	44	.337	.073	81	.1780	36	.1430	2.98	3.20	0.0073
24CB	45	.309	.064	81	.1780	36	.1430	2.07	3.22	
24CA	46	.336	.061	81	.1780	36	.1430	1.17	3.24	0.0061
26CB	49	1.100	.091	51	.1730	25	.1400	4.50	4.27	
26CB	50	1.158	.087	51	.1730	25	.1400	3.02	4.27	
26CB	51	1.075	.088	51	.1730	25	.1400	1.58	4.25	
28CB	55	1.175	.088	55	.1830	64	.1590	4.76	4.25	
28CB	56	1.079	.090	55	.1830	64	.1590	3.09	4.27	
28CB	57	1.052	.093	55	.1830	64	.1590	1.42	4.22	
30CA	61	1.156	.080	54	.1760	28	.1320	3.10	3.84	0.0078
30CA	62	1.122	.071	54	.1760	28	.1320	1.54	3.80	0.0095
33CA	69	1.125	.073	49	.1870	65	.1250	4.98	3.85	0.0117
33CA	70	1.150	.072	49	.1870	65	.1250	3.31	3.87	0.0126
33CA	71	1.184	.070	49	.1870	65	.1250	1.60	3.85	0.0154
36CB	77	1.010	.105	53	.2050	20	.1660	1.48	4.40	
36CB	78	.987	.103	53	.2050	20	.1660	3.01	4.40	
36CB	79	.919	.105	53	.2050	20	.1660	4.43	4.40	
37CB	80	.916	.104	52	.1890	40	.1820	4.48	4.39	
37CB	81	.890	.102	52	.1890	40	.1820	2.83	4.41	
37CB	82	.850	.104	52	.1890	40	.1820	1.13	4.41	
38CB	83	.825	.120	62	.2050	40	.1430	5.21	4.40	
38CB	84	.790	.117	62	.2050	40	.1430	3.53	4.40	
38CB	85	.935	.118	62	.2050	40	.1430	1.95	4.40	
45CA	103	.885	.035	94	.1620	40	.1430	3.20	4.07	0.0269
45CA	104	.929	.041	94	.1620	40	.1430	1.59	4.07	0.0225
52CB	119	.698	.083	62	.1780	25	.1520	3.19	4.32	
54CB	121	.734	.088	55	.1660	60	.1440	3.36	4.31	
54CB	122	.788	.089	55	.1660	60	.1440	1.86	4.29	
55CB	123	.742	.069	50	.1750	55	.1480	2.88	4.29	
55CB	124	.749	.073	50	.1750	55	.1480	1.39	4.29	
56CB	125	1.075	.104	50	.1560	35	.1180	2.57	4.30	
58CB	127	1.124	.083	51	.1590	40	.1230	3.49	4.32	
60CB	129	1.158	.097	54	.1460	40	.1170	3.04	4.32	
60CB	130	1.105	.091	54	.1460	40	.1170	1.57	4.32	
69CA	142	.372	.059	115	.1740	35	.1430	2.99	3.40	0.0159
70CA	143	.320	.055	100	.1650	45	.1490	2.90	3.45	0.0359
72CA	146	.297	.070	71	.1630	40	.1470	4.64	3.43	0.0197
72CA	147	.288	.054	71	.1630	40	.1470	3.77	3.42	0.0259
73CA	148	.322	.058	112	.1670	40	.1390	3.02	3.44	0.0176
73CA	149	.267	.057	112	.1670	40	.1390	2.12	3.42	0.0171
73CA	150	.343	.053	112	.1670	40	.1390	1.23	3.42	0.0225
74CA	151	.262	.060	105	.1620	35	.1490	4.82	3.42	0.0220
74CA	152	.250	.052	105	.1620	35	.1490	3.92	3.42	0.0285
74CA	153	.243	.050	105	.1620	35	.1490	3.04	3.42	0.0235
77CA	156	1.014	.046	91	.1430	150	.1330	3.51	4.34	0.0244
78CA	157	.986	.046	86	.1470	150	.1210	4.78	4.33	0.0246
80CA	160	.961	.049	40	.1430	150	.1260	4.09	4.34	0.0214
80CA	161	.943	.050	40	.1430	150	.1260	2.58	4.33	0.0203
85CA	166	.874	.057	145	.1640	125	.1370	3.74	4.27	0.0153
85CA	167	.921	.065	145	.1640	125	.1370	2.26	4.27	0.0174
86CA	168	.781	.049	46	.1620	115	.1400	2.73	4.27	0.0172
86CA	169	.809	.049	46	.1620	115	.1400	1.27	4.27	0.0204
88CA	173	.812	.085	39	.1620	150	.1450	4.45	4.32	
88CA	174	.825	.080	39	.1620	150	.1450	2.79	4.32	0.0117
88CA	175	.858	.074	39	.1620	150	.1450	1.05	4.34	0.0225
94CA	186	.266	.075	40	.1790	140	.1600	1.94	3.30	0.0345
98CA	194	.277	.077	46	.1710	115	.1250	3.31	3.21	
98CA	195	.280	.070	46	.1710	115	.1250	3.31	3.21	
98CA	196	.288	.083	46	.1710	115	.1250	1.51	3.23	
99CA	197	.717	.097	92	.1910	22	.1480	2.86	4.30	0.0023
99CA	198	.638	.101	92	.1910	22	.1480	1.29	4.30	0.0063
107CB	214	.649	.062	105	.1710	160	.1400	4.53	4.38	
108CB	215	.724	.088	92	.1800	36	.1360	3.70	4.43	
108CA	216	.676	.073	92	.1800	36	.1360	1.80	4.44	
111CB	220	1.210	.075	76	.1440	130	.1260	3.23	4.21	
112CB	221	1.184	.077	68	.1500	20	.1250	4.00	4.39	
114CB	223	1.271	.097	74	.1430	25	.1220	3.54	4.43	
114CB	224	1.245	.099	74	.1430	25	.1220	2.12	4.44	
115CB	225	1.226	.073	111	.1410	54	.1150	4.01	4.38	
115CB	226	1.216	.070	111	.1410	54	.1150	2.55	4.38	
1CA	501	.516	.028	120	.4830	160	.4470	2.96	4.28	0.1594
9CA	509	.369	.070	230	.4950	60	.4650	3.94	4.30	0.1435
11X	510	.261	.032	230	.4980	45	.4660	3.47	4.26	
11CA	511	.393	.048	230	.4980	45	.4660	3.82	4.26	0.1543
16CB	516	.338	.064	175	.4850	130	.4450	2.99	4.31	

Table IV-I (Continued)

17CA	517	.688	.077	82	.4850	55	.4550	2.50	4.52	
19CA	519	.511	.079	77	.4850	45	.4590	2.30	4.53	
20OB	520	.708	.090	115	.4860	45	.4360	1.96	4.48	
21OB	521	.362	.061	70	.4750	70	.4610	2.26	4.53	
22OB	522	.494	.052	57	.4800	85	.4610	3.61	4.38	
23OB	523	.419	.070	47	.4780	60	.4510	3.66	4.40	
24OB	524	.562	.078	50	.4880	40	.4660	2.62	4.45	
24X	525	.483	.160	50	.4880	40	.4660	4.40	4.45	
28OB	528	.686	.078	47	.4890	22	.4630	1.88	4.47	
28X	529	.145	.028	47	.4890	22	.4630	4.18	4.45	
28X	530	.112	.027	47	.4890	22	.4630	4.44	4.45	
36OB	536	.964	.117	44	.5090	45	.4690	2.46	4.44	
42CA	542	.214	.024	79	.4910	84	.4630	3.03	4.25	0.1655
43CA	543	.116	.009	82	.4840	70	.4540	2.89	4.30	0.1690
44CA	544	.173	.032	80	.4870	52	.4550	2.95	4.25	0.1497
45CA	545	.033	.014	39	.4860	50	.4540	2.96	4.30	0.1148
48CA	548	.094	.005	74	.4780	40	.4370	3.11	4.30	0.1581
50CA	550	.900	.039	52	.4830	45	.4530	2.91	4.29	0.1723
59CA	559	.872	.069	72	.4850	125	.4600	2.28	4.23	0.1228
60CA	560	.889	.063	73	.4870	60	.4560	3.64	4.25	0.1508
63CA	563	.870	.058	127	.4810	45	.4560	2.11	4.23	0.1280
64CA	564	.435	.071	87	.4780	80	.4520	4.52	4.37	
64OB	565	.391	.081	87	.4780	80	.4520	3.08	4.37	
64OB	566	.440	.076	87	.4780	80	.4520	1.54	4.37	
66OB	568	.482	.094	60	.4920	55	.4620	3.50	4.40	
66OB	569	.430	.096	60	.4920	55	.4620	2.47	4.40	
67OB	570	.531	.085	63	.4800	80	.4660	3.87	4.43	
67OB	571	.568	.081	63	.4800	80	.4660	2.88	4.43	
68C	572	.488	.087	69	.4740	35	.4550	4.36	4.43	
68C	573	.454	.095	69	.4740	35	.4550	3.30	4.43	
68C	574	.518	.090	69	.4740	35	.4550	2.30	4.44	
69OB	575	.506	.077	82	.4620	78	.4580	4.42	4.43	
69OB	576	.601	.071	82	.4620	78	.4580	3.43	4.43	
69OB	577	.568	.071	82	.4620	78	.4580	2.39	4.43	
70C	578	.632	.069	53	.4750	90	.4480	4.36	4.40	
70OB	579	.611	.105	53	.4750	90	.4480	3.12	4.40	
71OB	580	.672	.075	63	.4720	36	.4550	4.14	4.40	
71OB	581	.699	.078	63	.4720	36	.4550	2.92	4.40	
71OB	582	.690	.072	63	.4720	36	.4550	1.74	4.40	
72OB	583	.706	.087	77	.4910	54	.4650	4.68	4.40	
72C	584	.730	.083	77	.4910	54	.4650	3.47	4.40	
72OB	585	.630	.077	77	.4910	54	.4650	2.25	4.38	
73C	586	.672	.091	45	.4840	45	.4540	4.27	4.35	
73OB	587	.652	.098	45	.4840	45	.4540	3.10	4.35	
73C	588	.688	.087	45	.4840	45	.4540	1.87	4.35	
77OB	594	.688	.101	52	.4710	55	.4370	2.42	4.21	
78OB	595	.682	.127	60	.4850	80	.4600	3.47	4.05	
81OB	598	.670	.128	29	.4730	45	.4330	2.97	4.15	
94C	619	.483	.040	45	.4830	45	.4540	4.14	4.35	0.1651
94C	620	.474	.035	45	.4830	45	.4540	2.97	4.35	0.1441
95C	621	.665	.061	58	.4790	62	.4630	4.04	4.34	0.1155
95C	622	.675	.065	58	.4790	62	.4630	2.83	4.34	0.1265
95C	623	.541	.041	58	.4790	62	.4630	1.69	4.34	0.1353
97C	627	.659	.063	37	.4950	35	.4570	4.07	4.35	0.1456
97C	628	.671	.060	37	.4950	35	.4570	2.86	4.35	0.1518
97C	629	.562	.063	37	.4950	35	.4570	1.72	4.35	0.1444
98C	630	.945	.083	41	.4920	75	.4640	3.95	4.40	0.1218
98C	631	.737	.061	41	.4920	75	.4640	2.78	4.40	0.1253
100C	634	1.121	.065	105	.4810	125	.4500	3.80	4.25	0.1302
100C	635	1.020	.069	105	.4810	125	.4500	1.84	4.25	0.1350
102C	639	1.041	.069	140	.4850	90	.4690	5.15	4.25	0.1479
102C	640	1.075	.058	140	.4850	90	.4690	3.40	4.25	0.1361
102C	641	1.075	.060	140	.4850	90	.4690	1.60	4.25	0.1341
104C	644	.943	.048	55	.4920	40	.4590	5.27	4.25	0.1356
104C	645	.993	.062	55	.4920	40	.4590	3.42	4.25	0.1352
104C	646	.846	.054	55	.4920	40	.4590	1.69	4.25	0.1370
105C	647	.122	.012	51	.4800	82	.4600	4.41	4.37	0.1682
105C	648	.177	.027	51	.4800	82	.4600	2.86	4.37	0.1510
107C	651	.259	.020	165	.4990	95	.4700	3.17	4.35	0.1608
107C	642	.132	.033	165	.4990	95	.4700	2.14	4.35	0.1693
108C	653	.285	.038	90	.4970	65	.4670	2.48	4.35	0.1426
108C	654	.183	.026	90	.4970	65	.4670	1.48	4.35	0.1475
109C	655	.289	.035	44	.4870	48	.4550	4.78	4.35	0.1664
109C	656	.198	.032	44	.4870	48	.4550	3.79	4.35	0.1642
109C	657	.196	.013	44	.4870	48	.4550	2.76	4.35	0.1640
112C	661	.621	.061	115	.4270	48	.4550	2.93	4.40	0.1588
112X	662	.645	.064	115	.4270	48	.4550	4.10	4.40	0.1502
126C	675	1.050	.077	85	.4880	32	.4670	3.63	4.35	0.1114
128C	677	1.093	.054	53	.4880	30	.4700	3.70	4.34	0.1368
132C	681	.431	.037	64	.4810	150	.4530	4.27	4.50	0.1429
4CA	301	.529	.044	-0	*	-0	*	.99	-0.	
4CA	302	.535	.038	-0	*	-0	*	2.68	-0.	
4CA	303	.515	.029	-0	*	-0	*	4.39	-0.	
11CA	304	.514	.053	-0	*	-0	*	1.73	-0.	

Table IV-1 (Concluded)

11CA	305	.461	.044	-0	*	-0	*	3.23	-0.		
14DB	306	.294	.051	-0	*	-0	*	2.10	-0.		
53DB	307	.773	.091	-0	*	-0	*	4.16	-0.		
100DB	308	.799	.099	-0	*	-0	*	1.47	-0.		
100DB	309	.750	.096	-0	*	-0	*	2.93	-0.		
100DB	310	.732	.096	-0	*	-0	*	4.39	-0.		
102DB	311	.628	.097	-0	*	-0	*	1.03	-0.		
102DB	312	.733	.094	-0	*	-0	*	2.71	-0.		
102DB	313	.706	.097	-0	*	-0	*	4.45	-0.		
105DB	314	.637	.088	-0	*	-0	*	2.61	-0.		
109DB	315	.660	.088	-0	*	-0	*	1.83	-0.		
109DB	316	.712	.089	-0	*	-0	*	3.35	-0.		
4	317	.529	.044	-0	*	-0	*	.99	-0.		
4	318	.535	.038	-0	*	-0	*	2.68	-0.		
4	319	.515	.029	-0	*	-0	*	4.39	-0.		
11	320	.514	.053	-0	*	-0	*	1.73	-0.		
11	321	.461	.044	-0	*	-0	*	3.23	-0.		
14	322	.294	.051	-0	*	-0	*	2.10	-0.		
53	323	.773	.091	-0	*	-0	*	4.16	-0.		
100	324	.799	.099	-0	*	-0	*	1.47	-0.		
100	325	.750	.096	-0	*	-0	*	2.93	-0.		
100	326	.732	.096	-0	*	-0	*	4.39	-0.		
102	327	.628	.097	-0	*	-0	*	1.03	-0.		
102	328	.733	.094	-0	*	-0	*	2.71	-0.		
102	329	.706	.097	-0	*	-0	*	4.45	-0.		
105	330	.637	.088	-0	*	-0	*	2.61	-0.		
109	331	.660	.088	-0	*	-0	*	1.83	-0.		
109	332	.712	.089	-0	*	-0	*	3.35	-0.		
2CB	801	.498	.052	-0	*	-0	*	2.63	-0.		
13CB	802	.250	.035	-0	*	-0	*	3.68	-0.		
55CB	803	.907	.068	-0	*	-0	*	2.94	-0.		
90DB	804	1.292	.117	-0	*	-0	*	1.58	-0.		
90DB	805	1.327	.124	-0	*	-0	*	3.33	-0.		
90DB	806	1.412	.120	-0	*	-0	*	5.15	-0.		
91DB	807	1.171	.115	-0	*	-0	*	1.38	-0.		
91DB	808	1.487	.113	-0	*	-0	*	3.31	-0.		
91DB	809	1.498	.127	-0	*	-0	*	5.04	-0.		
93DB	810	1.257	.118	-0	*	-0	*	1.68	-0.		
93DB	811	1.783	.117	-0	*	-0	*	3.22	-0.		
93DB	812	1.878	.122	-0	*	-0	*	5.10	-0.		
110CB	813	.293	.040	-0	*	-0	*	2.35	-0.		
110CB	814	.242	.043	-0	*	-0	*	3.31	-0.		
110CB	815	.207	.034	-0	*	-0	*	4.32	-0.		
117DB	816	1.365	.127	-0	*	-0	*	3.78	-0.		
124CB	817	1.104	.082	-0	*	-0	*	3.76	-0.		
2	818	.496	.052	-0	*	-0	*	2.63	-0.		
13	819	.250	.035	-0	*	-0	*	3.68	-0.		
55	820	.907	.068	-0	*	-0	*	2.94	-0.		
90	821	1.292	.117	-0	*	-0	*	1.58	-0.		
90	822	1.327	.124	-0	*	-0	*	3.33	-0.		
90	823	1.412	.120	-0	*	-0	*	5.15	-0.		
91	824	1.171	.115	-0	*	-0	*	1.38	-0.		
91	825	1.487	.113	-0	*	-0	*	3.31	-0.		
91	826	1.498	.127	-0	*	-0	*	5.04	-0.		
93	827	1.257	.118	-0	*	-0	*	1.68	-0.		
93	828	1.783	.117	-0	*	-0	*	3.22	-0.		
93	829	1.878	.122	-0	*	-0	*	5.10	-0.		
110	830	.293	.040	-0	*	-0	*	2.35	-0.		
110	831	.242	.043	-0	*	-0	*	3.31	-0.		
110	832	.207	.034	-0	*	-0	*	4.32	-0.		
177	833	1.365	.127	-0	*	-0	*	3.78	-0.		
124	834	1.104	.082	-0	*	-0	*	3.76	-0.		

Table IV-2 lists nondestructive test observations as ordered according to the actual flaw length. Table IV-3 lists nondestructive test observations by the penetrant method as ordered according to actual open flaw length. Sequence 10 denotes the inspection cycle which we performed in the "as produced" condition, and after etching. Sequence 15 denotes the inspection cycle which was performed after scarfing one crown off the panels. Sequences 2 and 3 are inspections performed after etching the scarfed panels and after proof loading the panels. Sequences 2 and 3 inspections were performed with the panels in the same condition as noted for ultrasonic, eddy current and x-ray inspections performed in the same cycle. A "0" indicates that there were no misses by and of the three NDT observers. Conversely, a "3" indicates that the flaw was missed by all of the observers. A "-0" indicates that no NDT observations were made for the sequence.

2. Data Ordering

Actual flaw data (Table IV-1) were used as a basis for all subsequent calculation, ordering, and analysis. Flaws were initially ordered by decreasing actual flaw length, depth, and area. These data were then stored for use in statistical analysis sequences.

3. Data Analysis and Presentation

The same statistical analysis, plotting methods, and calculation of one-sided confidence limits described for the integrally stiffened panel data were used in analysis of the LOP detection reliability data.

4. Ultrasonic Data Analysis

Initial analysis of the ultrasonic testing data revealed a discrepancy in the ultrasonic data. Failure to maintain the detection level between sequences and to detect large flaws was attributed to a combination of panel warpage and human factors in the inspections. To verify this discrepancy and to provide a measure of the true values, 16 additional LOP panels containing 33 flaws were selected and subjected to the same Sequence 1 and Sequence 3 inspection cycles as the completed panels. An additional optimization cycle performed resulted in changes in the NDT procedures for the LOP panels. These changes are shown as Amendments A and B to the Appendix E procedure. The inspection sequence was repeated twice (double inspection in two runs),

Table IV-2 NDT Observations, LOP Panels

		ULTRASONIC			EDDY CURRENT			X-RAY		
INSPECTION SEQUENCE		1	2	3	1	2	3	1	2	3
CRACK NUMBER	ACTUAL VALUE									
223	1.271	3	0	0	0	3	3	1	0	0
224	1.245	0	0	0	1	3	3	1	0	0
225	1.226	3	3	0	3	1	2	0	0	0
226	1.218	3	3	0	1	1	2	0	0	0
220	1.210	3	3	0	0	3	2	2	0	0
71	1.184	2	0	0	3	3	3	0	0	0
221	1.184	3	3	0	0	1	0	0	0	0
55	1.175	3	3	0	1	0	0	0	0	0
50	1.158	3	3	0	1	3	3	0	0	0
129	1.158	3	0	0	3	3	0	0	0	3
61	1.156	3	0	0	3	3	0	0	0	0
70	1.150	2	3	0	3	3	0	0	0	0
69	1.125	1	3	0	3	3	3	0	0	1
127	1.124	3	3	0	0	2	0	0	0	0
62	1.122	3	3	0	3	3	1	0	0	0
634	1.121	0	0	0	3	3	3	0	0	0
130	1.105	1	0	0	1	3	0	0	0	3
49	1.100	3	3	0	2	3	3	0	0	0
677	1.093	1	0	0	3	3	3	0	0	0
56	1.079	3	3	0	0	0	0	0	0	0
125	1.075	3	1	0	0	3	3	2	0	0
640	1.075	3	1	0	1	2	2	3	2	0
641	1.075	2	1	1	1	1	3	1	1	0
51	1.075	3	3	3	2	2	3	0	0	0
57	1.052	3	2	0	3	2	0	0	0	0
675	1.050	2	3	0	2	1	2	2	2	0
639	1.041	3	3	0	3	3	1	3	3	1
635	1.020	3	2	0	3	2	3	2	2	0
156	1.014	3	0	0	3	3	3	0	0	0
77	1.010	0	0	0	1	0	0	0	0	0
645	.993	2	1	0	3	3	3	3	3	0
78	.987	0	0	0	0	0	1	0	0	0
157	.986	3	1	0	2	3	3	1	0	0
536	.964	3	3	0	0	3	0	3	2	0
160	.961	3	0	0	3	3	3	0	0	0
630	.945	3	3	0	2	2	2	2	1	0
644	.943	2	0	0	3	3	3	3	2	0
161	.943	3	0	0	2	3	2	0	0	0
85	.935	0	0	0	0	0	0	0	0	3
104	.929	3	2	0	3	3	3	0	0	0
167	.921	3	3	0	3	3	0	0	0	0
79	.919	0	0	0	1	0	1	0	0	0
80	.916	1	0	0	0	3	1	0	0	0
550	.900	3	3	0	1	3	0	3	3	1
81	.890	0	0	0	0	0	1	0	0	0
560	.889	1	1	0	3	3	1	1	0	0
103	.885	3	3	0	3	3	3	0	0	0

Table IV-2 (Continued)

CK NO	ACI VAL									
		1	2	3	1	2	3	1	2	3
166	.874	3	0	0	1	3	0	0	0	0
559	.872	3	3	0	3	3	3	2	2	0
563	.870	1	0	0	2	3	3	1	1	0
175	.858	3	3	0	3	3	0	0	0	3
82	.850	1	0	0	2	0	0	0	0	0
646	.846	3	0	0	2	2	2	3	3	0
174	.825	3	3	0	3	3	0	0	0	3
83	.825	0	0	0	1	3	0	0	0	3
173	.812	3	3	0	3	0	0	0	0	3
169	.809	3	2	0	3	2	3	0	0	0
84	.790	0	0	0	0	3	0	0	0	3
122	.788	3	3	0	1	3	3	0	0	0
168	.781	2	3	0	2	0	1	0	0	0
124	.749	3	0	0	2	3	0	0	0	0
123	.742	3	3	0	2	3	0	0	0	0
631	.737	3	3	0	3	2	1	3	1	0
121	.734	3	0	0	1	0	3	0	0	0
584	.730	3	2	0	2	3	0	0	1	0
215	.724	3	3	0	2	3	3	1	1	0
197	.717	1	3	0	1	3	3	0	0	0
520	.708	3	2	0	1	3	0	0	2	0
583	.706	3	1	0	0	3	0	0	1	2
581	.699	3	3	0	3	2	0	0	0	0
119	.698	3	3	0	1	3	3	0	0	0
582	.690	3	0	0	2	2	0	0	1	0
517	.688	1	3	0	1	3	3	3	0	0
588	.688	1	0	0	3	3	3	1	1	0
594	.688	3	3	0	3	3	0	1	2	0
528	.686	3	3	0	0	3	0	3	2	0
595	.682	3	1	0	0	3	3	1	1	0
216	.676	3	3	0	2	3	3	1	0	0
622	.675	0	0	0	3	3	1	2	1	0
580	.672	3	3	0	2	2	0	1	1	0
586	.672	3	1	0	1	3	3	1	2	0
628	.671	3	1	0	3	1	3	3	1	0
598	.670	3	3	0	2	3	3	1	1	0
621	.665	0	0	0	2	3	3	0	1	0
627	.659	3	1	0	3	2	2	1	1	0
587	.652	2	0	0	2	2	3	0	0	0
214	.649	3	3	0	3	3	0	0	0	0
662	.645	3	3	3	3	3	3	3	3	3
198	.638	0	1	0	2	3	3	0	0	0
578	.632	0	0	0	2	1	3	0	0	0
585	.630	3	0	0	2	0	0	0	1	0
661	.621	3	3	3	3	3	3	3	3	3
579	.611	0	0	0	1	3	3	0	1	0
576	.601	1	0	0	1	0	0	0	0	0
20	.569	3	3	0	3	3	3	0	0	0
571	.568	3	3	0	2	3	0	1	1	0

Table IV-2 (Continued)

CK NO	ACT VAL									
		1	2	3	1	2	3	1	2	3
577	.568	0	0	0	1	0	0	1	0	0
524	.562	2	3	0	2	0	1	0	0	0
629	.562	3	1	0	3	2	3	3	1	0
17	.542	3	3	0	2	3	1	0	0	0
623	.541	0	0	0	3	0	3	3	2	0
570	.531	3	3	0	1	3	0	0	1	0
574	.518	2	3	0	3	2	2	0	1	0
1	.517	3	3	0	3	3	3	0	0	0
501	.516	3	3	0	3	0	3	3	2	0
519	.511	3	3	0	1	0	2	3	0	0
575	.506	0	0	0	1	0	0	0	0	0
2	.504	3	3	0	3	3	3	0	0	0
19	.498	3	3	0	2	3	3	0	0	0
522	.494	2	3	0	0	3	0	1	2	0
572	.488	0	0	0	0	2	3	0	1	0
525	.483	2	2	0	0	3	3	0	0	0
619	.483	3	3	1	3	3	0	3	3	2
568	.482	3	3	0	1	3	0	0	1	0
620	.474	3	0	0	1	1	0	3	3	0
573	.454	1	0	0	3	2	3	1	1	0
566	.440	0	0	0	2	3	2	0	0	1
564	.435	3	2	0	2	3	3	0	0	0
681	.431	3	3	0	2	1	3	3	2	0
569	.430	0	3	3	2	0	2	0	0	0
523	.419	0	0	0	0	3	0	0	0	0
511	.393	3	2	0	3	3	3	3	3	0
565	.391	1	0	0	2	2	3	0	0	0
142	.372	3	3	0	0	3	3	0	0	0
509	.369	3	3	0	3	3	2	3	3	0
521	.362	3	3	0	0	3	0	1	2	0
35	.346	0	0	0	3	3	3	0	0	0
39	.345	0	0	0	1	0	0	0	0	0
150	.343	3	3	3	2	3	3	0	0	0
38	.341	1	0	0	2	0	3	0	0	0
516	.338	0	0	0	2	3	3	0	1	0
44	.337	0	0	0	1	3	3	0	0	0
46	.336	3	2	0	2	3	2	0	0	0
148	.322	3	3	0	1	3	3	0	0	0
143	.320	3	3	0	0	3	3	1	0	0
36	.318	0	0	0	2	2	1	0	0	0
45	.309	0	1	0	2	3	1	0	0	0
146	.297	3	3	2	1	3	1	0	0	0
655	.289	3	3	0	2	3	3	3	0	0
147	.288	3	3	0	2	3	3	0	0	0
196	.288	3	3	3	2	3	2	0	0	0
653	.285	3	0	0	3	3	3	3	3	1
195	.280	0	3	0	3	3	1	0	0	0
194	.277	3	3	0	3	3	0	0	0	0
30	.268	3	1	0	1	2	0	0	0	0

Table IV-2 (Concluded)

CK NO	ACT VAL									
		1	2	3	1	2	3	1	2	3
186	.268	3	3	0	1	3	3	0	0	0
149	.267	3	3	0	3	3	3	0	0	0
37	.263	1	0	0	2	1	1	0	0	0
151	.262	3	3	0	1	3	3	0	0	0
510	.261	0	0	0	3	3	3	2	3	3
651	.259	3	3	0	2	1	3	3	2	0
40	.258	0	0	0	1	3	0	0	0	0
152	.250	3	3	0	3	3	3	0	0	0
153	.243	3	3	0	1	3	2	0	0	0
29	.231	3	3	0	2	3	0	0	0	0
542	.214	2	3	0	2	0	3	3	2	0
656	.198	3	3	0	3	2	3	0	1	0
657	.196	3	3	0	3	1	3	3	2	1
24	.194	3	3	0	2	0	3	0	0	0
654	.183	3	3	0	2	3	3	3	3	0
648	.177	3	0	0	1	3	0	2	2	0
544	.173	3	3	0	0	3	0	2	0	1
529	.145	2	3	0	2	3	3	3	2	2
28	.133	3	3	0	2	3	3	3	1	0
642	.132	-0	-0	-0	-0	-0	-0	-0	-0	-0
647	.122	1	3	2	3	3	2	2	2	3
543	.116	2	3	0	3	3	1	3	1	1
530	.112	0	0	0	2	3	0	1	2	0
548	.094	1	3	3	1	3	3	2	3	2
545	.033	3	3	1	2	2	3	3	1	3

Table IV-3 NDT Observations by the Penetrant Method, LOP Panels.

INSPECTION SEQUENCE		PENETRANT			
		10	15	2	3
CRACK NUMBER	ACTUAL VALUE				
223	1.271	1	3	3	0
224	1.245	1	3	3	0
225	1.226	1	3	2	0
226	1.218	1	2	3	0
220	1.210	0	3	3	0
221	1.184	1	3	3	0
55	1.175	3	3	3	0
50	1.158	3	3	3	3
129	1.158	2	3	3	-0
127	1.124	2	3	3	0
130	1.105	0	3	3	-0
49	1.100	3	3	3	3
56	1.079	3	3	3	0
125	1.075	1	3	2/	0
51	1.075	3	3	3	2
57	1.052	3	3	3	0
77	1.010	3	1	0	3
78	.987	0	1	0	1
85	.935	0	3	3	3
79	.919	0	2	0	1
80	.916	3	3	2	0
81	.890	0	0	0	0
82	.850	0	0	0	0
83	.825	0	3	3	-0
173	.812	3	3	2	-0
84	.790	0	3	3	3
122	.788	0	3	3	0
124	.749	1	3	2	0
123	.742	3	3	2	0
121	.734	0	3	3	1
584	.730	0	0	0	0
215	.724	2	3	3	2
520	.708	2	3	3	0
583	.706	0	3	2	0
581	.699	0	3	3	0
119	.698	2	3	3	0
582	.690	0	2	3	0
517	.688	0	3	3	0
588	.688	0	3	3	0
594	.688	0	3	3	0
595	.682	0	3	3	0

Table IV-3 (Concluded)

CK NO	ACT VAL	10	15	2	3
216	.676	0	3	3	1
586	.672	0	3	3	0
580	.672	0	3	3	2
598	.670	2	3	3	0
587	.652	0	3	3	0
214	.649	0	3	3	0
578	.632	0	3	3	0
585	.630	0	3	3	0
579	.611	0	3	2	0
576	.601	0	0	0	0
571	.568	0	2	1	0
577	.568	0	0	0	0
524	.562	3	2	1	0
570	.531	0	2	2	2
574	.518	0	3	3	0
519	.511	1	3	3	0
575	.506	0	0	0	0
522	.494	3	3	2	1
572	.488	0	3	3	1
525	.483	3	3	3	1
568	.482	3	3	3	0
573	.454	2	3	3	0
566	.440	0	3	3	0
564	.435	2	3	3	0
569	.430	1	3	3	0
523	.419	2	3	3	0
565	.391	0	2	3	0
521	.362	1	3	1	0
39	.345	3	0	0	0
38	.341	0	0	0	0
516	.338	0	3	3	0
196	.288	3	3	3	3
195	.280	3	3	3	2
194	.277	3	3	3	0
30	.268	3	3	3	2
37	.263	3	0	1	0
40	.258	3	3	3	0
29	.231	2	3	2	0
24	.194	3	3	1	1
28	.133	1	3	1	0

with three different operators making their own C-scan recordings, interpreting the results, and documenting the inspections. The operator responsible for the original optimization and recording sequences was eliminated from this repeat evaluation. Additional care was taken to align warped panels to provide the best possible evaluation.

The results of this repeat cycle showed a definite improvement in the reliability of the ultrasonic method in detecting LOP flaws. The two data files were merged on the following basis:

- Data from the repeat evaluation were ordered by actual flaw dimension;
- An analysis was performed by counting down from the largest flaw to the first "miss" by the ultrasonic method;
- The original data were truncated to eliminate all flaws larger than that of the first "miss" in the repeat data;
- The remaining data were merged and analyzed according to the original plan. The merged actual data file used for processing Sequences 1 and 3 ultrasonic data is shown in Table IV-1. Table IV-4 lists nondestructive test observations by the ultrasonic method for the merged data as ordered by actual crack length;
- The combined data base was analyzed and plotted in the same manner as that described for the integrally stiffened panels.

F. DATA RESULTS

The results of inspection and data analysis are shown graphically in Figures IV-7, IV-8, IV-9, and IV-10. Figure IV-7 plots NDT observations by the penetrant method for flaws open to the surface. Figure IV-8 plots NDT observations by the ultrasonic inspection method and includes the merged data from the original and repeat evaluations for Sequences 1 and 3. Sequence 2 is for original data only. Figures IV-9 and IV-10 are plots of NDT observations by the eddy current and x-ray methods for the original data only.

The results of these analyses show the influences of both flaw geometry and tightness and of the weld bead geometry variations as inspection variables. The benefits of etching and proof loading for improving NDT reliability are not as great as those observed for flat specimens. This is due to the

greater inspection process variability imposed by the panel geometries.

Eddy current data for the thin (1/8-in.) panels are believed to accurately reflect the expected detection reliabilities. The data are shown at the lower end of the plots in Figure IV-9. Eddy current data for the thick (1/2-in.) panels are not accurately represented by this plot due to the limited depth of penetration, approximately 0.084 inch at 200 kilohertz. No screening of the data at the upper end was performed due to uncertainties in describing the flaw length interrogated at the actual penetration depth.

Table IV-4 NDT Observations by the Ultrasonic Method, Merged Data, LOP Panels

		ULTRASONIC		
INSPECTION SEQUENCE		1	2	3
CRACK NUMBER	ACTUAL VALUE			
812	1.878	0	-0	0
829	1.878	0	-0	0
828	1.783	0	-0	0
811	1.783	0	-0	0
809	1.498	0	-0	0
826	1.498	0	-0	0
825	1.487	0	-0	0
808	1.487	0	-0	0
806	1.412	0	-0	0
823	1.412	0	-0	0
816	1.365	0	-0	0
833	1.365	0	-0	0
805	1.327	0	-0	0
822	1.327	0	-0	0
821	1.292	0	-0	0
804	1.292	0	-0	0
223	1.271	3	0	0
827	1.257	0	-0	0
810	1.257	0	-0	0
224	1.245	0	0	0
225	1.226	3	3	0
226	1.218	3	3	0
220	1.210	3	3	0
71	1.184	2	0	0
221	1.184	3	3	0
55	1.175	3	3	0
807	1.171	0	-0	0
824	1.171	0	-0	0
50	1.158	3	3	0
129	1.158	3	0	-0
61	1.156	3	0	0
70	1.150	2	3	0
69	1.125	1	3	0
127	1.124	3	3	0
62	1.122	3	3	0
634	1.121	0	0	0
130	1.105	1	0	-0
817	1.104	0	-0	0
834	1.104	0	-0	0
49	1.100	3	3	0
677	1.093	1	0	0
56	1.079	3	3	0
641	1.075	2	1	1
51	1.075	3	3	3

Table IV-4 (Continued)

CK NO	ACT VAL	1	2	3
125	1.075	3	1	0
640	1.075	3	1	0
57	1.052	3	2	0
675	1.050	2	3	0
639	1.041	3	3	0
635	1.020	3	2	0
156	1.014	3	0	0
77	1.010	0	0	0
645	.993	2	1	0
78	.987	0	0	0
157	.986	3	1	0
536	.964	3	3	0
160	.961	3	0	0
630	.945	3	3	0
644	.943	2	0	0
161	.943	3	0	0
85	.935	0	0	-0
104	.929	3	2	0
167	.921	3	3	0
79	.919	0	0	0
80	.916	1	0	0
820	.907	0	-0	0
803	.907	0	-0	0
550	.900	3	3	0
81	.890	0	0	0
560	.889	1	1	0
103	.885	3	3	0
166	.874	3	0	0
559	.872	3	3	0
563	.870	1	0	0
175	.858	3	3	-0
82	.850	1	0	0
646	.846	3	0	0
174	.825	3	3	-0
83	.825	0	0	-0
173	.812	3	3	-0
169	.809	3	2	0
308	.799	0	-0	0
324	.799	0	-0	0
84	.790	0	0	-0
122	.788	3	3	0
168	.781	2	3	0
323	.773	0	-0	0
307	.773	0	-0	0

Table IV-4 (Continued)

CK NO	ACT VAL	1	2	3
309	.750	0	-0	0
325	.750	0	-0	0
124	.749	3	0	0
123	.742	3	3	0
631	.737	3	3	0
121	.734	3	0	0
312	.733	0	-0	0
328	.733	0	-0	0
326	.732	0	-0	0
310	.732	0	-0	0
584	.730	3	2	0
215	.724	3	3	0
197	.717	1	3	0
316	.712	0	-0	0
332	.712	0	-0	0
520	.708	3	2	0
313	.706	0	-0	0
329	.706	0	-0	0
583	.706	3	1	0
581	.699	3	3	0
119	.698	3	3	0
582	.690	3	0	0
594	.688	3	3	0
517	.688	1	3	0
588	.688	1	0	0
528	.686	3	3	0
595	.682	3	1	0
216	.676	3	3	0
622	.675	0	0	0
580	.672	3	3	0
586	.672	3	1	0
628	.671	3	1	0
598	.670	3	3	0
621	.665	0	0	0
331	.660	0	-0	0
315	.660	0	-0	0
627	.659	3	1	0
587	.652	2	0	0
214	.649	3	3	0
662	.645	3	3	3
198	.638	0	1	0
314	.637	0	-0	0
330	.637	0	-0	0
578	.632	0	0	0
585	.630	3	0	0
327	.628	0	-0	0
311	.628	0	-0	0
661	.621	3	3	3
579	.611	0	0	0
576	.601	1	0	0
20	.569	3	3	0

Table IV-4 (Continued)

CK NO	ACT VAL	1	2	3
571	.568	3	3	0
577	.568	0	0	0
524	.562	2	3	0
629	.562	3	1	0
17	.542	3	3	0
623	.541	0	0	0
302	.535	0	-0	0
318	.535	0	-0	0
570	.531	3	3	0
317	.529	0	-0	0
301	.529	0	-0	0
574	.518	2	3	0
1	.517	3	3	0
501	.516	3	3	0
303	.515	0	-0	0
319	.515	0	-0	0
304	.514	0	-0	0
320	.514	0	-0	0
519	.511	3	3	0
575	.506	0	0	0
2	.504	3	3	0
19	.498	3	3	0
801	.498	3	-0	0
818	.498	3	-0	0
522	.494	2	3	0
572	.488	0	0	0
525	.483	2	2	0
619	.483	3	3	1
568	.482	3	3	0
620	.474	3	0	0
305	.461	0	-0	0
321	.461	0	-0	0
573	.454	1	0	0
566	.440	0	0	0
564	.435	3	2	0
681	.431	3	3	0
569	.430	0	3	3
523	.419	0	0	0
511	.393	3	2	0
565	.391	1	0	0
142	.372	3	3	0
509	.369	3	3	0
521	.362	3	3	0
35	.346	0	0	0
39	.345	0	0	0
150	.343	3	3	3
38	.341	1	0	0
516	.338	0	0	0
44	.337	0	0	0
46	.336	3	2	0
148	.322	3	3	0
143	.320	3	3	0

Table IV-4 (Concluded)

CK NO	ACT VAL	1	2	3
36	.318	0	0	0
45	.309	0	1	0
146	.297	3	3	2
306	.294	0	-0	0
322	.294	0	-0	0
813	.293	0	-0	0
830	.293	0	-0	0
655	.289	3	3	0
147	.288	3	3	0
196	.288	3	3	3
653	.285	3	0	0
195	.280	0	3	0
194	.277	3	3	0
30	.268	3	1	0
186	.268	3	3	0
149	.267	3	3	0
37	.263	1	0	0
151	.262	3	3	0
510	.261	0	0	0
651	.259	3	3	0
40	.258	0	0	0
802	.250	0	-0	0
819	.250	0	-0	0
152	.250	3	3	0
153	.243	3	3	0
814	.242	0	-0	0
831	.242	0	-0	0
29	.231	3	3	0
542	.214	2	3	0
815	.207	0	-0	0
832	.207	0	-0	0
656	.198	3	3	0
657	.196	3	3	0
24	.194	3	3	0
654	.183	3	3	0
648	.177	3	0	0
544	.173	3	3	0
529	.145	2	3	0
28	.133	3	3	0
642	.132	-0	-0	-0
647	.122	1	3	2
543	.116	2	3	0
530	.112	0	0	0
548	.094	1	3	3
545	.033	3	3	1

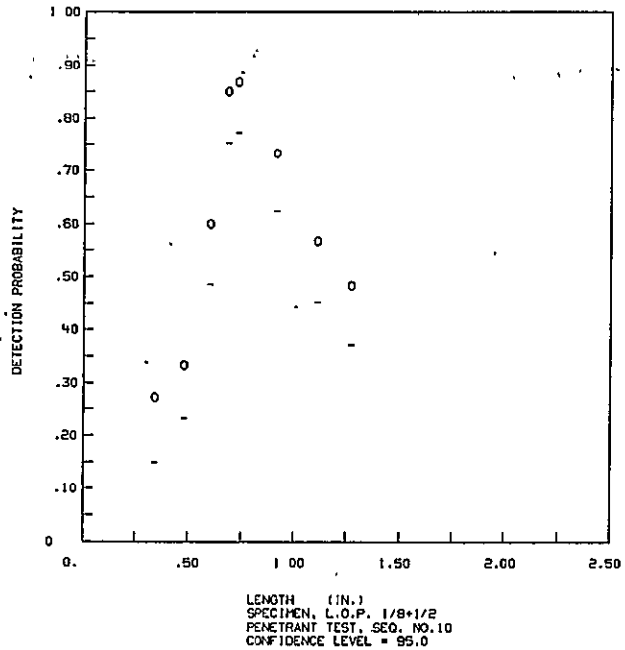

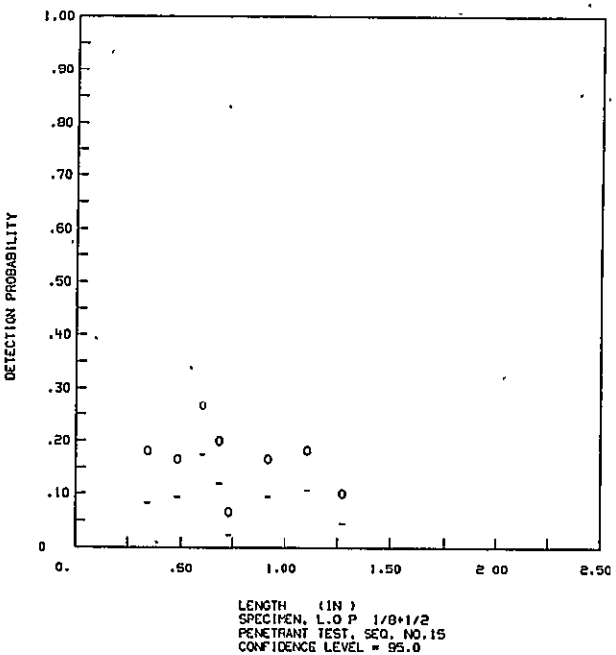

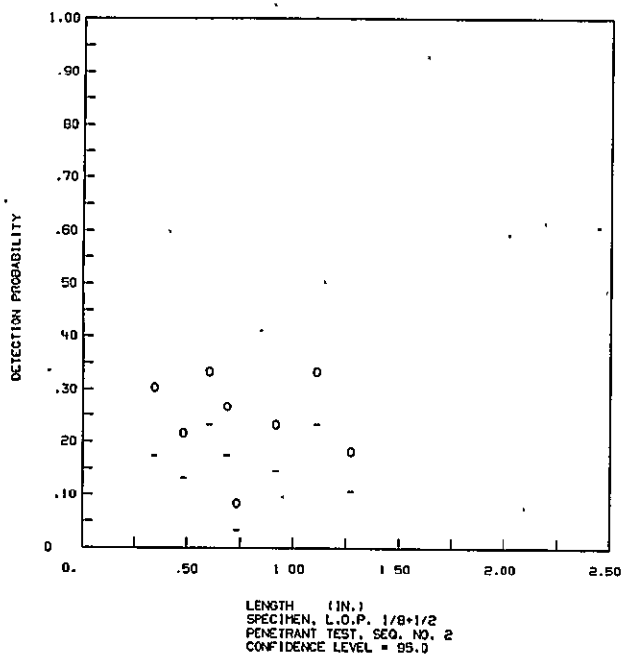

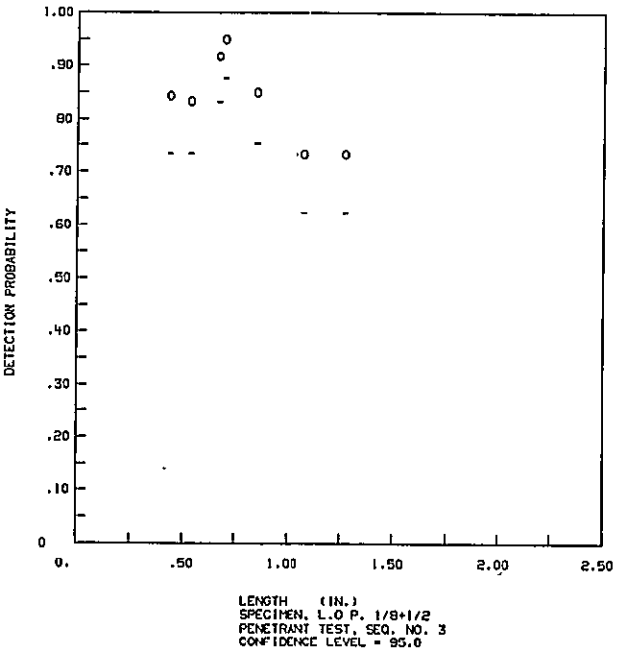

Figure IV-7 Flaw Detection Probability for LOP Panels by the Penetrant Method Plotted at 95% Probability and 95% Confidence

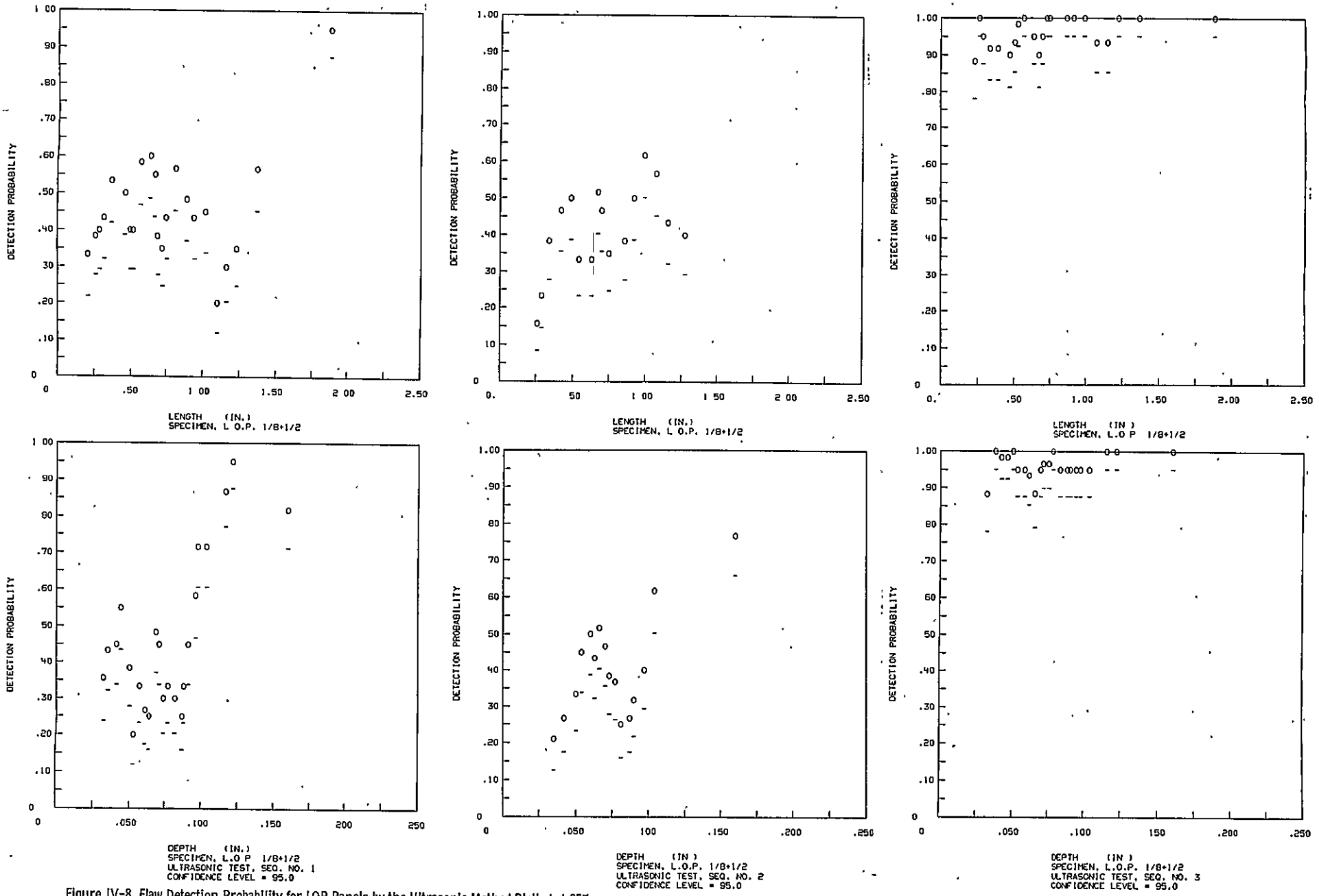

Figure IV-8 Flaw Detection Probability for LOP Panels by the Ultrasonic Method Plotted at 95% Probability and 95% Confidence

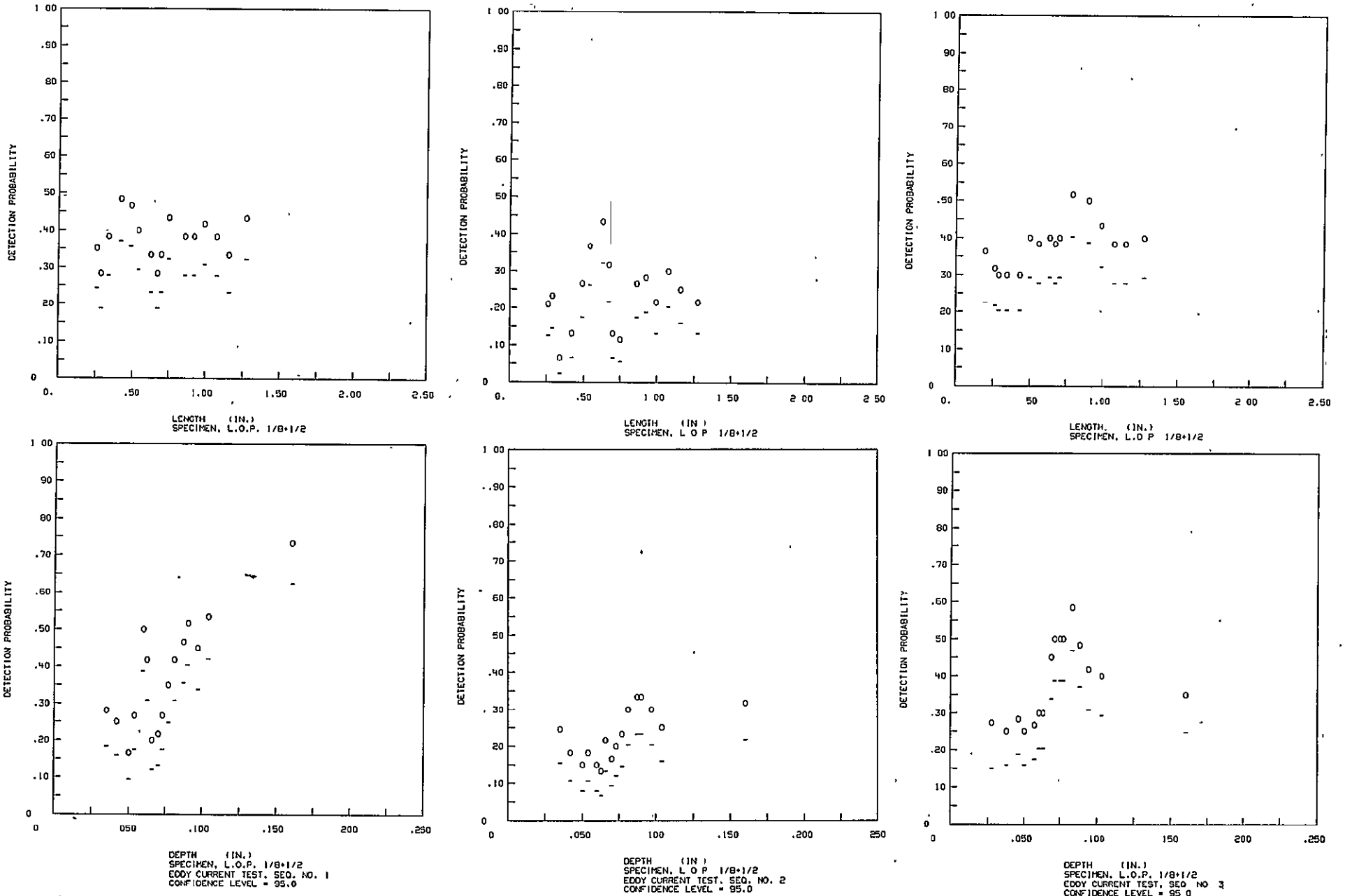

Figure IV-9 Flaw Detection Probability for LOP Panels by the Eddy Current Method Plotted at 95% Probability and 95% Confidence

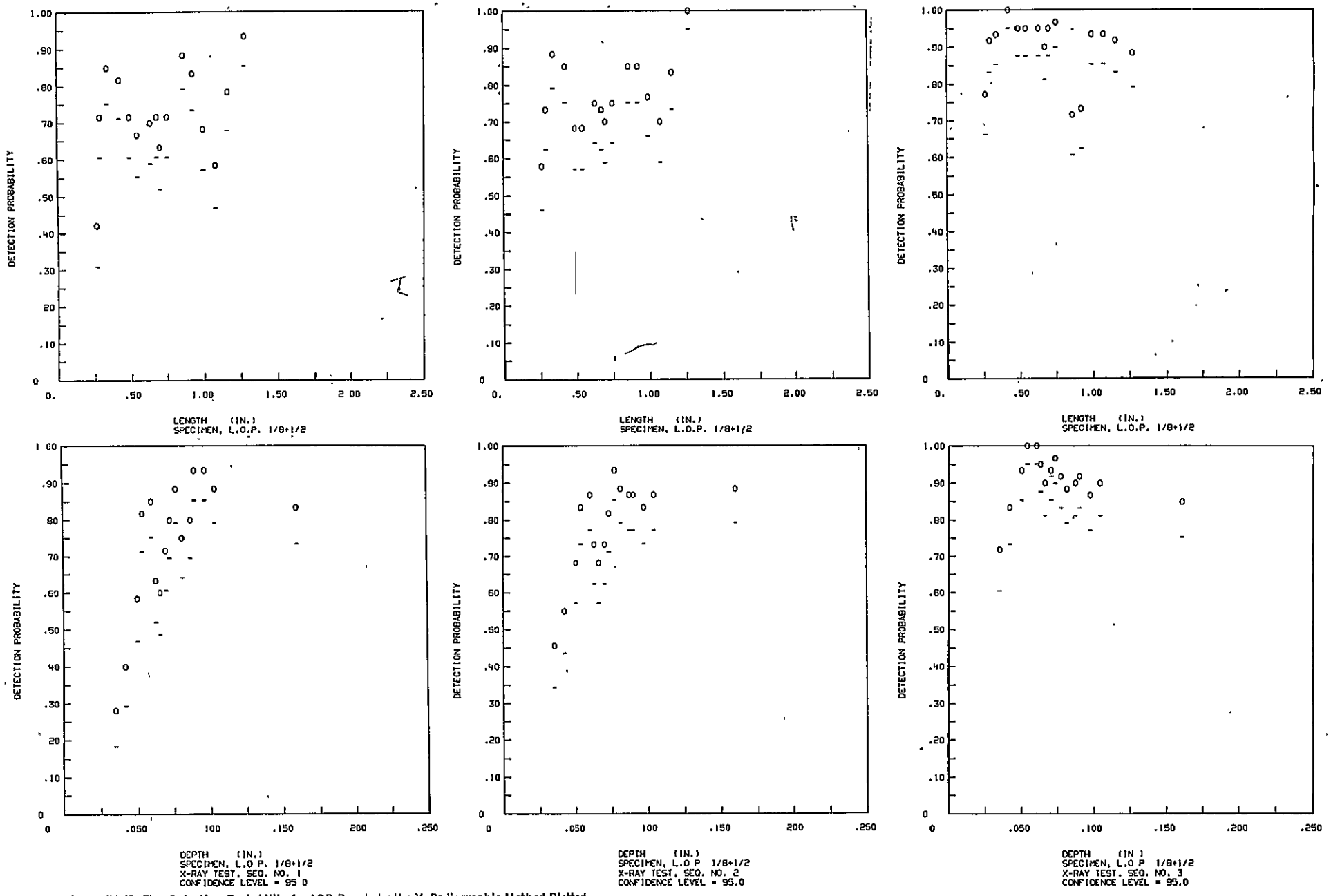

Figure IV-10 Flaw Detection Probability for LOP Panels by the X-Radiographic Method Plotted at 95% Probability and 95% Confidence

V FATIGUE-CRACKED WELD PANEL EVALUATION

Welding is a common method for joining parts in pressure vessels and other critical structural hardware. Weld cracking in structures during production, test, or service is a concern in design and service reliability analyses. Such cracking may be due to a variety of conditions and prevention of cracking is a primary responsibility and goal of the welding engineer. When such cracks occur, their detection early in the hardware life cycle is desirable and detection is the responsibility and goal of the nondestructive test engineer.

One difficulty in systematic study of weld crack detection has been in the controlled fabrication of samples. When known crack-producing parameters are vaired, the result is usually a gross cracking condition that does not represent the normal production variance. Controlled fatigue cracks may be grown in welds and may be used to simulate weld crack conditions for service-generated cracks. Fatigue cracks will approximate weld process-generated cracks without the high heat and compressive stress conditions that change the character of some weld flaws. Fatigue cracks in welds were selected for evaluation of NDT methods.

A program plan for preparation, evaluation, and analysis of fatigue cracked weld panels was established and is shown schematically in Figure V-1.

A. SPECIMEN PREPARATION

Weld panel blanks were produced in two different configurations in 0.317-centimeter (0.125-in.) and 1.27-centimeter (0.500 in.) nominal thicknesses. The panel material was 2219-T87 aluminum alloy with a fusion pass and a single 2319 aluminum alloy filler pass weld located in the center of each panel. Five panels of each thickness were chemically milled to produce a land area one inch from each side of the weld and to reduce the thickness of the milled area to one-half that in the land area. The specimen configuration is shown in Figure V-2.

Starter notches were introduced by electrodischarge machining (EDM) using shaped electrodes to control the final flaw shape. Cracks were then extended in fatigue and the surface crack length visually monitored and controlled to the required final flaw size and configuration requirements as shown schematically in Figure V-3. The flaws were oriented parallel to the weld bead

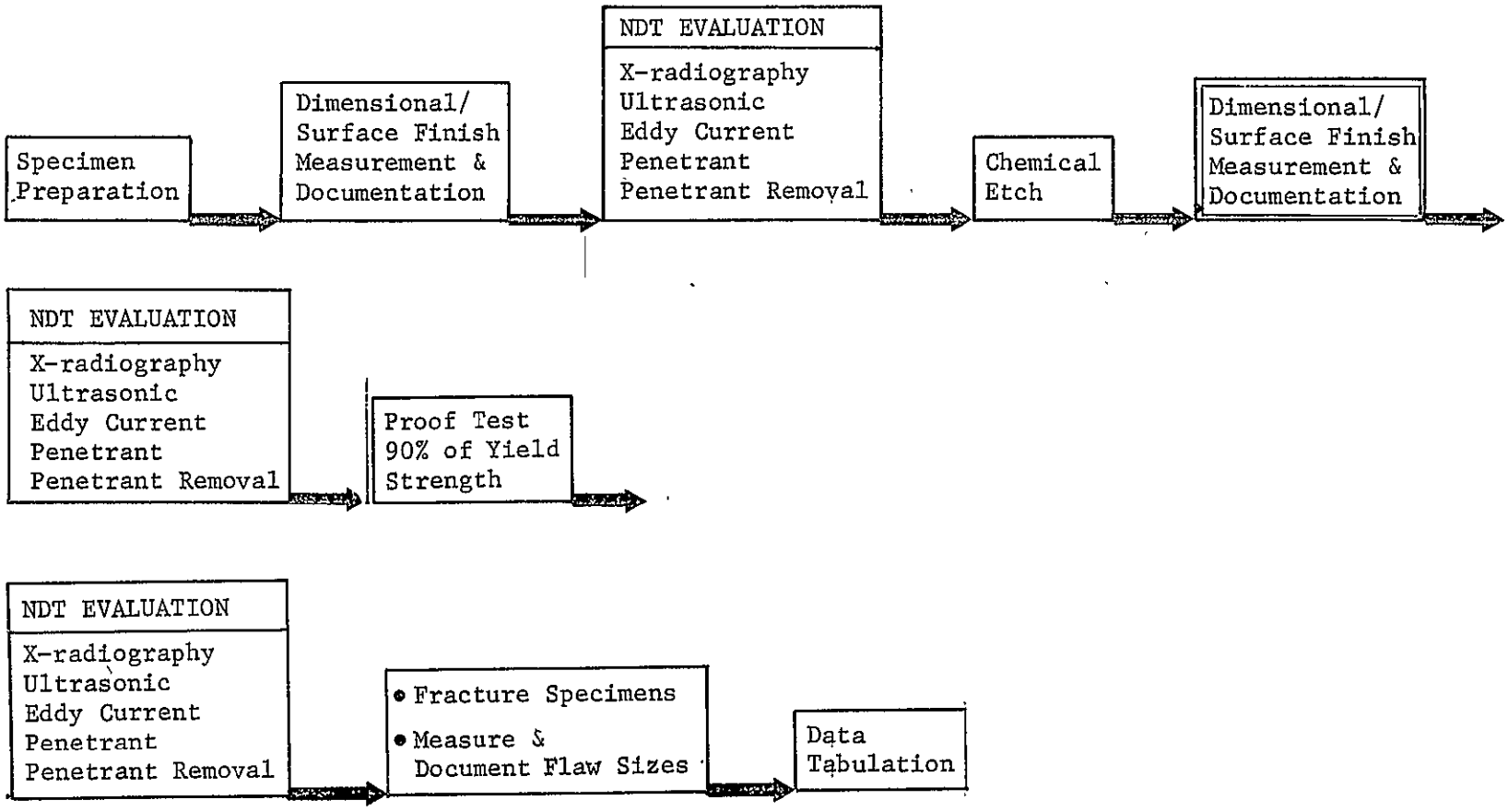

Figure V-1 NDT Evaluation Sequence for Fatigue-Cracked Welded Panels

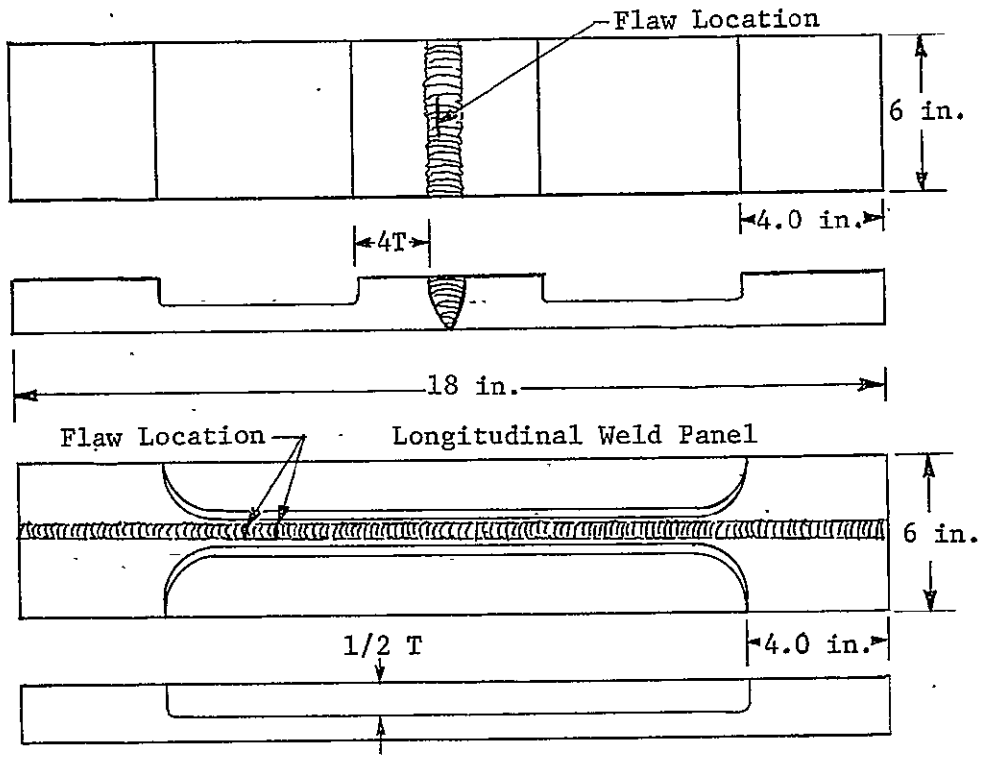

Figure V-2 Fatigue-Cracked Weld Panels

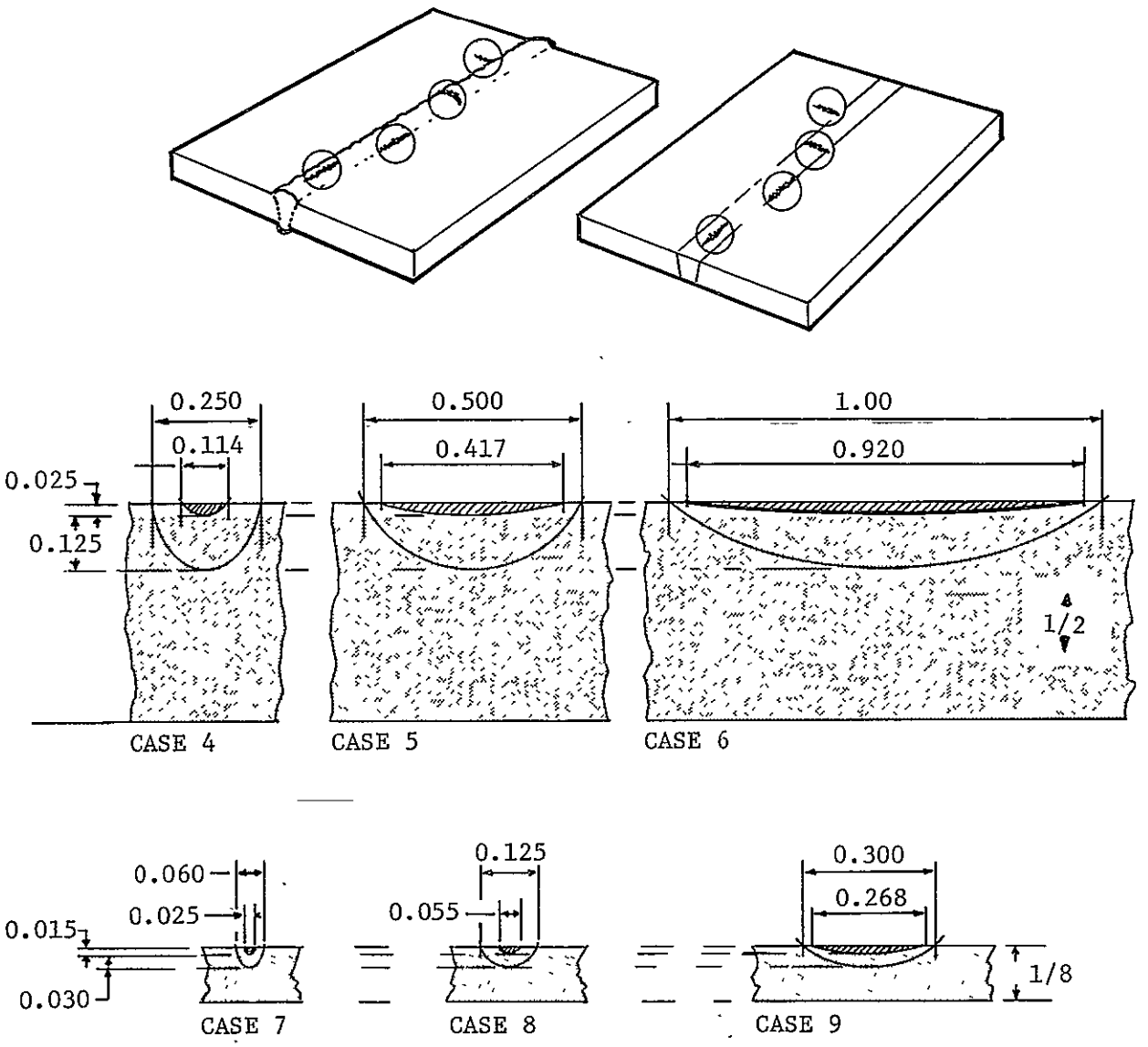

Note: All dimensions in inches.

Figure V-3
Schematic Side View of the Starter Flaw and Final Flaw Configuration for Fatigue-Cracked Weld Panels

in transverse weld panels and perpendicular to the weld bead in longitudinal weld panels. Flaws were randomly distributed in the weld bead centerline and in the heat-affected zone (HAZ) of both transverse and longitudinal weld panels.

Initial attempts to grow flaws without shaving (scarfing) the weld bead flush were unsuccessful. In the unscarfed welds, flaws would not grow in the cast weld bead material and several panels were failed in fatigue before it was decided to shave the welds. In the shaved weld panels, four of the six flaw configurations were produced in 3-point bend fatigue loading using a maximum bending stress of 1.4×10^8 N/m^2 (20 ksi). Two of the flaw configurations were produced by axially loading the panels to obtain the desired flaw growth. The flaw growth parameters and flaw distribution in the panels are shown in Table V-1.

Following growth of the flaws, panels were machined using a shell cutter to remove the starter flaws. The flush weld panel configurations were produced by uniformly machining the surface of the panel to the "as machined" flush configuration. This group of panels was designated as "fatigue-crack flawed, flush welds." Panels with the weld crown intact were produced by masking the flawed weld area and chemically milling the panel areas adjacent to the welds to remove approximately 0.076 centimeters (0.030 in.) of material. The maskant was then removed and the weld area hand-ground to produce a simulated weld bead configuration. This group of panels was designated the "fatigue-crack flawed welds with crowns." 117 fatigue cracked weld panels were produced containing 293 fatigue cracks. Panels were cleaned and submitted for inspection.

B. NDT OPTIMIZATION

Following preparation of the fatigue-crack flawed weld specimens, an NDT optimization and calibration program was initiated. Panels containing the smallest flaw size in each thickness group and configuration were selected for evaluation and comparison of NDT techniques.

1. X-radiography

X-radiographic exposure techniques established for the LOP panels were verified for sensitivity on the fatigue crack flawed weld panels. The techniques revealed some of the cracks and

Table V-1 Parameters for Fatigue-Crack Growth in Welded Panels

CASE #	STARTER DEPTH	DIM. WIDTH	FINAL FLAW WIDTH	TYPE OF LOADING	STRESS KSI	STRESS CYCLES (AVG.)		PANELS	FLAWS
4	.025	.114	.250	Axial	24	190,000	Transverse		
						45,000	Longitudinal		
5	.025	.417	.500	3-Point	24	100,000	Transverse	→ 60 1/2 inch Panels	157
						13,000	Longitudinal		
6	.025	.920	1.000	3-Point	22	100,000	Transverse		
						11,000	Longitudinal		
7	.015	.025	.060	Axial	24	169,000	Transverse		
						75,000	Longitudinal		
8	.015	.055	.125	3-Point	22	180,000	Transverse		
						13,000	Longitudinal	→ 57 1/8 inch Panels	136
9	.015	.268	.300	3-Point	25.6	60,000	Transverse		
						7,000	Longitudinal		

failed to reveal others. Failure of the techniques were attributed to the flaw tightness and further evaluation was not pursued. The same procedures used for evaluation of the LOP panels were selected for all weld panel evaluation. Details of this procedure are included in Appendix D.

2. Penetrant Evaluation

The penetrant inspection procedure used for evaluation of integrally stiffened panels and LOP panels was applied to the Fatigue-cracked weld panels. This procedure is shown in Appendix A.

3. Ultrasonic Evaluation

Single- and double-transducer evaluation techniques at 5, 10, and 15 megahertz were evaluated as a function of incident angle, flaw signal response, and the signal-to-noise ratio generated on the C-scan recording outputs. Each flaw orientation, panel configuration, and thickness required a different technique for evaluation. The procedures selected and used for evaluation of weld panels with crowns is shown in Appendix H. The procedure selected and used for evaluation of flush weld panels is shown in Appendix I.

4. Eddy Current Evaluation

Each flaw orientation, panel configuration, and thickness also required a different technique for eddy current evaluation. The procedures selected and used for evaluation of weld panels with crowns is shown in Appendix J. The spring-loaded probe holder used for scanning these panels is shown in Figure IV-4.

The procedure selected and used for evaluation of flush weld panels is shown in Appendix K. The spring-loaded probe holder used for scanning these panels is shown in Figure IV-5.

C. TEST SPECIMEN EVALUATION

Test specimens were evaluated by optimized penetrant, ultrasonic, eddy current, and x-radiographic inspection procedures in three separate inspection sequences. After familiarization with the specific procedures to be used, the 117 specimens were evaluated by three different operators for each inspection sequence.

Inspection records were analyzed and recorded by each operator without a knowledge of the total number of cracks present or of the previous inspection results.

1. Sequence 1 - Inspection of "As-Machined" Weld Specimens

The Sequence 1 inspection included penetrant, ultrasonic, eddy current, and x-radiographic inspection procedures.

Penetrant inspection of specimens in the "as-machined" condition was performed independently by three different operators who completed the entire penetrant inspection process and reported their own results. One set of C-scan ultrasonic and eddy current recordings were made. The recordings were then evaluated and the results recorded independently by three different operators. One set of x-radiographs was made. The radiographs were then evaluated independently by three different operators. Each operator interpreted the x-radiographic image and reported his own results.

Inspections were carried out using the optimized methods established and documented in Appendices A, D, H, I, J, and K.

2. Sequence 2 - Inspection after Etching

On completion of the first inspection sequence, the surface of all panels was given a light metallurgical ("Flicks" etchant) solution to remove the residual flowed material from the flaw area produced by the machining operations. Panels were then reinspected by the optimized NDT procedures.

Penetrant inspection was performed independently by three different operators who completed the entire penetrant inspection process and reported their own results.

One set of C-scan ultrasonic and eddy current recordings were made. The recording were then evaluated and the results recorded independently by three different operators. One set of x-radiographs was made. The radiographs were then evaluated by three different operators. Each operator interpreted the x-radiographic image and reported his own results.

Inspections were carried out using the optimized methods established and documented in Appendices A, D, H, I, J, and K.

3. Sequence 3 - Postproof-Load Inspection

Following completion of Sequence 3, the weld panels were proof-loaded to approximately 90% of the yield strength for the weld. This loading cycle was performed to simulate a proof-load cycle on functional hardware and to evaluate its benefit to flaw detection by NDT methods. Panels were cleaned and inspected by the optimized NDT methods.

Penetrant inspection was performed independently by three different operators who completed the entire penetrant inspection procedure and reported his own results. One set of C-scan ultrasonic and eddy current recording were made. The recordings were then evaluated independently by three different operators. One set of x-radiographs was made. This set was evaluated independently by three different operators. Each operator interpreted the information on the x-ray film and reported his own results.

Inspections and readout were carried out using the optimized methods established and documented in Appendices A, D, H, I, J, and K. The locations and relative magnitude of the NDT indications were recorded by each operator and were coded for data processing.

D. PANEL FRACTURE

Following the final inspection in the postproof-loaded configurations, the panels were fractured and the actual flaw sizes measured. Flaw sizes and locations were measured with the aid of a traveling microscope and the results were recorded in the actual data file.

E. DATA ANALYSIS

1. Data Tabulation and Ordering

Actual fatigue crack flaw data for the weld panels were coded, keypunched, and input to a computer for data tabulation, data ordering, and data analysis operations. Data were segregated by panel type and flaw orientation. Table V-2 lists actual flaw data for panels containing fatigue cracks in longitudinal welds with crowns. Table V-3 lists actual flaw data for panels containing fatigue cracks in transverse welds with crowns.

Table V-2 Actual Crack Data, Fatigue-Cracked Longitudinal Welded Panels with Crowns

PANEL NO.	CRACK NO.	CRACK LENGTH	CRACK DEPTH	INITIAL FINISH	INITIAL THICKNESS	FINAL FINISH	FINAL THICKNESS	CRACK POSITION X	CRACK POSITION Y
15	28	.305	.051	33	.1240	50	.1000	4.23	.05
16	29	.308	.040	32	.1220	42	.0980	1.94	.05
16	30	.239	.022	32	.1220	42	.0980	3.25	.05
16	31	.269	.029	32	.1220	42	.0980	4.58	.05
17	32	.070	.035	39	.1240	56	.1000	2.70	.01
17	33	.110	.040	39	.1240	56	.1000	4.04	.01
18	34	.094	.019	36	.1220	58	.0980	2.30	.01
18	35	.100	.019	36	.1220	58	.0980	4.04	.01
19P	36	.050	.010	49	.1220	64	.0970	1.80	.01
19P	37	.050	.010	49	.1220	64	.0970	3.48	.01
20	38	.099	.026	37	.1220	54	.0980	1.73	.05
20	39	.107	.032	37	.1220	54	.0980	3.04	.05
20	40	.095	.025	37	.1220	54	.0980	4.32	.05
21P	41	.051	.010	32	.1230	40	.0980	1.82	.09
21	42	.021	.007	32	.1230	40	.0980	2.40	.09
22	43	.324	.034	32	.1240	60	.0990	1.69	.01
22	44	.257	.038	32	.1240	60	.0990	2.99	.01
22	45	.291	.045	32	.1240	60	.0990	4.34	.01
23	46	.047	.007	50	.1230	46	.0990	1.53	.05
23	47	.120	.020	50	.1230	46	.0990	4.53	.05
24	48	.095	.018	50	.1230	38	.0990	1.47	.05
24	49	.117	.026	50	.1230	38	.0990	4.55	.05
25P	50	.050	.010	54	.1200	44	.0970	2.40	.09
25	51	.040	.020	54	.1200	44	.0970	3.61	.09
26	52	.079	.026	48	.1210	30	.0910	2.09	.05
26	53	.072	.026	48	.1210	30	.0910	3.90	.05
27	54	.283	.039	43	.1220	44	.0980	2.57	.01
27	55	.270	.035	43	.1220	44	.0980	3.99	.01
28	56	.090	.018	39	.1240	38	.1000	1.46	.05
28	57	.120	.027	39	.1240	38	.1000	2.81	.05
28	58	.102	.017	39	.1240	38	.1000	4.25	.05
29	59	.231	.018	38	.1220	38	.0970	3.33	.05
29	60	.287	.039	38	.1220	38	.0970	4.43	.05
40	80	.510	.116	27	.4670	28	.4700	4.35	.05
41	81	.165	.054	40	.4710	30	.4710	1.42	.05
41	82	.369	.178	40	.4710	30	.4710	2.94	.05
41	83	.110	.017	40	.4710	30	.4710	4.27	.05
42	84	.540	.133	64	.4680	24	.4700	3.55	.05
43	85	.530	.155	51	.4680	60	.4710	4.02	.09
44	86	.503	.154	45	.4700	48	.4700	2.26	.01
45	87	.480	.093	43	.4710	55	.4720	2.98	.05
46	88	.506	.124	58	.4680	70	.4720	4.30	.05
47	89	1.188	.215	57	.4700	54	.4710	2.88	.05
48	90	.984	.131	54	.4700	42	.4720	3.83	.05
49	91	.512	.153	53	.4710	38	.4710	4.13	.01
50	92	.494	.103	47	.4680	48	.4700	2.49	.05
51	93	.995	.173	47	.4710	45	.4720	1.72	.09
52	94	.981	.108	57	.4610	60	.4640	3.00	.05
53	95	.498	.103	61	.4700	58	.4700	3.09	.09
215	105	.112	.023	15	.1010	20	.0990	1.41	.05
215	106	.049	.007	15	.1010	20	.0990	3.23	.05
218	107	.284	.032	45	.1000	28	.0980	1.95	.05
716	112	.990	.160	22	.4480	25	.4580	1.78	.09
713	113	.493	.116	46	.4500	30	.4530	3.92	.09
1	201	.560	.045	-0	*	-0	*	2.17	-0.
1	202	.157	.023	-0	*	-0	*	3.20	-0.

Table V-2 (Concluded)

2	203	.043	.009	-0	*	-0	*	2.09	-0.
2	204	.104	.023	-0	*	-0	*	3.55	-0.
2	205	.072	.015	-0	*	-0	*	4.44	-0.
3	206	.622	.034	-0	*	-0	*	2.08	-0.
3	207	1.696	.084	-0	*	-0	*	3.61	-0.
4	208	.129	.029	-0	*	-0	*	1.51	-0.
4	209	.139	.036	-0	*	-0	*	2.68	-0.
4	210	.249	.055	-0	*	-0	*	3.64	-0.
1	214	.560	.045	-0	*	-0	*	2.17	-0.
1	215	.157	.023	-0	*	-0	*	3.20	-0.
2	216	.043	.009	-0	*	-0	*	2.09	-0.
2	217	.104	.023	-0	*	-0	*	3.55	-0.
2	218	.072	.015	-0	*	-0	*	4.44	-0.
3	219	.622	.034	-0	*	-0	*	2.08	-0.
3	220	1.692	.084	-0	*	-0	*	3.61	-0.
4	221	.129	.029	-0	*	-0	*	1.51	-0.
4	222	.139	.036	-0	*	-0	*	2.68	-0.
4	223	.249	.055	-0	*	-0	*	3.64	-0.
6	252	.368	.076	-0	*	-0	*	3.10	-0.
6	253	.276	.074	-0	*	-0	*	4.33	-0.
7	254	.181	.048	-0	*	-0	*	1.68	-0.
7	255	.417	.117	-0	*	-0	*	2.96	-0.
7	256	.273	.059	-0	*	-0	*	4.42	-0.
11	260	.160	.033	-0	*	-0	*	1.33	-0.
11	261	.270	.065	-0	*	-0	*	3.02	-0.
11	262	.305	.087	-0	*	-0	*	4.38	-0.
6	264	.368	.076	-0	*	-0	*	3.10	-0.
6	265	.267	.074	-0	*	-0	*	4.33	-0.
7	266	.181	.048	-0	*	-0	*	1.68	-0.
7	267	.417	.117	-0	*	-0	*	2.96	-0.
7	268	.273	.059	-0	*	-0	*	4.42	-0.
11	272	.160	.033	-0	*	-0	*	1.33	-0.
11	273	.270	.065	-0	*	-0	*	3.02	-0.
11	274	.305	.087	-0	*	-0	*	4.38	-0.

Table V-3 Actual Crack Data, Fatigue-Cracked Transverse Welded Panels with Crowns

PANEL NO.	CRACK NO.	CRACK LENGTH	CRACK DEPTH	INITIAL FINISH	INITIAL THICKNESS	FINAL FINISH	FINAL THICKNESS	CRACK POSITION X	CRACK POSITION Y
1	1	.047	.015	48	.1220	60	.0960	.09	6.17
1	2	.067	.019	48	.1220	60	.0960	.09	7.73
2	3	.067	.017	44	.1220	60	.0980	.05	6.36
2	4	.038	.010	44	.1220	60	.0980	.05	6.85
3	5	.100	.021	59	.1230	58	.0990	.05	4.33
3	6	.103	.024	59	.1230	58	.0990	.05	8.40
4	7	.033	.010	39	.1230	50	.1000	.05	6.20
4	8	.063	.017	39	.1230	50	.1000	.05	7.00
5	9	.111	.023	67	.1220	62	.0980	.05	7.56
6	10	.104	.038	51	.1220	54	.0990	.01	4.83
6	11	.128	.021	51	.1220	54	.0940	.01	7.86
7	12	.292	.045	58	.1220	68	.0970	.05	5.30
8	13	.286	.039	43	.1230	62	.0970	.05	4.03
8	14	.295	.039	43	.1230	62	.0970	.05	6.20
8	15	.282	.038	43	.1230	62	.0970	.05	8.22
9	16	.066	.013	44	.1220	56	.0990	.09	5.03
9	17	.047	.020	44	.1220	56	.0990	.09	6.29
9	18	.057	.013	44	.1220	56	.0990	.09	7.87
10	19	.172	.022	55	.1230	46	.0980	.05	4.65
10	20	.306	.048	55	.1230	46	.0980	.05	7.60
11	21	.283	.043	43	.1230	46	.0990	.05	5.09
11	22	.273	.041	43	.1230	46	.0990	.05	8.56
12	23	.279	.041	29	.1220	48	.1000	.09	8.06
13	24	.065	.029	39	.1220	52	.0980	.05	5.12
13	25	.061	.024	39	.1220	52	.0980	.05	6.58
13	26	.057	.030	39	.1220	52	.0980	.05	9.04
14	27	.101	.018	44	.1240	46	.0990	.09	6.70
30	61	1.032	.151	63	.4680	50	.4680	.05	6.12
31	62	.493	.083	38	.4670	26	.4680	.09	4.98
32	63	.234	.057	52	.4660	34	.4660	.05	6.94
32	64	.387	.147	52	.4660	34	.4660	.05	8.31
33	65	1.435	.235	69	.4710	38	.4700	.05	5.90
34	66	.498	.122	53	.4730	26	.4660	.05	4.90
35	67	.376	.138	53	.4690	42	.4760	.05	6.54
35	68	.341	.109	53	.4690	42	.4760	.05	10.71
36	69	.478	.107	64	.4690	48	.4710	.05	4.20
36	70	.478	.116	64	.4690	48	.4710	.05	8.94
36	71	.471	.130	64	.4690	48	.4710	.05	13.71
37	72	.985	.147	51	.4680	46	.4700	.09	5.07
37	73	.992	.129	51	.4680	46	.4700	.01	11.13
38	74	.930	.193	66	.4620	60	.4680	.05	4.58
38	75	1.085	.169	66	.4620	60	.4680	.05	8.45
38	76	1.076	.174	66	.4620	60	.4680	.05	12.59
39	77	.519	.091	56	.4680	55	.4670	.01	4.40
39	78	.498	.094	56	.4680	55	.4670	.01	9.06
39	79	.482	.085	56	.4680	55	.4670	.09	13.84
54	96	.113	.018	40	.4220	46	.0980	.01	4.61
54	97	.123	.036	40	.4220	46	.0980	.01	6.88
54	98	.112	.018	40	.4220	46	.0980	.09	9.11
55	99	.260	.045	35	.4250	36	.1010	.05	4.38
55	100	.126	.024	35	.4250	36	.1010	.05	6.38
55	101	.148	.029	35	.4250	36	.1010	.05	9.42
113	102	.229	.045	46	.1000	22	.0980	.09	5.32
113	103	.274	.035	46	.1000	22	.0980	.09	7.17
113	104	.288	.041	46	.1000	22	.0980	.09	9.73
505	109	.513	.122	19	.4650	30	.4670	.05	9.58
506	110	.485	.093	22	.4300	24	.4500	.09	4.18
506	111	.454	.087	22	.4300	24	.4500	.01	9.27
8	257	.233	.066	-0	*	-0	*	-0.	6.50
8	258	.065	.015	-0	*	-0	*	-0.	8.90
8	259	.152	.040	-0	*	-0	*	-0.	11.60
8	269	.233	.066	-0	*	-0	*	-0.	6.50
8	270	.065	.015	-0	*	-0	*	-0.	8.90
8	271	.152	.040	-0	*	-0	*	-0.	11.60

Table V-4 Actual Crack Data, Fatigue-Cracked Flush, Longitudinal Welded Panels with Crowns

PANEL NO.	CRACK NO.	CRACK LENGTH	CRACK DEPTH	INITIAL FINISH	INITIAL THICKNESS	FINAL FINISH	FINAL THICKNESS	CRACK POSITION X	CRACK POSITION Y
8	501	.070	.040	30	.1080	20	.1080	1.51	.05
8	502	.045	.009	30	.1080	20	.1080	2.58	.05
8	503	.063	.014	30	.1080	20	.1080	3.68	.05
8	504	.088	.025	30	.1080	20	.1080	4.37	.05
10	505	.083	.017	15	.1040	20	.1090	2.19	.05
10	506	.037	.009	15	.1040	20	.1090	4.48	.05
11	507	.043	.021	35	.1090	28	.1120	2.38	.01
11	508	.072	.015	35	.1090	28	.1120	3.16	.09
11	509	.085	.013	35	.1090	28	.1120	3.83	.01
11	510	.073	.021	35	.1090	28	.1120	4.14	.09
12	511	.396	.058	10	.1080	30	.0930	1.69	.05
12	512	.337	.058	10	.1080	30	.0930	2.46	.05
12	513	.347	.056	10	.1080	30	.0930	3.52	.05
12	514	.324	.043	10	.1080	30	.0930	4.33	.05
15	515	.089	.024	13	.1080	36	.1100	2.89	.05
15	516	.093	.020	13	.1080	36	.1100	3.74	.05
15	517	.075	.015	13	.1080	36	.1100	4.38	.05
18	518	.120	.030	14	.1070	20	.1100	1.95	.09
18	519	.064	.017	14	.1070	20	.1100	2.54	.09
18	520	.060	.016	14	.1070	20	.1100	3.31	.01
18	521	.068	.013	14	.1070	20	.1100	3.97	.05
19	522	.353	.058	18	.1080	30	.1120	1.53	.05
19	523	.323	.044	18	.1080	30	.1120	3.16	.05
19	524	.156	.012	18	.1080	30	.1120	4.85	.05
24	525	.070	.014	11	.1000	25	.1040	3.03	.05
24	526	.150	.045	11	.1000	25	.1040	4.49	.05
27	527	.212	.039	34	.1080	28	.1050	1.06	.09
27	528	.343	.058	34	.1080	28	.1050	2.28	.01
27	529	.271	.046	34	.1080	28	.1050	3.05	.09
27	530	.283	.051	34	.1080	28	.1050	4.06	.09
950	531	.348	.053	12	.0930	36	.1000	2.15	.01
950	532	.343	.065	12	.0930	36	.1000	2.95	.01
950	533	.378	.053	12	.0930	36	.1000	2.53	.09
950	534	.337	.060	12	.0930	36	.1000	3.45	.09
951	535	.157	.021	21	.1110	26	.1000	1.28	.05
951	536	.339	.049	21	.1110	26	.1000	2.62	.05
951	537	.300	.042	21	.1110	26	.1000	3.63	.05
30	538	.228	.084	21	.4350	20	.4350	1.29	.01
30	539	.194	.086	21	.4350	20	.4350	2.11	.09
30	540	.191	.070	21	.4350	20	.4350	3.62	.09
30	541	.193	.071	21	.4350	20	.4350	4.80	.01
34	542	.506	.138	16	.4400	18	.4400	1.35	.09
34	543	.708	.199	16	.4400	18	.4400	2.38	.01
34	544	.630	.179	16	.4400	18	.4400	3.76	.01
34	545	.502	.151	16	.4400	18	.4400	4.73	.09
35	546	.426	.073	23	.4450	28	.4400	.93	.05

Table V-4 (Concluded)

35	547	.598	.130	23	.4450	28	.4400	2.26	.05
35	548	.513	.103	23	.4450	28	.4400	3.48	.05
35	549	.446	.071	23	.4450	28	.4400	4.83	.05
36	550	1.009	.193	14	.4450	24	.4420	1.16	.05
36	551	1.176	.215	14	.4450	24	.4420	2.90	.05
36	552	1.562	.276	14	.4450	24	.4420	4.58	.05
37	553	.542	.153	14	.4430	20	.4420	1.92	.01
37	554	.606	.178	14	.4430	20	.4420	1.92	.09
37	555	.447	.115	14	.4430	20	.4420	2.97	.01
37	556	.526	.162	14	.4430	20	.4420	3.00	.09
38	557	1.037	.161	18	.4430	18	.4440	1.79	.05
38	558	1.224	.213	18	.4430	18	.4440	4.09	.05
39	559	.744	.119	21	.4430	30	.4410	1.90	.01
39	560	.937	.187	21	.4430	30	.4410	1.96	.09
39	561	1.098	.239	21	.4430	30	.4410	4.28	.01
39	562	.703	.106	21	.4430	30	.4410	4.40	.09
41	563	.130	.030	14	.4370	15	.4390	1.07	.05
41	564	.221	.071	14	.4370	15	.4390	2.52	.05
41	565	.224	.066	14	.4370	15	.4390	3.72	.05
41	566	.120	.033	14	.4370	15	.4390	4.87	.05
42	567	.280	.113	20	.4460	18	.4450	1.13	.05
42	568	.274	.104	20	.4460	18	.4450	2.04	.05
42	569	.319	.079	20	.4460	18	.4450	3.43	.05
42	570	.280	.097	20	.4460	18	.4450	4.63	.05
43	571	.217	.067	20	.4480	24	.4460	1.28	.05
43	572	.251	.086	20	.4480	24	.4460	2.86	.05
43	573	.161	.043	20	.4480	24	.4460	4.23	.05
43	574	.106	.018	20	.4480	24	.4460	5.13	.05
44	575	.210	.065	13	.4460	28	.4450	1.61	.05
44	576	.196	.057	13	.4460	28	.4450	2.74	.05
44	577	.264	.095	13	.4460	28	.4450	3.86	.05
44	578	.136	.037	13	.4460	28	.4450	4.91	.05
45	579	.149	.040	21	.4450	26	.4450	2.06	.09
45	580	.149	.035	21	.4450	26	.4450	3.04	.01
45	581	.148	.031	21	.4450	26	.4450	4.17	.01
45	582	.127	.029	21	.4450	26	.4450	4.94	.09
47	583	.760	.120	15	.4460	16	.4450	1.83	.09
47	584	1.119	.227	15	.4460	16	.4450	2.83	.01
47	585	.770	.120	15	.4460	16	.4450	3.91	.09
48	586	.895	.143	15	.4460	20	.4450	1.38	.05
48	587	1.289	.229	15	.4460	20	.4450	2.87	.05
48	588	1.110	.214	15	.4460	20	.4450	4.43	.05
49	589	.091	.021	22	.4470	18	.4470	2.25	.01
49	590	.379	.170	22	.4470	18	.4470	2.26	.09
49	591	.392	.182	22	.4470	18	.4470	3.73	.09
49	592	.100	.021	22	.4470	18	.4470	3.75	.01
50	593	.428	.070	14	.4450	25	.4430	1.18	.05
50	594	.479	.095	14	.4450	25	.4430	1.43	.05
50	595	.678	.178	14	.4450	25	.4430	3.67	.05
50	596	.417	.079	14	.4450	25	.4430	4.84	.05
51	597	1.061	.195	21	.4470	30	.4450	1.77	.05
51	598	1.088	.207	21	.4470	30	.4450	4.13	.05
52	599	.879	.154	45	.4450	40	.4430	1.84	.05
52	600	1.043	.215	45	.4450	40	.4430	3.93	.05
53	601	.479	.109	30	.4500	22	.4500	1.09	.05
53	602	.565	.137	30	.4500	22	.4500	2.22	.05
53	603	.616	.155	30	.4500	22	.4500	3.42	.05
53	604	.433	.083	30	.4500	22	.4500	4.81	.05
500	605	.139	.036	22	.4380	32	.4400	1.21	.05
500	606	.229	.080	22	.4380	32	.4400	2.29	.05
500	607	.218	.059	22	.4380	32	.4400	3.14	.05
500	608	.190	.055	22	.4380	32	.4400	4.62	.05
9	701	.089	.014	-0	*	-0	*	2.18	-0.
9	702	.108	.030	-0	*	-0	*	4.22	-0.
10	703	.073	.015	-0	*	-0	*	1.94	-0.
10	704	.113	.031	-0	*	-0	*	3.99	-0.
9	705	.089	.014	-0	*	-0	*	2.18	-0.
9	706	.108	.030	-0	*	-0	*	4.22	-0.
10	707	.073	.015	-0	*	-0	*	1.94	-0.
10	708	.113	.031	-0	*	-0	*	3.99	-0.

Table V-5 Actual Crack Data, Fatigue-Cracked Flush, Transverse Welded Panels

PANEL NO.	CRACK NO.	CRACK LENGTH	CRACK DEPTH	INITIAL FINISH	INITIAL THICKNESS	FINAL FINISH	FINAL THICKNESS	CRACK POSITION X	CRACK POSITION Y
960	609	.138	.059	20	.4320	26	.4430	.05	6.94
960	610	.178	.066	20	.4320	26	.4430	.05	7.92
960	611	.204	.069	20	.4320	26	.4430	.05	9.24
960	612	.308	.124	20	.4320	26	.4430	.05	10.30
960	613	.224	.079	20	.4320	26	.4430	.05	11.15
960	614	.235	.089	20	.4320	26	.4430	.05	12.10
961	615	.178	.054	16	.4410	18	.4420	.05	5.83
961	616	.495	.215	16	.4410	18	.4420	.05	7.01
961	617	.195	.078	16	.4410	18	.4420	.05	8.30
961	618	.182	.067	16	.4410	18	.4420	.05	9.58
961	619	.235	.099	16	.4410	18	.4420	.05	11.01
961	620	.297	.071	16	.4410	18	.4420	.05	12.36
962	621	.267	.115	15	.4560	20	.4530	.05	6.86
962	622	.225	.110	15	.4560	20	.4530	.05	7.58
962	623	.239	.103	15	.4560	20	.4530	.05	8.71
962	624	.158	.050	15	.4560	20	.4530	.05	9.94
962	625	.186	.063	15	.4560	20	.4530	.05	10.69
962	626	.160	.049	15	.4560	20	.4530	.05	12.06

Table V-4 lists actual flaw data for fatigue cracks in flush, longitudinal weld panels. Table V-5 lists actual flaw data for fatigue crack in flush, transverse weld panels.

NDT observations were also segregated by panel type and flaw orientation and were tabulated by NDT success for each inspection sequence according to the ordered flaw size. A "0" in the data tabulations indicates that there were no misses (failure to detect) by any of the three NDT observers. A "3" indicates that the flaw was missed by all observers. A "-0" indicates that no NDT observations were made for that sequence. Table V-6 lists NDT observations as ordered by actual flaw length for panels containing fatigue cracks in longitudinal welds with crowns. Table V-7 lists NDT observations as ordered by actual flaw length for panels containing fatigue crack in transverse welds with crowns. Table V-8 lists NDT observations as ordered by actual flaw length for fatigue cracks in flush, longitudinal weld panels. Table V-9 lists NDT observations as ordered by actual flaw length for fatigue cracks in flush, transverse weld panels.

Actual flaw data were used as a basis for all subsequent ordering, calculations, analysis, and data plotting. Flaws were initially ordered by decreasing flaw length, depth, and area. The data were then stored for use in statistical analysis sequences.

2. Data Analysis and Presentation

The same statistical analysis, plotting methods, and calculations of one-sided confidence limits described for use on the integrally stiffened panel data were used in analysis of the fatigue flaw detection reliability data.

3. Ultrasonic Data Analysis

Initial analysis of the ultrasonic testing data revealed a discrepancy in the data. Failure to maintain the detection level between sequences and to detect large flaws was attributed to a combination of panel warpage and human factors in the inspections. To verify this discrepancy and to provide a measure of the true values, 11 additional fatigue flawed weld panels containing 27 flaws were selected and subjected to the same Sequence 1 and Sequence 3 inspection cycles as the completed panels. An additional optimization cycle performed resulted in changes in the NDT procedures for the weld panels. These changes are shown as Amendments A and B to the Appendix procedure. The inspection sequence was repeated twice (double inspection in two runs), with three different operators making their

Table V-6 NDT Observations, Fatigue-Cracked Longitudinal Welded Panels with Crowns

		PENETRANT			ULTRASONIC			EDDY CURRENT			X-RAY		
INSPECTION SEQUENCE		1	2	3	1	2	3	1	2	3	1	2	3
CRACK NUMBER	ACTUAL VALUE												
207	1.696	-0	-0	-0	0	-0	0	-0	-0	-0	-0	-0	-0
220	1.692	-0	-0	-0	0	-0	0	-0	-0	-0	-0	-0	-0
89	1.188	1	0	0	2	0	0	2	0	3	1	0	0
93	.995	0	0	0	1	1	0	2	1	3	0	0	0
112	.990	1	2	0	0	0	3	0	3	3	1	1	0
90	.984	0	0	0	3	3	1	1	3	3	3	3	0
94	.981	0	0	0	2	2	0	1	1	0	3	3	0
219	.622	-0	-0	-0	0	-0	0	-0	-0	-0	-0	-0	-0
206	.622	-0	-0	-0	0	-0	0	-0	-0	-0	-0	-0	-0
201	.560	-0	-0	-0	0	-0	0	-0	-0	-0	-0	-0	-0
214	.560	-0	-0	-0	0	-0	0	-0	-0	-0	-0	-0	-0
84	.540	2	1	2	2	0	0	1	0	0	2	3	3
85	.530	1	1	0	3	3	0	2	1	3	3	3	0
91	.512	0	0	0	2	2	0	2	3	3	3	3	0
80	.510	1	2	0	2	2	0	1	3	1	3	3	3
88	.506	1	0	0	3	3	3	1	0	2	3	3	0
86	.503	0	2	0	2	3	3	3	3	3	1	0	0
95	.498	0	0	0	0	0	0	2	3	0	0	0	0
92	.494	1	1	0	3	3	3	0	0	0	3	2	3
113	.493	0	0	0	0	0	0	3	3	3	0	3	3
87	.480	0	0	0	0	0	0	0	0	0	3	1	0
255	.417	-0	-0	-0	0	-0	0	-0	-0	-0	-0	-0	-0
267	.417	-0	-0	-0	0	-0	0	-0	-0	-0	-0	-0	-0
82	.369	0	0	0	0	1	0	0	0	0	0	1	0
264	.368	-0	-0	-0	0	-0	0	-0	-0	-0	-0	-0	-0
252	.368	-0	-0	-0	0	-0	0	-0	-0	-0	-0	-0	-0
43	.324	2	2	0	3	0	1	3	3	3	1	0	1
29	.308	1	1	0	3	0	0	2	0	0	3	1	0
28	.305	2	1	0	3	3	2	3	3	3	3	2	1
262	.305	-0	-0	-0	0	-0	0	-0	-0	-0	-0	-0	-0
274	.305	-0	-0	-0	0	-0	0	-0	-0	-0	-0	-0	-0
45	.291	2	1	0	3	0	0	3	3	3	3	0	0
60	.287	1	1	0	0	0	0	0	0	3	3	3	3
107	.284	1	1	0	0	0	0	0	0	0	2	2	0
54	.283	0	1	0	3	2	3	1	3	-0	3	3	2
253	.276	-0	-0	-0	0	-0	0	-0	-0	-0	-0	-0	-0
268	.273	-0	-0	-0	3	-0	0	-0	-0	-0	-0	-0	-0
256	.273	-0	-0	-0	3	-0	0	-0	-0	-0	-0	-0	-0
261	.270	-0	-0	-0	0	-0	0	-0	-0	-0	-0	-0	-0
273	.270	-0	-0	-0	0	-0	0	-0	-0	-0	-0	-0	-0
55	.270	0	1	0	2	2	3	2	3	3	3	3	3
31	.269	2	1	0	3	3	0	1	3	3	2	1	0
265	.267	-0	-0	-0	0	-0	0	-0	-0	-0	-0	-0	-0
44	.257	2	2	0	3	0	0	3	3	3	3	0	0

Table V-6 (Concluded)

CK NO	ACT VAL	1	2	3	1	2	3	1	2	3	1	2	3
210	.249	-0	-0	-0	0	-0	0	-0	-0	-0	-0	-0	-0
223	.249	-0	-0	-0	0	-0	0	-0	-0	-0	-0	-0	-0
30	.239	3	0	0	2	0	0	2	3	3	2	2	0
59	.231	1	2	3	1	0	0	2	3	3	3	3	0
254	.181	-0	-0	-0	1	-0	0	-0	-0	-0	-0	-0	-0
266	.181	-0	-0	-0	1	-0	0	-0	-0	-0	-0	-0	-0
81	.165	0	0	0	0	0	0	2	0	0	2	3	3
260	.160	-0	-0	-0	0	-0	0	-0	-0	-0	-0	-0	-0
272	.160	-0	-0	-0	0	-0	0	-0	-0	-0	-0	-0	-0
215	.157	-0	-0	-0	0	-0	0	-0	-0	-0	-0	-0	-0
202	.157	-0	-0	-0	0	-0	0	-0	-0	-0	-0	-0	-0
222	.139	-0	-0	-0	0	-0	0	-0	-0	-0	-0	-0	-0
209	.139	-0	-0	-0	0	-0	0	-0	-0	-0	-0	-0	-0
208	.129	-0	-0	-0	0	-0	0	-0	-0	-0	-0	-0	-0
221	.129	-0	-0	-0	0	-0	0	-0	-0	-0	-0	-0	-0
47	.120	0	1	0	3	3	3	1	3	0	2	2	2
57	.120	0	3	3	1	1	3	1	2	2	3	1	3
49	.117	0	1	0	2	3	0	2	3	2	3	3	3
105	.112	0	3	0	0	1	0	0	3	3	3	3	3
33	.110	0	0	0	1	1	0	2	3	3	3	3	2
83	.110	0	0	0	1	3	3	2	0	0	3	2	2
39	.107	0	0	1	3	3	3	3	3	3	3	2	2
217	.104	-0	-0	-0	0	-0	0	-0	-0	-0	-0	-0	-0
204	.104	-0	-0	-0	0	-0	0	-0	-0	-0	-0	-0	-0
58	.102	0	3	3	3	3	3	2	3	2	3	3	3
35	.100	0	0	1	2	2	2	1	0	0	2	2	3
38	.099	0	0	1	1	3	3	2	3	0	2	3	1
48	.095	2	1	0	3	3	0	3	3	1	2	3	3
40	.095	0	0	0	1	1	1	1	3	0	2	2	2
34	.094	0	0	0	1	3	3	1	1	0	3	3	3
56	.090	0	3	3	1	3	3	1	1	1	3	3	3
52	.079	1	1	0	0	0	0	2	3	-0	0	2	0
53	.072	1	1	0	0	0	0	1	3	-0	0	1	0
205	.072	-0	-0	-0	3	-0	0	-0	-0	-0	-0	-0	-0
218	.072	-0	-0	-0	3	-0	0	-0	-0	-0	-0	-0	-0
32	.070	0	0	0	2	0	2	3	0	3	3	3	3
41	.051	0	0	0	3	3	3	3	3	3	3	2	2
36	.050	1	0	0	1	3	1	1	3	2	3	3	3
37	.050	3	1	2	2	1	2	2	3	3	3	3	2
50	.050	0	1	1	3	3	3	3	3	3	1	2	3
106	.049	1	3	3	3	1	0	3	3	3	3	3	3
46	.047	3	3	3	3	3	3	1	3	0	3	2	2
216	.043	-0	-0	-0	3	-0	0	-0	-0	-0	-0	-0	-0
203	.043	-0	-0	-0	3	-0	0	-0	-0	-0	-0	-0	-0
51	.040	0	1	1	3	3	3	2	3	3	2	2	3
42	.021	0	0	0	3	3	3	3	3	3	3	3	1

Table V-7 NDT Observations, Fatigue-Cracked Transverse Welded Panels with Crowns

		PENETRANT			ULTRASONIC			EDDY CURRENT			X-RAY		
INSPECTION SEQUENCE		1	2	3	1	2	3	1	2	3	1	2	3
CRACK NUMBER	ACTUAL VALUE												
65	1.435	0	0	0	1	0	0	0	0	0	0	0	0
75	1.085	0	0	0	0	0	0	0	0	1	3	3	2
76	1.076	0	0	0	0	0	0	1	0	0	3	2	2
61	1.032	0	0	0	0	0	0	0	0	0	3	3	0
73	.992	0	0	0	0	1	0	1	0	0	2	3	3
72	.985	0	0	0	0	0	1	0	0	0	0	0	1
67	.976	0	0	0	0	0	0	0	0	0	3	3	2
68	.941	0	0	0	1	0	0	0	0	0	3	3	3
74	.930	0	0	0	0	0	0	0	0	0	3	3	3
77	.919	0	0	0	1	0	0	0	0	0	3	3	3
109	.913	0	0	0	0	3	0	0	0	0	3	3	2
78	.898	0	0	0	0	0	1	1	0	0	3	3	3
66	.898	0	0	0	3	2	2	0	0	0	3	1	3
62	.893	0	2	0	3	3	3	0	3	3	3	1	3
110	.885	0	0	1	0	0	3	0	0	0	3	1	2
79	.882	0	0	0	2	0	3	1	0	1	3	3	3
69	.878	0	0	0	1	0	0	0	0	0	3	3	3
70	.878	0	0	0	0	0	0	0	0	0	0	0	0
71	.871	0	0	0	0	1	0	2	1	2	3	3	3
111	.854	0	0	0	0	1	3	0	0	3	1	1	2
64	.837	0	0	1	2	3	3	0	0	0	2	3	3
20	.836	0	0	0	1	0	0	1	0	2	0	0	0
14	.835	0	0	0	0	0	0	1	0	0	1	1	0
12	.832	0	0	0	0	0	0	0	0	3	3	0	0
104	.828	0	0	0	0	0	0	0	0	0	2	2	0
13	.826	0	0	0	0	0	0	1	0	0	2	0	1
21	.823	1	0	0	1	0	3	1	3	0	2	3	0
15	.822	0	0	0	0	0	0	1	0	0	2	1	0
23	.779	0	0	0	1	0	0	0	1	1	3	3	2
103	.774	0	0	0	0	0	0	0	0	0	1	1	0
22	.773	0	0	0	3	0	2	0	3	1	0	0	0
99	.760	0	1	0	1	0	0	0	1	0	0	0	0
63	.734	0	3	1	2	3	3	0	0	0	3	3	3
257	.733	-0	-0	-0	0	-0	0	-0	-0	-0	-0	-0	-0
269	.733	-0	-0	-0	0	-0	0	-0	-0	-0	-0	-0	-0
102	.729	0	0	0	0	0	0	0	1	0	2	2	0
19	.672	1	0	0	1	0	0	0	0	0	3	2	3
211	.656	-0	-0	-0	0	-0	0	-0	-0	-0	-0	-0	-0

Table V-7 (Concluded)

CK NO	ACT VAL											
		1	2	3	1	2	3	1	2	3	1	2	3
224	.156	-0	-0	-0	0	-0	0	-0	-0	-0	-0	-0	-0
259	.152	-0	-0	-0	0	-0	0	-0	-0	-0	-0	-0	-0
271	.152	-0	-0	-0	0	-0	0	-0	-0	-0	-0	-0	-0
101	.148	0	1	0	2	0	0	3	3	1	3	3	2
11	.128	0	0	0	0	0	1	3	0	3	2	3	3
100	.126	0	1	0	1	0	0	0	1	0	3	2	2
97	.123	0	3	3	3	3	3	3	0	2	3	3	3
225	.123	-0	-0	-0	0	-0	0	-0	-0	-0	-0	-0	-0
212	.123	-0	-0	-0	0	-0	0	-0	-0	-0	-0	-0	-0
96	.113	0	3	3	3	3	3	2	3	3	3	3	1
98	.112	0	3	3	1	1	3	1	1	0	3	2	2
9	.111	3	2	1	3	3	3	2	0	0	3	3	2
10	.104	0	0	0	1	3	3	2	3	3	3	3	3
6	.103	0	0	0	1	0	0	1	3	3	1	2	3
27	.101	0	1	0	3	3	3	2	3	1	2	3	3
5	.100	0	2	0	3	3	3	1	0	3	2	2	2
213	.093	-0	-0	-0	0	-0	0	-0	-0	-0	-0	-0	-0
226	.093	-0	-0	-0	0	-0	0	-0	-0	-0	-0	-0	-0
2	.067	0	2	2	1	0	3	3	3	3	3	3	1
3	.057	0	0	0	3	3	3	3	1	3	3	3	3
16	.056	0	2	2	3	3	3	3	1	3	3	2	3
258	.065	-0	-0	-0	3	-0	0	-0	-0	-0	-0	-0	-0
270	.065	-0	-0	-0	3	-0	0	-0	-0	-0	-0	-0	-0
24	.065	0	1	0	0	0	3	1	3	1	1	2	0
8	.063	0	1	1	3	3	3	3	0	3	3	3	2
25	.061	0	1	0	1	0	0	2	3	3	1	2	1
18	.057	0	1	0	3	3	3	2	3	3	3	3	3
26	.057	0	1	2	0	0	0	1	3	3	1	2	0
17	.047	0	2	2	3	2	3	3	1	3	3	3	3
1	.047	2	2	2	3	3	3	3	3	3	3	2	3
7	.039	3	2	2	2	0	0	3	3	0	3	2	3
4	.038	3	0	0	1	0	0	3	2	0	3	3	2

Table V-8 NDT Observations, Fatigue-Cracked Flush, Longitudinal Welded Panels

		PENETRANT			ULTRASONIC			EDDY CURRENT			X-RAY		
INSPECTION SEQUENCE		1	2	3	1	2	3	1	2	3	1	2	3
CRACK NUMBER	ACTUAL VALUE												
552	1.562	0	0	0	0	0	1	0	0	0	0	0	0
587	1.289	1	0	0	0	0	0	0	0	0	0	0	0
558	1.224	0	0	0	0	0	0	1	0	0	0	0	0
551	1.176	0	0	0	0	0	0	0	0	0	0	0	0
584	1.119	0	0	0	0	0	0	0	0	0	0	0	0
588	1.110	1	0	0	0	0	0	0	0	0	1	0	0
561	1.098	0	0	0	0	1	0	0	0	0	0	0	0
598	1.088	0	0	0	0	0	0	0	0	0	0	0	0
597	1.061	0	0	0	0	0	0	0	0	0	0	1	0
600	1.043	0	0	0	0	0	0	0	0	0	0	0	0
557	1.037	0	0	0	0	0	0	0	0	0	0	1	0
550	1.009	0	0	0	0	0	0	0	0	0	0	0	0
560	.937	0	0	0	0	0	0	0	0	0	3	3	0
586	.895	1	0	0	0	0	0	0	0	0	0	0	0
599	.879	0	0	0	0	0	0	0	0	0	0	0	0
585	.770	0	0	0	0	0	0	0	0	0	3	2	0
583	.760	0	0	0	0	0	0	0	0	0	3	3	0
559	.744	0	0	0	0	0	0	0	0	0	0	0	0
543	.708	1	0	0	0	0	0	0	0	0	0	0	0
562	.703	0	0	0	0	0	0	0	0	0	3	3	3
595	.678	0	0	0	0	0	0	0	0	0	1	1	0
544	.630	0	0	0	0	0	0	0	0	0	0	1	0
603	.616	0	0	0	0	0	0	0	0	0	0	0	0
554	.606	0	0	0	0	1	0	0	0	0	3	3	0
547	.598	0	0	0	0	0	0	0	0	0	0	2	0
602	.565	0	0	0	0	0	0	0	0	0	1	0	0
553	.542	0	0	0	0	0	0	0	0	0	0	1	0
556	.526	0	0	0	0	1	0	0	0	0	2	3	0
548	.513	0	0	0	0	0	0	0	0	0	3	3	0
542	.506	0	0	0	0	0	0	0	0	0	2	2	0
545	.502	0	0	0	2	1	0	0	0	0	3	3	1
594	.479	0	0	0	0	1	0	0	0	0	3	3	0
601	.479	0	0	0	0	0	0	0	0	0	3	1	0
555	.447	0	0	0	0	0	0	0	0	0	2	3	0
549	.446	0	0	0	0	0	0	0	0	0	3	3	3
604	.433	0	0	0	0	0	0	0	0	0	2	3	3
593	.428	0	0	0	0	0	0	0	0	0	3	3	0
546	.426	0	0	0	0	0	0	0	0	0	3	3	0

Table V-8 (Continued)

CK NO	ACT VAL													
		1	2	3	1	2	3	1	2	3	1	2	3
596	.417	0	0	0	0	0	0	0	0	0	3	3	3
511	.396	0	0	0	0	0	0	0	0	0	1	0	0
591	.392	0	0	0	0	2	0	0	0	0	0	0	0
590	.379	0	0	1	0	2	2	3	3	0	1	3	3
533	.378	0	0	0	0	0	0	0	0	0	0	0	0
522	.353	0	0	0	0	0	0	0	0	0	1	1	0
531	.348	0	0	0	0	0	0	0	0	0	0	0	0
513	.347	0	0	0	0	0	0	0	0	0	0	0	0
528	.343	0	0	0	0	0	0	0	0	0	0	0	0
532	.343	0	0	0	0	0	0	0	0	0	0	0	0
536	.339	0	0	0	0	0	0	0	0	0	3	2	0
512	.337	0	0	0	0	0	0	0	0	0	1	0	0
534	.337	0	0	0	0	0	0	0	0	0	0	0	0
514	.324	0	0	0	0	0	0	0	0	0	0	0	0
523	.323	0	0	0	0	0	0	0	0	0	0	1	0
569	.319	0	0	0	0	0	0	0	0	0	3	2	3
537	.300	0	0	0	0	0	0	0	0	0	3	3	0
530	.283	0	0	0	0	1	0	0	0	0	3	0	0
567	.280	0	1	0	0	0	0	0	0	0	0	1	3
570	.280	0	0	0	0	1	0	0	0	0	3	3	2
568	.274	0	0	0	0	0	0	0	0	0	2	1	3
529	.271	0	0	0	0	0	0	0	0	0	3	0	0
577	.264	0	0	0	0	0	0	0	0	0	3	2	2
572	.251	0	0	0	0	0	0	0	0	0	3	3	3
606	.229	0	1	1	0	0	0	0	0	0	2	2	3
538	.228	0	0	0	0	0	0	0	0	0	3	3	3
565	.224	0	0	0	0	0	0	0	0	0	2	3	3
564	.221	0	0	0	0	0	0	0	0	0	3	1	3
607	.218	0	0	0	0	0	0	0	0	0	3	3	3
571	.217	0	0	0	0	0	0	0	0	0	3	3	3
527	.212	0	0	0	0	0	0	1	0	0	3	3	1
575	.210	0	0	0	0	0	0	0	0	0	3	3	3
576	.196	0	0	0	0	0	0	0	0	0	3	3	3
539	.194	0	0	0	0	0	0	0	0	0	1	3	2
541	.193	0	0	0	0	0	0	0	0	0	3	3	3
540	.191	0	0	0	0	0	0	0	0	0	2	3	3
608	.190	0	0	1	0	0	2	0	0	0	3	3	3
573	.161	0	0	0	3	3	3	0	0	0	2	3	3
535	.157	0	0	0	0	0	0	0	3	3	3	3	0
524	.156	0	0	0	0	0	0	3	3	3	3	3	3
526	.150	0	0	0	3	0	0	0	0	0	3	2	1
580	.149	0	0	0	0	0	0	0	0	0	3	3	0
579	.149	0	0	2	1	1	0	0	3	0	0	0	0

Table V-8 (Concluded)

CK NO	ACT VAL												
		1	2	3	1	2	3	1	2	3	1	2	3
581	.148	0	0	0	0	0	0	0	0	0	3	3	3
605	.139	0	0	0	0	0	3	0	0	0	3	3	2
578	.136	0	1	3	0	0	0	0	0	0	3	3	3
563	.130	0	2	3	0	0	0	0	0	0	3	3	3
582	.127	0	0	0	3	1	3	0	1	0	3	3	3
566	.120	0	0	0	0	0	0	0	0	0	2	3	2
518	.120	0	0	0	3	0	0	0	0	0	3	2	1
704	.113	-0	-0	-0	0	-0	0	-0	-0	-0	-0	-0	-0
708	.113	-0	-0	-0	0	-0	0	-0	-0	-0	-0	-0	-0
706	.108	-0	-0	-0	0	-0	0	-0	-0	-0	-0	-0	-0
702	.108	-0	-0	-0	0	-0	0	-0	-0	-0	-0	-0	-0
574	.106	0	2	1	1	3	2	3	3	3	3	3	3
592	.100	0	3	1	0	0	3	3	3	0	3	3	3
516	.093	0	0	0	3	1	0	0	0	3	3	3	0
589	.091	0	3	1	0	0	0	0	0	0	2	0	0
705	.089	-0	-0	-0	0	-0	0	-0	-0	-0	-0	-0	-0
515	.089	0	0	0	3	0	0	0	0	3	3	3	1
701	.089	-0	-0	-0	0	-0	0	-0	-0	-0	-0	-0	-0
504	.088	1	0	0	3	3	0	0	3	3	3	3	0
509	.085	1	1	1	3	3	3	3	3	3	3	3	3
505	.083	0	0	0	3	0	0	0	0	0	3	2	3
517	.075	0	0	0	3	0	0	0	0	3	3	3	1
510	.073	0	0	0	0	1	3	0	0	0	3	3	3
707	.073	-0	-0	-0	3	-0	0	-0	-0	-0	-0	-0	-0
703	.073	-0	-0	-0	3	-0	0	-0	-0	-0	-0	-0	-0
508	.072	0	0	0	3	1	3	3	0	3	3	3	3
525	.070	0	0	0	3	3	0	0	0	3	3	2	2
501	.070	0	0	0	3	0	0	0	3	3	-0	3	0
521	.068	0	0	0	3	0	1	0	0	0	1	3	3
519	.064	0	0	0	2	0	2	0	0	0	3	3	3
503	.063	0	0	0	2	3	3	0	3	3	-0	3	3
520	.060	0	0	0	0	0	1	0	0	0	3	3	2
502	.045	0	1	0	0	0	3	0	3	3	-0	3	2
507	.043	1	2	1	3	2	3	3	0	3	3	3	3
506	.037	0	2	2	3	0	0	3	3	3	3	2	3

Table V-9 NDT Observations, Fatigue-Cracked Flush, Transverse Welded Panels

		PENETRANT			ULTRASONIC			EDDY CURRENT			X-RAY		
INSPECTION SEQUENCE		1	2	3	1	2	3	1	2	3	1	2	3
CRACK NUMBER	ACTUAL VALUE												
616	.495	0	0	0	0	0	3	0	0	0	3	0	0
612	.308	0	0	0	3	0	1	0	0	0	3	3	3
620	.297	0	0	0	0	0	3	0	0	0	3	3	3
621	.267	0	0	0	0	3	3	0	0	0	3	3	3
623	.239	0	0	0	0	0	2	0	0	0	3	3	3
619	.235	0	0	0	0	0	2	0	0	0	3	3	3
614	.235	0	0	0	3	0	3	0	0	0	3	3	3
622	.225	0	0	0	0	0	1	0	0	0	3	3	3
613	.224	0	0	1	3	0	1	0	0	0	3	3	3
611	.204	0	2	3	3	2	2	0	0	0	3	3	3
617	.195	0	0	0	0	0	3	0	0	0	3	3	3
625	.186	0	2	1	1	0	2	0	0	0	3	3	3
618	.182	0	0	0	0	0	3	0	0	0	3	3	3
615	.178	0	0	0	0	0	1	0	3	0	3	3	3
610	.178	0	0	0	3	0	1	0	0	0	3	3	3
626	.160	0	0	2	2	3	3	3	3	0	3	3	3
624	.158	0	1	0	0	0	2	3	3	0	3	3	3
609	.138	0	1	3	3	0	1	0	0	0	3	3	3

own C-scan recordings, interpreting the results, and documenting the inspections. The operator responsible for the original optimization and recording sequences was eliminated from this repeat evaluation. Additional care was taken to align warped panels to provide the best possible evaluation.

The results of this repeat cycle showed a definite improvement in the reliability of the ultrasonic method in detecting fatigue cracks in welds. The two data files were merged on the following basis:

- Data from the repeat evaluation were ordered by actual flaw dimension;
- An analysis was performed by counting down from the largest flaw to the first "miss" by the ultrasonic method;
- The original data were truncated to eliminate all flaws larger than that of the first "miss" in the repeat data;
- The remaining data were merged and analyzed according to the original plan. The merged actual data file used for processing Sequences 1 and 3 ultrasonic data is shown in Tables V-2 through V-4. Tables V-5 through V-9 list nondestructive test observations by the ultrasonic method for the merged data as ordered by actual crack length;
- The combined data base was analyzed and plotted in the same manner as that described for the integrally stiffened panels.

F. DATA RESULTS

The results of inspection and data analysis are shown graphically in Figures V-4 through V-19. Data are plotted by weld panel type and crack orientation in the welds. This separation and plotting shows the differences in detection reliability for the various panel configurations. An insufficient data base was established for optimum analysis of the flush, transverse panels at the 95% reliability and 95% confidence level. The graphical presentation at this level is shown and it may be used to qualitatively assess the etching and proof loading of these panels.

The results of these analyses show the influences of flaw geometry, flaw tightness and of inspection process influence on detection reliability.

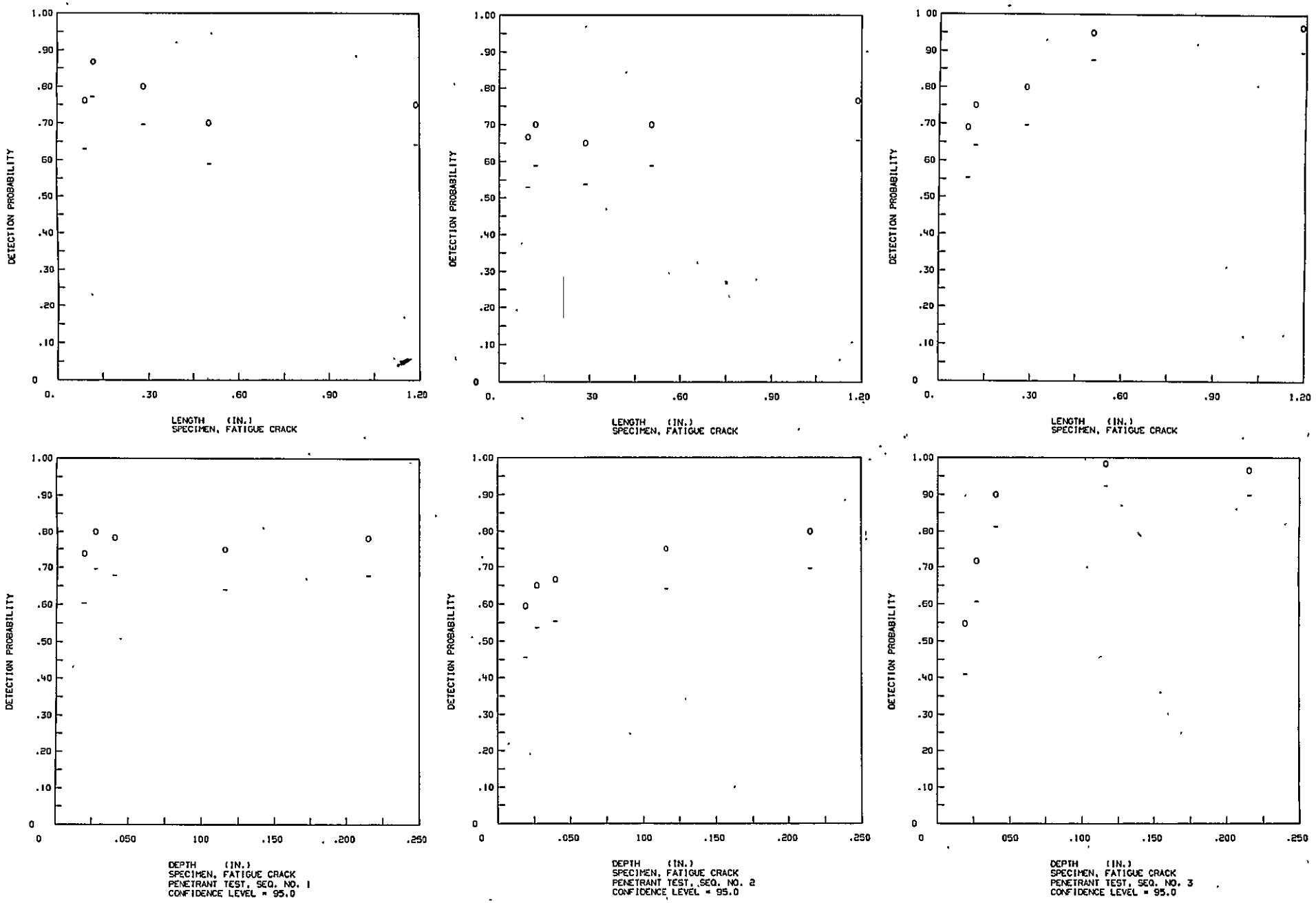

Figure V-4 Crack Detection Probability for Longitudinal Welds with Crowns by the Penetrant Method Plotted at 95% Probability and 95% Confidence

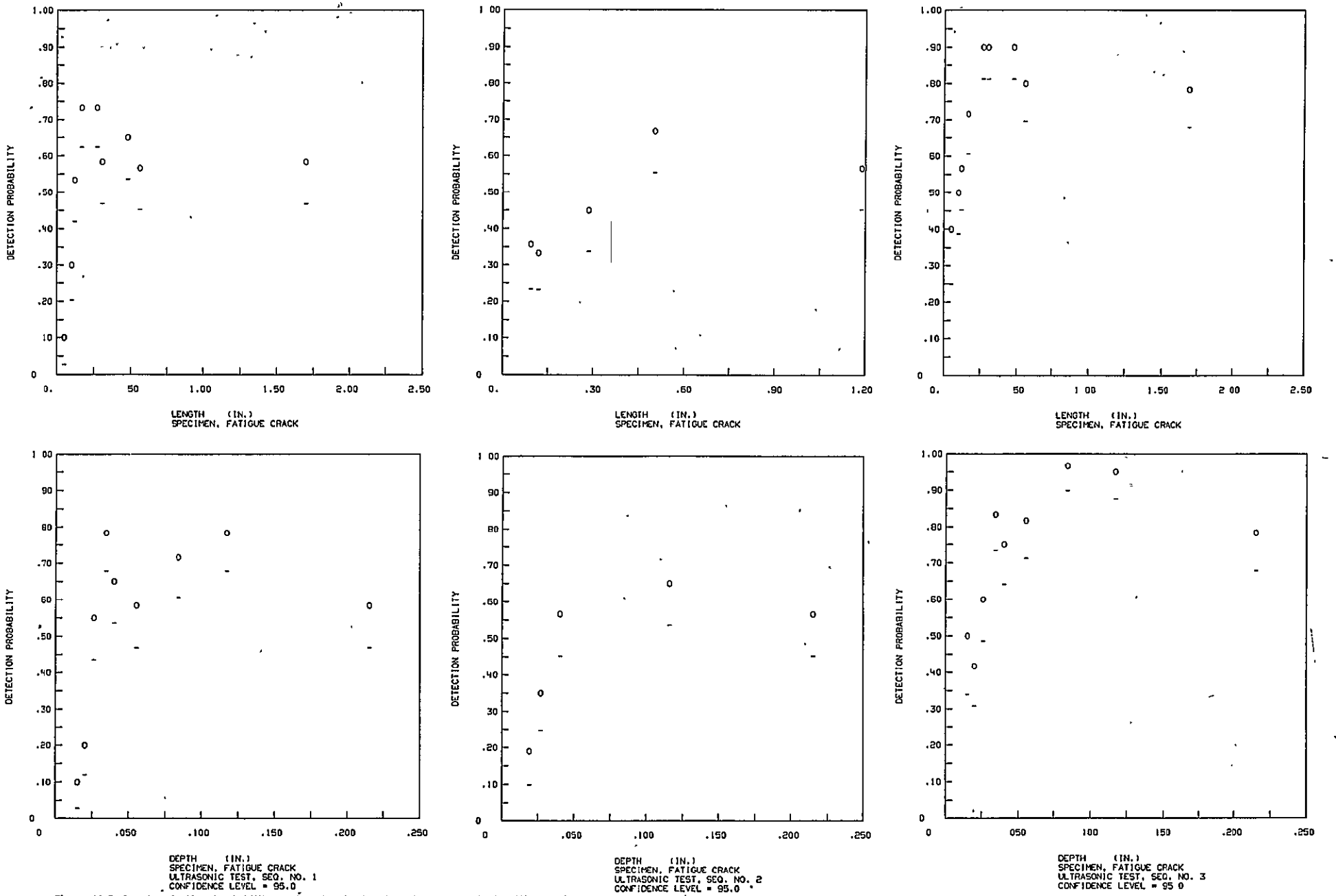

Figure V-5 Crack Detection Probability for Longitudinal Welds with Crowns by the Ultrasonic Method Plotted at 95% Probability and 95% Confidence

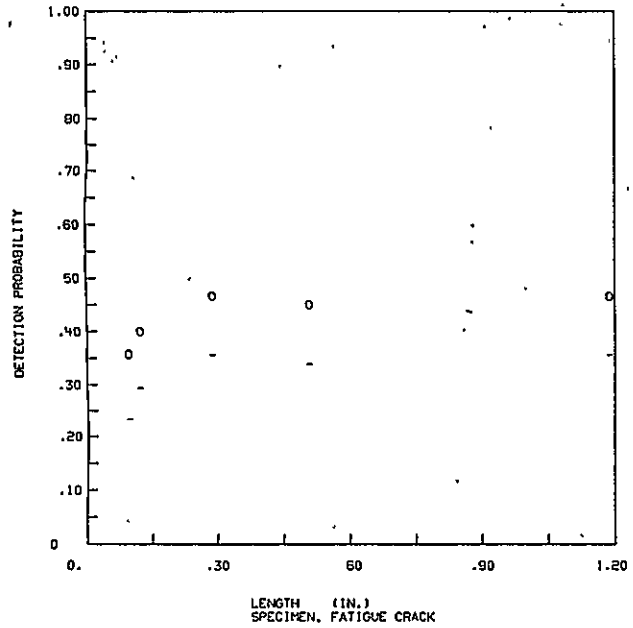

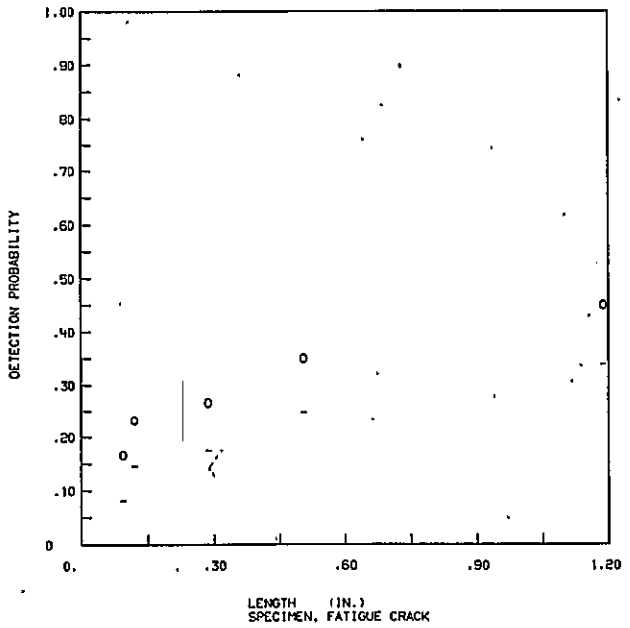

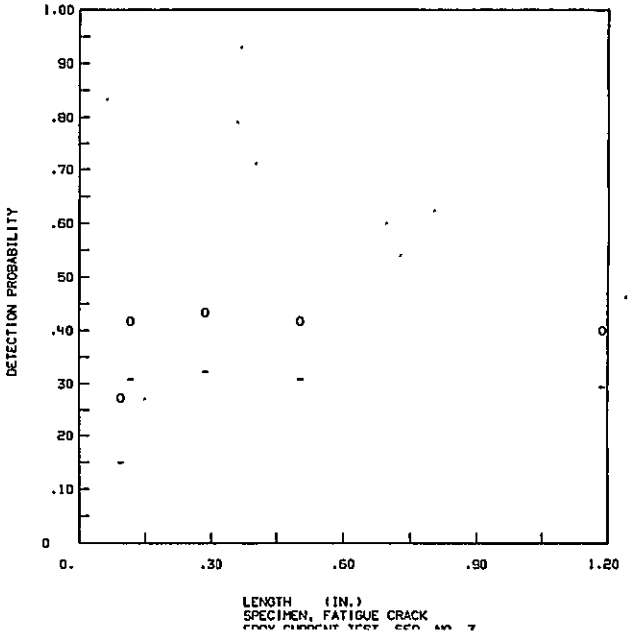

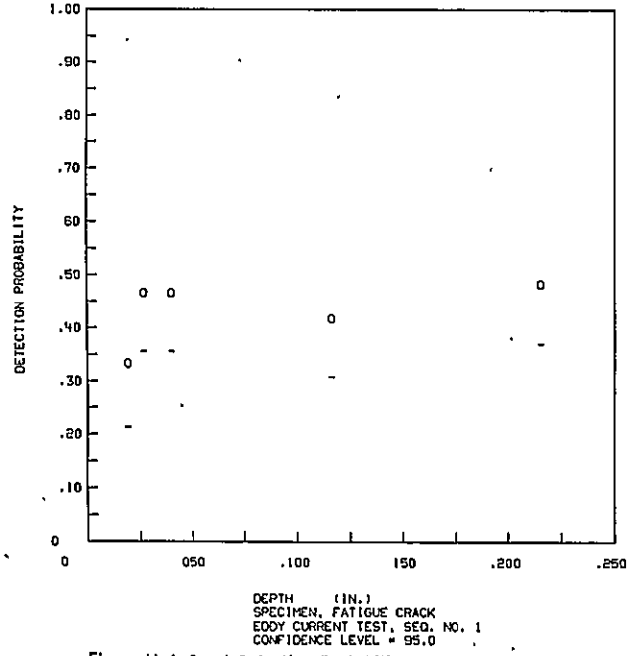

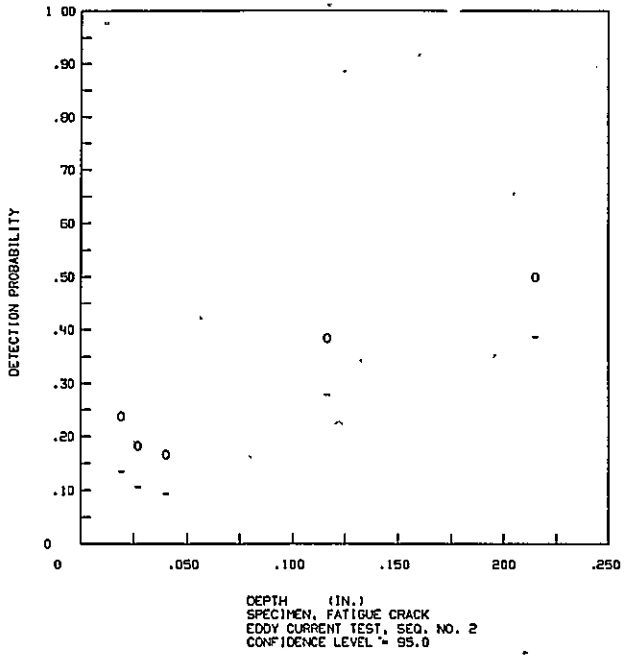

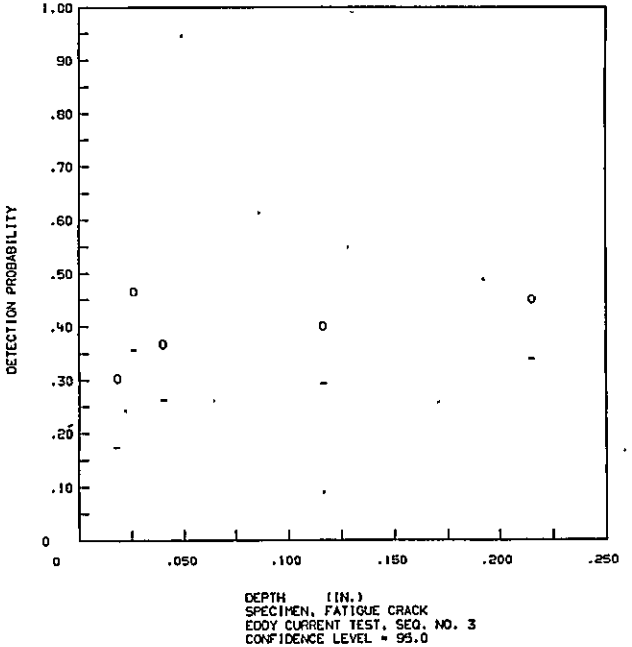

Figure V-6 Crack Detection Probability for Longitudinal Welds with Crowns by the Eddy Current Method Plotted at 95% Probability and 95% Confidence

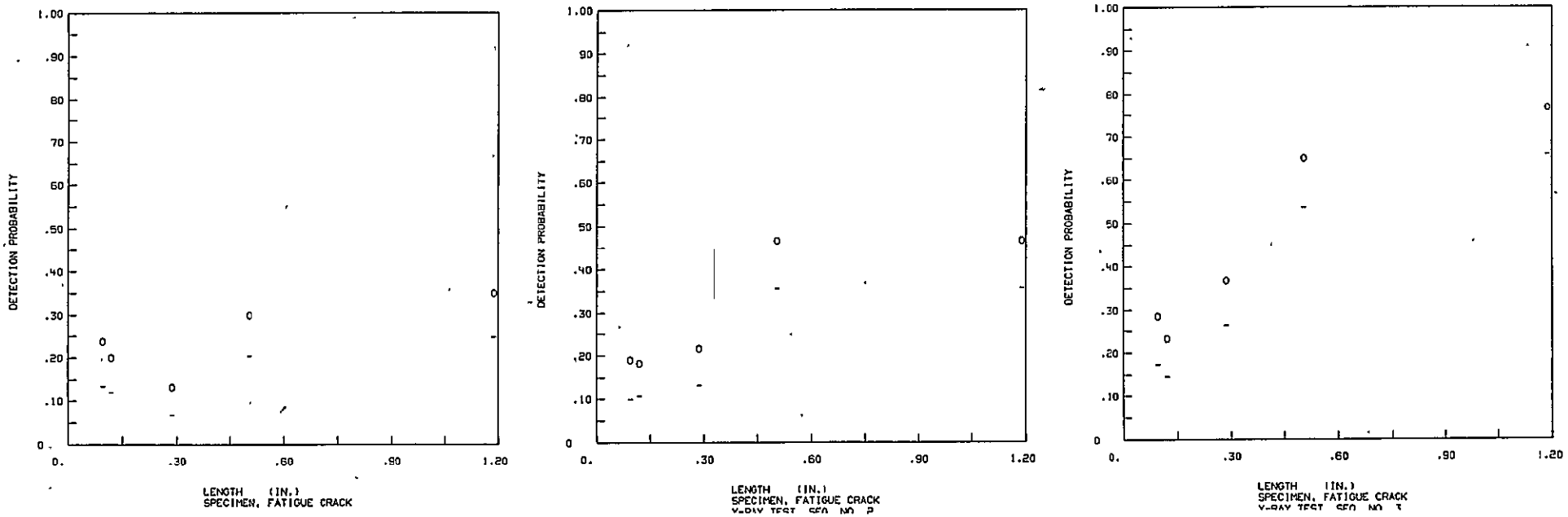

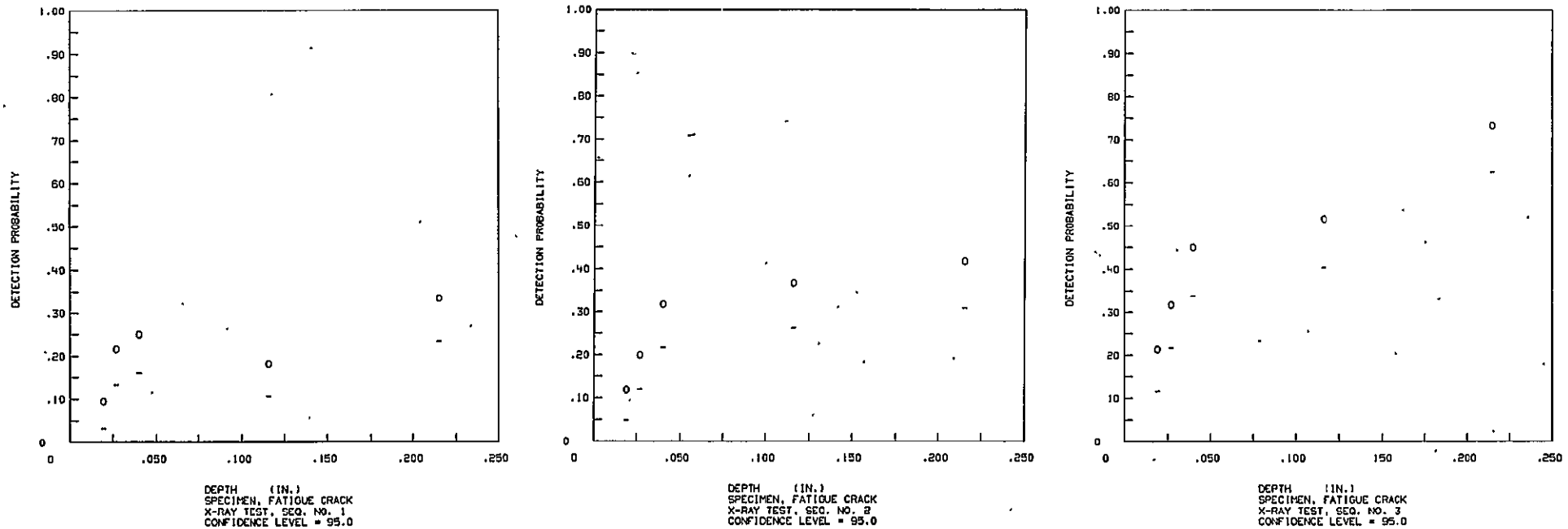

Figure V-7 Crack Detection Probability for Longitudinal Welds with Crowns by the X-Radiographic Method Plotted at 95% Probability and 95% Confidence

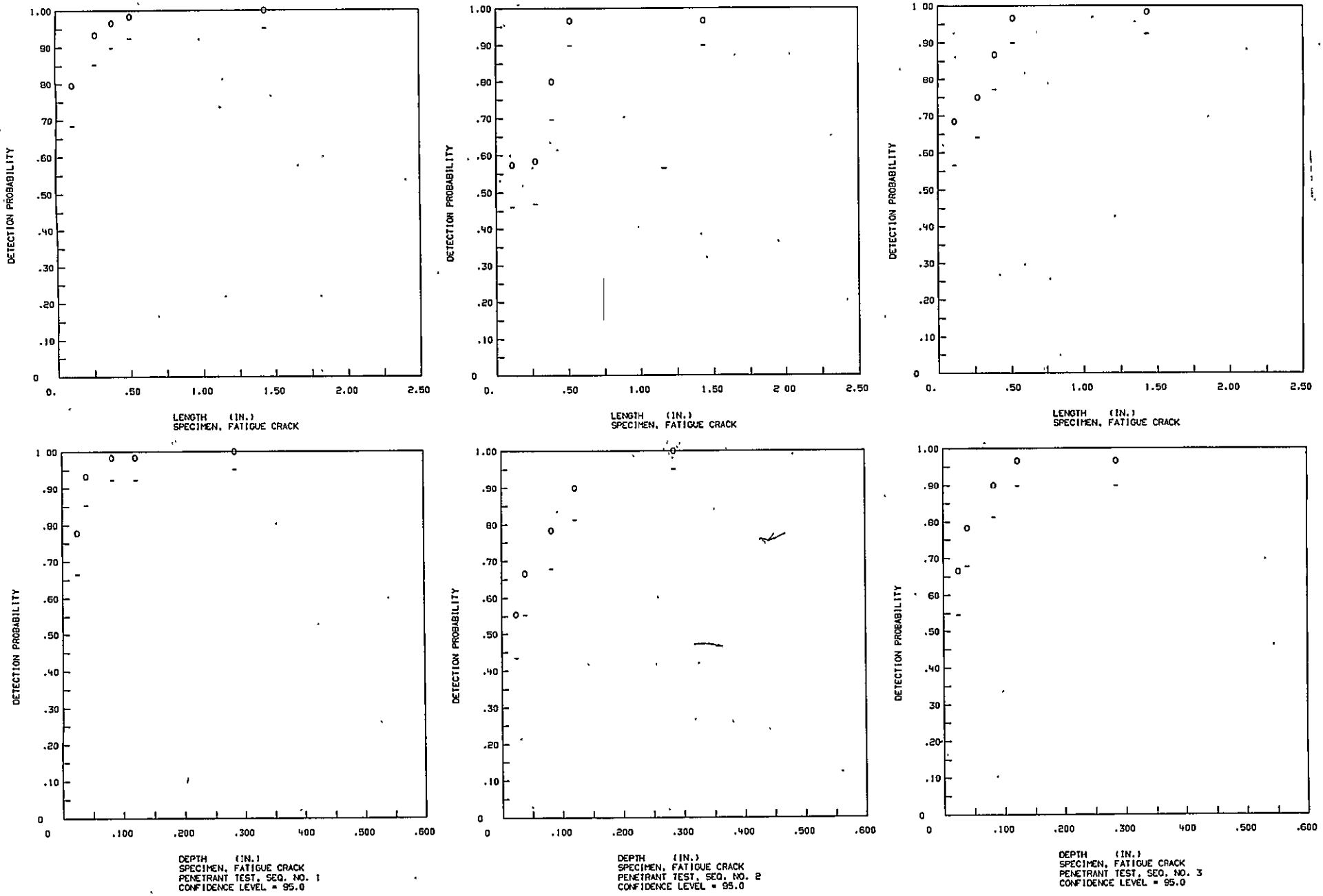

Figure V-8 Crack Detection Probability for Transverse Welds with Crowns by the Penetrant Method Plotted at 95% Probability and 95% Confidence

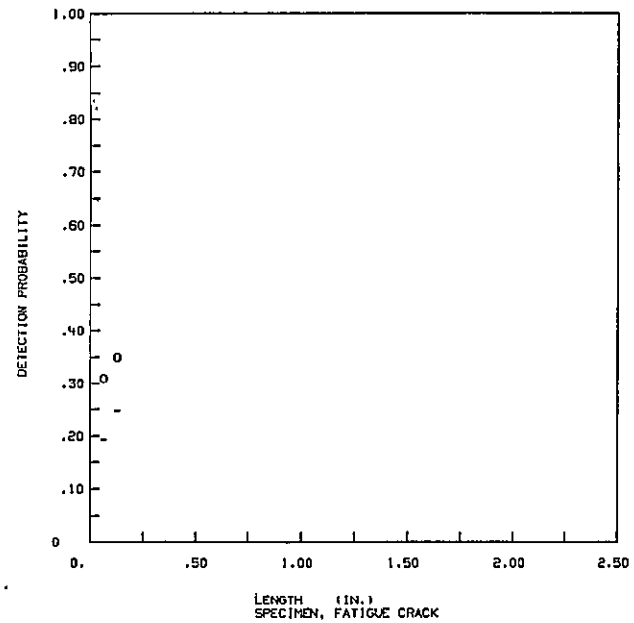

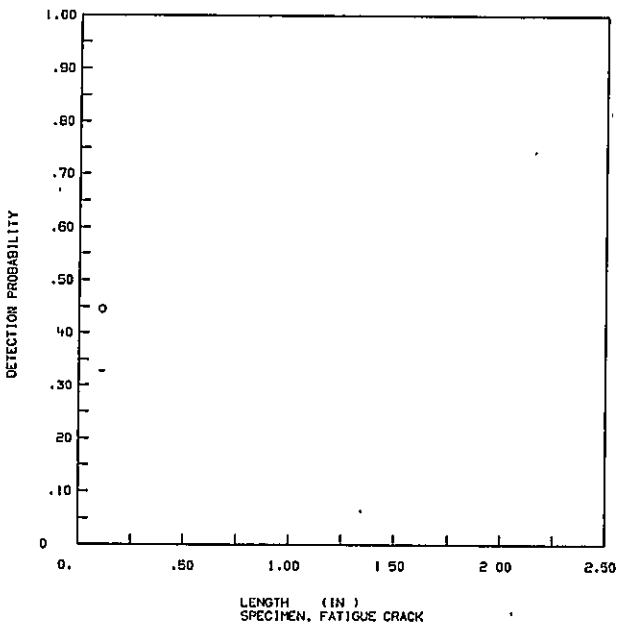

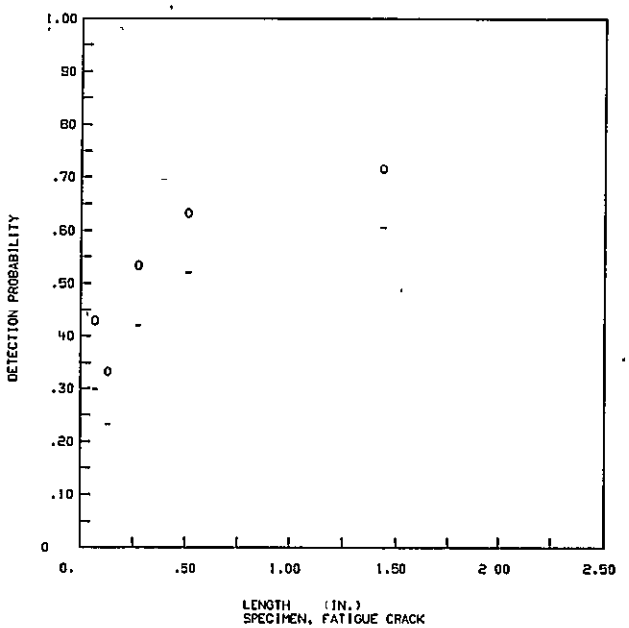

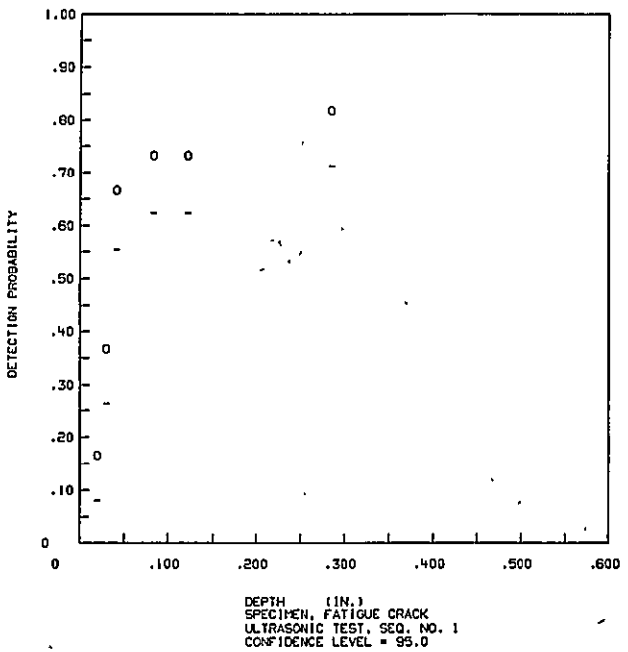

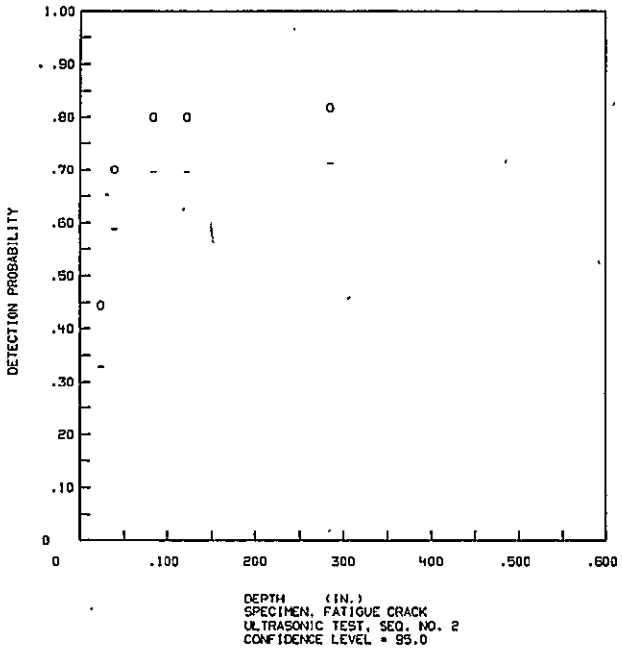

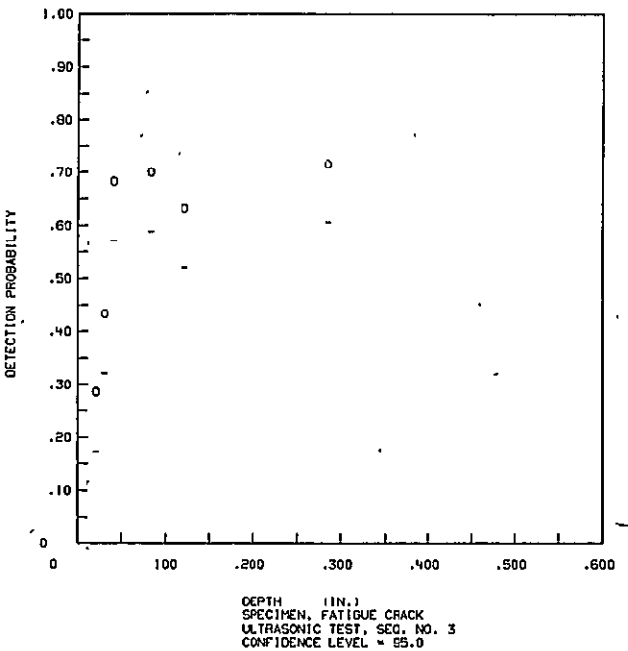

Figure V-9 Crack Detection Probability for Transverse Welds-with Crowns by the Ultrasonic Method Plotted at 95% Probability and 95% Confidence

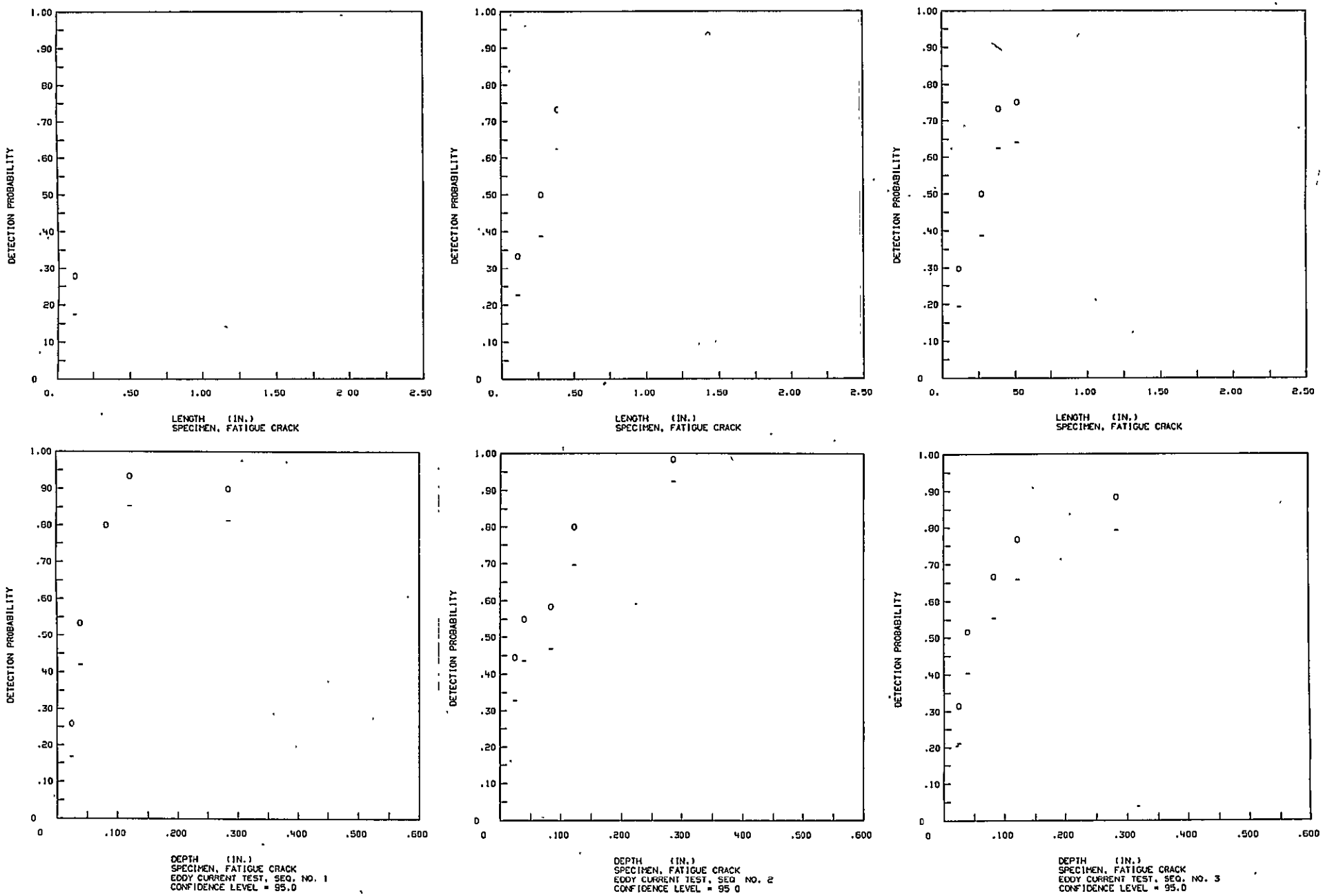

Figure V-10 Crack Detection Probability for Transverse Welds with Crowns by the Eddy Current Method Plotted at 95% Probability and 95% Confidence

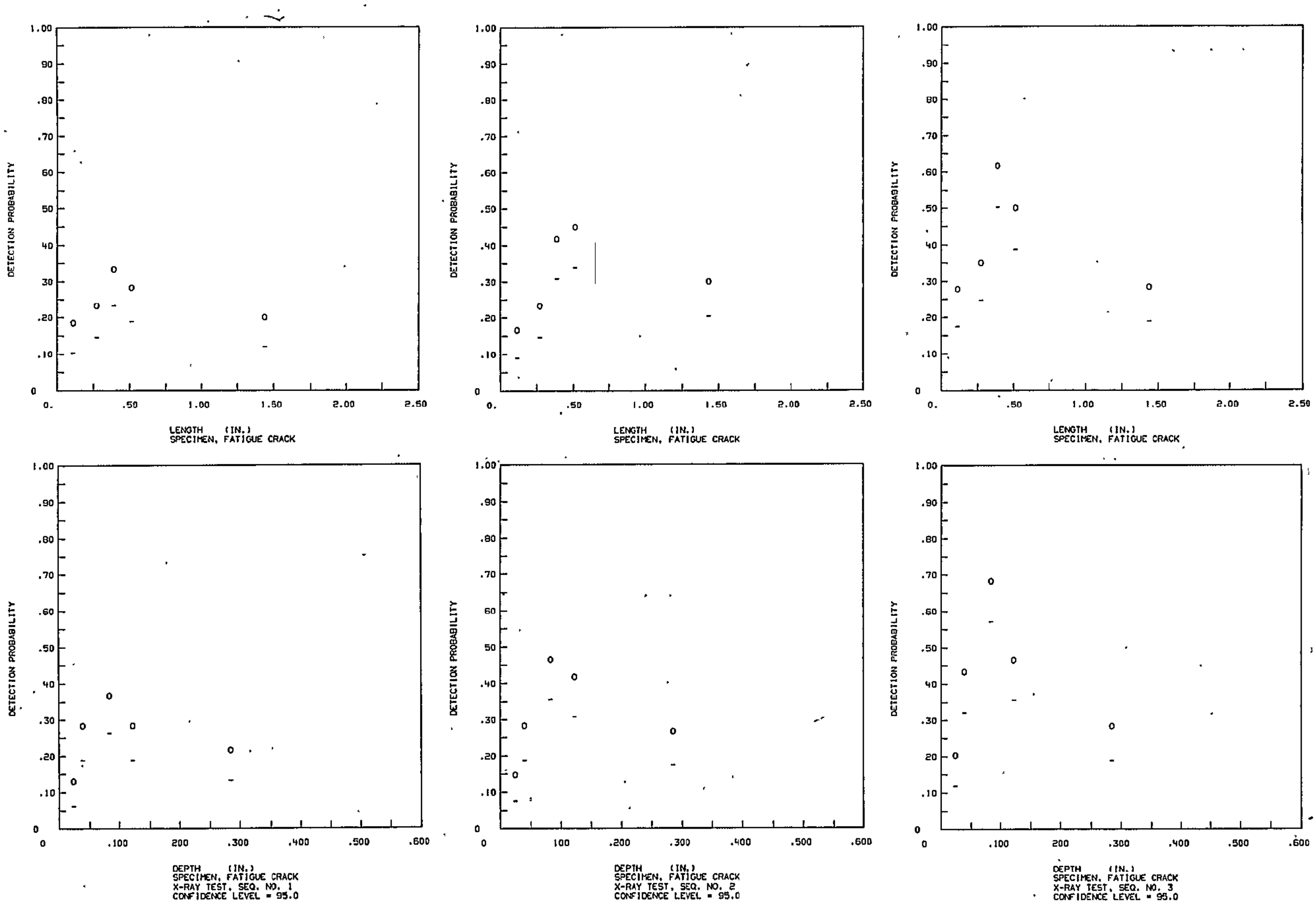

Figure V-11 Crack Detection Probability for Transverse Welds with Crowns by the X-Radiographic Method Plotted at 95% Probability and 95% Confidence

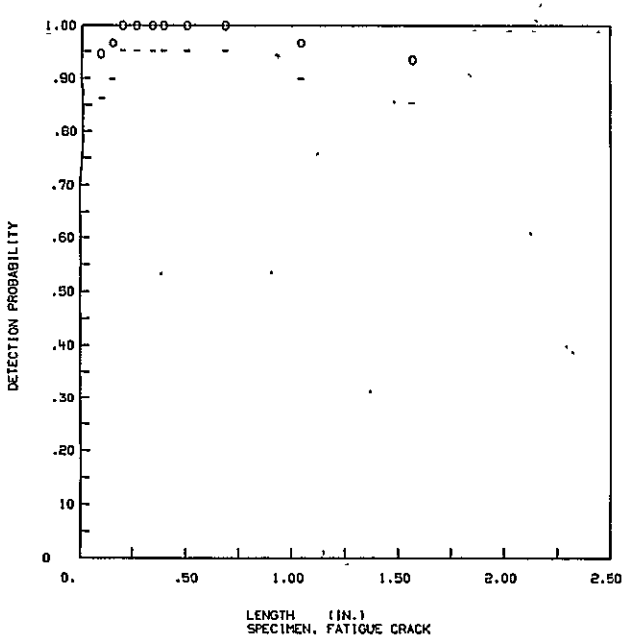

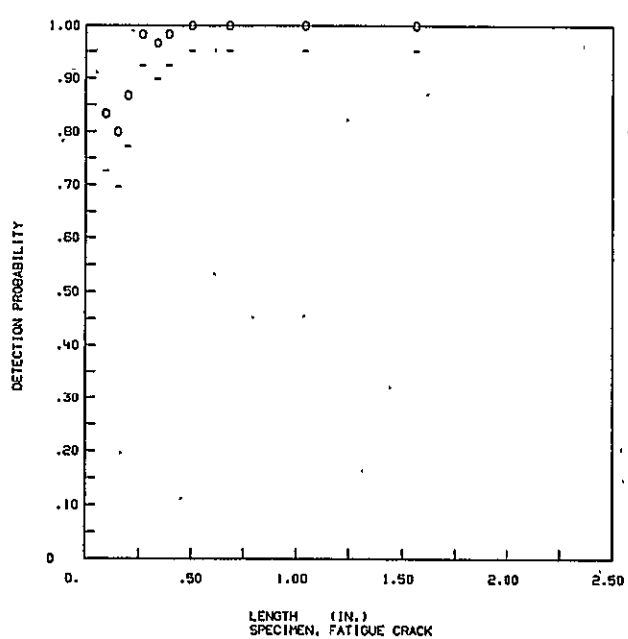

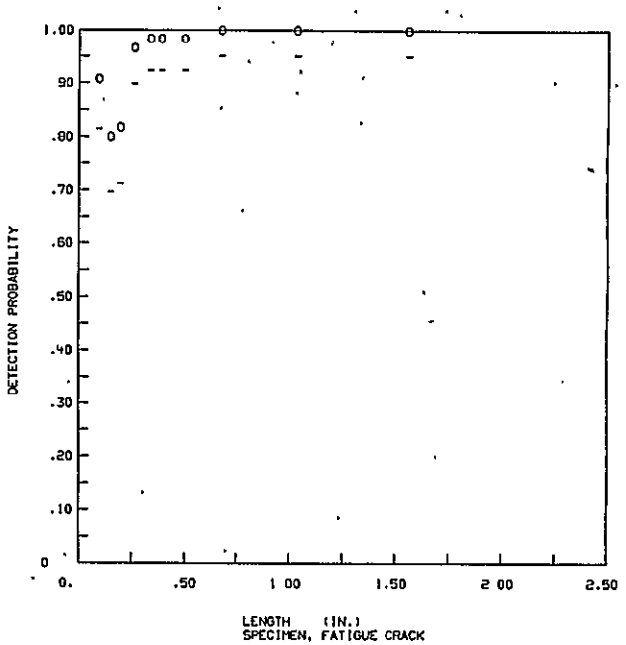

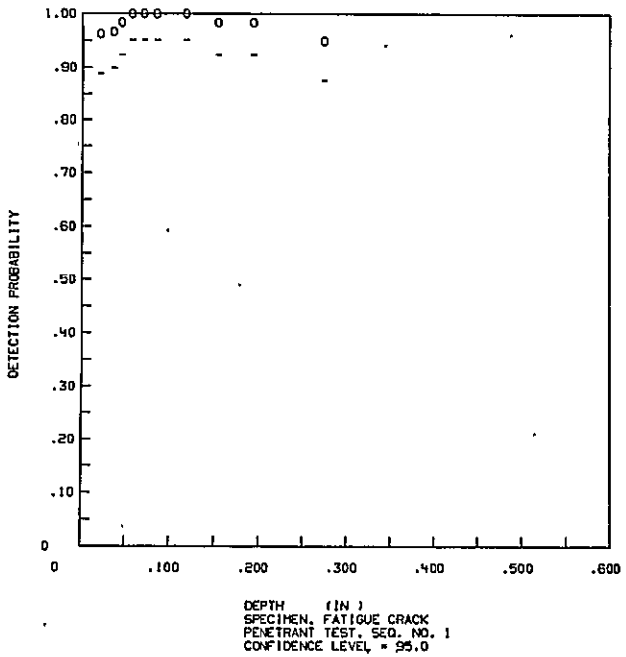

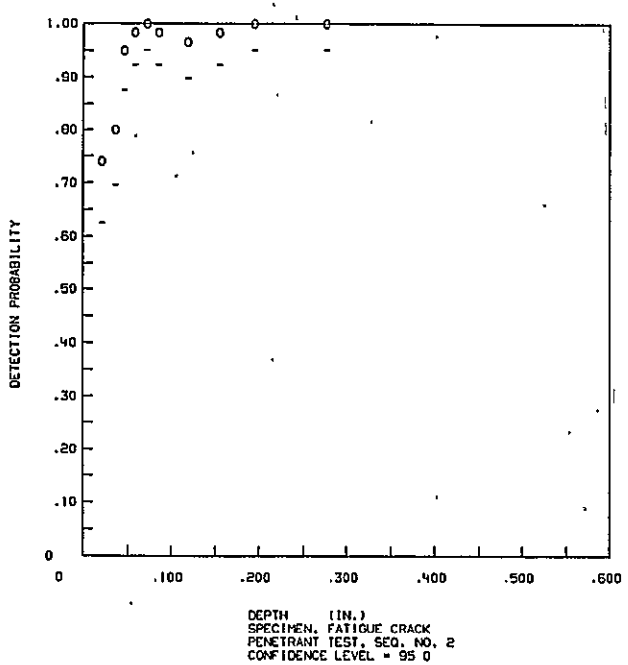

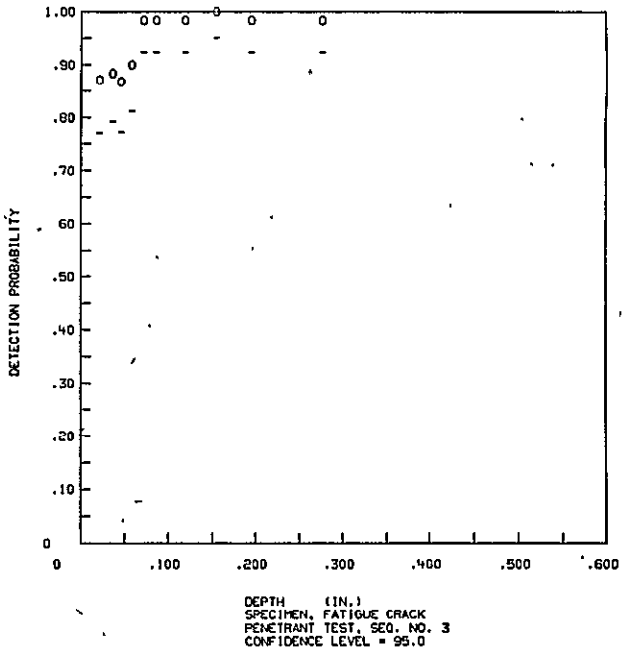

Figure V-12 Crack Detection Probability for Flush, Longitudinal Welds by the Penetrant Method Plotted at 95% Probability and 95% Confidence

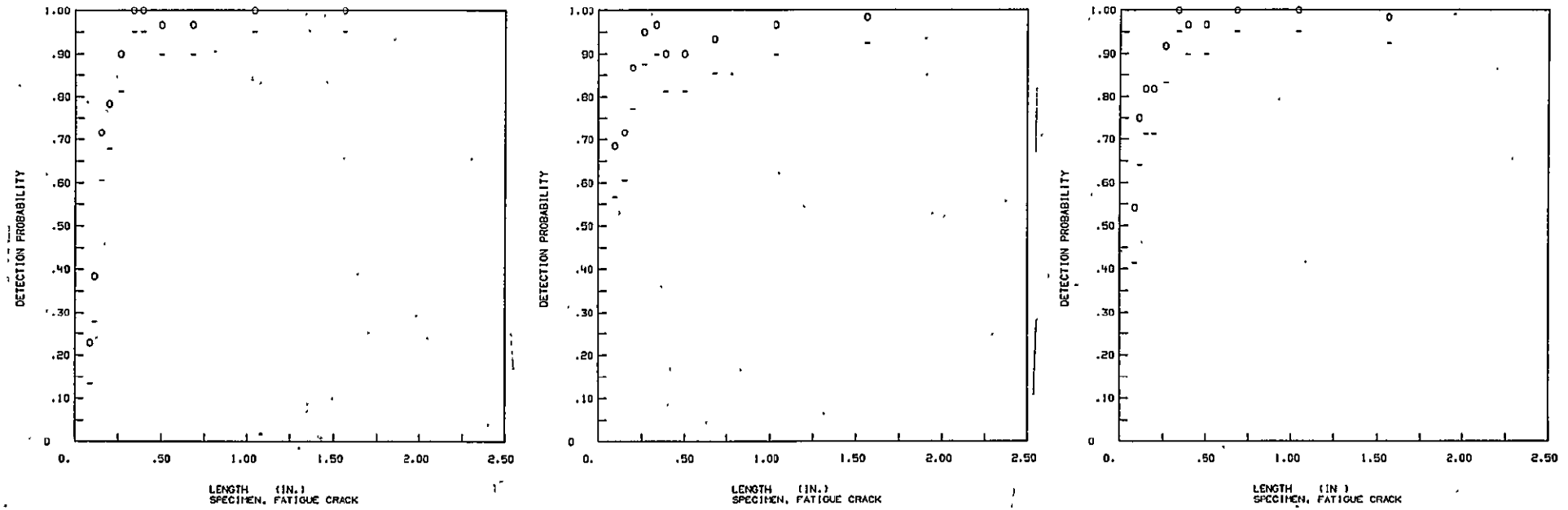

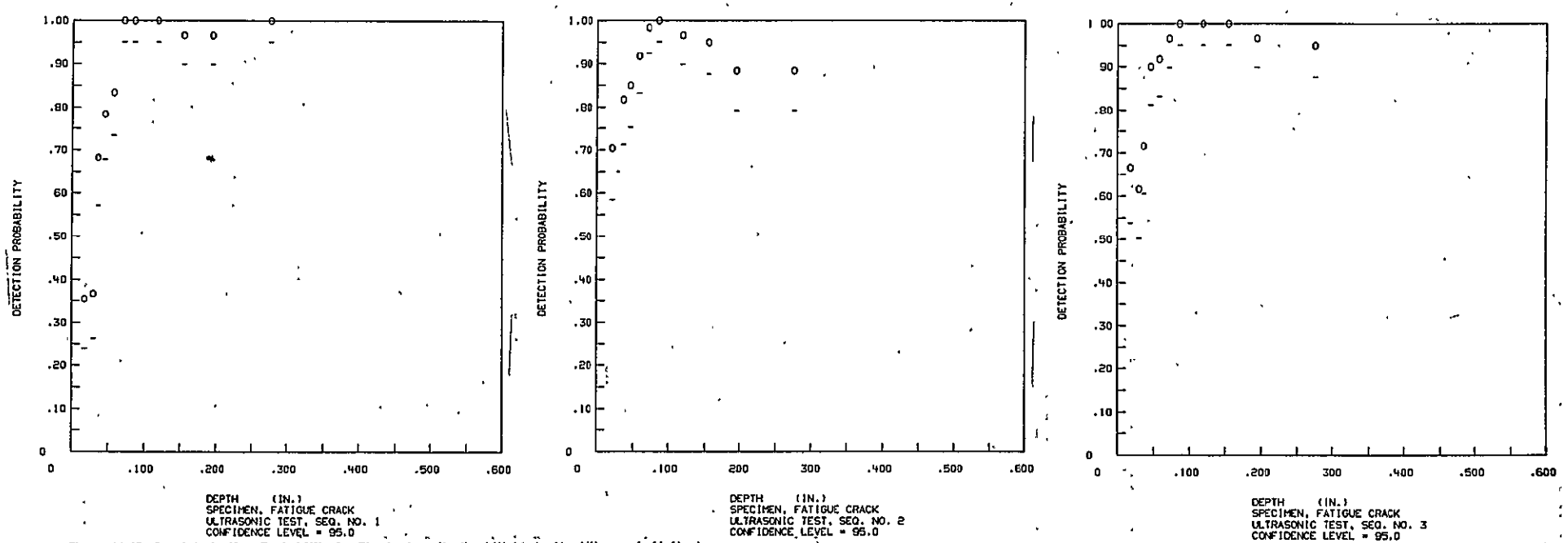

Figure V-13 Crack Detection Probability for Flush, Longitudinal Welds by the Ultrasonic Method Plotted at 95% Probability and 95% Confidence

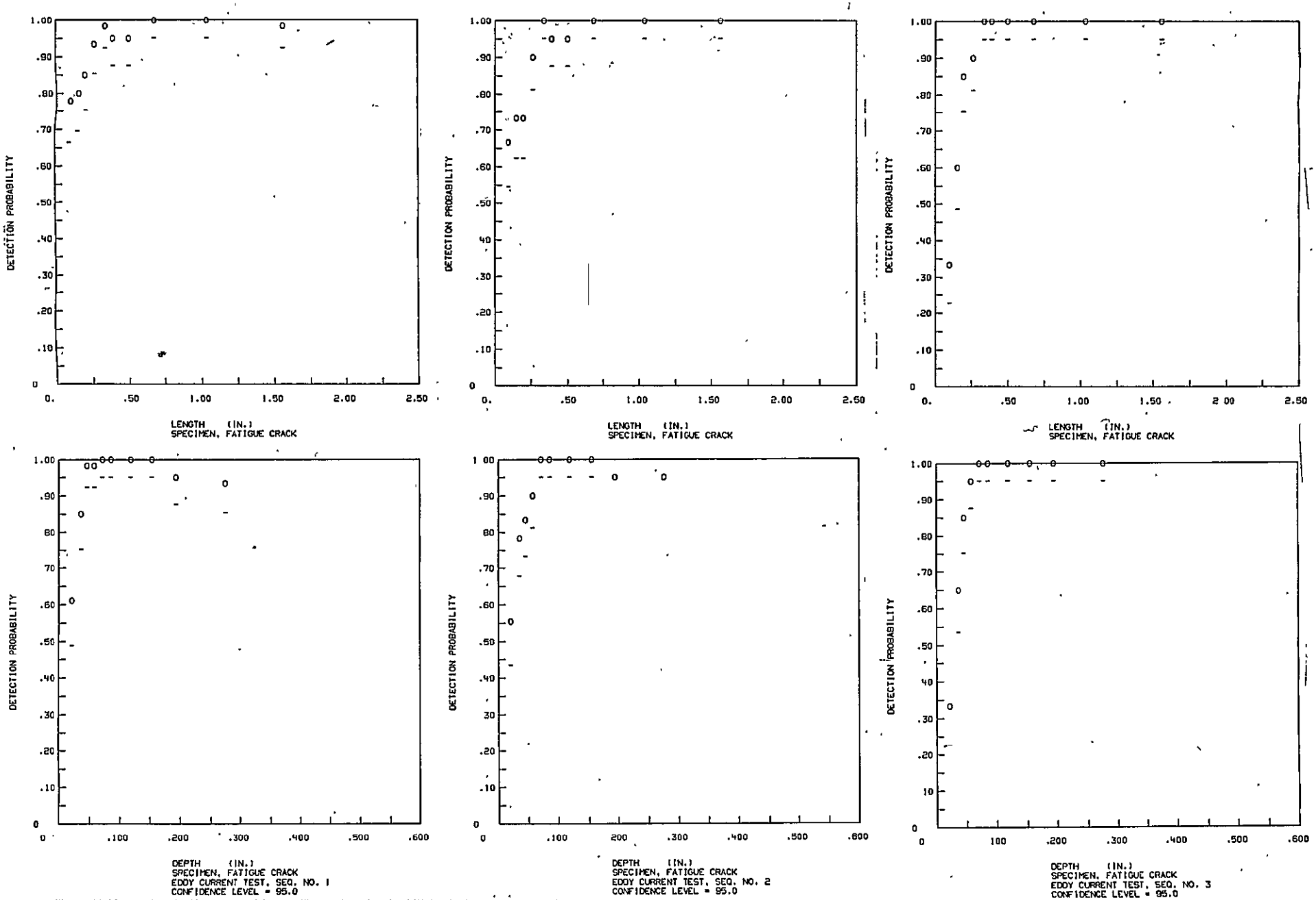

Figure V-14 Crack Detection Probability for Flush, Longitudinal Welds by the Eddy Current Method Plotted at 95% Probability and 95% Confidence

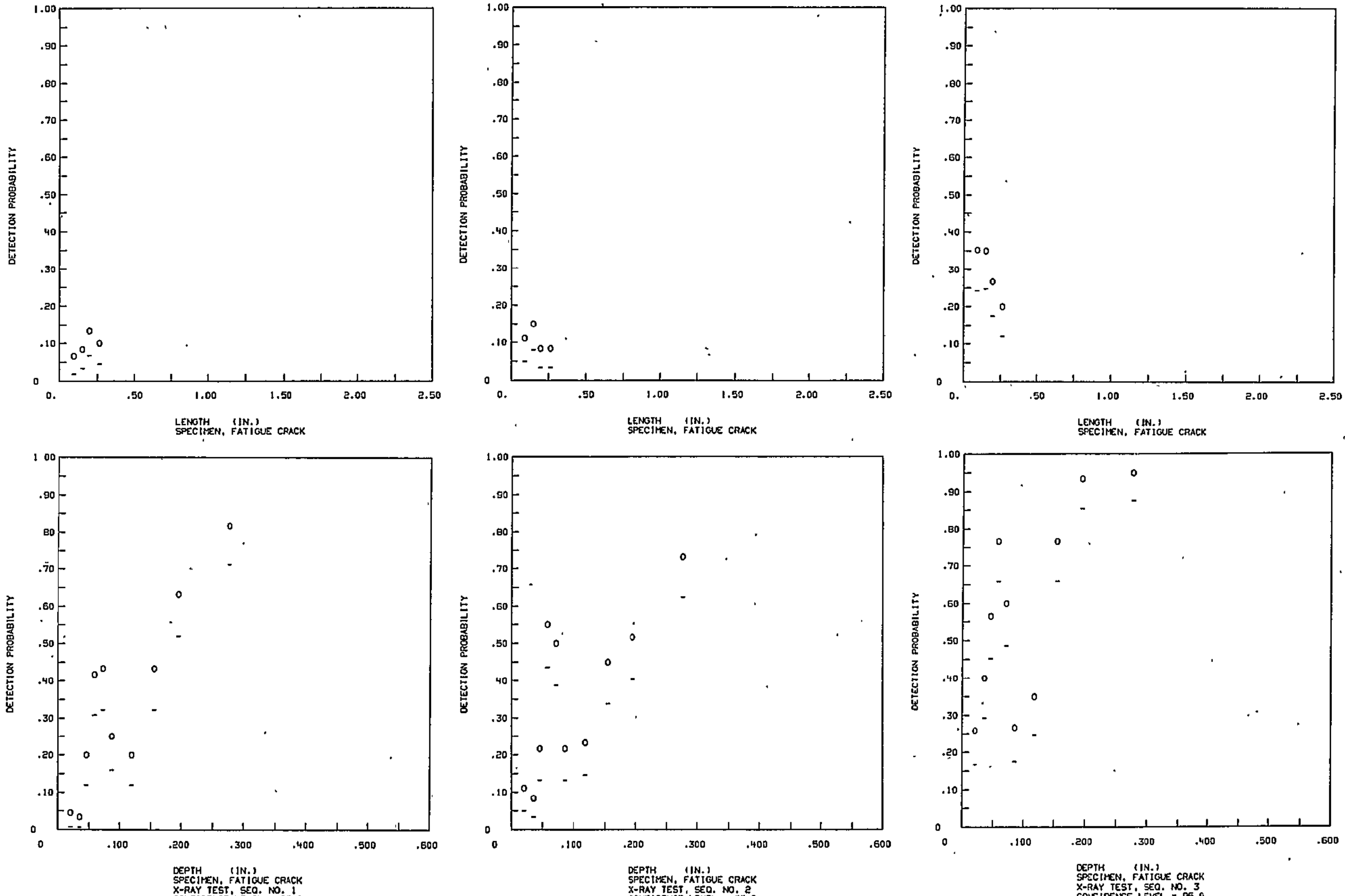

Figure V-15 Crack Detection Probability for Flush, Longitudinal Welds by the X-Radiographic Method Plotted at 95% Probability and 95% Confidence

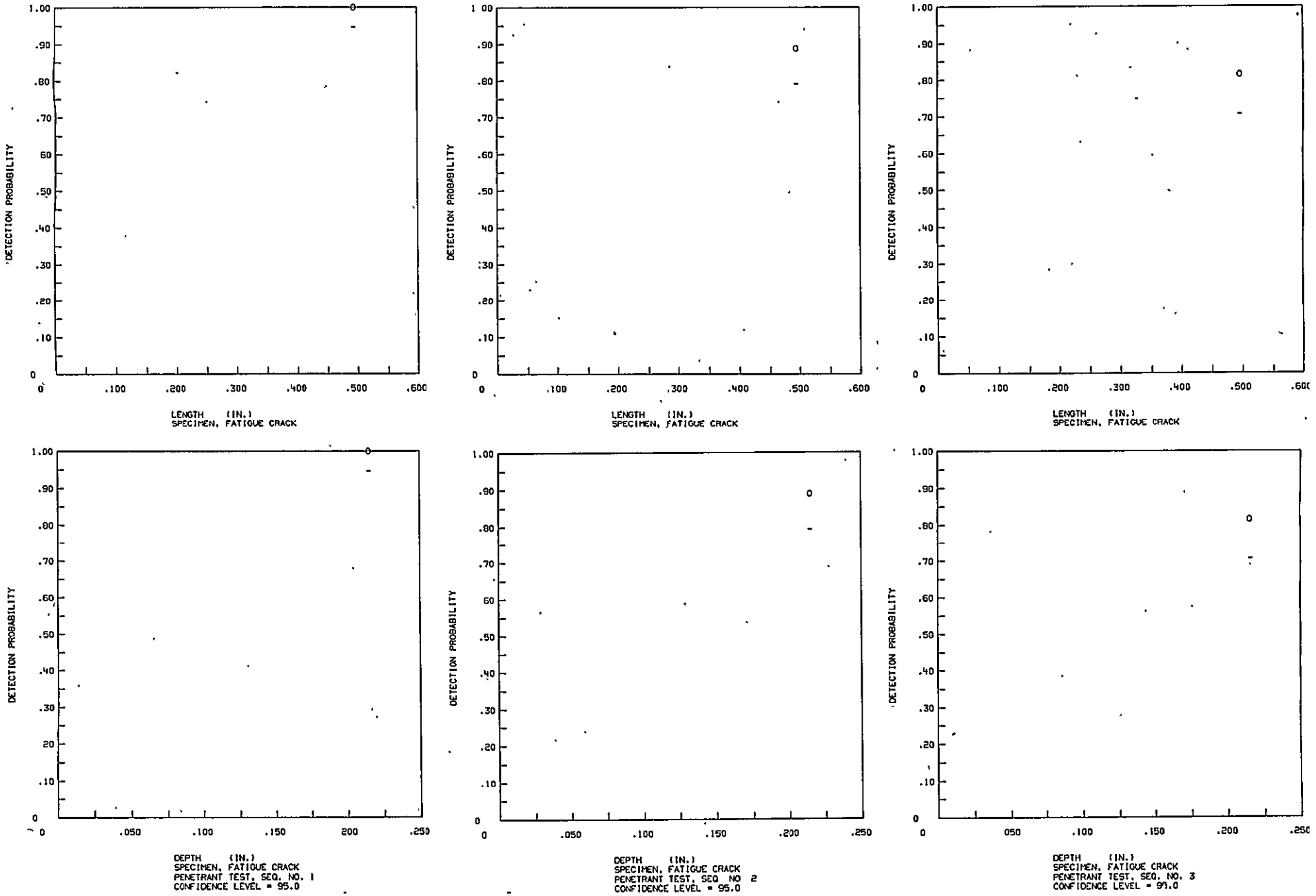

Figure V-16 Crack Detection Probability for Flush, Transverse Welds by the Penetrant Method Plotted at 95% Probability and 95% Confidence

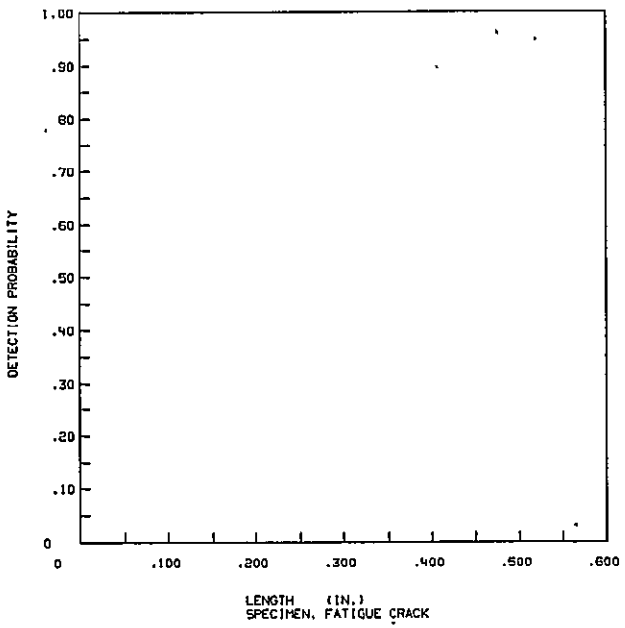

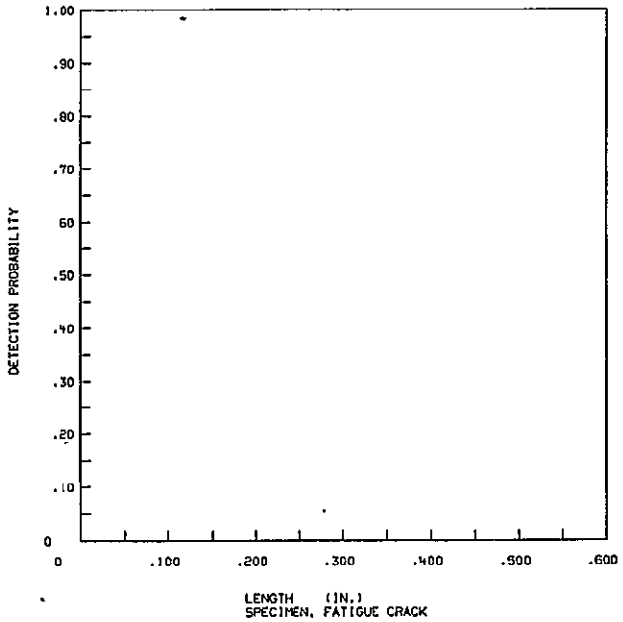

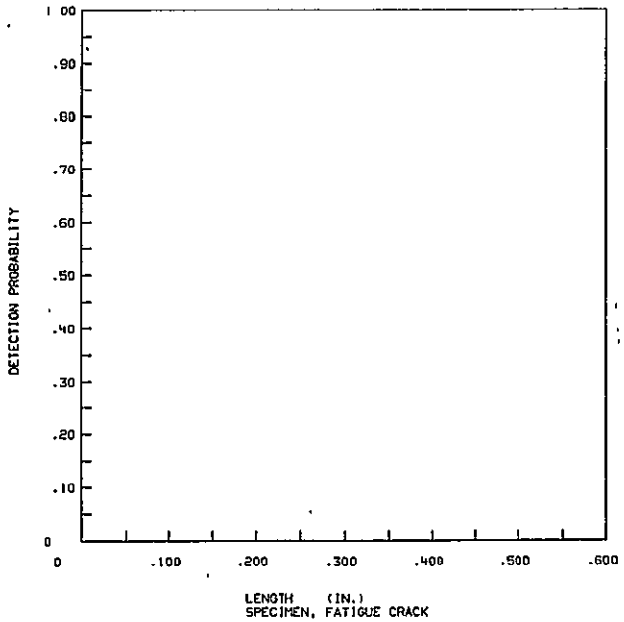

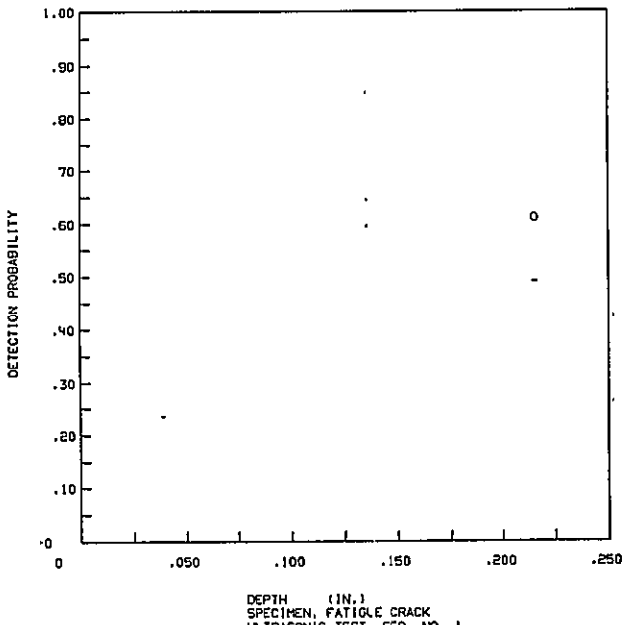

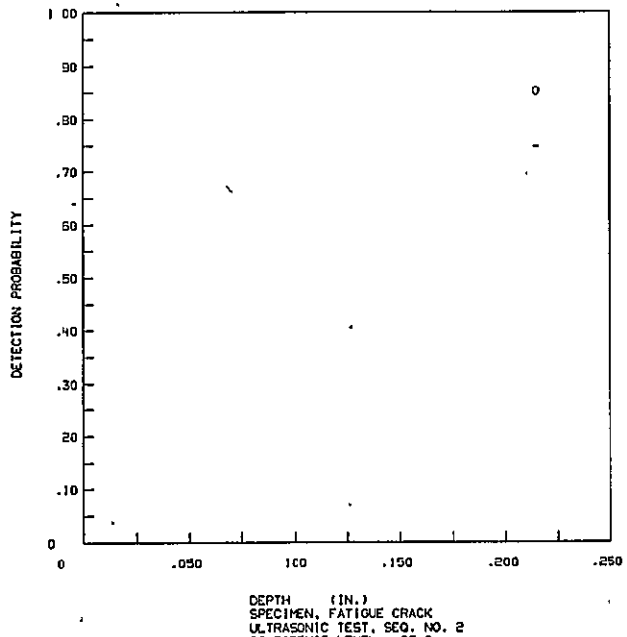

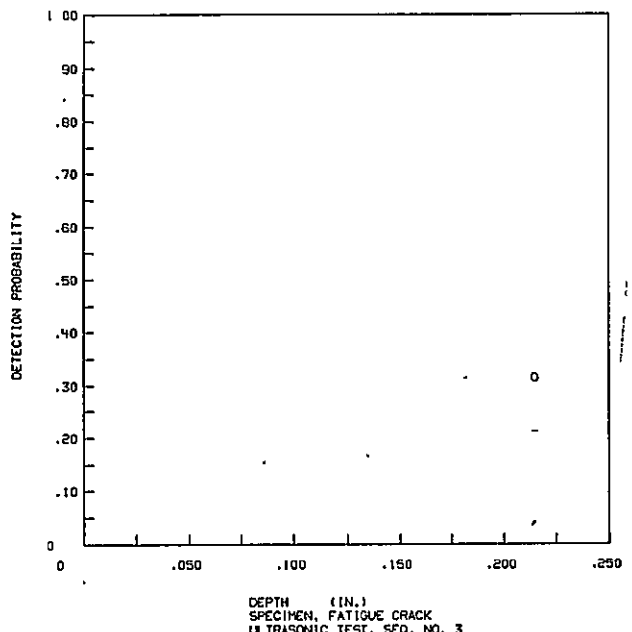

Figure V-17 Crack Detection Probability for Flush, Transverse Welds by the Ultrasonic Method Plotted at 95% Probability and 95% Confidence

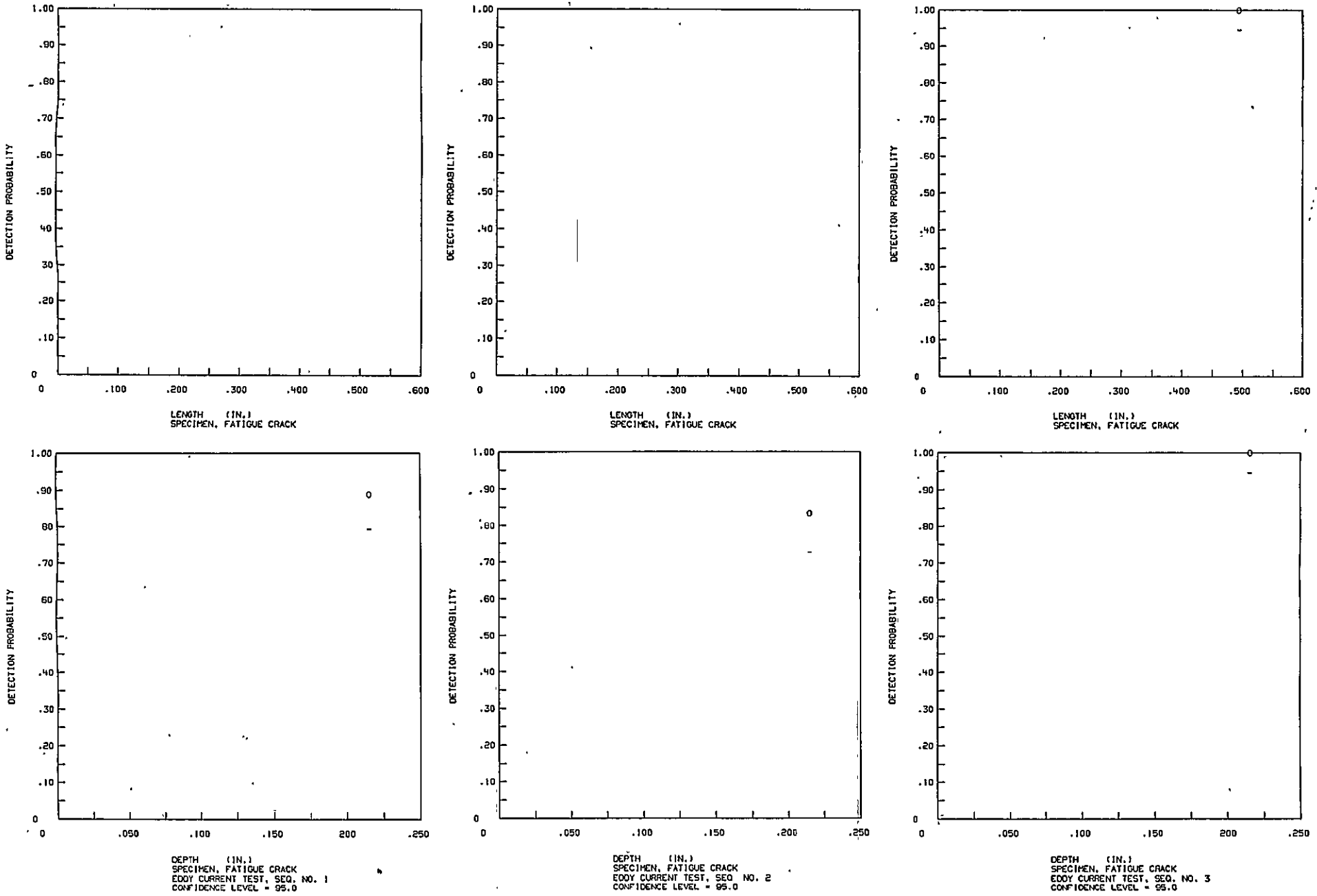

Figure V-18 Crack Detection Probability for Flush, Transverse Welds by the Eddy Current Method Plotted at 95% Probability and 95% Confidence

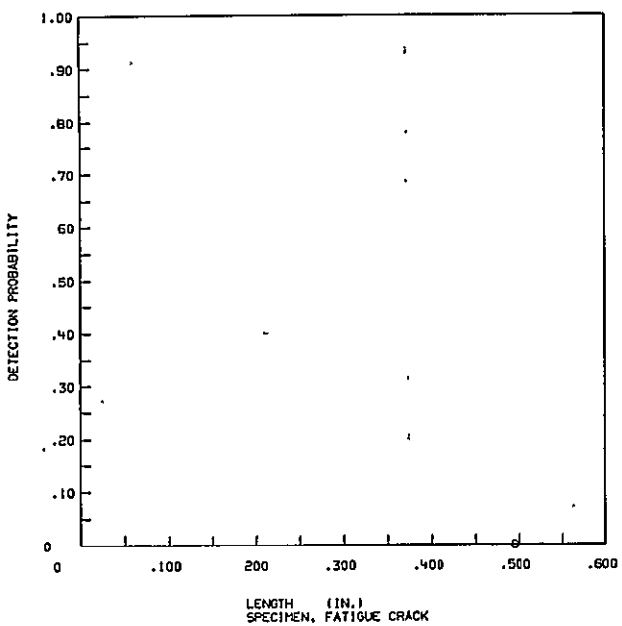

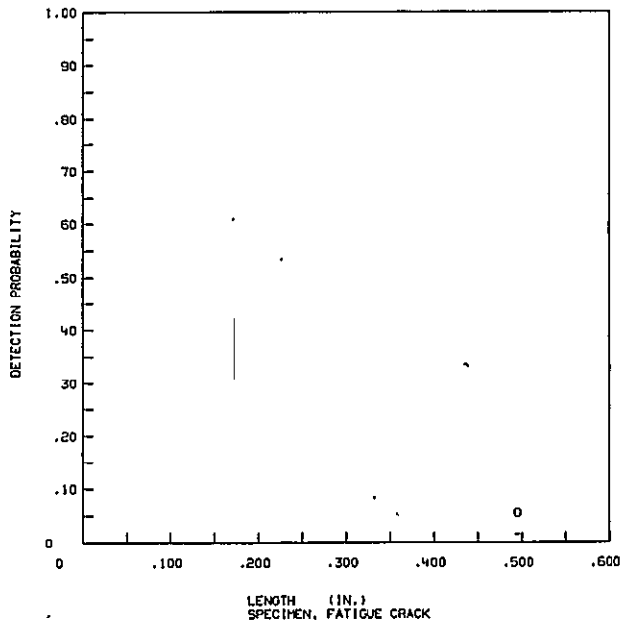

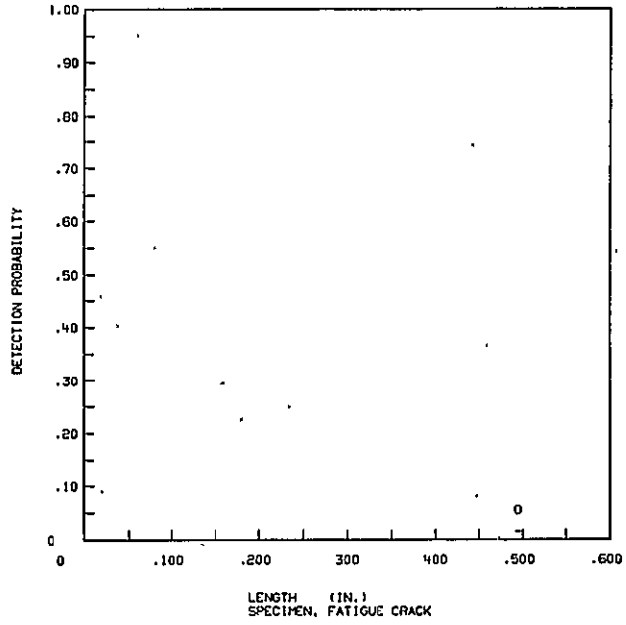

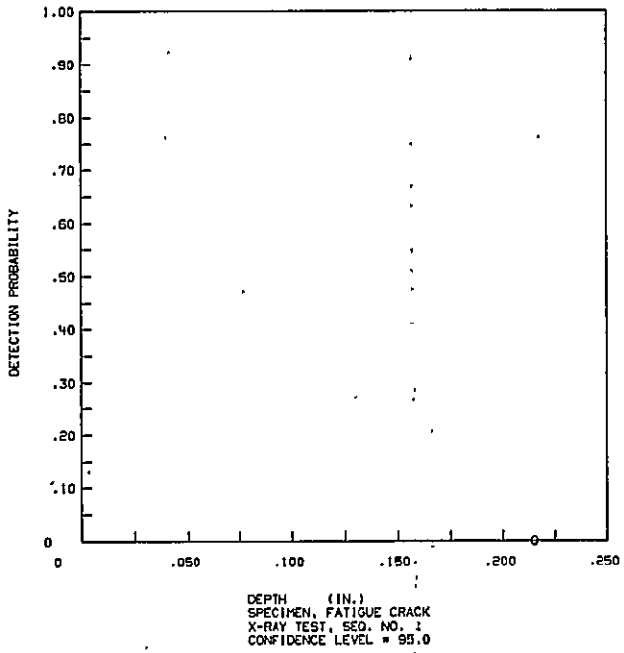

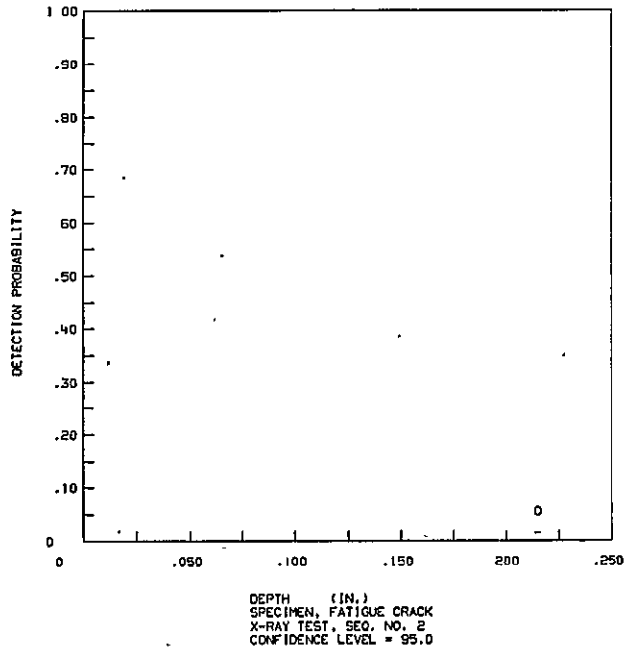

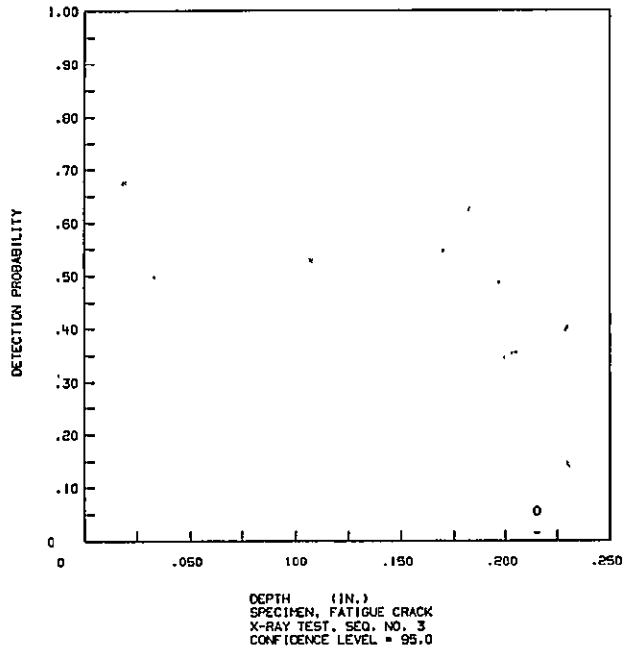

Figure V-19 Crack Detection Probability for Flush, Transverse Welds by the X-Radiographic Method Plotted at 95% Probability and 95% Confidence

VI. CONCLUSIONS AND RECOMMENDATIONS

Liquid penetrant, ultrasonic, eddy current and x-radiographic methods of nondestructive testing were demonstrated to be applicable and sensitive to the detection of small, tightly closed flaws in stringer stiffened panels and welds in 2219-T87 aluminum alloy. The results vary somewhat for that established for flat, parent metal panel data.

For the stringer stiffened panels, the stringer member in close proximity to the flaw and the radius at the flaw influence detection by all NDT methods evaluated. The data are believed to be representative of a production depot maintenance operation where inspection can be optimized to an anticipated flaw area and where automated C-scan recording is used.

LOP detection reliabilities obtained are believed to be representative of a production operation. The tightness of the flaw and diffusion bond formation at the flaw could vary the results considerably. It is evident that this type of flaw challenges detection reliability and that efforts to enhance detection should be used for maximum detection reliability.

Data obtained on fatigue cracked weld panels is believed to be a good model for evaluating the detection sensitivity of cracks induced by production welding processes. The influence of the weld crown on detection reliability supports a strong case for removing weld bead crowns prior to inspection for maximum detection reliability.

The quantitative inspection results obtained and presented herein add to the nondestructive testing technology data bases in detection reliability. These data are necessary to implement fracture control design and acceptance criteria on critically loaded hardware. Data may be used as a design guide for establishing engineering acceptance criteria. This use should however, be tempered by considerations of material type, condition and configuration of the hardware and also by the controls maintained in the inspection processes. For critical items and/or for special applications, qualification of the inspection method is necessary on the actual hardware configuration. Improved sensitivities over that reflected in these data may be expected if rigid configurations and inspection methods control are imposed.

The nature of inspection reliability programs of the type described herein requires rigid parameter identification and control in order to generate meaningful data. Human factors in the inspection process and inspection process control will influence the data

output and is not readily recognized on the basis of a few samples. A rationale and criteria for handling descrepant data needs to be developed. In addition, documentation of all parameters which may influence inspection results is necessary to enable duplication of the inspection methods and inspection results in independent evaluations. The same care in analysis and application of the data must be used in relating the results obtained to a fracture control program on functional hardware.

-APPENDIX A-

LIQUID PENETRANT INSPECTION PROCEDURE FOR WELD PANELS, STIFFENED PANELS, AND LOP PANELS

1.0 SCOPE

1.1 This procedure describes liquid penetrant inspection of aluminum for detecting surface defects (fatigue cracks and LOP at the surface).

2.0 REFERENCES

2.1 Uresco Corporation Data Sheet No. PN-100

2.2 Nondestructive Testing Training Handbooks P1-4-2, Liquid Penetrant Testing, General Dynamics Corporation, 1967.

2.3 Nondestructive Testing Handbook, McMasters Ronald Press, 1959, Volume I, Sections 6, 7 and 8.

3.0 EQUIPMENT

3.1 Uresco P-149 High Sensitive Fluorescent Penetrant

3.2 Uresco K-410 Spray Remover

3.3 Uresco D499C Spray Developer

3.4 Cheese Cloth

3.5 Ultraviolet light source (Magnaflux Black-Ray B-100 with General Electric H-100, FL-4, Projector flood lamp and Magnaflux 3901 filter.

3.6 Quarter inch paint brush

3.7 Isopropyl Alcohol

3.8 Rubber Gloves

3.9 Ultrasonic Cleaner (Sonogen Ultrasonic Generator, Mod. G1000)

3.10 Light Meter, Weston Model 703, Type 3A

4.0 PERSONNEL

4.1 The liquid penetrant inspection shall be performed by technically qualified personnel.

5.0 PROCEDURE

5.1 Clean panels to be penetrant inspected by immersing in isopropyl alcohol in the ultrasonic cleaner and running for 1 hour; stack on tray and air dry.

5.2 Lay panels flat on work bench and apply P-149 penetrant using a brush to the areas to be inspected. Allow a dwell time of 30 minutes.

5.3 Turn on the ultraviolet light and allow a warm up of 15 minutes.

5.3.1 Measure the intensity of the ultraviolet light and assure a minimum reading of 125 foot candles at 15" from the filter. (or 1020 micro watts per cm^2)

5.4 After the 30 minute penetrant dwell time, remove the excess penetrant remaining on the panel as follows:

5.4.1 With dry cheese cloth, remove as much penetrant as possible from the surfaces of the panel.

5.4.2 With cheese cloth, dampened with K-410, remover wipe remainder of surface penetrant from the panel.

5.4.3 Inspect the panel under ultraviolet light. If surface penetrant remains on the panel, repeat step 5.4.2.

NOTE: The check for cleanliness shall be done in a dark room with no more than two foot candles of white ambient light.

5.5 Spray developer D-499c on the panels by spraying from the pressurized container. Hold the container 6 to 12 inches from the area to be inspected. Apply the developer in a light, thin coat sufficient to provide a continuous film on the surface to be inspected.

NOTE: A heavy coat of developer may mask possible defects.

5.6 After the 30 minute bleed out time, inspect the panels for cracks under black light. This inspection will again be done in a dark room.

5.7 On data sheet record the location of the crack giving "X" dimension to center of fault and the length of the cracks. Also record location as to near, center or far as applicable. See paragraph 5.8.

5.8 Panel orientation and dimensioning of the cracks.

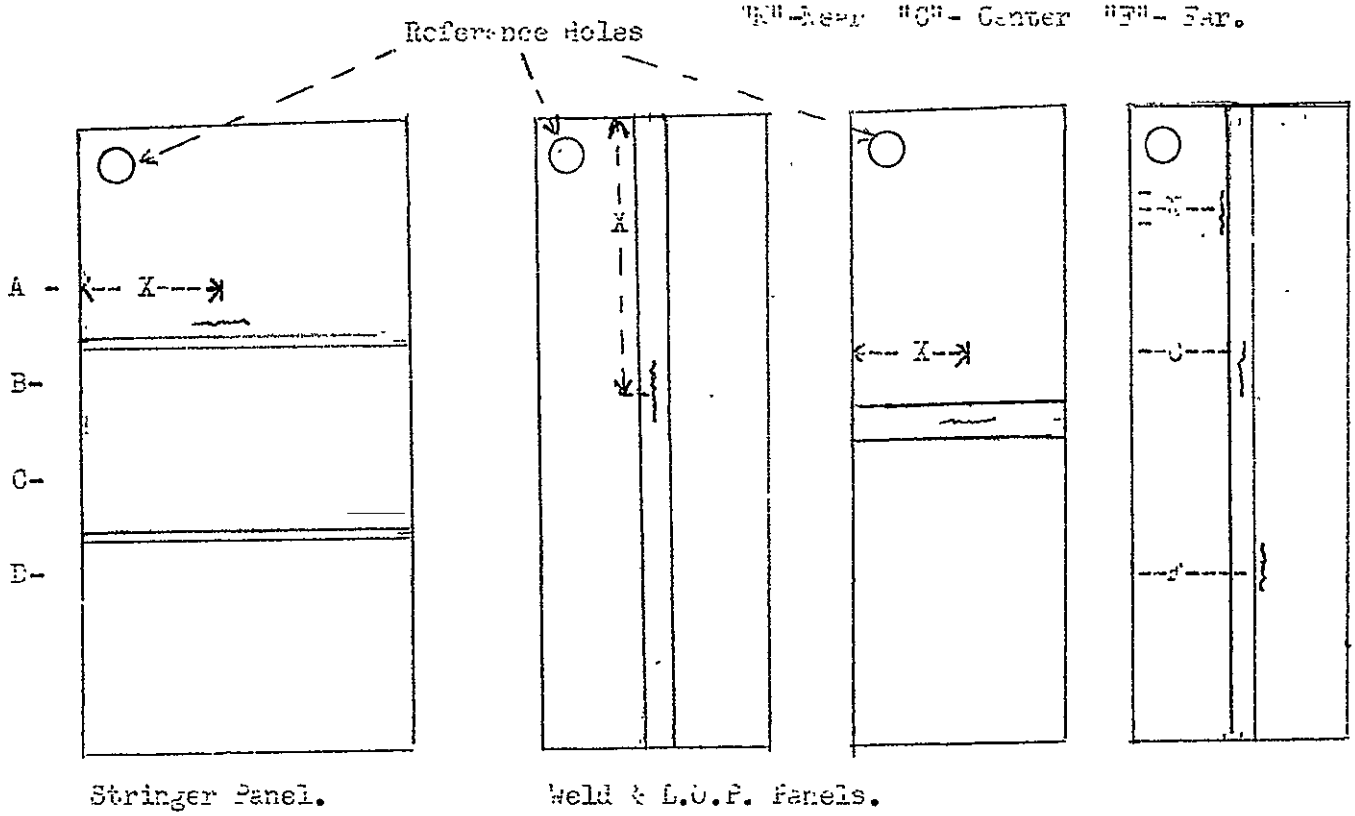

5.9 After read out is completed repeat paragraph 5.1 and turn off ultraviolet light.

-APPENDIX B-

ULTRASONIC INSPECTION FOR "TIGHT FLAW DETECTION BY NDT" PROGRAM - INTEGRALLY STIFFENED PANELS

1.0 SCOPE

1.1 This procedure covers ultrasonic inspection of stringer panels for detecting fatigue cracks located in the radius root of the web and oriented in the plane of the web.

2.0 REFERENCES

2.1 Manufacturer's instruction manual for the UM-715 Reflectoscope instrument.

2.2 Nondestructive Testing Training Handbook, P1-4-4, Volumes I, II and III, Ultrasonic Testing, General Dynamics, 1967.

2.3 Nondestructive Testing Handbook, McMasters, Ronald Press, 1959, Volume II, Sections 43-48.

3.0 EQUIPMENT

3.1 UM-715 Reflectoscope, Automation Industries

3.2 10N Pulser/Receiver, Automation Industries

3.3 E-550 Transigate, Automation Industries

3.4 SIJ-385, .25 inch diameter, flat, 10.0 MHz Transducer; Automation Industries

3.5 SR 150 Budd, Ultrasonic Bridge

3.6 319 DA Alden, Recorder

3.7 Reference Panel - Panel #1 (Stringer)

3.8 Attenuator, Arenberg Ultrasonic Labs (0 db to 122 db)

4.0 PERSONNEL

4.1 The ultrasonic inspection shall be performed only by technically qualified personnel.

5.0 PROCEDURE

5.1 Set up equipment per set up sheet, page 3.

5.2 Submerge the stringer reference panel in a water filled inspection tank. (panel 1). Place the panel so the bridge indexes away from the reference hole.

5.2.1 Scan the web root area "B" to produce an ultrasonic "C" scan recording of this area (see panel layout on page 4).

5.2.2 Compare this "C" scan recording, web root area "B", with the reference recording of the same area (see page 5). If the comparison is favorable, precede with paragraph 5.3.

5.2.3 If the comparison is not favorable, adjust the sensitivity control as necessary until a favorable recording is obtained.

5.3 Submerge, scan and record the stringer panels two at a time. Place the stringers face up.

5.3.1 Scan and record areas in the following order: "C", "A", "B" and "D".

5.3.2 Identify on the ultrasonic "C" scan recording each web root area and corresponding panel tag number.

5.3.3 On completion of the inspection or at the end of the day, whichever occurs first, rescan the web root area of the stringer panel 1 and compare with reference recording.

5.4 When removing panels from water, thoroughly dry each panel.

5.5 Complete the data sheet for each panel inspected. (If no defects are noted, so indicate on the data sheet.)

5.5.1 The "X" dimension is measured from right to left for web root areas "C" and "A", and from left to right for web root areas "B" and "D". Use the extreme edge of the stringer indication for zero reference.

NOTE: Use decimal notation for all measurements.

5.6 After completing the Data Sheet, roll up ultrasonic recording and on the outside of the roll record the following information:

a) Date

b) Name (your)

c) Panel Type (stringer, weld, LOP)

d) Inspection name (ultrasonic, eddy current, etc.)

e) Sequence nomenclature (before chemical etch, after chemical etch, after proof test, etc.).

ULTRASONIC SET-UP SHEET

DATE: 02/12/74

METHOD: Pulse/Echo @ 18° incident angle in water

OPERATOR: Todd and Rathke

INSTRUMENT: UM 715 Reflectoscope with 10N Pulser/Receiver or see attached set-up sheet for UFD-1.

PULSE LENGTH: Min. ⊗

PULSE TUNING: ⊗ For Max. signal

REJECT: ⊗

SENSITIVITY: 2.0 X 10.0 (Note: Insert 6 db into attenuator and adjust the sensitivity control to obtain a 1.8" reflected signal from the class 1 defect in web root area "B" of panel 1. (See Figure 1.) Take 6db out of system before scanning the panels.

FREQUENCY: 10 MHz

GATE START: 4 ⊗

GATE LENGTH: 2 ⊗

TRANSDUCER: —SLJ 385; .25/10.0; S/N 24061

WATER PATH: 1 1/4" when transducer was normal to surface

WRITE LEVEL: + Auto Reset ⊗ SYNC: Main Pulse

PART: Integrally Stiffened Fatigue Crack Panels

SET-UP GEOMETRY:

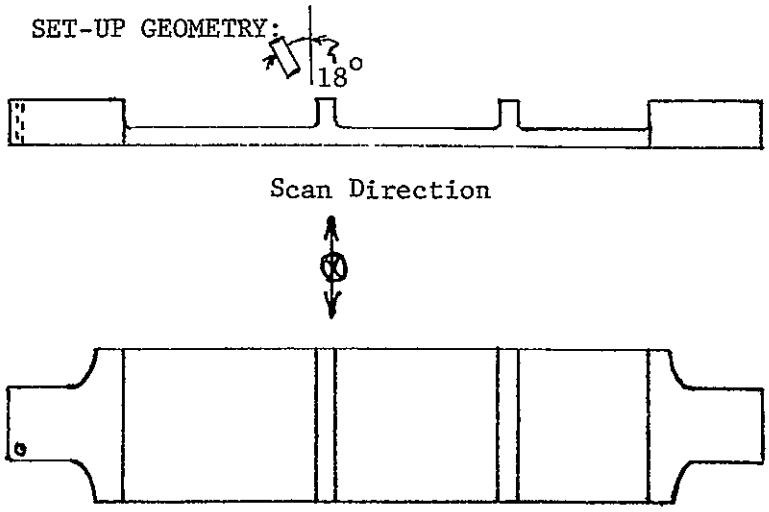

Bridge Controls

Carriage Speed	.033
Index	
Rate	.015 to .20
Step Increment	.032

LAY-OUT SHEET

Reference

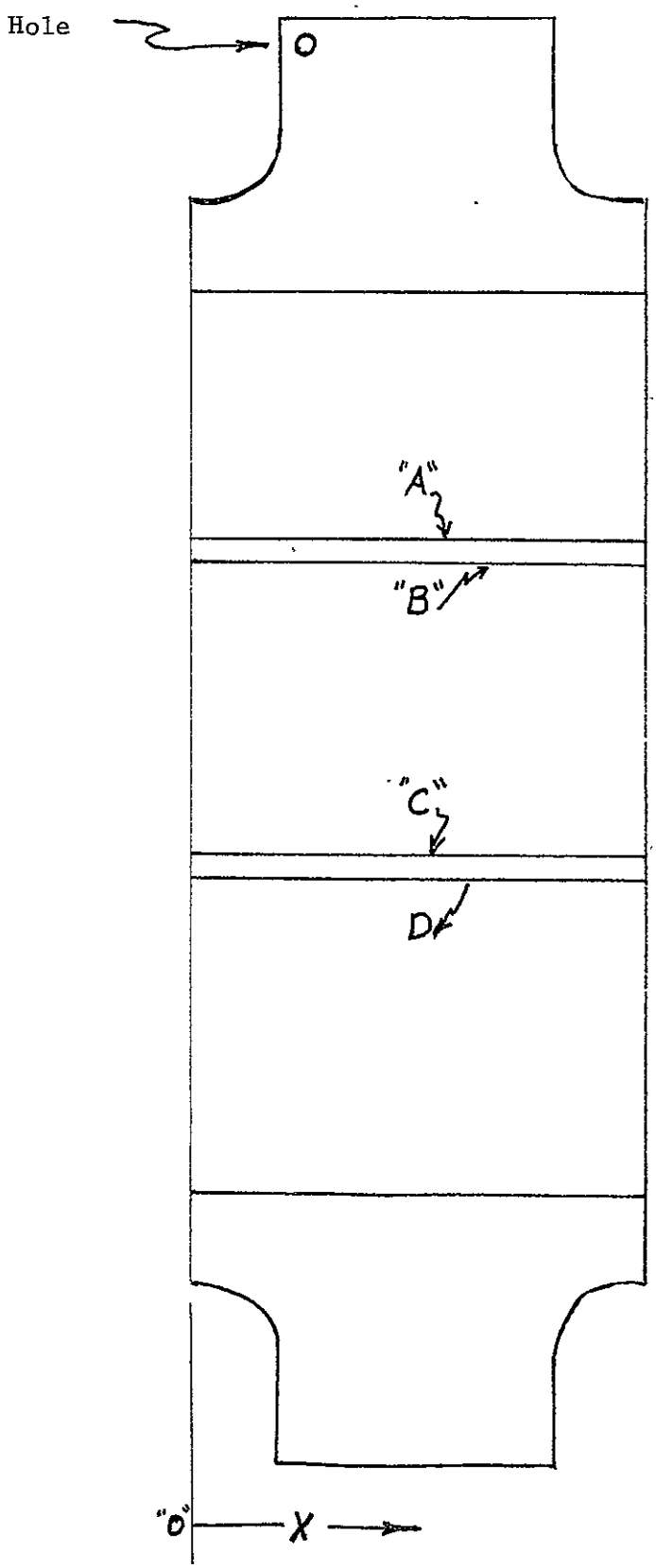

REFERENCE RECORDING SHEET

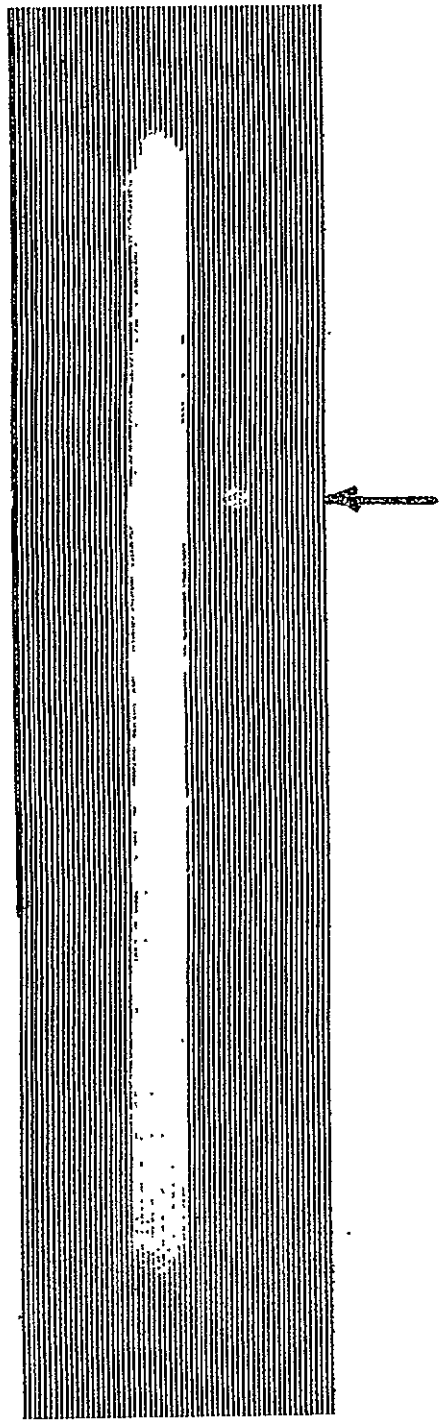

Case
1
Defect

WEB ROOT AREA

"B"

Panel 1.

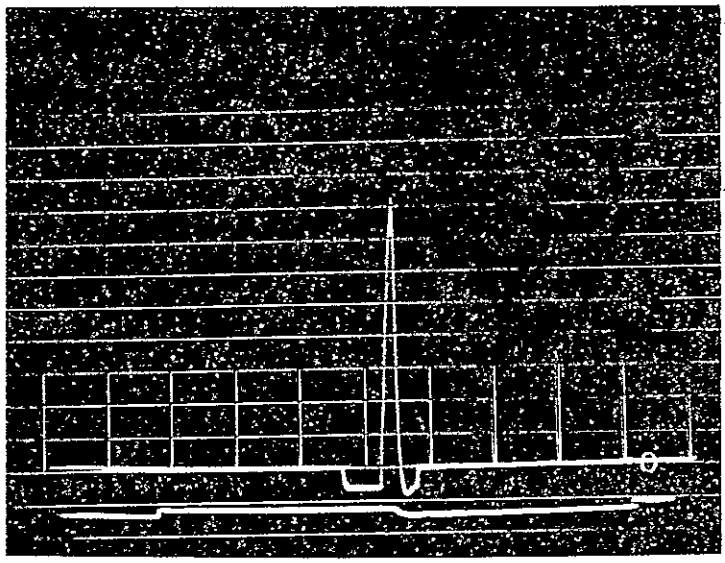

FIGURE 1: Scope Presentation for the Adjusted Sensitivity to 1.98".

-APPENDIX C -

EDDY CURRENT INSPECTION AND RECORDING FOR INTEGRALLY STIFFENED ALUMINUM PANELS.

1.0 SCOPE

1.1 This procedure covers eddy current inspection for detecting fatigue cracks in integrally stiffened aluminum panels.

2.0 REFERENCES

2.1 Manufacturer's instruction manual for the NDT Instruments Model Vector 111 Eddy Current Instrument.

2.2 Nondestructive Testing Training Handbooks, P1-4-5 Volumes I & II, Eddy Current Testing, General Dynamics, 1967.

2.3 Nondestructive Testing Handbook, McMasters, Ronald Press, 1959, Volume II, Sections 35-41.

3.0 EQUIPMENT

3.1 NDT Instruments Vector III Eddy Current Instrument.

3.1.1 100KHz Probe for Vector 111, Core diameter 0.063 inch.

NOTE: This is a single core, helically wound coil.

3.2 NDE Integrally Stiffened Reference Panel #4, web B.

3.3 SR 150 Budd, Ultrasonic Bridge.

3.4 319DA Alden, Recorder.

3.5 Special Probe Scanning Fixture #2.

3.6 Special Eddy Current Recorder Controller Circuit.

3.7 Dual DC Power Supply; 0-25V, 0-2A (HP Model 6227B).

4.0 PROCEDURE

4.1 Connect 100 KHz Probe to Vector 111 instrument.

4.2 Turn instrument power on and set sensitivity course control to position 1.

4.3 Check batteries by operating power switch to BAT position. Batteries should be checked every two hours of use.

4.3.1 Meter should read above 70.

4.4 Connect Recorder controller circuit

4.4.1 Set Power Supply for +16 volts and -16 volts.

4.5 Place Fluorolin tape on vertical and horizontal (2 places) tracking surfaces of scanning block. Trim tape to allow probe penetration.

4.5.1 Replace tape as needed.

4.6 Set up panel scanning support fixture spacers and shims for a two panel inspection, inner stringer faces.

4.7 Place the reference panel (#4, web B, Case 1, crack) and one other panel in support fixture for B stringer scan. Align panels carefully for parallelism with scan path. Secure panels in position with weights or clamps.

4.8 Manually place scan probe along the reference panel stringer face at least one inch from the panel edge.

4.8.1 Adjust for vector III meter null indication by alternately using X and R controls with the sensitivity control set at 1. Use Scale control to maintain readings on scale.

4.8.2 Alternately increase the course sensitivity control and continue to null the meter until a sensitivity level of 8 is reached with fine sensitivity control at 5. Note the final indications on X and R controls.

4.8.3 Repeat steps 4.8.1 and 4.8.2 while a thin non-metallic shim (3 mils thickness) is placed between the panel horizontal surface and the probe block. Again note the X and R values.

4.8.4 Set the X and R controls to preliminary lift-off compensation values based on data of steps 4.8.2 and 4.8.3.

4.8.5 Check the meter indications with and without the shim in place. Adjust the X and R controls until the meter indication is the same for both conditions of shim placement. Record the final settings:

"X" 160.0 These are approximate settings and are given here for reference purposes only.

"R" 319.5

SENSITIVITY:

COURSE 8

FINE 5

4.9 Set the Recorder controls for scanning as follows:

Index Step Increment	.020
Carriage Speed	.029
Scan Limits	set to scan 1 inch beyond panel edge.
Bridge	OFF and bridge mechanically clamped.

4.10 Manually move the probe over panel inspection region to determine scan background level. Adjust the Vector 111 Scale control to set the background level as close as possible to the Recorder Controller switching point (meter indication is 20 for positive-going indication and 22 for negative-going indication).

4.11 Initiate the Recorder Scan function.

4.12 Verify that the flaw in "B" stringer of the reference panel is clearly displayed in the recording. Repeat step 4.10 if required.

4.13 Repeat step 4.10 and 4.11 for the second panel in the fixture. Annotate recordings with panel/stringer identification.

4.14 Reverse the two panels in the support fixture to scan the "C" stringer. Repeat steps 4.7, 4.10, 4.11, 4.13, and 4.14 for the remaining panels.

4.15 Set up panel scanning support fixture, spacers and shims for outer stringer faces. Relocate scan bridge as required and clamp.

4.16 Repeat steps 4.7, 4.10, 4.11, 4.13, and 4.14 for all panels for A and D stringer inspections.

4.17 Evaluate recordings for flaws and enter panel, stringer, flaw location and length on applicable data sheet. Observe correct orientation of reference edge of each panel when measuring location of a flaw.

5.0 PERSONNEL

5.1 Only qualified personnel shall perform inspections.

6.0 SAFETY

6.1 Operation should be in accordance with Standard Safety Procedure used in operating any electrical device.

AMENDMENT A

APPENDIX C

NOTE

This amendment covers changes in procedure from raster recording to analog recording.

4.4.2 Connect Autoscaler circuit to Vector 111 and set back panel switch to AUTO.

4.8 Initiate the Recorder Scan function. Set the Autoscaler switch to RESET.

4.9 Adjust the Vector 111 Scale control to set the recorder display for no flaw or surface noise indications.

4.10. Set the Autoscaler switch to RUN.

4.11 When all of the signatures of the panels are indicated (all white display), stop the recorder. Use the carriage Scan switch on the Recorder Control Panel to stop scan.

4.12 Annotate recordings with panel/side/thickness/reference edge identification data.

-APPENDIX D-

X-RADIOGRAPHIC INSPECTION PROCEDURES FOR DETECTION OF FATIGUE CRACKS AND LOP IN WELDED PANELS

1.0 SCOPE

To establish a radiographic technique to detect fatigue cracks and LOP in welded panels.

2.0 REFERENCES

2.1 MIL-STD-453.

3.0 EQUIPMENT AND MATERIALS

3.1 Norelco X-ray machine 150 KV, 24MA.

3.2 Balteau X-ray machine, 50 KV, 20MA.

3.3 Kodak Industrial Automatic Processor Model M3.

3.4 MacBeth Quantalog Transmission Densitometer, Model TD-100A.

3.5 Viewer, High Intensity, GE Model BY-Type 1 or equivalent.

3.6 Penetrameters - in accordance with MIL-STD-453.

3.7 Magnifiers, 5X and 10X pocket comparator or equivalent.

3.8 Lead numbers, lead tape and accessories.

4.0 PERSONNEL

Personnel performing radiographic inspection shall be qualified in accordance with MIL-STD-453.

5.0 PROCEDURE

5.1 An optimum and reasonable production technique using Kodak, Type M Industrial X-ray film shall be used to perform the radiography of welded panels. The rationale for this technique is based on the results as demonstrated by the radiographs and techniques employed on the actual panels.

5.2 Refer to Table 1 to determine the correct setup data necessary to produce the proper exposure except:

Paragraph (h) Radiographic Density shall be: 2.5 to 3.5

Paragraph (i) Focal Spot size shall be: 2.5 mm

Collimation 1-1/8" diameter lead diaphram at the tube head.

5.3 Place the film in direct contact with the surface of the panel being radiographed.

5.4 Prepare and place the required film identification on the film and panel .

5.5 The appropriate penetrameter (MIL-STD-453) shall be radiographed with each panel for the duration of the exposure.

5.6 The penetrameters shall be placed on the source side of the panels.

5.7 The radiographic density of the panel shall not vary more than ± 15 percent from the density at the MIL-STD-453 penetrameter location.

5.8 Align the direction of the central beam of radiation perpendicular and to the center of the panel being radiographed.

5.9 Expose the film at the selected technique obtained from Table 1.

5.10 Process the exposed film through the Automatic Processor (Table 1).

5.11 The radiographs shall be free from blemishes or film defects which may mask defects or cause confusion in the interpretation of the radiograph for fatigue cracks.

5.12 The density of the radiographs shall be checked with a densitometer (Ref. 3.3) and shall be within a range of 2.5 to 3.5 as measured over the machined area of the panel.

5.13 Using a viewer with proper illumination (Ref. 3.4) and magnification (5X and 10X Pocket Comparator or equivalent) interpret the radiographs to determine the number, location, and length of fatigue cracks in each panel radiographed.

TABLE 1

DETECTION OF LOP - X-RAY

Type of Film: Eastman Kodak Type M

Exposure Parameters: Optimum Technique

(a) Kilovoltage:

.130 - 45 KV
.205 - 45 KV
.500 - 70 KV

(b) Milliamperes:

.130-.205 - 20 MA
.500 - 20 MA

(c) Exposure Time:

.130-.145 - 1½ Minutes
.146-.160 - 2 Minutes
.161-.180 - 2¼ Minutes
.181-.190 - 2½ Minutes
.190-.205 - 3 Minutes
.500 - 2½ Minutes

(d) Target/Film Distance:

48 Inches

(e) Geometry or Exposure:

Perpendicular

(f) Film Holders/Screens:

Ready Pack/No Screens

(g) Development Parameters:

Kodak Model M3 Automatic Processor
Development Temperature of 78°F

(h) Radiographic Density:

.130 - 3.0
.205 - 3.0
.500 - 3.0

TABLE 1 (Continued)

(i) Other Pertinent Parameters/Remarks:

Radiographic Equipment
Norelco 150 KV 24 MA
Beryllium Window
.7 and 2.5 Focal Spot

WELD CRACKS

Exposure Parameters: Optimum Technique

(a) Kilovoltage:

1/8" - 45 KV
1/2 " - 70 KV

(b) Milliamperes:

1/8" - 20 MA
1/2" - 20 MA

(c) Exposure Time:

1/8" - 1½ Minutes
1/2" - 2¼ Minutes

(d) Target/Film Distance:

48 Inches

(e) Geometry or Exposure:

Perpendicular

(f) Film Holders/Screens:

Ready Pack/No Screens

(g) Development Parameters:

Kodak Model M3 Automatic Processor
Development Temperature at 78°F

(h) Radiographic Density:

.060 - 3.0
.205 - 3.0

(i) Other Pertinent Parameters/Remarks:

Radiographic Equipment
Norelco 150 KV 24 MA
Beryllium Window
.7 and 2.5 Focal Spot

APPENDIX E

ULTRASONIC INSPECTION FOR "TIGHT FLAWS DETECTION BY NDT" PROGRAM -

L.O.P. PANELS

1.0 SCOPE

1.1 This procedure covers ultrasonic inspection of LOP panels for detecting lack of penetration and subsurface defects in Weld area.

2.0 REFERENCE

2.1 Manufacturer's instruction manual for the UM-715 Reflectoscope instrument, and Sonatest UFD 1 instrument.

2.2 Nondestructive Testing Training Handbook, P1-4-4, Volumes I, II and III, Ultrasonic Testing, General Dynamics, 1967.

2.3 Nondestructive Testing Handbook, McMasters, Ronald Press, 1959, Volume II, Sections 43-48.

3.0 EQUIPMENT

3.1 UM-715 Reflectoscope, Automation Industries

3.2 10N Pulser/Receiver, Automation Industries

3.3 E-550 Transigate, Automation Industries

3.4 SIJ-360 .25 inch diameter, flat, 5.0 MHZ Transducer Automation Ind.
SIL-57A2772 .312 inch diameter, flat 5.0 MHZ Transducer Automation Ind.

3.5 SR 150 Budd, Ultrasonic Bridge

3.6 319 DA Alden, Recorder

3.7 Reference Panels. Panels #24 & 36 for 1/8" Panels and #42 and #109 for 1/2 inch panels.

4.0 PERSONNEL

4.1 The ultrasonic inspection shall be performed only by technically qualified personnel.

5.0 PROCEDURE

5.1 Set up equipment per applicable setup sheet. (page 4)

5.2 Submerge the applicable reference panel for the thickness being inspected. Place the panel so the least panel conture is on the bottom.

5.2.1 Scan the weld area to produce an ultrasonic "C" scan recording of this area. (See panel layouts on page 4).

5.2.2 Compare this "C" scan recording with the referenced recording of the same panel (See page 5 and 6). If the comparison is favorable, presede with paragraph 5.3.

5.2.3 If comparison is not favorable, adjust the controls as necessary until a favorable recording is obtained.

5.3 Submerge, scan and record the panels two at a time. Place the panels so the least panel conture is on the bottom.

5.3.1 Identify on the ultrasonic "C" scan recording the panel number and reference hole orientation.

5.3.2 On completion of the inspection or at the end of shift, whichever occurs first, rescan the reference panel and compare with reference recording.

5.4 When removing panels from water, thoroughly dry each panel.

5.5 Complete the data sheet for each panel inspected.

5.5.1 The "x" dimension is measured from end of weld, starting zero at end with reference hole. (Use decimal notation for all measurements).

5.6 After completing the data sheet, roll up ultrasonic recording and on the outside of the roll record the following information.

A - Date

B - Name of Operator

C - Panel Type

D - Inspection Name

E - Sequence Nomenclature

Date. Oct. 1, 1974

Method- Pitch And Catch

Operator- H. Lovisone

Instrument- UM-715 Reflectoscope, 10N Pulser/Receiver.

	1/8"	1/2"
Pulse Length-	Min.	Min.
Pulse Tuning-		
Reject-	10 O'Clock	12 O'Clock
Sensitivity-	5 X 1	3.1 X 10
Frequency-	5 MHZ	5 MHZ
Gate Start-	4	4
Gate Length-	3	3

Transducer- Transmitter- SIL 5.0 S/N 39090
- Receiver- SIL 5.0 S/N 15926

Water Path- 2-11/16"

Write Level

Part - 1/8" & 1/2" L.O.P. Panels

Sweep delay - 2

Sweep

Max. 1

1

Set-Up Geometry-

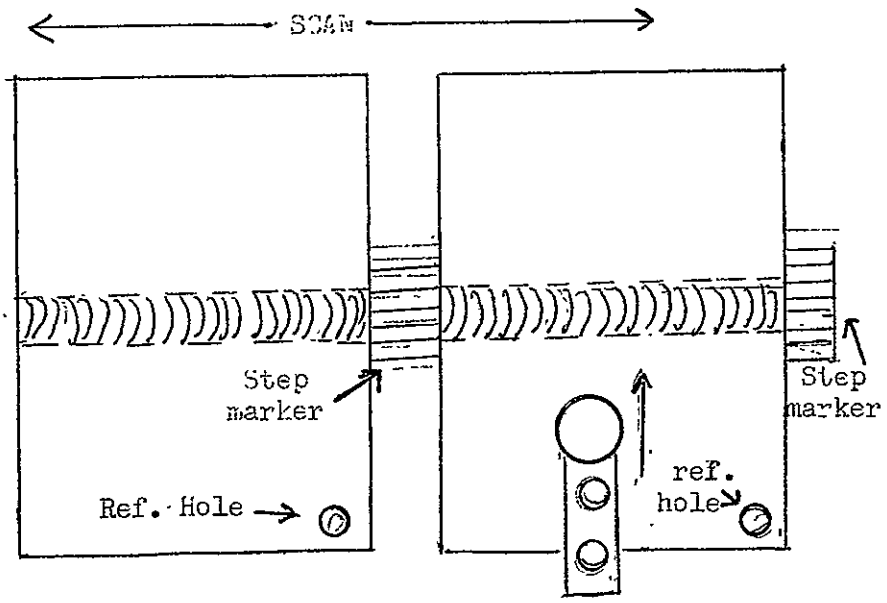

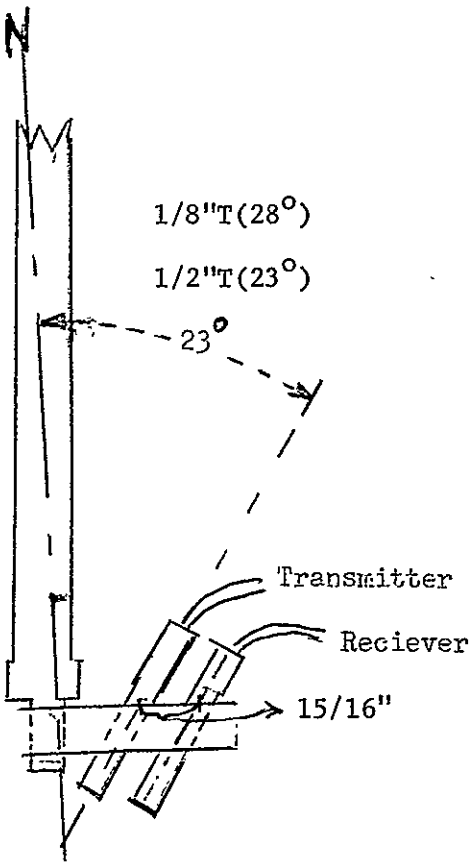

Use a N/G transducer to hold bracket

1/8" LOP REFERENCE PANEL #24

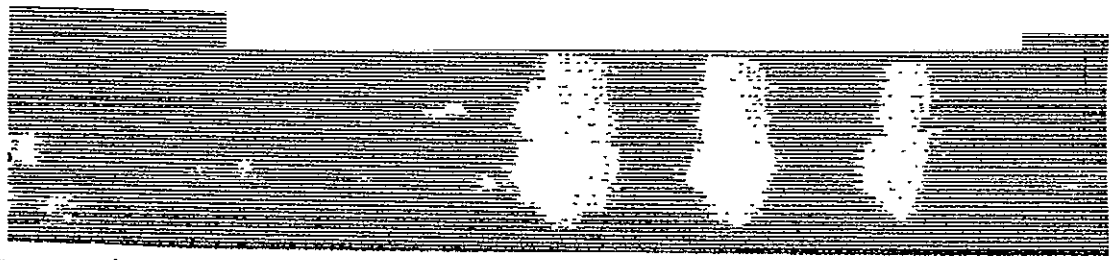

REFERENCE HOLE

1/8" LOP REFERENCE PANEL #36

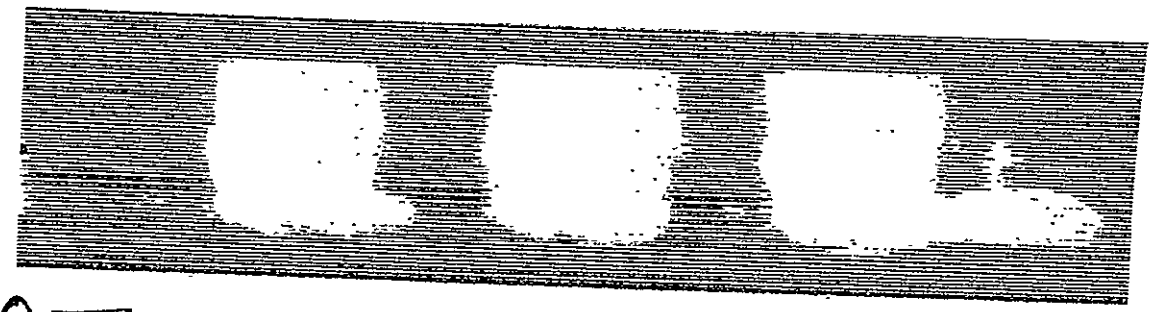

REFERENCE HOLE

1/2" LOP REFERENCE PANEL #42

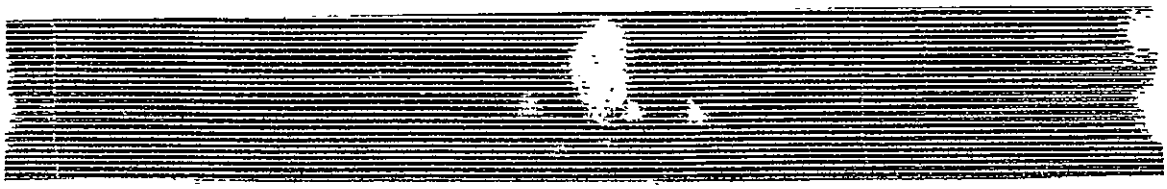

REFERENCE HOLE

1/2" LOP REFERENCE PANEL # 109

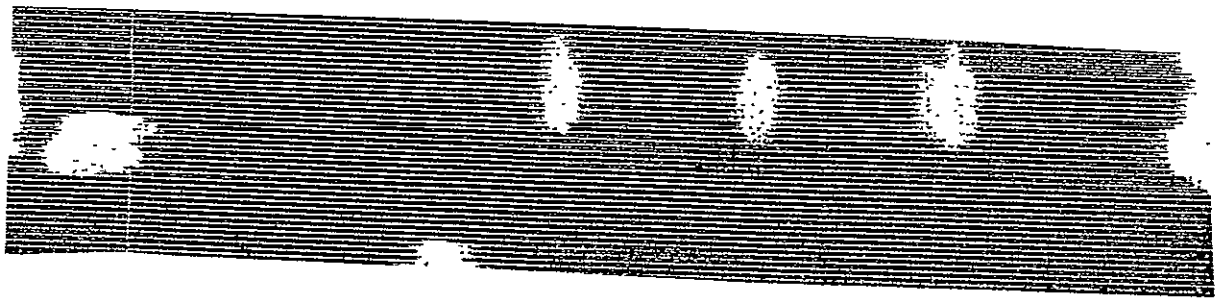

REFERENCE HOLE

AMENDMENT A

APPENDIX E

SET-UP FOR 1/8" LOP PANELS

DATE:	08/11/75
METHOD:	Pitch-Catch, Pulse-echo @ 27 3/4° incident angle of transmitter and receiver in water (angle indicator - 4 3/4°)
OPERATOR:	Steve Mullen
INSTRUMENT:	UM 715 Reflectoscope with 10 N/Pulser/Receiver
PULSE LENGTH:	Min.
PULSE TUNING:	for Max signal
REJECT:	10:00 o'clock
SENSITIVITY:	5 x 10
FREQUENCY:	5 MHz
GATE START:	4
GATE LENGTH:	3
TRANSDUCER:	Tx-SIZ-5; S/N 26963; RX-SIZ-5, S/N 35521
WATER PATH:	1.9" from Transducer Housing to part Transducer inserted into housing completely
WRITE LEVEL:	Reset + auto
PART:	1/8" LOP Panels for NAS 9-13578

SET-UP GEOMETRY:

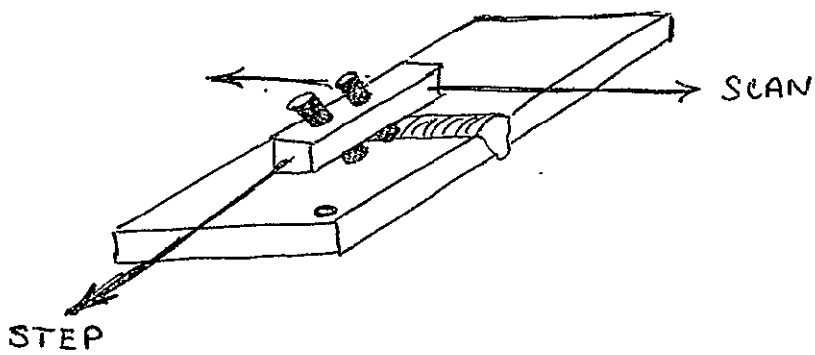

1/8" LOP REF PANELS

DRILL HOLE REF PANEL #28

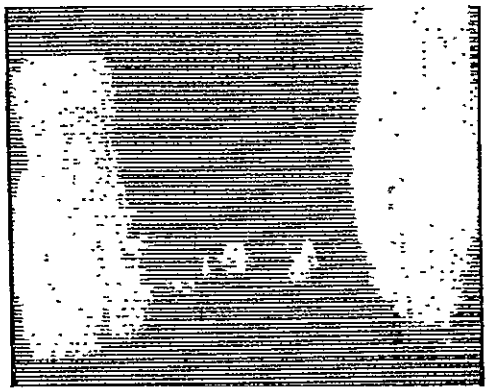

LOP REF PANEL #51

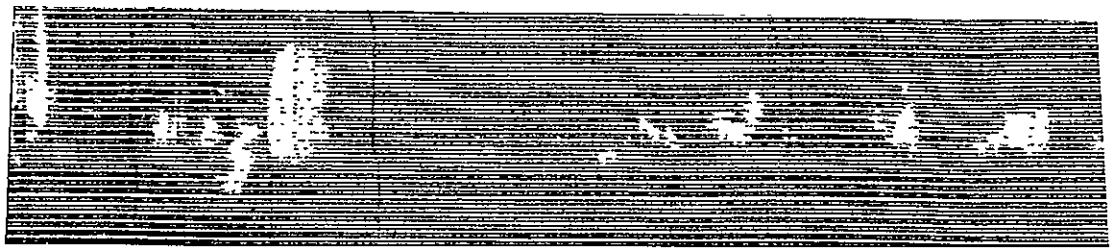

AMENDMENT B

APPENDIX E

SET UP FOR 1/2" LOP PANELS

DATE:	08/12/75
METHOD:	Pitch-Catch, Pulse-Echo @ 27° incident angle of Transmitter and Receiver in Water (angle indicator = 4°)
OPERATOR:	Steve Mullen
INSTRUMENT:	UM-715 Reflectoscope with 10N/Pulser/Receiver
PULSE LENGTH ⊗	Min.
PULSE TUNING: ⊗	For Max signal
REJECT:	10:00 o'clock
SENSITIVITY:	5 x 10
FREQUENCY:	5 MHz
GATE START:	4
GATE LENGTH:	3
TRANSDUCER:	TX-SIZ-5; SN26963; Rx-SIZ-5, S/N 35521
WATER PATH:	1.6" from Transducer Housing to Part Transducer inserted into housing completely
WRITE LEVEL:	Reset ~~1~~ auto
PART:	1/2" LOP Panels for NAS 9-13578

SET-UP GEOMETRY:

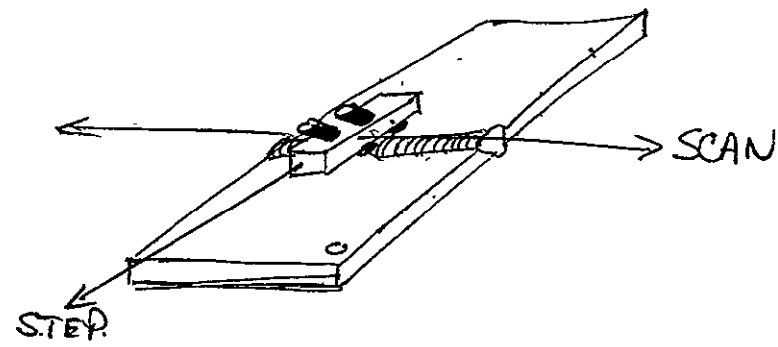

1/2" LOP Reference Panels

Drill Hole, Reference Panel #19

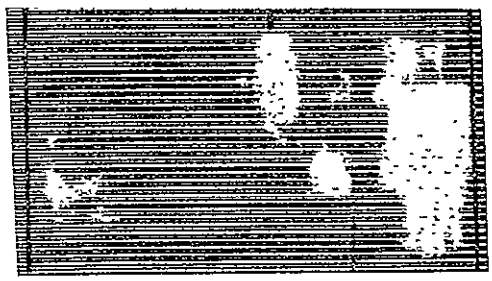

LOP, Reference Panel #118

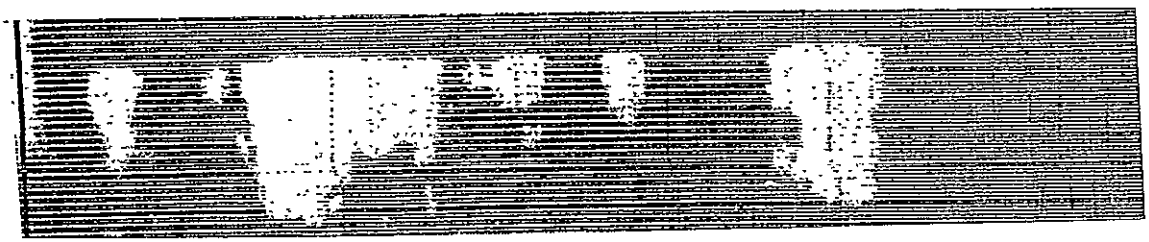

APPENDIX F

EDDY CURRENT INSPECTION AND RECORDING OF LACK OF PENETRATION (LOP) ALUMINUM PANELS, UNSCARFED CONDITION

1.0 SCOPE

1.1 This procedure covers eddy current inspection for detecting lack of penetration flaws in welded aluminum panels.

2.0 REFERENCES

2.1 Manufacturer's instruction manual for the NDT Instruments Model Vector 111 Eddy Current Instrument.

2.2 Nondestructive Testing Training Handbooks P1-4-5, Volumes I and II, Eddy Current Testing, General Dynamics, 1967.

2.3 Nondestructive Testing Handbook, McMasters, Ronald Press, 1959, Volume II, Sections 35-41.

3.0 EQUIPMENT

3.1 NDT Instruments Vector 111 Eddy Current Instrument.

3.1.1 20 KHz Probe for Vector 111, Core Diameter 0.250 inch.

NOTE: This is a single core helically wound coil.

3.2 NDE LOP Reference Panels.

3.2.1 1/2 inch panels Nos. 1 and 2.

3.2.2 1/8 inch panels Nos. 89 and 115.

3.3 SR 150 Budd, Ultrasonic Bridge.

3.4 319DA Alden, Recorder.

3.5 Special Probe Scanning Fixture No. 1 for LOP Panels.

3.6 Special Eddy Current Recorder Controller Circuit.

3.7 Dual DC Power Supply; 0-25V, 0-1A (Hp Model 6227B or equivalent).

3.8 Special Autoscaler/Eddy Current Meter Circuit.

4.0 PROCEDURE

4.1 Connect 20 KHz Probe to Vector 111 instrument.

4.2 Turn instrument power on and set Sensitivity Course control to position #1.

4.3 Check batteris by operating power switch to BAT position. (These should be checked every two hours to use).

4.3.1 Meter should read above 70.

4.4 Connect Recorder Controller circuit

4.4.1 Set Power Supply for +16 volts and -16 volts.

4.4.2 Connect Autoscaler Circuit to Vector 111 and set back panel switch to AUTO.

4.5 Set up weld panel scanning support fixture, shims and spacers as follows:

4.5.1 Clamp an end scan plate (of the same thickness as welded panel) to the support fixture. Align the end scan plate perpendicular to the path that the scan probe will travel over the entire length of the weld bead. Place two weld panels side by side so that the weld beads are aligned with the scan probe. Secure the LOP panels with weights/clamps as required. Verify that the scan probe holder is making sufficient contact with the weld bead such that the scan probe springs are unrestrained by limiting devices. Secure an end scan plate at opposite end of LOP panels. Verify that scan probe holder has sufficient clearance for scan travel.

4.5.2 Use shims or clamps to provide smooth scan probe transition between weld panels and end scan plates.

4.6 Set Vector 111 controls as follows:

"X" 134.0

"R" 517.0

Sensitivity, Course 8, Fine 5.

4.7 Set the Recorder Controls for scanning as follows:

Index Step Increment - .020 inch.

Carriage Speed - 029

Scan Limits - set to scan $1\frac{1}{2}$ inches beyond the panel edges.

Bridge - OFF and bridge mechanically clamped.

4.8 Initiate the Recorder/Scan function. Set the Autoscaler switch to RESET. Adjust the Vector 111 Scale control to set the recorder display for no flow or surface noise indications.

4.9 Set the Autoscaler switch to RUN.

4.10 When all of the signatures of the panels are indicated (white display) stop the Recorder. Use the Carriage Scan switch on the Recorder control panel to stop scan.

4.11 Annotate recordings with panel/side/thickness/reference edge identification data.

4.12 Repeat 4.5, 4.8, through 4.11 with panel sides reversed for back side scan

4.13 Evaluate recordings for flaws and enter panel, flaw location and length on applicable data sheet. Observe correct orientation of reference hole edge of each panel when measuring location of a flaw.

5.0 PERSONNEL

5.1 Only qualified personnel shall perform inspections.

6.0 SAFETY

6.1 Operation should be in accordance with Standard Safety Procedure used in operating any electrical device.

APPENDIX G

EDDY CURRENT INSPECTION AND C-SCAN RECORDING OF LOP, ALUMINUM PANELS, SCARFED CONDITION

1.0 SCOPE

1.1 This procedure covers eddy current C-scan inspection detecting LOP in Aluminum panels with scarfed welds.

2.0 REFERENCES

2.1 Manufacturer's instruction manual for the NDT instruments Model Vector 111 Eddy Current Instrument.

2.2 Nondestructive Testing Training Handbooks, P1-4-5, Volumes I and II, Eddy Current Testing, General Dynamics, 1967.

2.3 Nondestructive Testing Handbook, McMasters, Ronald Press, 1959, Volume II, Sections 35-41.

3.0 EQUIPMENT

3.1 NDT Instruments Vector 111 Eddy Current Instrument.

3.1.1 20 KHz probe for Vector 111, Core diamter 0.250 inch

Note: This is a single core helically wound coil.

3.2 SR 150 Budd, Ultrasonic Bridge.

3.3 319DA Alden, Recorder.

3.4 Special Probe Scanning Fixture for Weld Panels. (#5).

3.5 Dual DC Power Supply; 0-25V, 0-1A (HP Model 6227B or equivalent).

3.6 NDE reference panel no. 4, LOP reference panels no. 20($\frac{1}{2}$") and No. 36(1/8").

3.7 Special Eddy Current Recorder Controller circuit.

4.0 PROCEDURE

4.1 Connect 20 KHz probe to Vector 111 instrument.

4.2 Turn instrument power on and set SENSITIVITY COURSE control to position 1.

4.3 Check batteries by operating power switch to BAT position. Batteries should be checked every two hours of use. Meter should read above 70.

4.4 Connect C-scan/Recorder Controller Circuit

4.4.1 Set Power Supply for +16 volts and -16 volts.

4.4.2 Set "/S E/C" siwtch to E/C.

4.4.3 Set OP AMP switch to OPR.

4.4.4 Set RUN/RESET switch to RESET.

4.5 Set up weld panel scanning support fixture as follows:

4.5.1 Clamp an end scan plate of the same thickness as the weld panel to the support fixture. One weld panel will be scanned at a time.

4.5.2 Align the end scan plate, using one weld panel so that the scan probe will be centered over the entire length of the weld bead.

4.5.3 Use shims or clamps to provide smooth scan transition between weld panel and end plates.

4.5.4 Verify that scan probe is making sufficient contact with panel.

4.5.5 Secure the weld panel with weights or clamps as required.

4.5.6 Secure an end scan plate at opposite end of weld panel.

4.6 Set Vector 111 controls as follows:

"X" 050.0

"R" 424.0

SENSITIVITY, COURSE 8, FINE 4.

MANUAL/AUTO switch to MAN.

4.7 Set the Recorder controls for scanning as follows:

Index Step Increment - .020 inch

Carriage Speed -.029

Scan Limits - set to scan 1½ inches beyond the panel edge.

Bridge -

4.8 Manually position the scan probe over the center of the weld.

4.9 Manually scan the panel to locate an area of the weld that contains no flaws (decrease in meter reading).

With the probe at this location, adjust the Vector 111 Scale control to obtain a meter indication of 10 (meter indication for switching point is 25).

4.10 Set Bridge switch to OFF and locate probe just off the edge of the weld.

4.11 Set the Bridge switch to BRIDGE.

4.12 Initiate the Recorder/Scan function.

4.13 Annotate recordings with panel reference edge and serial number data.

4.14 Evaluate recordings for flaws and enter panel, flaw location and length data on applicable data sheet. Observe correct orientation of reference hold edge of each panel when measuring location of flaws.

5.0 PERSONNEL

5.1 Only qualified personnel shall perform inspection.

6.0 SAFETY

6.1 Operation should be in accordance with Standard Safety Procedure used in operating any electrical device.

APPENDIX H

ULTRASONIC INSPECTION FOR "TIGHT FLAWS DETECTED BY NDT" PROGRAM - WELD PANELS HAVING CROWNS

1.0 SCOPE

1.1 This procedure covers ultrasonic inspection of weld panels for detecting fatigue cracks located in the Weld area.

2.0 REFERENCES

2.1 Manufacturer's instruction manual for the UM-715 Reflectoscope instrument.

2.2 Nondestructive Testing Training Handbook, P1-4-4, Volumes I, II and III, Ultrasonic Testing, General Dynamics, 1967.

2.3 Nondestructive Testing Handbook, McMasters, Ronald Press, 1959, Volume II, Sections 43-48.

3.0 EQUIPMENT

3.1 UM-715 Reflectoscope, Automation Industries

3.2 10N Pulser/Receiver, Automation Industries

3.3 E-550 Transigate, Automation Industries

3.4 UFD-1 Sonatest, Baltue

3.5 SIJ-385, .25 inch diameter, flat, 10.0 MHz Transducer; Automation Industries.

3.6 SR 150 Budd, Ultrasonic Bridge

3.7 319 DA Alden, Recorder

3.8 Reference Panels - For thin panels use #8 for transverse cracks and #26 for longitudinal cracks. For thick panels use #36 for transverse carcks and #41 for longitudinal cracks.

4.0 PERSONNEL

4.1 The ultrasonic inspection shall be performed only by technically qualified personnel.

5.0 PROCEDURE

5.1 Set up equipment per setup sheet on page 3.

5.1.1 Submerge panels. Place the reference panels, (for the material thickness and orientation to be inspected) so the bridge indices toward the reference hole. Produce a "C" scan recording and compare with the reference recording.

5.1.1.1 If the comparison is not favorable, adjust the controls as necessary until a favorable recording is obtained.

5.2 Submerge, scan the weld area and record in both the longitudinal and transverse directions. Complete one direction then change bridge controls and complete the other direction (see page 3 & 4).

5.2.1 Identify on the recording the starting edge of the panel, location of Ref. hole and direction of scanning with respect to the weld. (Longitudinal or transverse)

5.3 On completion of the inspection or at the end of shift, whichever occurs first, rescan the reference panel, (for the orientation and thickness in progress), and compare recordings.

5.3.1 When removing panels from water, thoroughly dry each panel.

5.4 Complete the data sheet for each panel inspected.

5.4.1 The "X" dimension is measured from the edge of panel. Zero designation is the edge with the reference hole.

5.5 After completing the data sheet, roll up recordings, and on the outside of roll record the following information:

A. Date

B. Name of Operator

C. Panel Type (stringer, weld, LOP, etc.)

D. Inspection Name (U.S., E/C, etc.)

E. Sequence Nomenclature

ULTRASONIC SET-UP SHEET

DATE: 07/16/74

METHOD: Pulse/Echo @ 32° incident angle in water

OPERATOR: Lovisone.

INSTRUMENT: UM 715 Reflectoscope with 10N Pulser/Receiver.

PULSE LENGTH: Min.

PULSE TUNING: For Max. Signal.

REJECT: Three O'Clock.

SENSITIVITY: Using the ultrasonic fat crack Cal. Std. panel add shims for correct thickness of panels to be inspected. Align transducer on small hole of the Std. and adjust sensitivity to obtain a signal of 1.6 inches for transverse and 0.4 inches for longitudal.

FREQUENCY: 10 MHZ.

GATE START: 4

GATE LENGTH: 2

TRANSDUCER: SIJ 385 .25/10.0 S/N 24061.

WATER PATH: 1.7" measured @ 32° tilt, center of transducer to top of panel.

WRITE LEVEL: Auto Reset.

PART: FATIGUE crack weld p anels with crown.

BRIDGE CONTROLS: Carriage Speed 0.30 , Step Increment 0.30.

SET-UP GEOMETRY:

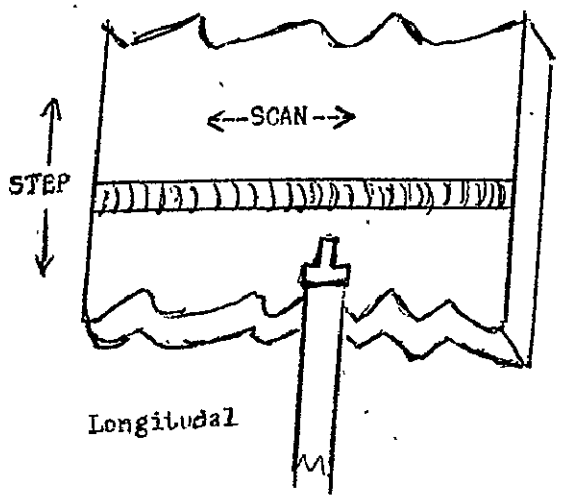

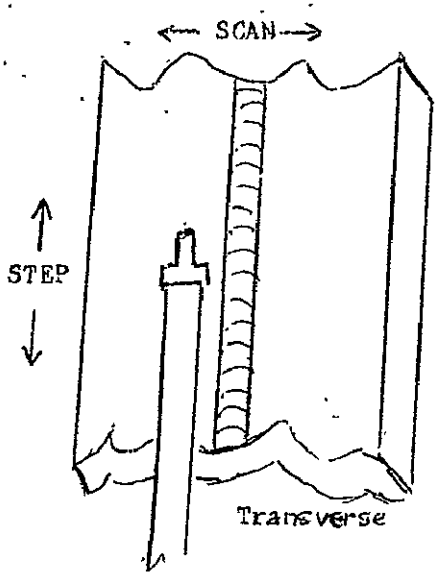

ULTRASONIC SET-UP TECHNIQUE PROGRA WELD VECTOR

DATE 12-10-74

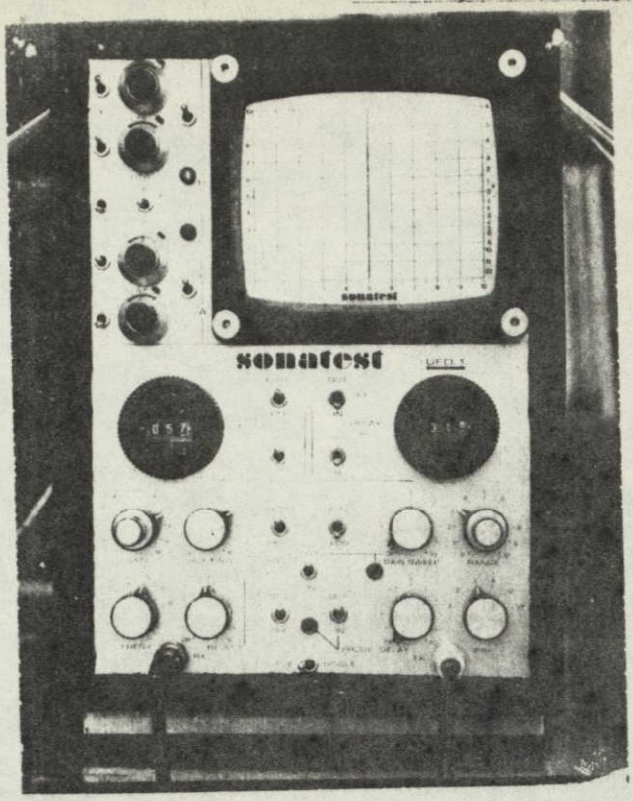

SONATEST

TRANSDUCER:

X1
X10
DELAY
+
-
X1
X10
TB
E
TX
WIDTH
SENSITIVITY
A+B
A
A-B
9
7
DELAY
67
3.5
+
-
X1
X10

GATE WIDTH MM
015

GATE
OUT
OFF
IN
XO.1
X1
XO.1
X1

UFD. 1
DELAY MM
09.85

70
60
GAIN
AUX. GAIN

DISPLAY
NORM.
S.P.
LIN.
REST.
LOG.

1.5
OFF
GAIN SWEEP
4
9
RANGE

OUT
IN
ON
OFF
OUT
IN

10
8
FREQ.
H-4
RX
REJECT

DOUBLE
SINGLE

4
OFF
PROBE DELAY
TX
P.R.F.

H-4

H-4

PANEL #8 FOR TRANSVERSE SCAN OF WELD AREA.

DEFECT 4.4" FROM REFERENCE END.

REF. END.

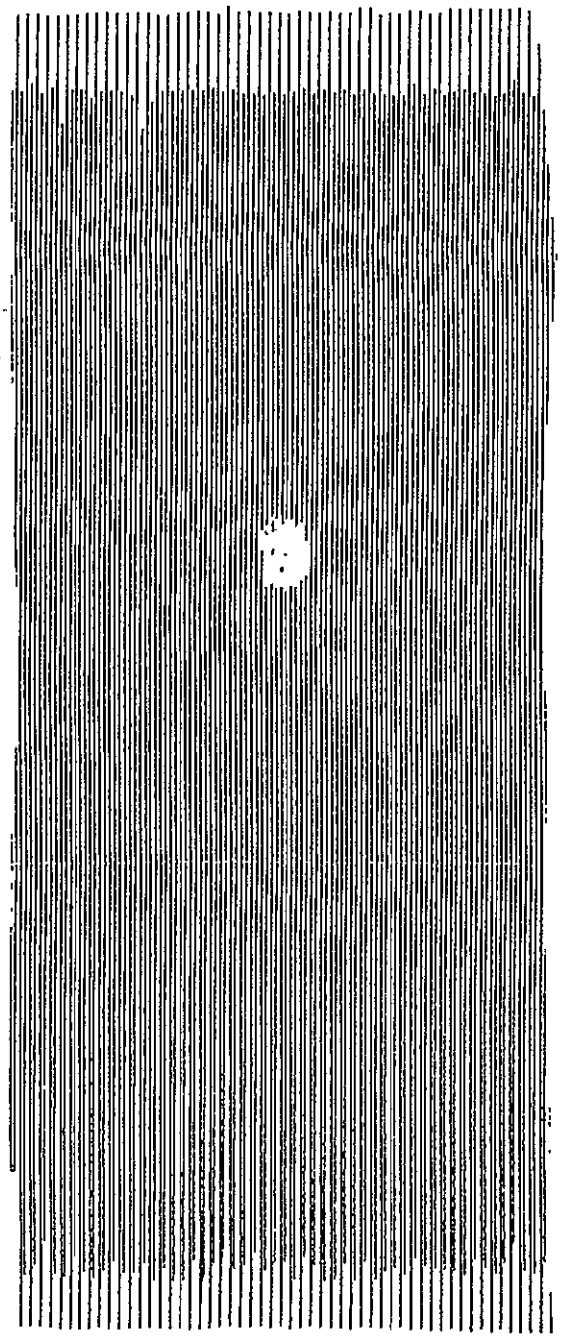

PANEL #36 FOR TRANSVERSE SCAN OF WELD AREA.

DEFECT 4.1" FROM REFERENCE END.

REF. END.

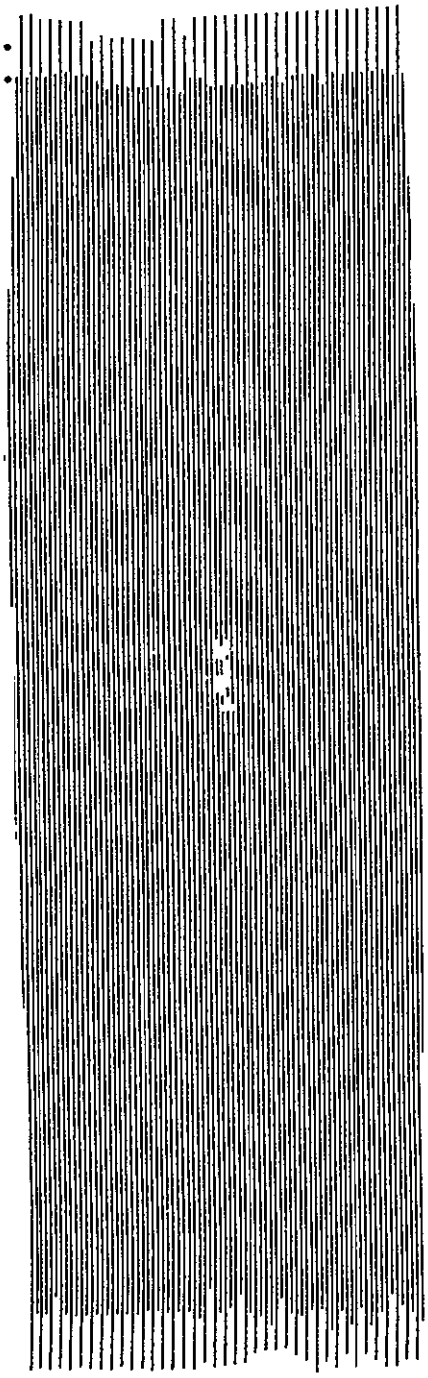

PANEL #26 REFERENCE RECORDING FOR LONGITUDAL SCAN OF WELD AREA.

REFERENCE END.

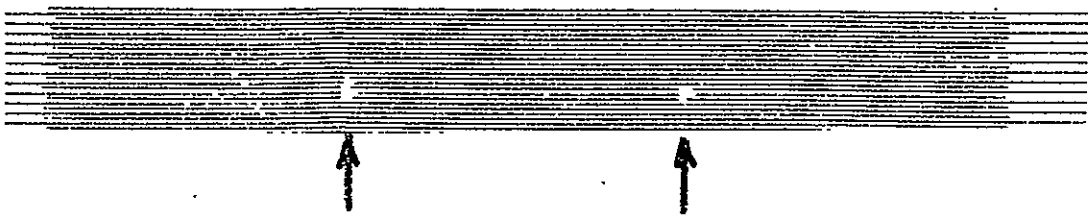

DEFECT MEASUREMENTS -- 1.9 --- 3.7

PANEL #41 REFERENCE RECORDING FOR LONGITUDAL SCAN OF WELD AREA.

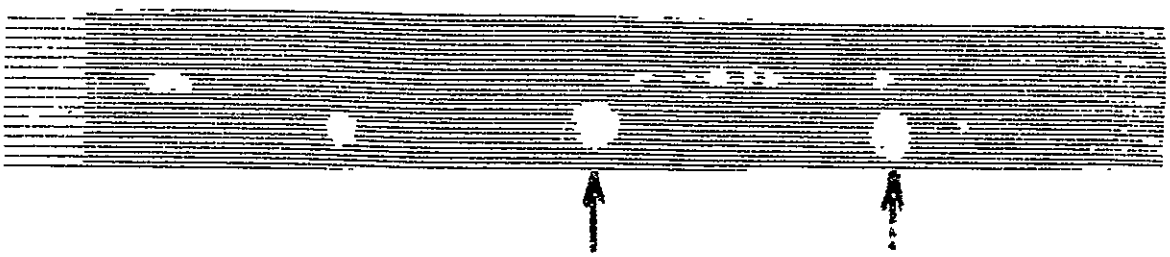

DEFECTS 2.95 1.4

AMENDMENT A

APPENDIX H

SET-UP FOR 1/8" WELDED FATIGUE CRACK PANELS

DATE:	08/29/75
METHOD:	Pitch-Catch, Pulse-Echo @ 27 1/2" Incident Angle Angle Indicator + 4 1/2°
OPERATOR:	Steve Mullen
INSTRUMENT:	UM 715 Reflectoscope with 16N/Pulser/Receiver
PULSE LENGTH:	Max
PULSE TUNING:	MAX Signal
REJECT:	Weld with Crown Flush Weld
SENSITIVITY:	10 x 10
FREQUENCY:	15 MHZ
GATE START:	W/Crown: 4 Flush: 4
GATE LENGTH:	3 3
TRANSDUCER:	Transmitter: 464-15 MHZ, S/N 6391, Flat Receiver: SIZ-15 MHz, S/N 10755, Flat
WATER PATH:	1" From Transducer Housing to Panel
WRITE LEVEL:	+ Auto Reset
PART:	1/8" Weld Panels

SET-UP GEOMETRY:

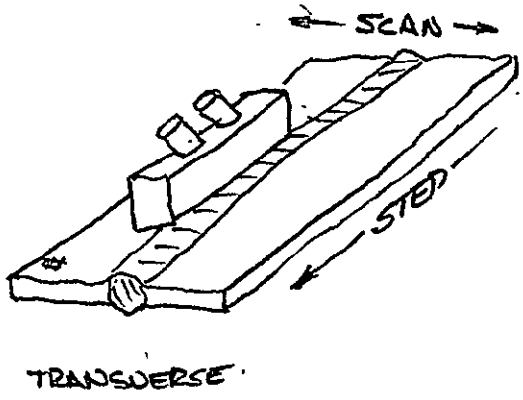

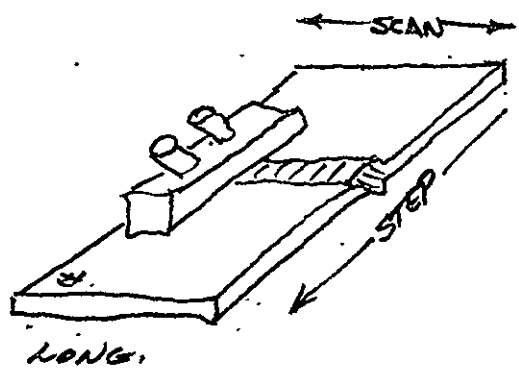

1/8" WELDED PANELS

REF CRACK PANEL #3 ACP

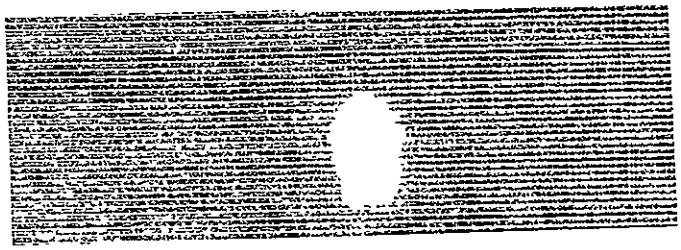

APPENDIX H

SET-UP FOR 1/2", WELDED FATIGUE CRACK PANELS

DATE: 08/15/75

METHOD: Pitch-Catch, Pulse-Echo @ 21 1/2° incident angle for long defect @ 18° incident angle for transverse scan in water,
Angle Indicator
Long = -2 1/2°
Trans= -5°

OPERATOR: Steve Mullen

INSTRUMENT: UM-715 Reflectoscope with 10N/Pulser/Receiver

PULSE LENGTH: 3:00 o'clock

PULSE TUNING: For Max Signal

REJECT: 10:00 o'clock

SENSITIVITY: 2 x 10

FREQUENCY: 5 MHz

GATE START: 4

GATE LENGTH: 3

TRANSDUCER: TX-SIZ-5, S/N 26963, RX-SIZ-5, S/N 35521

WATER PATH: 1.6" From Transducer Housing to the panel

WRITE LEVEL: + Auto
Reset

PART: 1/2" Fatigue Crack Welded Panels

SET-UP GEOMETRY: 1/2" Weld Panel

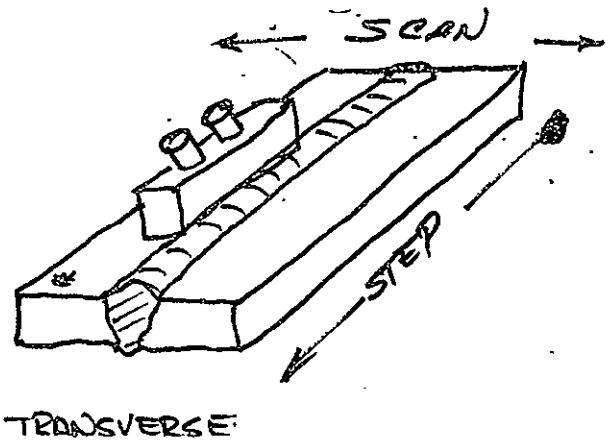

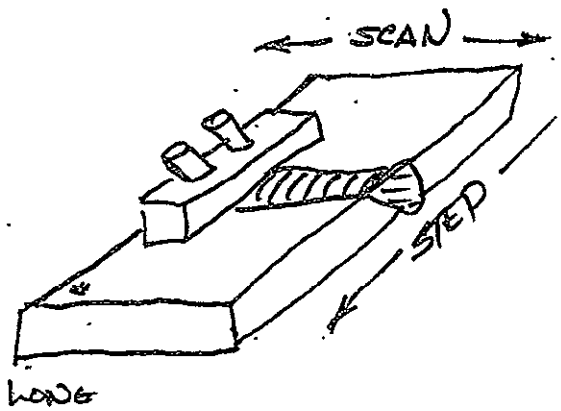

1/2" WELD PANEL

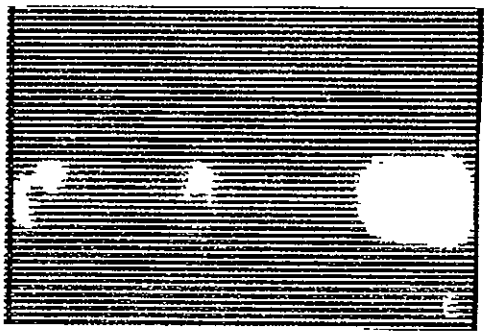

REF PANEL #19 WITH DRILL HOLE

APPENDIX I

ULTRASONIC INSPECTION FOR TIGHT FLAWS IN PANELS WITH FLUSH WELDS

1.0 SCOPE

1.1 This procedure covers ultrasonic inspection of weld panels with flush welds.

2.0 REFERENCES

2.1 Manufacturer's instruction manual for the UM-715 Reflectoscope instrument.

2.2 Nondestructive Testing Training Handbook, P1-4-4, Volumes I, II and III, Ultrasonic Testing, General Dynamics, 1967.

2.3 Nondestructive Testing Handbook, McMasters, Ronald Press, 1959, Volume II, Section 43-48.

2.4 Manufacturer's instruction manual for the Sonatest Flaw Detector, UFD 1.

3.0 EQUIPMENT

3.1 UM-715 Reflectoscope, Automation Industries or Sonatest Flaw Detector UFD-1 with Recorder Interface.

3.2 ION Pulser/Receiver, Automation Industries. (UM-715 only)

3.3 E-550 Transigate, Automation Industries. (UM-715 only)

3.4 SIJ-385, .25 inch diameter, flat, 10.0 MHz Transducer: Automation Industries.

3.5 SR 150 Budd, Ulatrasonic Bridge

3.6 319 DA Alden, Recorder

3.7 Reference Panels - For thin panels use #15 and for thick panels use #30.

4.0 PERSONNEL

4.1 The ultrasonic inspection shall be performed only by technically qualified personnel.

5.0 PROCEDURE

5.1 Set up equipment per setup sheet on page 3 for UM-715 Reflectoscope or page 4 for Sonatest equipment.

5.1.1 Submerge panels. Place the reference panels for the thickness and orientation to be inspected so the bridge steps away from the reference hole. Produce a C-scan recording and compare with the reference recording.

5.1.2 If the comparison is not favorable, adjust the controls (excluding controls on the Pulser/Receiver unit) as necessary until a favorable recording is obtained.

5.2 Submerge, scan the weld area and record in both the longitudinal and transverse directions. Complete one direction then change bridge controls and complete the other direction (see set up sheets).

5.3 Identify on the recording the starting edge of the panel, location of reference hole and direction of scanning with respect to the weld (longitudinal or transverse).

5.4 Upon completion of the inspection or at the end of the shift, whichever occurs first, rescan the reference panel and compare to the reference recording.

NOTE

Dry each panel thoroughly after removing from water.

5.5 Complete the data sheet for each panel inspected.

5.5.1 The "X" dimension is measured from the edge of the panel. Zero designation is the edge with the reference hole.

5.6 After completing the data sheet, roll up recordings, and on the outside of roll record the following information:

A. Date
B. Name of Operator
C. Panel type (Flush weld)
D. Inspection Name (U/S)
E. Inspection Sequence

Ultrasonic setup sheet for
UM-715 Reflectoscope.

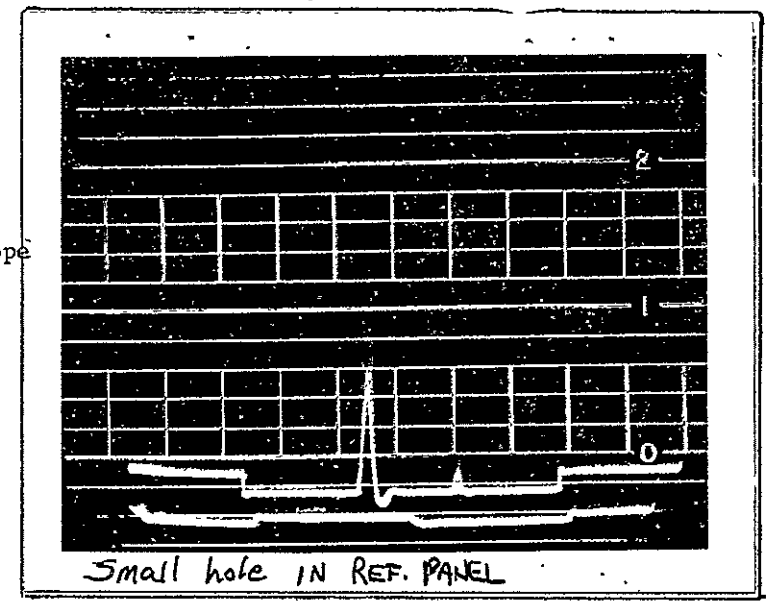

DATE: 07-16-74
METHOD: Pulse/Echo@ 32° L
OPERATOR: Lovisone
INSTRUMENT: UM-715 Reflectoscope

PULSER/RECEIVER UNIT

PULSE LENGTH: Min.
PULSE TUNING: For Max. sig.
REJECT: Ten O'Clock
FREQUENCY: 10 MHz
SENSITIVITY: Using the Ultrasonic Fat. crack Cal. Std. panel, add shims for correct thickness of panels to be inspected. Align transducer on small hole of the Std Panel and adjust sensitivity to obtain a signal of 1.6 inches for transverse scan and 0.4 inches for longitudal scan. (Sensitivity adjustment made with gate turned OFF).

TRANSIGATE UNIT

GATE START: 4
GATE LENGTH: 2
WRITE LEVEL: Auto Reset +
SYNC: Main Pulse

TRANSDUCER: SIJ 385 .25/10.0 S/N 24061
WATER PATH: 1.7" measured @ 32° tilt, center of transducer to panel.
BRIDGE CONTROLS: Carriage Speed 0.30, Step Increment 0.30
PART TYPE: Fatigue crack weld panels with crown and flush welds, 1/8" and 1/2" thickness.
SET-UP GEOMETRY:

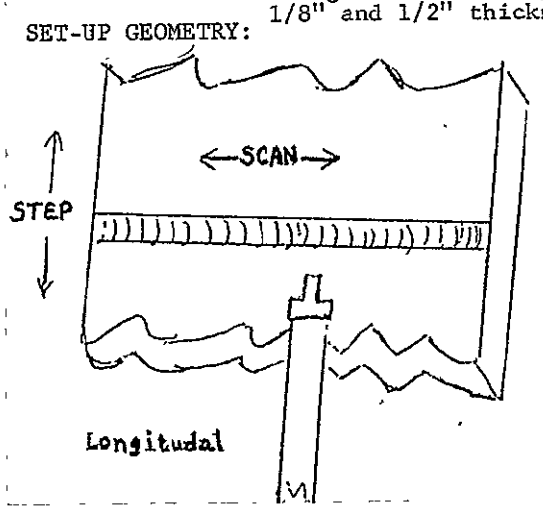

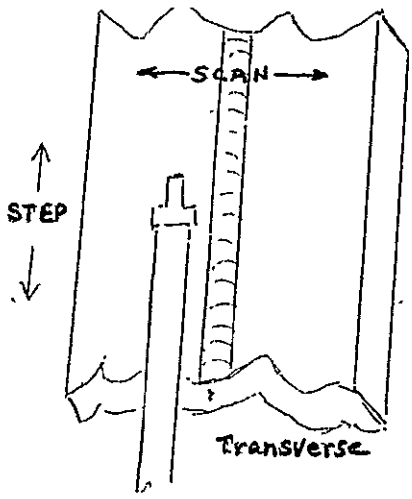

ULTRASONIC SET-UP TECHNIQUE PROGRAM 1/8" Flush Weld

DATE 12/3/74

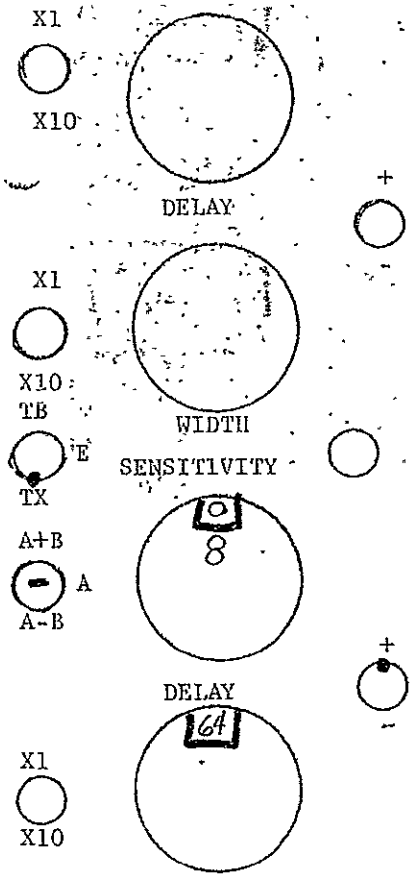

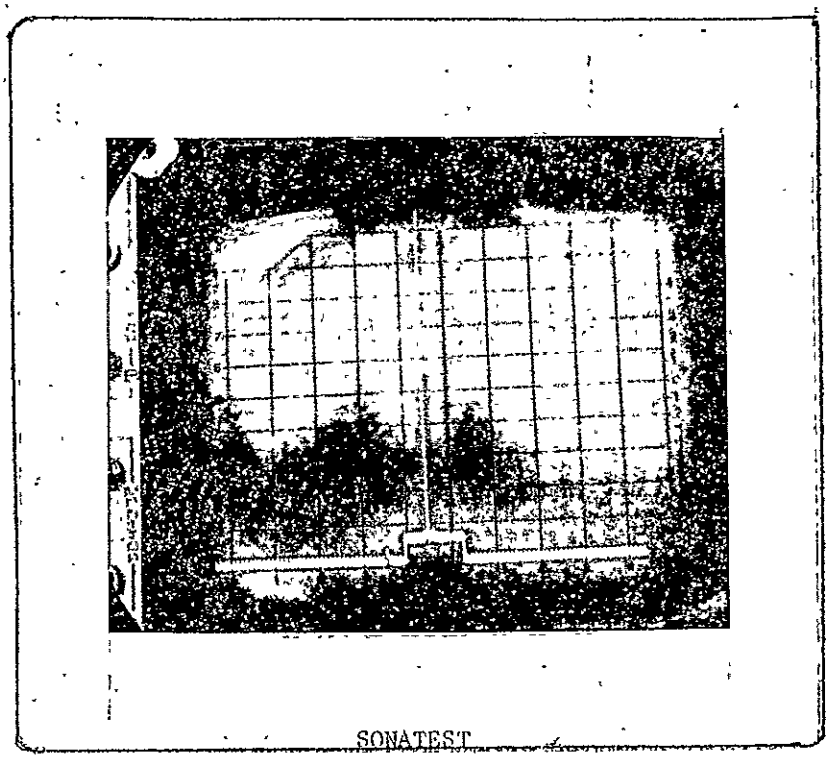

TRANSDUCER:

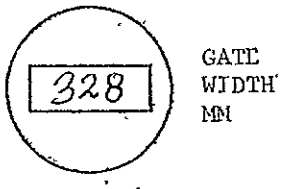

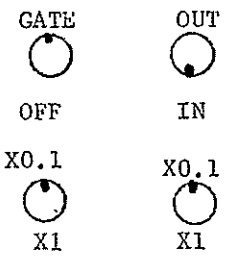

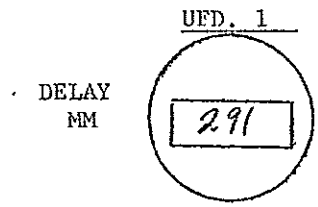

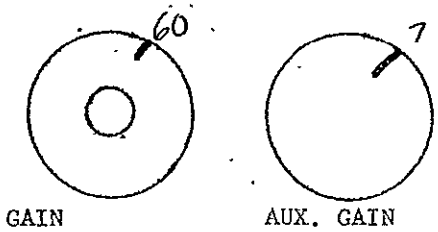

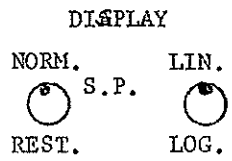

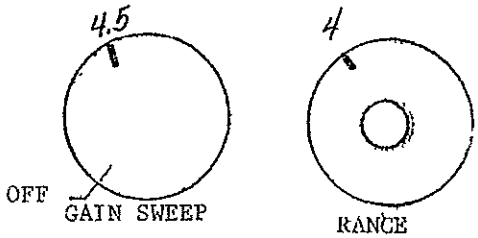

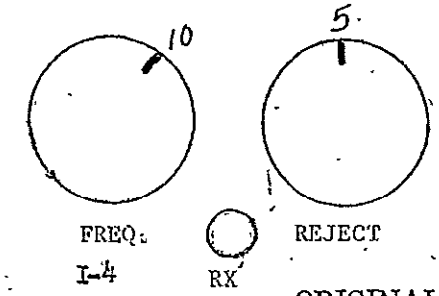

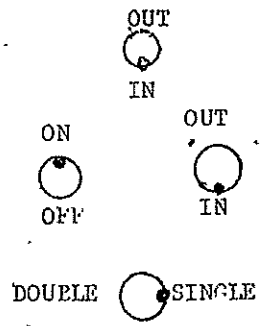

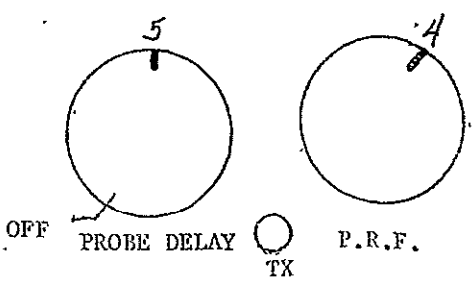

ORIGINAL PAGE IS
OF POOR QUALITY

ULTRASONIC SET-UP TECHNIQUE PROGRAM 1/2" Flush Weld

DATE 12/5-/74

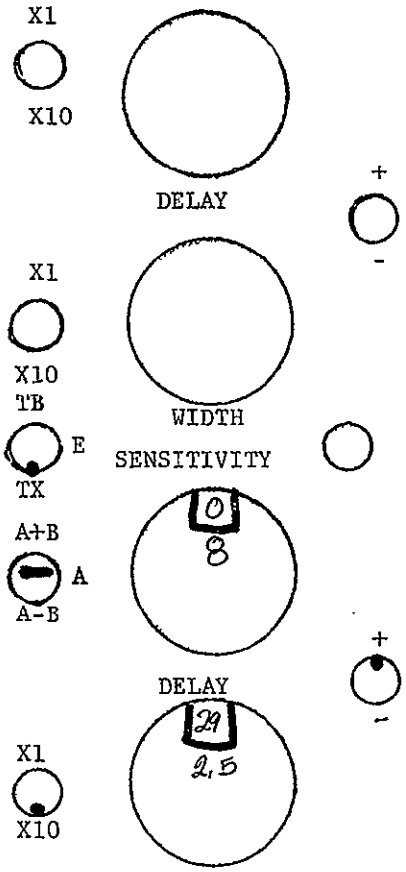

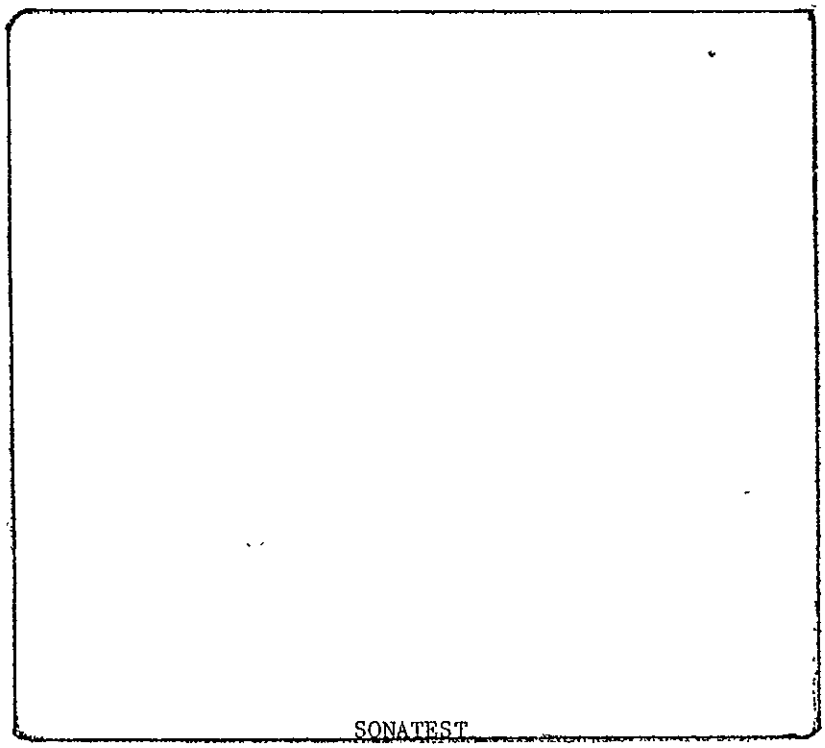

TRANSDUCER:

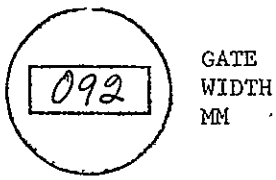

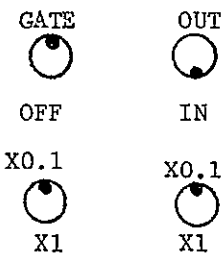

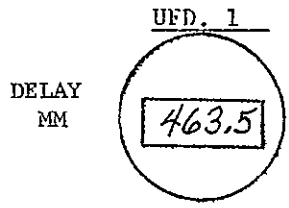

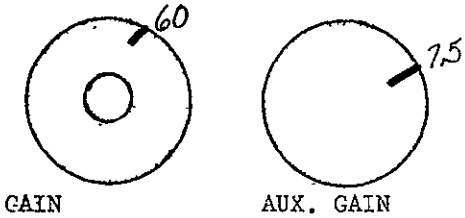

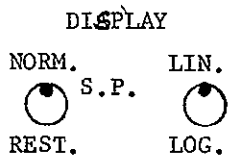

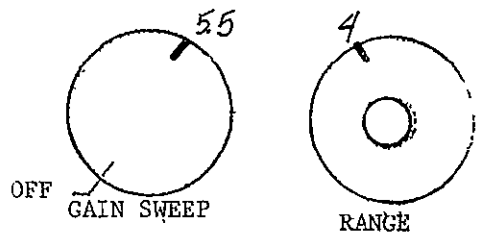

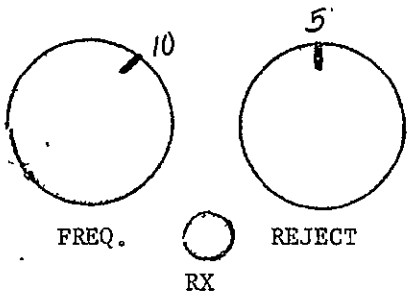

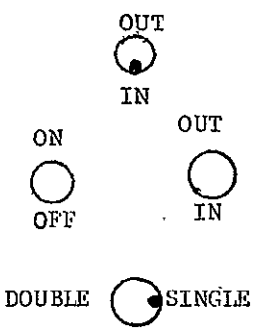

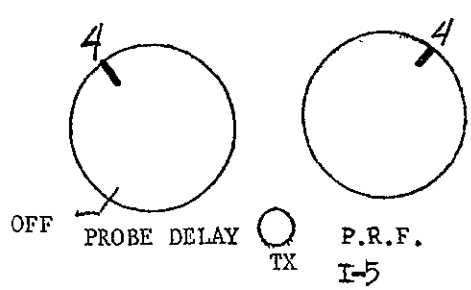

REFERENCE PANEL #15, 1/8" Flush

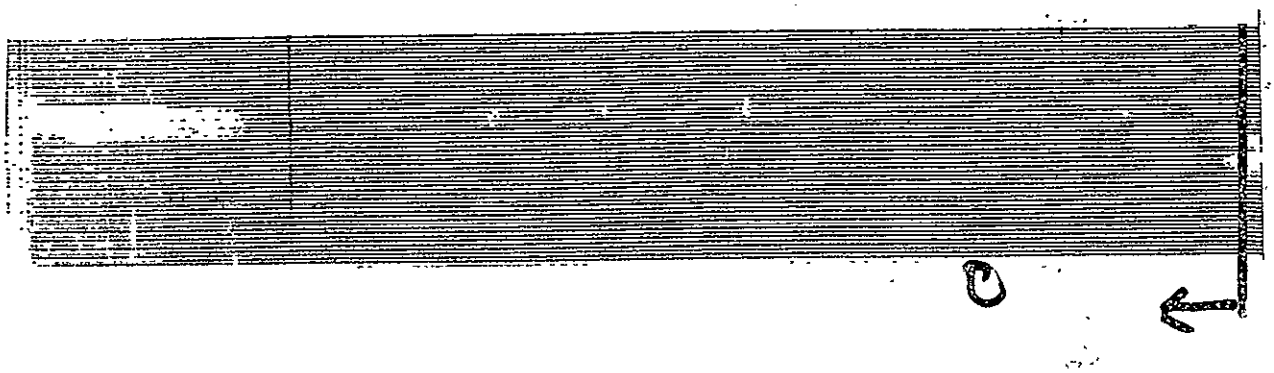

REFERENCE PANEL #30, 1/2" Flush

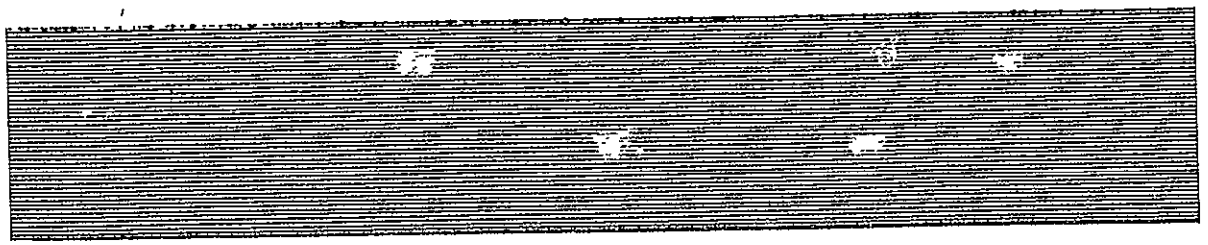

ORIGINAL PAGE IS
OF POOR QUALITY

- APPENDIX J -

EDDY CURRENT INSPECTION AND RECORDING OF
WELD CRACK ALUMINUM PANELS HAVING CROWNS

1.0 SCOPE

1.1 This procedure covers eddy current recorded inspection for detecting cracks in welded aluminum panels having crowns.

2.0 REFERENCES

2.1 Manufacturer's instruction manual for the NDT Instruments Model Vector 111 Eddy Current Instrument.

2.2 Nondestructive Testing Training Handbooks, P1-4-5, Volumes I and II, Eddy Current Testing, General Dynamics, 1967.

2.3 Nondestructive Testing Handbook, McMasters, Ronald Press, 1959, Volume II, Sections 35-41.

3.0 EQUIPMENT

3.1 NDT Instruments Vector 111 Eddy Current Instrument.

3.1.1 100 KHz Probe for Vector 111. Core diameter 0.063 inch.

NOTE: This is a single core, helically wound coil.

3.2 NDE Reference Panel #4, Flaw Length .155 inch.

3.3 SR 150 Budd, Ultrasonic Bridge.

3.4 319DA Alden, Recorder.

3.5 Special Probe Scanning Fixture for Weld Crack Panels. (#2)

3.6 Special Eddy Current Recorder Controller Circuit.

3.7 Dual DC Power Supply; 0-25V, 0-1A (Hp Model 6227B or equivalent).

4.0 PROCEDURE

4.1 Connect 100KHz Probe to Vector 111 instrument.

4.2 Turn instrument power on and set Sensitivity Course control to position #1.

4.3 Check batteries by operating power switch to BAT position. These should be checked every two hours of use.

4.3.1 Meter should read above 70.

4.4 Connect Recorder Controller circuit

4.4.1 Set Power Supply for +16 volts and -16 volts.

4.5 Set up weld panel scanning support fixture, shims and spacers as follows:

4.5.1 If longitudinal welded panels are being scanned, clamp an end plate of the same thickness as welded panel to the support fixture. Align the end scan plate, using one weld panel so that the scan probe will be centered over

the entire length of the weld bead. Secure the weld panel with weights/clamps as required. Verify that the scan probe holder is making sufficient contact with the weld bead such that the scan probe springs are unrestrained by limiting devices. Secure an end scan plate at opposite end of weld panel. Verify that scan probe holder has sufficient clearance for scan travel. One logitidinal welded panel will be scanned at a time.

4.5.2 If transverse welded panels are being scanned, set up as in 4.5.1, except that two weld panels are placed side by side so that the weld beads are aligned with the scan probe.

4.5.3 Use shims or clamps to provide smooth scan probe transition between weld panel and end plates.

4.6 Set Vector 111 controls as follows:

X 189.7

R 404.0

Sensitivity, Course 8, Fine 5.

4.7 Set the Recorder controls for scanning as follows:

Index Step Increment	.020 inch
Carriage Speed	.029
Scan Limits	set to scan 1½ inches beyond the panel edges
Bridge	OFF and bridge mechanically clamped.

4.8 Manually move the scan probe over panel inspection region to determine background level as close as possible to the Recorder Controller switching point (meter indication for switching point is 40 for positive-going indication of a flaw, 42 for negative-going indication).

4.9 Initiate the Recorder/Scan function.

4.10 Vary the Vector 111 Scale control as required to locate flaws. Use the Carriage Scan switch on the Recorder control panel to stop scan for resetting of background level.

4.11 Repeat step 4.8 (background level determination) and 4.9 for the second panel if located in the support fixture. Annotate recordings with panel identification data.

4.12 Evaluate recordings for flaws and enter panel and flaw location on applicable data sheet. Observe correct orientation of reference hole edge of each panel when measuring location of a flaw.

5.0 PERSONNEL

5.1 Only qualified personnel shall perform inspections.

6.0 SAFETY

6.1 Operation should be in accordance with Standard Safety Procedure used in operating any electrical device.

AMENDMENT A

- APPENDIX J -

NOTE

This amendment covers changes in procedure from raster scan recording to analog recording.

4.4.2 Connect Autoscaler circuit to Vector 111 and set back panel switch to AUTO.

4.8 Initiate the Recorder Scan function. Set the Autoscaler switch to RESET.

4.9 Adjust the Vector 111 Scale control to set the recorder display for no flaw or surface noise indications.

4.10 Set the Autoscaler switch to RUN.

4.11 When all of the signatures of the panels are indicated (all white display), stop the recorder. Use the carriage Scan switch on the Recorder Control Panel to stop scan.

4.12 Annotate recordings with panel/side/thickness/reference edge identification data.

4.13 Evaluate recordings for flaws and enter panel and flaw location on applicable data sheet. Observe correct orientation of reference hole edge of each panel when measuring location of a flaw.

-APPENDIX K -

EDDY CURRENT INSPECTION AND C-SCAN RECORDING OF FLUSH WELD ALUMINUM PANELS

1.0 SCOPE

1.1 This procedure covers eddy current C-scan inspection detecting fatigue cracks in Aluminum panels with flush welds.

2.0 REFERENCES

2.1 Manufacturer's instruction manual for the NDT instruments Model Vector 111 Eddy Current Instrument.

2.2 Nondestructive Testing Training Handbooks, P1-4-5, Volumes I and II, Eddy Current Testing, General Dynamics, 1967.

2.3 Nondestructive Testing Handbook, McMasters, Ronald Press, 1959, Volume II, Sections 35-41.

3.0 EQUIPMENT

3.1 NDT Instruments Vector 111 Eddy Current Instrument.

3.1.1 100 KHz probe for Vector 111. Core diameter 0.063 inch

NOTE: This is a single core, helically wound coil.

3.2 SR 150 Budd, Ultrasonic Bridge.

3.3 319DA Alden, Recorder.

3.4 Special Probe Scanning Fixture for Weld Panels. (#5)

3.5 Dual DC Power Supply; 0-25V, 0-1A (HP Model 6227B or equivalent).

3.6 NDE reference panel no. 41.

3.7 Special Eddy Current Recorder Controller circuit.

4.0 PROCEDURE

4.1 Connect 100 KHz probe to Vector 111 instrument.

4.2 Turn instrument power on and set SENSITIVITY COURSE control to position 1.

4.3 Check batteries by operating power switch to BAT position. Batteries should be checked every two hours of use. Meter should read above 70.

4.4 Connect C-scan/Recorder Controller Circuit

4.4.1 Set Power Supply for +16 volts and -16 volts.

4.4.2 Set "U/S E/C" switch to E/C.

4.4.3 Set OP AMP switch to OPR.

4.4.4 Set RUN/RESET switch to RESET.

4.5 Set up weld panel scanning support fixture as follows:

4.5.1 Clamp an end scan plate of the same thickness as the weld panel to the support fixture. One weld panel will be scanned at a time.

4.5.2 Align the end scan plate, using one weld panel so that the scan probe will be centered over the entire length of the weld bead.

4.5.3 Use shims or clamps to provide smooth scan transition between weld panel and end plates.

4.5.4 Verify that scan probe is making sufficient contact with panel.

4.5.5 Secure the weld panel with weights or clamps as required.

4.5.6 Secure an end scan plate at opposite end of weld panel.

4.6 Set Vector 111 controls as follows:

"X" 189.5

"R" 404.0

SENSITIVITY, COURSE 8, FINE 4.

MANUAL/AUTO switch to MAN.

4.7 Set the Recorder controls for scanning as follows:

Index Step Increment .020 inch

Carriage Speed .029

Scan Limits set to scan 1½ inches beyond the panel edge.

Bridge BRIDGE

4.8 Manually position the scan probe over the center of the weld.

4.9 Manually scan the panel to locate an area of the weld that contains no flaws (decrease in meter reading).

With the probe at this location, adjust the Vector 111 Scale control to obtain a meter indication of 10 (meter indication for switching point is 25).

4.10 Set Bridge switch to OFF and locate probe just off the edge of the weld.

4.11 Set the Bridge switch to BRIDGE.

4.12 Initiate the Recorder/Scan function.

4.13 Annotate recordings with panel reference edge and serial number data.

4.14 Evaluate recordings for flaws and enter panel, flaw location and length data on applicable data sheet. Observe correct orientation of reference hole edge of each panel when measuring location of flaws.

5.0 PERSONNEL

5.1 Only qualified personnel shall perform inspection.

6.0 SAFETY

6.1 Operation should be in accordance with Standard Safety Procedure used in operating any electrical device.